AGARD-LS-191

AGARD

ADVISORY GROUP FOR AEROSPACE RESEARCH & DEVELOPMENT
7 RUE ANCELLE 92200 NEUILLY SUR SEINE FRANCE

AGARD LECTURE SERIES 191

Non Linear Dynamics and Chaos

(La Dynamique Non-Linéaire et le Chaos)

The material in this publication was assembled to support a Lecture Series under the sponsorship of the Guidance and Control Panel of AGARD and the Consultant and Exchange Programme of AGARD which it was planned to present in Stanford, United States and Sophia Antipolis, France in June 1993.

North Atlantic Treaty Organization
Organisation du Traité de l'Atlantique Nord

The Mission of AGARD

According to its Charter, the mission of AGARD is to bring together the leading personalities of the NATO nations in the fields of science and technology relating to aerospace for the following purposes:

- Recommending effective ways for the member nations to use their research and development capabilities for the common benefit of the NATO community;
- Providing scientific and technical advice and assistance to the Military Committee in the field of aerospace research and development (with particular regard to its military application);
- Continuously stimulating advances in the aerospace sciences relevant to strengthening the common defence posture;
- Improving the co-operation among member nations in aerospace research and development;
- Exchange of scientific and technical information;
- Providing assistance to member nations for the purpose of increasing their scientific and technical potential;
- Rendering scientific and technical assistance, as requested, to other NATO bodies and to member nations in connection with research and development problems in the aerospace field.

The highest authority within AGARD is the National Delegates Board consisting of officially appointed senior representatives from each member nation. The mission of AGARD is carried out through the Panels which are composed of experts appointed by the National Delegates, the Consultant and Exchange Programme and the Aerospace Applications Studies Programme. The results of AGARD work are reported to the member nations and the NATO Authorities through the AGARD series of publications of which this is one.

Participation in AGARD activities is by invitation only and is normally limited to citizens of the NATO nations.

Published June 1993

ISBN 92-835-0714-2

Printed by Specialised Printing Services Limited
40 Chigwell Lane, Loughton, Essex IG10 3TZ

Abstract

In the last decade many efforts have been oriented towards the understanding of the unexpected behaviour of systems — linear or non-linear. These could be large (weather systems, biological life) or small (automatic pilot). A new branch of dynamics is now considered; it is called "Chaos". Some general theories have emerged and reconsideration of concepts of non-linear control to determine the stability of such systems is now intensively studied in the scientific community.

It is planned that the following topics will be covered:

— Linear (including time varying coefficients equations) vs non-linear systems. Types of non-linearity: curved characteristics, jumps, bifurcation

— Non linear dynamics; sensibility to initial conditions and/or uncertainties on the system parameters. Robustness

— Neuronal-type machines

— Chaos — Random process behaviour

— Reversibility and irreversibility; Newtonian mechanics and thermodynamics

— Fractals

— Applications:
  — Fluid mechanics, meteorology
  — Aircraft behaviour
  — Mechanical systems.

Abrégé

Au cours de la dernière décennie des efforts considérables ont été consacrés à la compréhension du comportement imprévisible des systèmes linéaires et non-linéaires. De tels systèmes peuvent être de grande taille (systèmes météo, vie biologique) ou petits (pilote automatique).

Une attention particulière est actuellement accordée à une nouvelle branche de l'aérodynamique; elle s'appelle "le chaos". Un certain nombre de théories générales se sont dégagées et les concepts du contrôle non-linéaire pour la détermination de la stabilité de tels systèmes ont été remis à l'étude de façon intensive par la communauté scientifique.

Les sujets suivants seront examinés:

— Les systèmes linéaires (y compris les équations à coefficient variable dans le temps) comparés aux systèmes non-linéaires. Les différents types de non-linéarité: les caractéristiques courbes, les sauts, la bifurcation.

— La dynamique non-linéaire; sensibilité aux conditions initiales et/ou incertitudes concernant les paramètres du système. Robustesse.

— Les machines du type neuronales

— Le chaos — le comportement des procédés aléatoires

— La reversibilité et l'irréversibilité; la mécanique Newtonienne et la thermodynamique

— Les fractales

— Applications:
  — la mécanique des fluides, la météorologie
  — le comportement des aéronefs
  — les systèmes mécaniques.

List of Authors/Speakers

Lecture Series Director

Dr Marc Pelegrin
Honorary Scientific Adviser
ONERA CERT
BP 4025
31055 Toulouse Cedex
France

Prof. P. Coullet
Université de Nice
Institut Non-Linéaire de Nice
UMR CNRS 129
Parc Valrose
Sophia Antipolis
(near Cannes)
France

Prof. C. Houpis
Air Force Institute of Technology
ENG
Wright Patterson AFB.
Ohio 45433
United States

Prof. Ph. Guicheteau
ONERA
BP 72
92322 Châtillon Cedex
France

Prof. J.J. Slotine
Ecole Polytechnique
91128 Palaiseau Cedex
France

Contents

* These papers have already been published in the textbook "Applied Nonlinear Control" by Slotine and Li (Prentice-Hall).

INTRODUCTION TO LECTURE SERIES 191 ON NON LINEAR DYNAMICS AND CHAOS

Dr Marc PELEGRIN
Honorary Scientific Adviser
ONERA / CERT
B P 4025
31055 TOULOUSE CEDEX
FRANCE

I do not intend to give a summary of what Prof P. Coulet, Ph. Guicheteau, C. Houpis and J.J. Slotine will talk about during this Lecture Series - it's merely a matter for the Conclusions.

I will try to mention some aspects of non-linear dynamics and/or chaos which perhaps are marginal with regard to the core of the subject which will be developed during these 3 days; eventually they could be commented on or discussed during the Round Table.

Most of us are involved in engineering studies or designs; although aeronautics and space are not mentioned in the title of the LS, it is pertinent that these two fields will be dominant during the lectures. However, it is always fruitful to look around and compare the different approaches to the subject. This is why Prof Houpis and Guicheteau will speak mainly about aeronautics and space-related problems, Prof Slotine will comment about robotics and Prof Coulet will cover the general subject both from a theoretical viewpoint and on application in various domains (fluid flows, optics, chemical and biological systems).

1. SOME BASIC DEFINITIONS AND COMMENTS[1/]

A system is an ensemble of components well delimited in space and time; outside the system is the external world. If there is no mass transfer across the delimiting surface the system is said to be "closed"; if there is no heat transfer - or more generally no radiation exchanged with the external world, the system is said to be "isolated".

The complexity of the system is difficult to precise; it implies the specification of observability scales; a trivial example is the difference in the concept used for the engineer who designs a turbine and the physicist who studies molecular transformations; both of them use the entropy concept. For the engineer, entropy S is defined as $dS=dQ/T$ Q heat flux exchanged T absolute temperature; for the physicist entropy is the logarithm of the probability that an event of a given complexion (in terms of molecule arrangement) happens. This notion of scale is of prime importance as we will see later.

The correlation concept is very useful in the study of systems (see, for example, the proceedings of the International Symposium on "The correlation" ref[2]).

Correlation apparently bears different meanings for mathematicians, physicists and engineers. The correlation is commonly used as a device to quantify an uncertainty in physics phenomena. The uncertainty can be a fundamental one, like in the quantum mechanics, or can be produced by the large number of parameters which are considered, or it can simply be an appearance like in phenomena linked to the determinist chaos. To understand such situations, it is necessary to enlarge the concept of correlation and even to go beyond its limits (concept of linkage, resemblance, distance). That's why it seems worthwhile considering the question.

Finally the perception and comprehension mechanism of the human brain, as well as the "neuronal machines" which are being developed, encourage us to examine the importance of the part played by the correlation.

The next concept to be introduced is order and disorder. Complete disorder is independence. All other definitions are merely negative such as this one: a sufficient (but not necessary) condition to say that a system is not disorganized is that correlations between the fluctuating parameters - if any - are not null.

Hazard is generally associated to probability; however, complete disorder is considered to be a manifestation of hazard, but, from a stochastic point of view, complete disorder escapes from laws of probability: there is a contradiction.

Then we arrive at chaos, which is normally associated with disorder.

The deterministic chaos has been introduced by Poincaré around 1892 in his famous books (3 volumes) on "Les Méthodes Nouvelles de la mécanique céleste" 1892-93-99 reprinted by Dover Publications Inc., 1957.

It seems that nobody has really considered the problem stated by Poincaré until the '60s though the Bénard's curls have been deeply studied both on an experimental and a theoretical basis. Nobody questioned - and still questions - the fact that organized large motions of molecules (water, for example) appear gently from completely unorganized motions when external parameters (the heat flux in that case) varies continuously in one direction; it is worthwhile noting that the container in which the Bénard's curls appear is not an isolated system.

Major works have been provided by Lorentz on the Rayleigh-Bénard convection and by Ruelle and Takens[2/] on the turbulence in the '60s. At that time high subsonic civilian planes and supersonic ones in the military domain came into being. The power of the jet engine and their high consumption (double flux jet engines did not yet exist) imposed a careful study of the aerodynamic drag of the plane. It was recognized that the big problem was in the boundary layer and, in particular, the transition laminar/turbulent in the extrados of the wings. Aerodynamists shall try to arrive at a full laminar boundary layer along the entire wing chord.

The transition is not yet fully understood but progress is made every day, perhaps thanks to scientists working on chaos, as this transition belongs to a more general phenomena, contrary to the Bernard's curls, the passage from organized flow structure to unorganized flow structure.

Extreme chaos is the molecular chaos which is an undeterministic chaos governing thermodynamics. We will come back to it a little further on.

A pure determinist chaos is represented in certain types of "fractals". Discovered - or rediscovered - in 1975 by Benoit Mendelbrot, fractals can have regular but incredibly complex structures (such ones issue from a triangle) or fully irregular structures though issued from a mathematical iteration.

1/ For further details see ref [1] the paper presented by A. Favre "Correlations Spatio-Temporelles, determinisme et chaos".

2/ For bibliographic references see Footnote under Paragraph 6.

Initially fractals did not seem to have any application except, perhaps, in the beauty of the presentation. Later on, it was recognized that, firstly fractals may represent a good approximation of real features such as maritime coast, secondly, that the "auto-similarity" which can be considered as the intrinsic property of fractals, is certainly a general property of nature. For examples, the structure of a tree is about the same if we look at it from very far or very near; types of ramifications are similar; the cosmos structure seems to comply with the rule of auto-similarity (star with planets; galaxy with stars, cluster of galaxies...).

A fractal dimension has been defined (the fractal dimension of the coast of Brittany is 1.26 and the "dust of Caritov" has a fractal dimension of 0.6309).

Another apparent contradiction lies in the dimension of a structure and in 1890 G. Peano described a geometrically defined curve which can cover a square completely: any point of the square can be reached by the curve. Then, what is the dimension of a square, 2 as normally assumed or 1 because it is anything else than a curve?

On the other hand, a phenomenon that can be called anti-turbulence has been discovered and studied by John Russel in 1834. This is the soliton wave which is an isolated wave whose amplitude can be large (a few decimeters on a canal 5m wide). This wave can travel thousands of meters without any modification in shape. The two problems rising from this fact are that first, how is the wave produced and second, how can it travel without a quick damping? The answers are not yet well established. It seems that the soliton starts from the complex and apparently unorganized turbulence which is created in front of an old-fashioned boat. This is why we have said above that such a phenomenon is sometimes associated with anti-turbulence. As to the absence of degradation of this isolated wave, we can only say that some non-linear interaction should be produced between the bottom of the canal and the wave.

Indeed it is rather difficult to produce a soliton in the laboratory; some success has been obtained with large canals; it has always been noted that the energy involved in this process is quite a critical parameter: too little energy causes a quick dumping of the wave produced, too much energy creates just turbulent motion. Some non-linear partial derivative equations give an acceptable representation of the phenomenon (KdV equation of D.J. Kortweg and C. de Vries).

It is time now to comment about the contradiction between the classical mechanics (which implies reversibility) and thermodynamics (which implies irreversibility, the entropy of an isolated system can only increase).

As a first remark, is the assumption that molecules, at least monoatomic ones, behave like interacting bodies in macroscopic mechanics absolutely true? If we answer yes, then thermodynamics should be reversible and the entropy should no longer be a monotonous quantity. If we answer no, then thermodynamics is a separate branch of physics and everything has to be reconsidered from the molecule behaviour.

Today and for the next 2 days, I propose to you that the answer is yes. How to justify this worldwide accepted assumption? The basic point is Poincaré's statement according to which a closed and isolated system will necessarily pass in the "vicinity" of any initial configuration from which it started [1]. I am unable to comment about "vicinity", however, it does not cancel what is said below.

In the famous statement called Maxwell's devil, two vessels initially at different pressures (or temperatures) communicate through a small hole. Everybody knows that after a while the pressure will be the same in the two vessels. Poincaré's statement says - just wait and in some moments pressure (or temperature) will be different. Nobody has yet observed such a phenomenon.

The devil was looking at the speed of molecules; he let pass through the hole only those which had a "great velocity". If pressure in the vessels was equal in the beginning, they will not be after a while... An explanation may come from the fact that there are $6.023.10^{23}$ molecules per mol [2]. Can the "classical mechanics" be extended to such numbers of "components"? Previously we said yes, but if we now compute the time it can take to arrive at an "abnormal" molecule repartition, we find (from C. Marchal):

- Initial pressures in the vessels $1.4\ 10^5$ Pa [3] and $0.6\ 10^5$ Pa.
- The mode of choice of molecules which passes through the hole does not notably influence the results.
- If we measure the pressure with 10^{-3} Pa accuracy, we can notice fluctuations with regard to the average solution at a rate of about once per two years.
- If we look for variations of 5m Pa the probability of finding such a division is 10^{-20^7} before $1.4\ 10^{322}$ years.
- The a priori probability that the pressure in one vessel would be $1.4\ 10^6$ Pa or higher is 10^{-M} with $M=3.5\ 10^{16}$: it is not zero!...

It is hard to say that this is a final answer to the dilemma. However, we could not deny that the return time to initial conditions (Poincaré's return time) exists; unfortunately we could not pass from macroscopic systems to microscopic systems on a continuous basis. State vector of dimension 100, even 1,000 are now considered (flexible structures, for example) in the macroscopic domain; in fluid dynamics state vectors are on the order of 6.023×10^{23} per mole!

The last concept we want to mention is the stability concept. At first glance stability and chaos seem opposite - like stability and instability: this is not always true.

Is stability a measurable quantity - like mass, or an identifiable quantity - like temperature? There are many definitions of stability, sometimes contradictory: in fact, it is a subjective quality which should be defined in the context of the field considered. The reference system in which the system evolves should be defined: stability may well exist in a given reference system, but no longer exist in another reference system. Stability seems to be a dominant factor in aircraft or missile control - or for that matter, of any type of vehicle. However, stability and manoeuvrability are two opposing factors which intervene in aircraft control: for civilian aircraft, stability is the dominant factor; for military aircraft or missiles, manoeuvrability is the dominant factor. The above are some of the reasons which led to the organization of a Workshop on "Stability" for the AGARD community.[2]

Basically, stability is related to irreversibility, which means no energy dissipation for linear systems. While linear systems are very rare, they often represent a suitable approximation of non-linear systems. Stability is also a matter of accuracy. Take, for example, the rotation of the earth: is it stable or unstable? This question has no meaning unless the range of accuracy we are looking for, and in fact, the whole context can be specified. Thanks to the accuracy of existing atomic clocks, it can be demonstrated that daily variations of the order of 1ms yearly or pluri-annual variations of the order of tens of ms, occur in a pseudo periodic manner. However, angular velocity is necessarily decreasing long-term; this is mainly due to the water/earth friction in tides. In the pre-Cambrian period (400 M years ago) the day was only 15 hours long (that is 1ms lost every 10 years)! What has been said about the angular velocity of the earth could also be said about the direction of the earth's momentum. At the pole, (the trace of the rotational vector moves continuously in a circle of about 2m in diameter. However, for all human activities the earth's rotation is considered stable (except by some astronomers).

Poincaré studied stability for non-autonomous and autonomous problems in the 1870's. Lyapounov in the 1900's introduced a way of proving whether or not stability exists. It was sufficient, but not the necessary condition. Following this, the behaviour of a system in the vicinity of an "equilibrium point" was studied in detail by Poincaré and equilibrium points or "singularities" were classified as nodes-summits-focus-saddle.

1/ For more details see the paper presented by C. Marchal "Chaos Entropy and Irreversibility: a Simple Example", which appears in ref[2].

2/ A mole (mol) corresponds to the number of atoms of 0.012kg of C12.

3/ 1 Pa (Pascal) is approximately 10^5 bar.

A variety of possible behaviour patterns in the vicinity of a point, the limit cycles, which can be stable or unstable, were introduced; they

generalized the point of stability by letting a periodic motion, normally of a small amplitude, around the point of stability (in the phase plane or space). More recently, new vocabulary has been introduced "strange attractor" instead of point of equilibrium or limit cycle.

All aspects of physics are affected by the concepts of stability. Mechanical systems were the first to be affected by Poincaré's approach. Theories and studies concern non-linear systems. All that can be said about linear systems has been said. At the present time theories and studies concern non-linear systems. No global solution is expected. The robustness concept of a control system is an extension of linear systems studies. This concept is important for applications in industry or vehicle control. Robustness can be defined as the capacity to achieve the specified performances in spite of some unknown concerning the parameters which define the system to be controlled - or sometimes, the control parameters themselves. Obviously, a linear differential equation with such uncertainties on coefficients is no longer a linear equation. In fact, even in the early days of linear system studies "phase margin" and "gain margin" were used to compensate for some errors in system description. Nowadays more elaborate techniques such as H∞ optimization enable us to deal with multi-input, multi-output systems.

We can probably say that the dilemma "stability-instability" has made most progress in fluid mechanics, aero- and hydro-dynamics and spectacular (in both meanings of the word) results arose from the Benard's curls.

Nonetheless, in this domain, the aerodynamic flow around a wing can be stable, though instability may appear locally in the boundary layer; during a "normal flight" the boundary layer becomes turbulent (i.e., locally unstable) somewhere between one-half or two-thirds of the wing chord. Buffer phenomena is due to the escape of curls from the boundary layer, a phenomena which should be avoided for aircraft performance and passenger comfort. Flutter phenomena which are very dangerous, are due to aero-elastic coupling between air flow and wing elasticity: it appears when the frequencies of 2 modes converge to a unique frequency (normally the 1st bending and 1st torsion modes). This is typically a case of instability which can gradually emerge from stability when some flight parameters vary (velocity and/or load factor).

Stability - or instability - also has a meaning in static structures (bridges [1/], buildings, dams, earth embankments, ship or aircraft structures, etc.) when loads reach a given value: this is buckling. Even in the earth's crust, instability appears (earthquakes). Roughly speaking, it can be said that as a result of tectonic plate motions, when, in a given location, the friction constraint is surpassed, the sliding effect or the elastic deformation of a part of the ground is suddenly transformed into a jump.

To conclude, I would like to briefly mention atmospheric conditions. Does stability have a meaning? Probably not, though in many countries, like those in the temperate zone, weather has a certain degree of stability: if you say "Tomorrow the weather will be like today's" you are not making a bad forecast! (The probability of success is well above 50% since in these countries weather does not change every day - a certain degree of stability exists.) Weather is a consequence of air movement over the world; it should be predictable as for any system for which the equations are known. Unfortunately, air movement is governed by partial derivative equations - they are known with reasonable certainty - but a set of homogeneous initial conditions (3-D) remains to be acquired even by meteorological satellites. Meteorologists proceed by region (they use some grids, ranging in size from a few kilometers to hundreds or thousands of kilometers) and try to start with coherent sets of initial conditions on the boundaries of these grids. The computer then solves the equations and they arrive at a correct(?) forecast for 24 or now 48 hours. Their goal is to achieve predictions with the same degree of accuracy for a 72-hour period before the end of the century.

In the following paragraphs we will touch upon the coupling between the local atmosphere in which a plane flies and the plane itself.

2. THE RANDOM ENVIRONMENT OF A PLANE

This is probably the main characteristic of aeronautics. Marine and space activities have to face adverse conditions, but probably not on the same level as aeronautics.

To start the design and computation of a plane, a "standard atmosphere" has been specified (Fig. 1). Assuming that the plane flies within such an atmosphere, aerodynamic forces and eventually their associated phenomenas such as buffeting (called "buffet") or flutter (an aeroelastic coupling between the airflow and the structure) can be precisely computed, hence the attitude and motion of the plane. The flight envelopes (Fig. 2) are used by airline operators, air traffic control or military people for the safe and optimum management of the aircraft.

But the real atmosphere departs from the standard atmosphere in a way which is difficult to specify in the vicinity of the plane.

The atmosphere is composed of - the troposphere a 8,000-11,000m high layer around the earth in which there are vertical motions namely in active cumulo-nimbus clouds - the stratosphere, just above the troposphere, in which air motions are mainly horizontal.

The separation is called tropopause, it is a transition layer in which both characteristics are present. The position and thickness of this layer varies with the latitude and the seasons.

In the troposphere, strong turbulence even in clear sky may exist. Active cumulo-nimbus are dangerous for a plane due to the turbulence, the vertical velocities (20m/s in the core of the ascending mass of air-/water), lightning, icing...

If a plane enters such a cloud, it is like entering into chaos at least for the passengers, (the crew tries just to maintain an acceptable angle of attack and to stabilize the roll motion of the plane).

In the stratosphere, jet streams are frequent; there are "tubes" of some hundreds of meters or of a few kilometers diameter of air; the flow can be laminar and clear but the transition is highly turbulent.

Until the last few years, the only measurable parameters on board were static pressure p_s, dynamic pressure p_d and total temperature T_s. From there data true airspeed (TAS) and Mach number should be derived by St Venaud or Rayleigh formulaes according to the Mach number.

Lastly, the scales of turbulence could vary from some meters to some kilometers and stationarity is normally not the rule.

To be certified, a plane must experience no damage (more precisely, it should stay in the "elastic domain") when crossing a gust or when flying in a turbulent area. Gusts are defined by "specifications" which vary - slightly - among the countries who certify planes. In France, two major conditions to be satisfied are:

- a vertical gust of "1 - cos" type

$$\begin{cases} w(t) = 0 & t < 0 \\ w(t) = \frac{W_m}{2}\left(1 - \cos\frac{2\pi v t}{d_m}\right) & \text{for } 0 < t < \frac{d_m}{v} \\ w(t) = 0 & t > \frac{d_m}{v} \end{cases}$$

W_m gust amplitude (m/s)

d_m gust length wind (m)

1/ The Tacoma suspension bridge which collapsed on 7 Nov 1940 was subjected to a relatively low wind (18.7 m/s). It was a typical phenomenon similar to flutter (conjecture of 2 vibrating modes).

- a van Karman spectrum

$$\phi_w(\omega) = \sigma^2_w \frac{L_w}{v} \frac{1+\frac{8}{3}\,[1{,}339\frac{L_w}{v}\omega]^2}{[1+1.339\frac{L_w}{v}\omega]^{11/6}}$$

with $$\sigma^2_w = \frac{1}{2T}\int_{-\infty}^{+\infty}\phi_w(\omega)d\omega$$

L_w : turbulence scale
σ_w^2: velocity mean square value
ω : pulsation

It is important to note that the numerical values which appear in the above equations must be revised according to the safety level reached at a time. As this safety level increases, one must look for the amplitude of the gust or turbulent spectra which have a probability of the same value as the safety level of the plane.

3. WHEN CHAOS BECOMES DOWNBURSTS

"Some aircraft accidents that occurred at low altitudes during convective activity were regarded as pilot error without blaming the weather systems as major contributing factors" from Theodore Fujita "The Downburst", University of Chicago 1985[3]. He proved that the "inquiry board" was wrong!

It is estimated that 1 to 3 commercial planes are lost each year because of windshears due to downbursts (Russia and China are not accounted for). Downbursts result from the sudden instability of a cold mass of air coming normally from a cloud; however, a downburst can be accompanied by a shower (sometimes very strong), it can be dry or be accompanied by showers only in its upper part i.e. the droplets evaporate in between the cloud and the ground. Fig. 3 modelizes a microburst and a tornado.

I'll give two examples to point out the quasi-impossibility for a pilot first to understand what is happening, and second to control the plane in order to avoid a fatal accident. The 2 examples are extracted from "The Downburst" (Theodore Fujita).

a) Take-off accident: Continental 426, Denver Colorado, 7 August 1975

Two planes took off just before Continental 426. Both pilots reported "windshears during and immediately after take-off". "Continental 426 took off with the maximum takeoff thrust. It entered rain shortly before the liftoff. After a normal liftoff, the aircraft climbed with a 14° pitch attitude. Then all of a sudden, it lost 42 kts (22 m/sec) IAS in less than 10 seconds. The captain lowered the pitch attitude to about 10°, but the aircraft continued to descend to the ground (Fig. 4).

The maximum divergence at the surface inside the Continental 426 microburst was estimated to be 150-250 per hour (0.04-0.07 per second). If we assume that this magnitude of divergence extended up to an estimated maximum height of 150 ft (45 m) AGL, the downflow speeds at various AGL heights were

2-4 fps (1-2 kts) at 50 ft (15 m)
4-7 fps (2-4 kts) at 100 ft (30 m)
6-11 fps (3-6 kts) at 150 ft (45 m)

The loss of lift at a 10° pitch attitude is 2.5% per knot. This will result in a maximum of 15% loss of lift at 150 ft (45 m) due to the encountered downflow. The 42 kts (20 m/ec) loss of IAS was very serious in this case, because it could induce the loss of lift as much as 55%.

How can we make a decision, prior to takeoff, whether or not to fly into such a severe windshear? Obviously, the use of radar may hold the key to such a decision. Radar photographs taken by the National Weather Service, Limon radar (10 cm) show a number of small echoes scattered all over the Denver area. The first echo of the Continental 426 microburst cloud was photographed at 1606 MDT, five minutes before the accident. The echo reached the maximum size and intensity at 16h12, one minute after the accident. Thereafter, the echo split into two parts and weakened. This evidence presents a difficult problem of identifying microburst echoes by non-Doppler radars."

b) The second accident I will mention here is the Royal Jordanian 600 at Doha, Quatar, on May 1976 in its final approach.

"Doha Airport has only one runway, oriented in a 160°-340° direction. At 0208 LST, the pilot wanted to land towards the south. Runway 16 was requested and was cleared for a visual approach. As the aircraft began descending toward the requested runway, the wind direction changed from 90° at 17kts to 340° at 6 kts. At that point, the pilot had not seen the runway. A missed approach was initiated and a new approach to Runway 34 was requested.

At 0235 LST when the aircraft completed the turn and the field was in sight, landing clearance was given. However, the runway wind changed again to 180° at 6 kts, which is a tailwind on Runway 34. The rain was very heavy and visibility at the tower was less than 1,000 m (0.6 mile). Before reaching the decision height, a second missed approach was initiated at 0237:19 LST at about 300 ft (90 m) AGL. The pilot then requested clearance to Daran.

The aircraft began climbing at a 12° pitch attitude at 1,300 fpm (6.6 m/sec) rate of climb. During this climb, IAS kept decreasing to 140 kts. Upon reaching 750 ft (230 m) AGL, the aircraft began to descend until it struck the ground with a vertical speed of 4,200 fpm (21 m/sec). During the last 7 seconds, the IAS increased rapidly to 170 kts, while the ground proximity warning system (GPWS) gave a continuous warning 11 seconds prior to the impact.

The author's analysis in Fig. 5 shows that the aircraft experienced a 28 kts increase of the headwind from 151 to 170 kts. It is likely that the aircraft flew beneath a roll vortex. When the second go-around was initiated at 0237:19, the aircraft was at the dead center of the downflow, without realizing that it was penetrating the second tailwind of the micro-burst. As the aircraft was flying out of the microburst, the IAS was lost to the point that the aircraft could no longer maintain its altitude. After reaching its peak altitude, the aircraft kept losing altitude until ground impact at 0237:58 LST."

What to conclude from these accidents? They are the result of an unpredictable airflow pattern with high velocity gradients; due to the inertia of the plane, its true air speed varies accordingly to these gradients and the plane may go to stall. In the Continental 426 accident the plane lost 42 kts (IAS) in less than 10 s. In addition, vertical descending winds may reach 20-25 m/s, a velocity higher than the maximum vertical velocity of plane in calm air.

When this mass of cold air reaches the ground, at first a giant toric vortex is generated and, as time passes, secondary, tertiary ..., vortices appear.

This is a non-deterministic chaos (or stochastic chaos) that the human brain can hardly identify and, even if well identified, there are major difficulties to counter the quickly varying random disturbances and to exit from them. Specific modes in the automatic pilot already exist

and they behave quite well 1/; it is, however, necessary to detect such a phenomena in due time. It can be done by putting sensors on the plane (a difficult problem and an expensive solution) or by equipping airports with sensors and processors to detect the possibility of downbursts with a high probability and a very low rate of false alarms.

This is a very complex non-linear flow dynamics problem as it is impossible to get a set of boundary conditions reset at a common instant (4-D problem).

Currently, a heavy emphasis is on the sensors problems (lidars, radar, infrared sensors, acoustic sensors, etc.).

There are many attempts to modelize windshears and downbursts. They use Navier-Stokes, 3-D, non-stationary and incompressible flow. From these equations the presence of droplets and their density, sometimes even their size is possible to ascertain.

ONERA has studied some models and Fig. 6 gives the current lines in an axisymmetrical plane at two times (26mn and 43 mn) [5]. The flow was located in a 8km x 8 km x 5km (height) parallelipiped (cloud base at 5 km). The characteristic length is the radius of the cloud (1 km) the characteristic velocity is the maximum axial velocity at the base of the cloud (0.02 km/s). The Reynolds number is 5.10^3.

Fig. 6a shows the birth of two vortices, same axis but opposite in sign. Fig. 6b clearly shows the development of the two vortices. There is a good correlation with the experimental data related in Fujita's book [3] [4].

4. STRANGE BEHAVIOUR OF LINEAR SYSTEMS

When linear systems behave chaotically the basic property of linear systems is: if $s_1(t)$ is the response to input $e_1(t)$ and $s_2(t)$ the one to $e_2(t)$ then $\alpha e(t) + \beta s_2(t)$ gives an output of: $\alpha s_1(t) + \beta s_2(t)$ (Superposition principle).

A linear system such as

$$S_\alpha(t) = \Sigma a_i(t) \frac{d^i e_i(t)}{dt^i}$$

satisfies this condition.

Lets now return to the basic stability concept when using the transfer function of the systems even if with a disturbance as additional input, if any. Let's first suppose that the coefficients are constant. A system is stable if the poles of the transfer function lie in the left half plane (abs: real part of the pole; ordinate imaginary frequencies). Stability means that if the system is temporarily departed from a stable state, it will come back to its stable state after a while (Lyapounov's asymptotic stability). If poles lie in the right half plane, the output will tend towards infinity which means toward saturation or permanent oscillations because some non-linearities will happen somewhere.

This old-fashioned concept - still valid - is too far from reality and from the user's point of view stability is normally attached to input-output correlation. If poles are closed to the imaginary axis, stability is poor and the answer to a Dirac input is a low damped oscillation (in case of no disturbances). If the input is a permanently varying signal, the output will vary, but with a poor correlation.

If one now supposes that coefficients are time dependent, but assuming that in any case they always stay in the left half plane, the system is linear and stable Let's suppose that all poles are complex (no real pole). If the pole Wi varies slowly with time with regard to $1/w_i$ sinusoidally at frequency Ω_i ($\Omega_i << Wi$) then the system behaves like a collection of fixed coefficients and input-output corellation is very slightly modified. If Ω_i is much greater than co_i, the output will apparently be subjected to an additional noise and input-output correlation will only be slightly affected. In both cases we assumed that the energy contained in the input signal (spectrum) in $d\Omega_i$ is very small. This is the usual case.

If Ω_i is close to w_i or if the spectrum of the input signal contains significant energy at $d\Omega_i$, then input-output correlation may disappear completely and the response to an input may appear as unrelated to it; it's a kind of deterministic chaos.

In fact, this example calls for two comments. First, it is assumed that a model exists without any uncertainty about the values of the coefficients at each instant; in other words the structure of the system is perfectly known, it enters into the classical $X = AX + Bu$ equation in which the coefficients of A depend on time. In any applications, uncertainties on these coefficients make the time-varying assumption weak. Modern concepts in automatic control imply robustness concept as the choice of B in such a way that uncertainties or coefficients of A do not reflect more than a given quantity on the output vector y ($y=CX$). Secondly, the transfer function concept or the pole localisation concept does not account for pole variation and it is unfair to mix the superposition principle and the stability concept (poles in the right left plane).

Nevertheless, parametric systems - such was the name given to these linear systems with time-varying coefficients - are no longer studied and when they were, some 20-25 years ago, chaos was not yet rediscovered. It seems to me that some academic studies on parametric systems could be worthwhile in a "chaotic approach".

5. BRAIN DYNAMICS AND DETERMINISTIC CHAOS

I would like to touch on this subject although it is not in the field of my activities. A chaotic system in a stationary state is unstable on its attractor, and it thus possesses the lability and capabilities of exploring phase space that one might expect for the nervous system. The idea that brain dynamics, in some of its aspects, could be chaotic and of small dimension, has aroused various speculations and attempts to interpret the electro-encephalographic (EEG) signal in terms of deterministic chaos. It is expected to find a strange attractor in almost every α signal (frequencies in 8-13 Hz).

One major difficulty in studying EEG is the non-stationarity of the signal; it should be sampled in short duration time signal and thus limit the dimensions of the attractor. Can we conclude that this non-stationarity can be interpreted as the proof of the fugitive character of brain attractors? Or, in other words, attractors are specific of the matter considered by the brain at a given instant (or during a period of time).

6. CONCLUSIONS

Stochastic consideration in engineering systems were really introduced by Norbert Wiener in the 40s (remember his famous book on cybernetics?). The first applications concerned the behaviour of deterministic systems subject to stochastic perturbations; at the same time predicting linear networks were designed and worked well for stationary random input function. While at the same time, Claude Shanon introduced the information theory and the decade 50-60 confirmed the well-founded statement of the stochastic approach in the engineer's activities.

Later on, engineers asked for more; they noted that linear systems are rare (but don't forget that often they are still considered as good approximations of non-linear systems) and stationarity is rare except

---

1/ It is surprising that the Autopilot reacts better than a pilot: this is partially due to the fact that the immediate action that the pilot should take is contrary to common sense: the plane is descending and he must use full power immediately in order to increase the plane's total energy. The Auto-pilot does not hesitate!

2/ From: Compte Rendu Académie des Sciences, Paris t.311, Serie II, pp. 1037-1044, 1990, Roger Cerf et al. Among the bibliographic references cited in the Compte Rendu I mention:
E.N. Loretz, J. Atmosph Sci 20, 1963, pp. 130-141.
D. Ruelle and F. Takens, Commun. Math. Phys. 20, 1971, pp. 167-192.
D. Ruelle, Proc. Roy. Soc. Lond A 427 1990, pp 261-268.
P. Grassberger and I. Procaccia, Physic. 9D, 1983, pp. 189-208
J. Theiler, Phys. Review A 34, 1986, pp. 2427-2432.

in some kind of perturbations such as those issuing from the granular structure of electricity.[1/] If the signal considered is not stationary, it cannot be approximated by stationary signals.

Nowadays, engineers are familiar with random functions and random process: the Kalman filters with many variants is fitted in GPS receivers, in automatic pilots in any intelligent mobile robot. However, the tremendous increase in processor capability makes the engineer dissatisfied. He knows that the models he was using were approximations of the real systems as well as the type of signals which enter the system (inputs or perturbations). The concept of robustness was introduced some 20 years ago and new optimization algorithms were used to accept some uncertainties on parameters.

Chaos then arrived or re-emerged because as we said it was mentioned by Poincaré more than 100 years ago. This is probably the biological universal law concerning the evolution of a population of "living beings" which lead scientists to study carefully this simple equation (Verhult's equation) $\chi_{n+1} = \alpha \chi_n (1 - \chi_n)$ and all the consequences on non-linear system behaviour[2/].

From all this baggage a more structured theory on non-linear dynamics which includes chaos has been elaborated on and elaborations continue. The lectures which follow will develop the main features of this new chapter in view of the applications in the engineering field.

1/ Across a resistance R, at temperature T, the voltage fluctuates in a stationary way. If ΔF is the frequency band in which the signal is observed, the quadratic fluctuations are given by $e^2 = 4\ k\ RT\Delta F$ k Boltzman's constant ($1.380\ 10^{-23}$ JK^{-1}).

2/ This equation is well commented on in ref [6] when Ω varies from 0 to 3.56'99 ....

REFERENCES

[1] La Corrélation, Académie des Science et Académie Nationale de l'Air et de l'Espace, International Symposium, Toulouse, Nov. 1991, Cepadues Ed. Toulouse or write to ANAE, 1 Avenue Camille Flammarion, 31500 Toulouse.

[2] GCP Workshop on Stability in Aerospace Systems, AGARD Report 789, Feb. 1993.

[3] "The Downburst", Theodore Fujita, 1985, University of Chicago.

[4] "DFW Microburst", Theodore Fujita, 1986, University of Chicago.

[5] "Modelisation des cisaillements de vent", B. Cantaloube, T.H. Le, Nov. 1990, ONERA rapport 12/3619 SYA.

[6] "Turbulent Mirror", John Briggs, F. David Peat, 1989 (Harper and Row),
"Un miroir turbulent", version française, 1991, (Interédition).

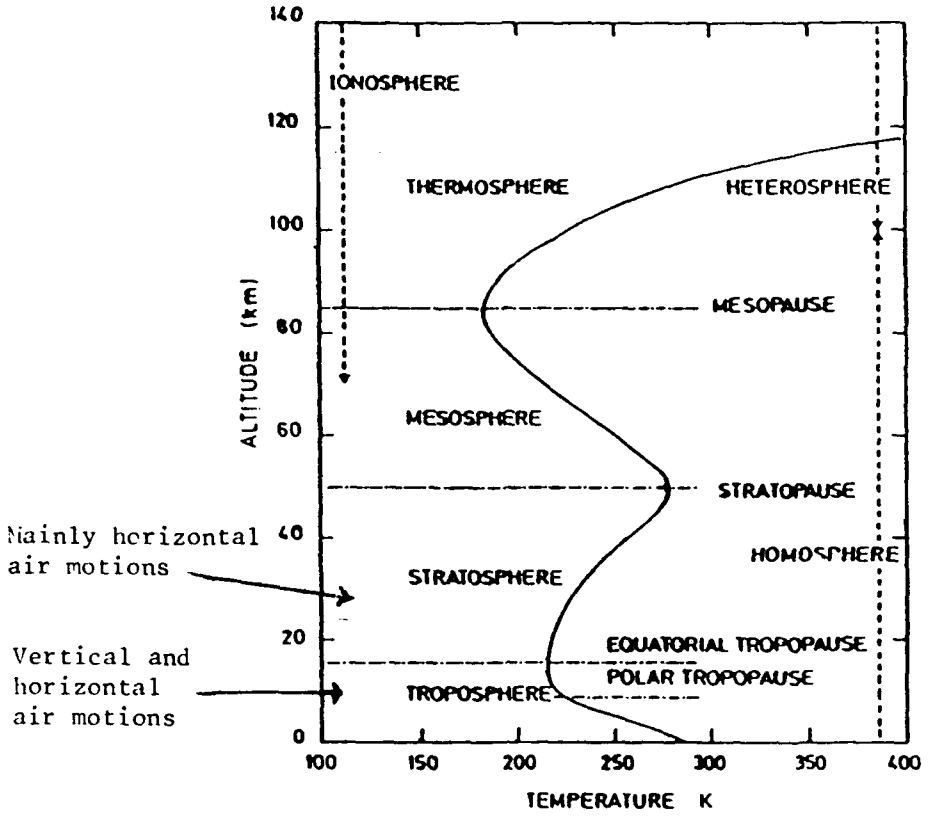

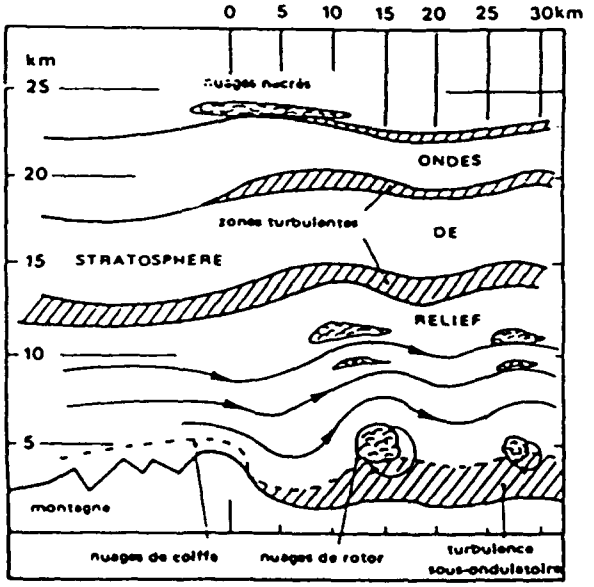

Fig.1 The Atmostphere - turbulent zones
L'atmosphère - zones de turbulence

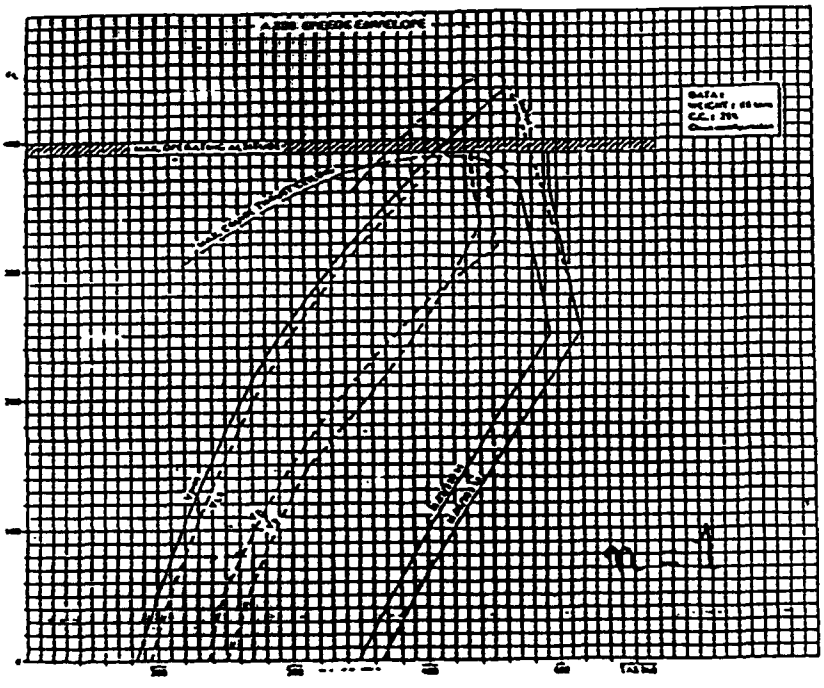

SPEEDS DEFINITION

Vls : Lowest selectable speed. It corresponds to 1.13 Vs during take-off
or following touch and go. It becomes 1.23 Vs as soon as any flap/slat selection is made.

Va : Design speed for maneuver

Vb : Design speed for max. gust intensity and rough air speed
(JAR 24.335 (d))

High speed protection:

MMO/VMO : M.82/350 kt
MMO+0.04/VMO+15 kt : max steady speed with full nose down stick

High angle of attack protection:

This protection has priority over all other protections.
V prot : min speed .(corresponding angle of attack : alpha prot)
If alpha prot is exceeded, the angle of attack returns to and maintains alpha prot.

Fig. 2 Flight envelope (A320)

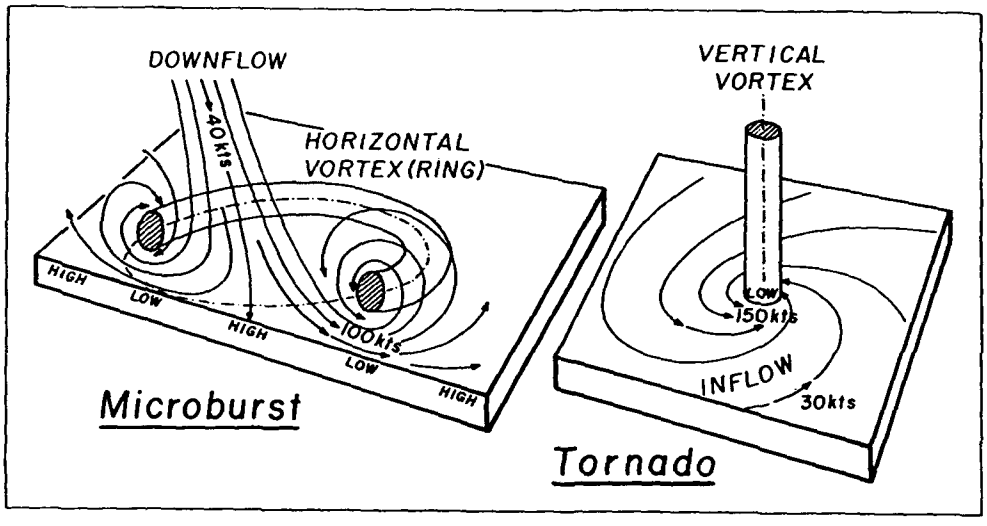

Fig. 3 *Simplified models of a vertical vortex in a tornado and a horizontal vortex in a microburst.* FROM FUJITA

Modèles simplifiés d'un vortex vertical dans une tornade et un vortex horizontal dans un "microburst".

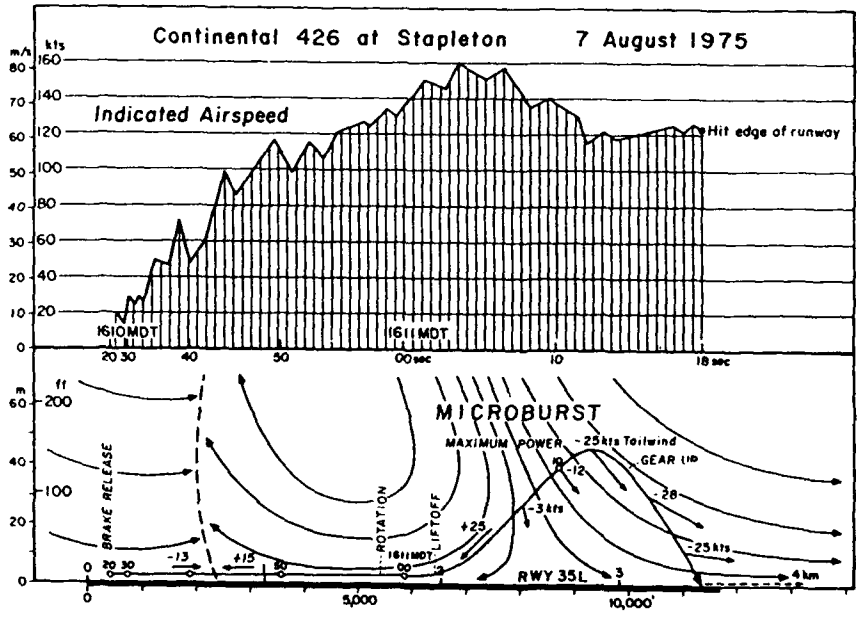

Fig. 4 *Flight path and indicated airspeed of Continental 426 at Stapleton Airport, Denver, Colorado on 7 August 1975.*

FROM FUJITA

Trajectoire et vitesse indiquée du Continental 426 à Stapleton, Denver, Colorado le 7 août 1975 (d'après Fujita)

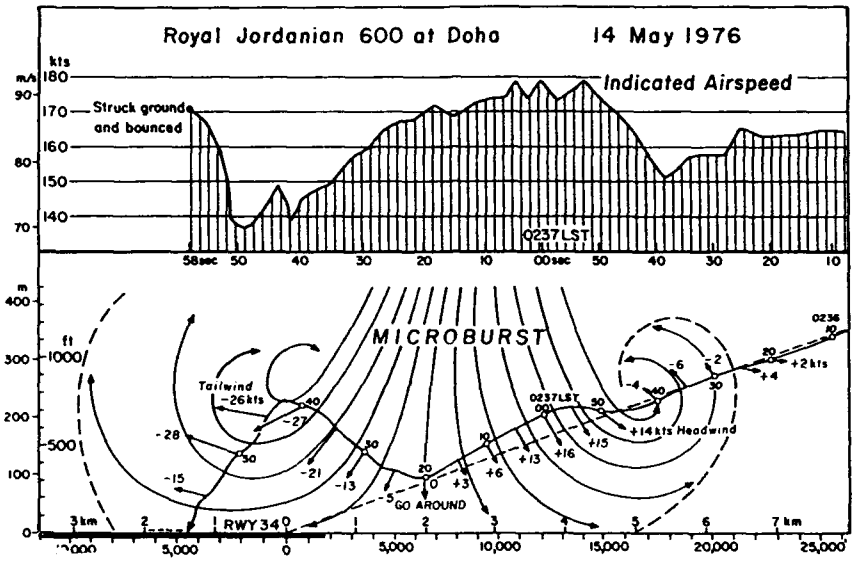

Fig. 5 *The flight path of Royal Jordanian 600, which crash landed at Doha Airport, Qatar at 0238 LST 14 May 1976. According to the author's analysis, the aircraft flew into a strong tailwind inside the horizontal vortex of a strong microburst.* FROM FUJITA

Fig. 5 Trajectoire du Royal Jordanian 600 qui percuta le sol à Doha, Qatar le 14 mai 1976. Selon l'auteur Dr Fujita, l'avion a volé dans une zone à vent arrière à l'intérieur d'un vortex d'axe horizontal provenant d'un "downburst".

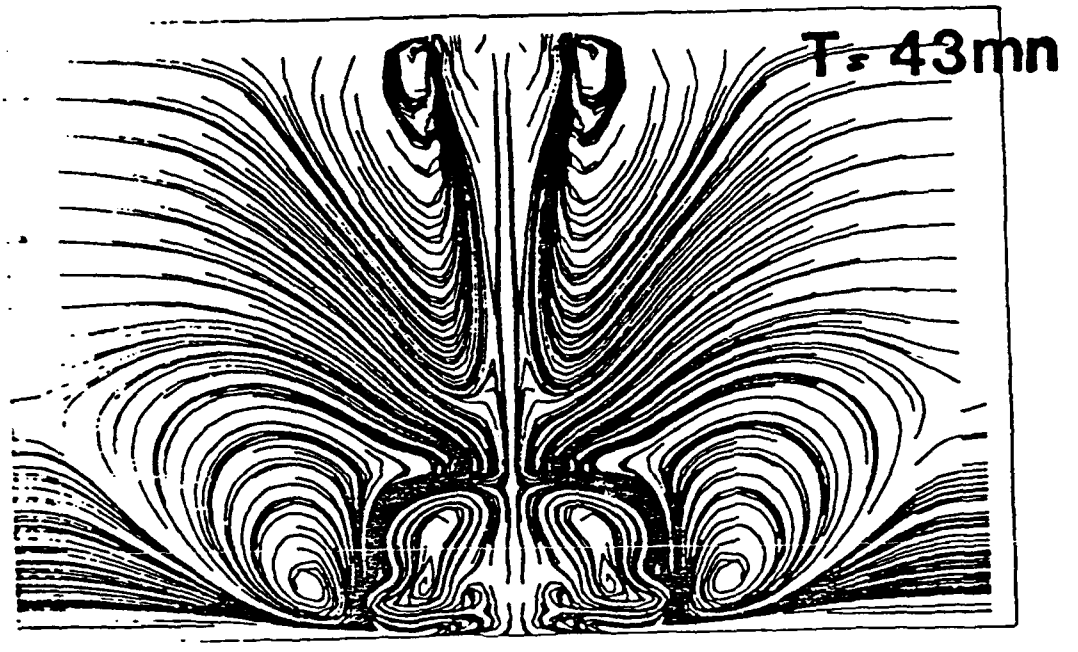

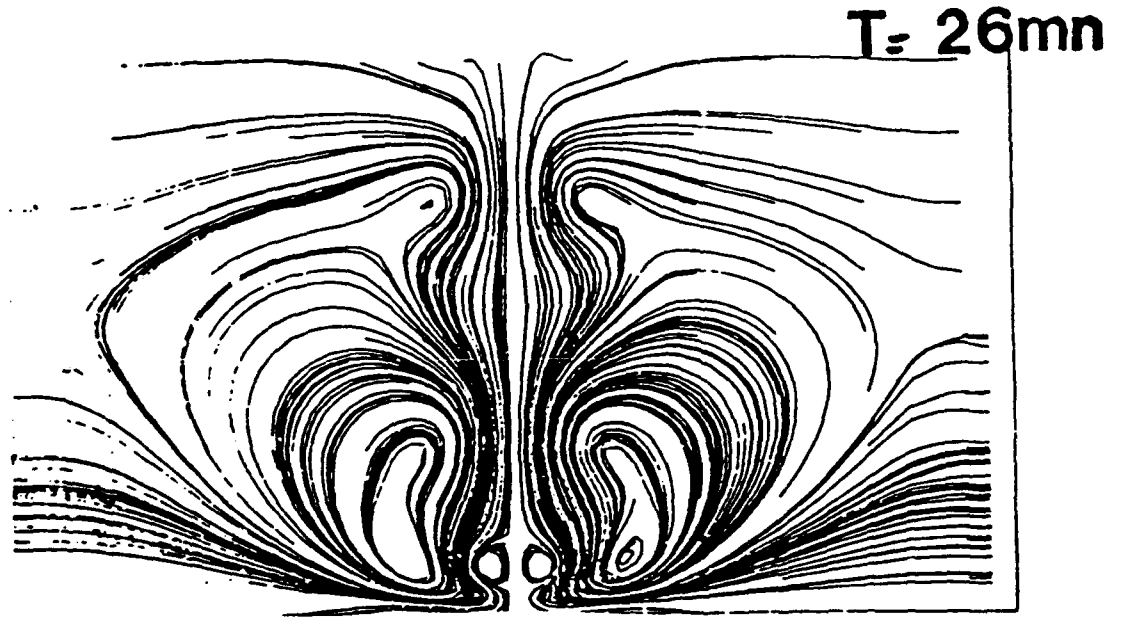

Fig. 6 Downburst simulation from (5)
Simulation de "downburst" de (5)

Introduction à la "Lecture Series" LS 191

Marc J. Pélegrin
Haut Conseiller Scientifique
ONERA - CERT
B.P. 4025
31055 Toulouse Cédex
France

Il n'est pas dans mes intentions de résumer ce que les Professeurs P. Coulet, Ph. Guicheteau, C. Houpis et J.J. Slotine vont vous dire durant cette "lecture series". Ce serait plus un sujet pour la conclusion.

Je vais essayer de souligner quelques aspects de la dynamique non linéaire et du chaos qui, peut être, sont marginaux par rapport au cœur du sujet qui sera développé durant ces 3 jours ; ces aspects pourront faire l'objet de discussions durant les tables rondes de ces journées.

La plupart d'entre nous sont engagés dans des activités d'ingénierie ou de recherche ; bien que l'Aéronautique et l'Espace ne soient pas mentionnés dans le titre de la "L.S.", il est clair que ces 2 domaines resteront dominants durant ces 2 1/2 jours. Mais il est souvent profitable de regarder autour de soi et de comparer les différentes approches possibles du sujet. C'est pourquoi les Prof. Houpis et Guicheteau parleront principalement de sujets liés à l'Aéronautique et l'Espace ; Prof. Slotine parlera, entre autres, de robotique et le Prof. Coulet couvrira l'ensemble du domaine, à la fois d'un point de vue théorique et d'un point de vue applicatif dans divers domaines (mécanique des fluides, optique, systèmes chimiques et biologiques).

1Quelques définitions et commentaires[1]

Un système est un ensemble de composants clairement délimités dans le temps et dans l'espace ; le système est contenu à l'intérieur de sa frontière. S'il n'y a pas de transferts de masse à travers cette frontière le système est dit fermé ; s'il n'y a pas d'échange de chaleur, ou, plus généralement s'il n'y a pas de radiation échangée avec le monde extérieur, le système est dit isolé (condition plus théorique que réaliste ...)

La complexité d'un système est difficile à préciser : elle implique la définition des échelles d'observation ; un exemple trivial est la différence de conception qu'utilise l'ingénieur qui dessine une turbine et le physicien qui étudie une transformation moléculaire : tous les deux utilisent la notion d'entropie. Pour le 1er l'entropie est définie par ds = dQ/T Q flux de chaleur échangé, T température absolue (processus réversible), pour le second l'entropie est le logarithme de la probabilité d'apparition d'un état de complexion donnée (en termes d'arrangement des molécules). La notion d'échelle est de première importance, ainsi que nous le verrons plus tard.

Le concept de corrélation est très utile dans l'étude des systèmes (voir, par exemple, les compte-rendus du Symposium International sur "La Corrélation" réf. [2].

Le concept de corrélation est utilisé par les mathématiciens, les physiciens et les ingénieurs. La corrélation est un outil couramment utilisé pour tenter de quantifier une incertitude apparaissant dans de nombreux phénomènes physiques. Cette incertitude peut avoir un caractère fondamental, comme celle rencontrée en mécanique quantique, être liée au trop grand nombre de paramètres à considérer, ou n'être qu'une apparence comme dans les phénomènes liés au chaos déterministe. La compréhension de telles situations nécessite parfois l'extension du concept de corrélation et même son dépassement (concept de liaison, de ressemblance, de distance). Il paraît donc utile de faire le point sur la question.

Enfin, le mécanisme de perception et de compréhension du cerveau humain, tout autant que les "machines neuronales" en cours de développement, conduisent à s'interroger sur l'importance que peut y jouer la corrélation.

[1] pour plus de détails voir en ref. [1] l'article de A. Favre "Corrélation spatio-temporelle".

Il faut ensuite parler du concept d'ordre et de désordre. Le désordre complet est l'indépendance de tous les composants du système. Toutes les autres définitions sont plutôt négatives, par exemple celle-ci : une condition suffisante (mais non nécessaire) pour dire qu'un système n'est pas désorganisé et que les corrélations entre les différents paramètres qui caractérisent son évolution -s'ils sont accessibles- ne sont pas nulles.

Le hasard est généralement associé à la notion de probabilité ; cependant le désordre complet est considéré comme une manifestation du hasard et, d'un point de vue stochastique, le désordre complet échappe aux lois de probabilité : il y a contradiction !

Et l'on arrive au chaos qui est normalement associé au désordre.

Le chaos déterministe a été introduit par H. Poincaré aux environs de 1892 dans son fameux livre (2 tomes) sur : "Les méthodes nouvelles de la mécanique céleste" 1892 - 93 - 99, réédité par Dover Publications Inc., 1957.
Il semble que personne, depuis cette date, n'ait réellement repris le problème formulé par Poincaré jusqu'aux années 60 bien que les tourbillons de Bénard aient été étudiés très en profondeur tant du point de vue expérimental que du point de vue théorique. Personne ne mettait en cause -et ne met en cause encore aujourd'hui- que des mouvements organisés, à grande échelle, de particules (molécules d'eau par exemple) apparaissent progressivement à partir de mouvements complètement désorganisés, quand un paramètre extérieur (le flux de chaleur dans ce cas) varie de façon continue dans un sens. Il est cependant important de noter que le récipient dans lequel les tourbillons de Benard apparaissent ne constitue pas un système isolé.

Des travaux importants ont été faits dans les années 60 par Lorentz sur la convection de Rayleigh, Benard et par Ruelle et Takins [2] sur la turbulence. A cette époque, les avions civils à Mach subsonique élevé et les avions supersoniques du domaine militaire entraient en service opérationnel. La poussée des réacteurs et leur forte consommation (les réacteurs double-flux n'existaient pas encore) imposaient des études fines sur les causes de la trainée aérodynamique des avions. Il fut confirmé que le problème résidait principalement dans la nature de la couche limite et principalement dans la transition laminaire-turbulent sur l'extrados de l'aile. Encore aujourd'hui le problème est d'actualité et les aérodynamiciens essayent d'obtenir une aile à écoulement complètement laminaire sur toute la corde de l'aile.

La transition n'est pas encore parfaitement expliquée mais la connaissance du phénomène s'accroit chaque jour, peut être, grâce aux scientifiques qui étudient le chaos, parce que cette transition appartient à un phénomène très général, à l'opposé des tourbillons de Benard : c'est le passage d'un mouvement organisé à une structure totalement désorganisée.

Le chaos extrême est le chaos moléculaire, c'est un chaos non déterministe qui préside à toute la thermodynamique ; nous reviendrons plus tard sur cet aspect.

Un chaos purement déterministe est celui des fractals (tout au moins de certains types de fractals). Découverts ou plus précisément re-découverts par Benoît Mendelbrot, les fractals peuvent avoir des structures parfaitement régulières mais incroyablement complexes, telle celle par exemple issue d'un triangle équilatéral. Elles peuvent avoir aussi des structures complètement irrégulières bien qu'elles soient issues d'itérations mathématiques.

Au début, les fractals ne paraissaient avoir aucune application, excepté peut être dans l'exploitation de leur beauté. Plus tard il fut reconnu que, d'une part les fractals pouvaient être une bonne approximation d'objets réels - par exemple une côte maritime, d'autre part que l'auto-similarité, qui peut être considéré comme la propriété intrinsèque de leur structure, est aussi une propriété fréquente dans la nature. La structure non dimensionalisée d'un arbre, par exemple, est la même qu'on le regarde de loin ou au contraire de très près : les types de ramification sont les mêmes. De même la structure du cosmos semble satisfaire la loi d'autosimilarité des fractals : étoile avec ses planètes, galaxie avec ses étoiles, amas de galaxies avec ses galaxies ...

Une dimension fractale a été définie (la dimension fractale de la côte bretonne est de 1,26 ; celle de la poussière de Cantor est de 0,6309).

---

[2] voir le rappel en bas de page du § 5 pour les références bibliographiques.

Une autre contradiction -tout au moins apparente- est liée à la dimension d'une structure ; en 1890 G. Peano décrit une courbe, géométriquement définie, qui peut complètement couvrir un carré (la courbe passe nécessairement par n'importe quel point donné à l'intérieur du carré). Dès lors, quelle est la dimension du carré : 2 comme il est usuellement affirmé ou bien 1 car ce n'est autre chose qu'une courbe ?

A l'opposé, un phénomène qu'on peut appeler anti-turbulence, a été découvert et étudié par John Russel en 1834. C'est la vague soliton. Il s'agit d'une vague isolée, d'amplitude importante (quelques décimètres dans un canal de 5 m de largeur). Cette vague peut se propager sur des milliers de mètres sans modification de forme, c'est-à-dire sans amortissement notable. Deux problèmes émergent de cette observation. D'abord comment la vague est-elle produite, ensuite comment peut-elle se propager sans amortissement ? Les réponses ne sont pas encore très bien établies. Il semble que le soliton apparaît dans la turbulence apparemment très désorganisée que l'on rencontre devant l'étrave d'un bateau mal caréné, tel celle des vieux bateaux. C'est pourquoi nous avons dit que, quelquefois, ce phénomène est associé à l'anti-turbulence. Quant à l'absence de dégradation de forme de cette vague isolée on ne peut arguer que d'interactions non-linéaires entre le fond du canal et la vague.

En fait, l'expérience est difficile à réaliser au laboratoire ; quelques succès ont été obtenus dans des canaux larges ; il a toujours été noté que l'énergie mise en jeu dans la production d'une telle vague est un paramètre critique ; si l'énergie est trop faible il se produit une vague qui est sujette à un fort amortissement ; si l'énergie fournie est trop grande, un mouvement turbulent est produit sans création d'une vague isolée. Des équations non linéaires aux dérivées partielles donnent une représentation acceptable du phénomène (équation KdV de D.J. Kortweg et C. de Vries).

Il est temps maintenant de commenter à propos de la contradiction entre la mécanique classique qui, pour les systèmes non dissipatifs, implique la reversibilité et la thermodynamique qui implique l'irréversibilité : l'entropie d'un système isolé ne peut que croître).

L'hypothèse selon laquelle les molécules se comportent comme des corps en interaction parfaitement élastique, comme dans le domaine macroscopique est-elle absolument exacte ?

Si la réponse est oui, alors la themrodynamique doit être réversible et l'entropie n'est plus une grandeur à variation monotone.

Si la réponse est non, alors la thermodynamique est une branche séparée de la Physique et tout doit être reconsidéré à partir du comportement de la molécule.

Aujourd'hui et pour les 2 jours qui suivent je vous propose d'accepter la réponse oui. Mais alors comment justifier cette hypothèse mondialement acceptée.

Le point de départ de l'affirmation de Poincaré selon laquelle, dans un système fermé et isolé une trajectoire de phase passera nécessairement "dans le voisinage" d'un point quelconque, par exemple la condition initiale d'où le système est parti [3] (je ne peux pas commenter le terme "voisinage" car H. Poincaré lui-même ne l'a pas précisé. De toute façon je ne crois pas que cette "indétermination" rende caduc ce qui suit).

Le fameux démon de Maxwell contrôle un trou entre 2 récipients qui contiennent initialement un gaz à des pressions (ou températures différentes). Chacun sait qu'après un certain temps la pression sera la même dans les 2 récipients. Poincaré dit : attendez et il arrivera un instant où les pressions (ou les températures) deviendront différentes. Personne n'a observé un tel phénomène.

Une explication possible vient du fait qu'il y a $6{,}023\ 10^{23}$ molécules par mole [4]. La "mécanique classique" peut-elle être étendue à un tel nombre de "composants". Nous avons dit précédemment oui ... mais alors si à partir de ce nombre on calcule le temps qu'il faudra pour arriver à une répartition "anormale" des molécules, on trouve sur un exemple les valeurs suivantes (cf. C. Marchal) : pression initiale dans les récipients : $1{,}4.10^5$ Pa [5] et $0{,}6.10^5$ Pa. La loi de probabilité définissant le mode de

---

[3] pour plus de détails voir réf. [2], conférence présentée par Ch. Marchal "Chaos Entropy and Irreversibility a simple example".

[4] une mole correspond au nombre d'atomes contenu dans 0,012 kg de C12

[5] 1 Pa (Pascal) vaut 10^{-5} bar.

choix des molécules qui passent à travers le trou n'a pas grande influence sur le résultat.

Si on effectue les mesures de pression avec une précision de 10^{-3} Pa, on peut déceler des fluctuations de la pression par rapport à la solution moyenne environ 1 fois tous les 2 ans. Si l'on adopte une précision de 5 m Pa la probabilité de rencontrer un tel écart est de 10^{-200} avant $1{,}4.10^{322}$ années ... La probabilité a priori que la pression dans l'un des récipients soit $1.4\ 10^{6}$ Pa (ou plus grande) est 10^{-M} où $M = 3{,}5\ 10^{16}$ ... ce n'est pas zéro !

Il est difficile de dire si cet exemple est une réponse finale au dilemme énoncé plus haut. On ne peut pas, cependant nier que le temps de retour aux conditions initiales (le temps de retour de Poincaré) existe. On ne peut pas, malheureusement passer d'un système macroscopique à un système microscopique de façon continue. Des vecteurs d'état de dimension 100, voire 1000 sont maintenant couramment utilisés dans différentes techniques (structures flexibles par exemple) du domaine macroscopique ; en mécanique des fluides les vecteurs d'état sont de l'ordre de 6.10^{23} par mole.

Le dernier concept que je voudrais mentionner est celui de la stabilité. Au premier abord, la stabilité et le chaos semblent exclusifs comme la stabilité et l'instabilité. Ce n'est pas toujours vrai.

La stabilité est-elle une grandeur mesurable comme la masse, ou bien une grandeur repérable comme la température (le zéro n'existe pas) ?. Il y a de nombreuses définitions de la stabilité, quelquefois contradictoires : en fait, c'est une quantité subjective qui doit être définie dans le contexte du domaine considéré. Le système de référence dans lequel le système évolue doit être défini ; la stabilité peut exister dans un système de référence et ne pas exister dans un autre système de référence.

La stabilité est un critère dominant dans le domaine de la commande des avions ou des missiles, ou plus généralement pour la commande tout véhicule. Cependant, stabilité et manœuvrabilité sont deux propriétés opposées qui interviennent dans la commande des avions; pour les avions civils la stabilité est le facteur dominant, pour les avions militaires, c'est la manœuvrabilité qui domine. Ce sont ces deux aspects qui ont conduit AGARD/GCP à organier un Atelier sur la Stabilité en Juin 1992 [2].

Fondamentalement la stabilité est liée à l'irreversibilité, c'est-à-dire à la dissipation d'énergie pour les systèmes linéaires. Bien que les systèmes linéaires soient très rares, ils représentent souvent une bonne approximation de systèmes non-linéaires.

La stabilité est aussi une question de précision. Prenons par exemple la rotation de la terre. Est-ce une propriété stable ou instable ? Cette question n'a pas de sens tant qu'on a pas spécifié la précision avec laquelle on observe le phénomène et, en fait, le problème plus général qu'on étudie. Grâce à la précision des horloges atomiques d'aujourd'hui, il est prouvé que des variations journalières de l'ordre de 1 ms par an et des variations de l'ordre de 10 ms sur plusieurs années, existent de façon pseudo périodiques. Cependant, la vitesse de rotation décroît nécessairement à long terme à cause, principalement, du frottement eau/terre résultant des marées. A l'époque pré-cambrienne (400 M années) la durée du jour était de 15 heures (le ralentissement global sur cette période correspond à 0,1 ms par an).

Ce qui a été dit à propos de la vitesse de rotation de la terre aurait pu être dit à propos de la direction de l'axe de rotation. Au pôle, la trace de l'axe de rotation se déplace constamment dans un cercle d'environ 2 m de diamètre. Et pourtant, pour toutes les activités humaines le vecteur rotation de la terre est considéré comme stable (sauf pour certains astronomes ...).

Poincaré étudia la stabilité des systèmes autonomes et non autonomes dans les années 1870 ; Ljapounov, dans les années 1900, introduisit une condition suffisante mais non nécessaire permettant de dire si un système est stable (fonctions de Ljapounov). A partir de ces notions, la stabilité d'un système au voisinage d'un point d'équilibre fut étudiée en détail par Poincaré et les points d'équilibre ou singularités furent classés en nœuds - sommets - foyers - col.

Une variante possible de l'évolution d'un système dans l'espace des phases au voisinage d'un point sont les cycles limites qui peuvent être stables ou instables ; ils généralisent la notion de stabilité ponctuelle en acceptant un mouvement périodique, généralement de faible

amplitude, autour du point de stabilité. Un nouveau vocabulaire a été introduit, il s'agit d'attracteur, éventuellement étrange ...

Tous les aspects de la physique sont concernés par le concept de stabilité. Les systèmes mécaniques, fussent-ils célestes, ont été les premiers à être concernés par l'approche de Poincaré. Tout ce qui pouvait être dit sur les systèmes linéaires a été dit. Les théories et études concernent maintenant les systèmes non linéaires. Aucune solution globale ne peut être espérée pour les systèmes non-linéaires.

Le concept de "robustesse" pour la commande d'un système est une extension des études de systèmes linéaires. Ce concept est important pour les applications dans l'industrie ou dans la commande des véhicules. La robustesse peut être définie comme la capacité de répondre à des spécifications de performance malgré des incertitudes sur la valeur des paramètres qui définissent le système à contrôler, et quelquefois aussi les incertitudes sur les paramètres du "contrôleur". Evidemment une équation différentielle linéaire avec incertitudes sur la valeur de certains coefficients n'est plus une équation différentielle linéaire. En fait, déjà dès le début de l'étude des systèmes linéaires, les notions de marge de gain et marge de phase étaient utilisées pour pallier ces incertitudes. Aujourd'hui des concepts plus élaborés tels que l'optimisation $H\infty$ permet de traiter ce problème pour des systèmes multivariables.

Nous pouvons probablement dire que le dilemme "stabilité - instabilité" a fait le plus de progrès en mécanique des fluides (aéro et hydro-mécanique). Des résultats spectaculaires (aux deux sens du terme) concernent les tourbillons de Benard.

Il n'en reste pas moins vrai que l'écoulement de l'air autour d'une aile peut être considéré comme stable bien que des instabilités puissent exister localement dans la couche limite ; lors d'un vol en croisière, considéré par tous comme stable, la couche limite devient turbulente (c'est-à-dire localement instable) quelque part entre la moitié et les 2/3 de la corde.

Le phénomène de tremblement est dû à un degré plus grand de cette instabilité puisqu'il s'agit du détachement de tourbillons qui s'échappent par paquet de la couche limite ; ce phénomène doit être évité pour les performances de l'avion et le confort des passagers.

Le flottement est un phénomène dangereux dû au couplage aéro-élastique entre l'air et l'aile ; il apparaît normalement quand la fréquence de 2 modes de vibration convergent en une unique fréquence (il s'agit généralement du 1er mode de flexion et du 1er mode de torsion). C'est typiquement un phénomène instable qui peut apparaître graduellement lorsqu'un paramètre de vol varie, par exemple vitesse ou facteur de charge.

Stabilité et instabilité ont aussi un sens dans le domaine statique (ponts [6], bâtiments, barrages, digues, structures de navires ou d'avions) lorsque les charges atteignent une valeur critique : c'est le flambage. Même dans la croûte terrestre, l'instabilité existe (tremblements de terre). Approximativement on peut dire que la résultante du mouvement des plaques tectoniques fait apparaître des contraintes de frottement qui dépassent le seuil, le glissement ou la déformation élastique d'une partie du sol donne lieu, soudainement à un saut.

Pour conclure ce paragraphe et introduire le suivant, je voudrais mentionner brièvement les mouvements de l'atmosphère. La stabilité, dans ce domaine, a-t-elle un sens ? Probablement non, bien qu'en de nombreuses contrées, principalement celles de la zone tempérée, un certain degré de stabilité existe. Si vous dites "demain il fera le même temps qu'aujourd'hui" vous ne faites pas une mauvaise prédiction (la probabilité de succès est bien supérieure à 0,5 car, dans ces contrées le temps ne change pas chaque jour, c'est dire qu'un certain degré de stabilité existe).

Le temps résulte de mouvements de masses d'air sur la surface du globe. Il devrait être prédictible comme pour tous les systèmes pour lesquels les équations qui les régissent sont connues. Malheureusement c'est un système d'équations aux dérivées partielles qui est connu avec une bonne approximation, mais pour le résoudre il faut disposer d'un ensemble homogène de conditions initiales (3-D) ; il est difficile de les acquérir même avec des satellites. Les météorologues procèdent par régions (les grilles qu'ils utilisent vont de quelques km jusqu'à des centaines ou des

---

[6] Le pont suspendu du Tacoma qui s'est écroulé le 7 Novembre 1940 l'a été alors qu'il était soumis à un vent relativement modeste 18,7 m/s. C'est typiquement un phénomène similaire à celui du flottement (conjonction de 2 modes de vibrations).

milliers de km et intègrent les équations à partir des données supposées convenablement connues sur la grille considérée. L'aide de processeurs, parmi les plus puissants, conduit à une prévision bonne sur 24 H, acceptable sur 48 H. L'objectif est d'atteindre le même degré de précision sur 72 H avant la fin du siècle

Dans le paragraphe suivant nous allons développer quelque peu le couplage qui existe entre l'atmosphère locale dans laquelle l'avion vole et l'avion lui-même.

2. L'environnement stochastique d'un avion

C'est probablement la caractéristique principale de l'Aéronautique. La Marine et l'Espace ont aussi à faire face à des conditions adverses difficiles mais probablement pas du même niveau que l'Aéronautique.

L'étude et le calcul d'un avion nécessite, initialement qu'une "atmosphère standard" ait été précisée (Fig. 1). En supposant que l'avion vole dans une atmosphère conforme à celle-ci, les forces aérodynamiques et éventuellement leurs phénomènes associés tels que le tremblement ou le flottement peuvent être calculés avec précision et, par suite, l'attitude et le mouvement de l'avion. Les domaines de vol (Fig. 2) sont utilisés par les compagnies aériennes, le contrôle du trafic aérien et les militaires pour la gestion optimale de l'avion.

Mais l'atmosphère réelle diffère de l'atmosphère standard d'une façon telle qu'il est difficile de le préciser dans le voisinage de l'avion.

L'atmosphère est composée de :
- la troposphère, une couche de 8 à 11 km d'épaisseur autour de la terre dans laquelle il y a des mouvements horizontaux et verticaux, ceux-ci exacerbés dans les cumulo-nimbus actifs,

- la stratosphère, au-dessus de la troposphère, dans laquelle les mouvements sont principalement parallèles à la surface de la terre.

La séparatrice est appelée tropopause, c'est une zone de transition dans laquelle les 2 caractéristiques sont présentes. La position et l'épaisseur de la tropopause varient avec la latitude et les saisons.

Dans la troposphère, une turbulence sévère, même parfois en ciel clair, peut exister. Les cumulo-nimbus actifs sont dangereux pour un avion, à cause de la turbulence, des vitesses des masses d'air (ou d'eau, gouttes de pluie) dans le centre du nuage : des vitesses ascensionnelles de 20 m/s peuvent être atteintes au centre de la colonne, avec des éclairs et du givrage.

Si un avion pénètre dans un tel nuage, c'est comme s'il entrait dans le chaos... tout au moins pour les passagers ; le pilote (le pilotage manuel, par rapport au pilotage automatique est recommandé) essaye de maintenir l'incidence de l'avion à une valeur acceptable, sans tenter de stabiliser l'altitude ; il essaye aussi de contrôler au mieux le roulis.

Dans la stratosphère, des "jet streams" sont fréquents ; ce sont des "tubes" de quelques centaines de mètres ou quelques km de diamètre correspondant à un déplacement quasi-horizontal très rapide de masses d'air. Le flux à l'intérieur de ce tube peut être laminaire mais évidemment la transition vers l'extérieur est fortement turbulente.

Jusqu'à ces dernières années, les seuls paramètres mesurables à bord étaient la pression statique p_s, la pression dynamique p_d et la température totale T_a. De ces données on peut calculer la vitesse propre et le nombre de Mach par les équations de St Venant (subsonique) ou Rayleigh (supersonique).

L'échelle de turbulence peut varier de quelques mètres à plusieurs km et la stationnarité de la turbulence n'est, en général, pas acquise.

Pour être certifié un avion ne doit pas subir de dommage (plus précisément, doit rester dans le domaine élastique) lorsqu'il rencontre une rafale ou lorsqu'il vole dans une zone turbulente.

Les rafales sont définies par des "spécifications" qui varient légèrement selon les pays qui ont une autorité de certification. Pour la France la rafale "type" est du type "1-cos"

$$w(t) = 0 \quad t < 0$$

$$w(t) = \frac{W_n}{2}\left(1-\cos\frac{2\pi v t}{dm}\right) \quad \text{for } 0 < t < \frac{d_m}{v}$$

$$w(t) = 0 \quad t > \frac{d_m}{v}$$

W_n amplitude de la rafale vitesse (m/s)
d_m longueur caractéristique (m)

- un spectre de von Karman

$$\phi_w(\omega) = \sigma^2_w \frac{L_w}{\upsilon} \frac{1+\frac{8}{3}\,[1{,}339\frac{L_w}{v}\,\omega]^2}{[1+1.339\,\frac{L_w}{v}\,\omega]^{11/6}}$$

avec $$\sigma^2_w = \frac{1}{2T'} \int_{-\infty}^{+\infty} \phi_w(\omega)d\omega$$

L_w = échelle de turbulence
$\sigma\omega^2$ = valeur quadratique moyenne de la vitesse
ω = pulsation

Il est important de noter que ces valeurs numériques doivent être révisées en fonction du niveau de sécurité atteint par le matériel. Lorsque ce niveau s'améliore, il faut chercher quelle est la valeur de l'amplitude (vitesse) de la rafale ou les paramètres du spectre qui ont la même probabilité d'occurence que le niveau de sécurité de l'avion.

3. Lorsque le chaos devient "downbursts"

"Quelques accidents d'avion qui se sont produits à basse altitude alors qu'une activité convective régnait, furent considérés comme dûs à une erreur de pilotage sans référence aux conditions atmosphériques comme cause possible" ; de Théodore Fujita "The downburst", Université de Chicago, 1985 [3]. Il a démontré que la commission d'enquête était dans l'erreur pour de nombreux accidents.

On estime actuellement que 1 à 3 appareils commerciaux sont perdus chaque année à cause de cisaillements de vent dus aux "downbursts" (Russie et Chine non comptées).

Les "downbursts" proviennent d'une instabilité soudaine d'une masse d'air froid, provenant normalement d'un nuage ; un "downburst" peut être accompagné d'une pluie (quelquefois très forte) ou peut être sec, ou peut être accompagné de pluie seulement dans sa partie supérieure, c'est-à-dire que les gouttes de pluie s'évaporent entre le nuage et le sol.

La Fig. 3 modélise une tornade (masse d'air chaud ascendante) et un microburst (masse d'air froid descendante).

Je vais donner 2 exemples qui montreront la quasi impossibilité pour un pilote de comprendre la situation et de contrôler l'avion afin d'éviter un accident fatal. Ces 2 exemples sont extraits de "The Downburst" de Th. Fujita.

a) accident au décollage. Continental 426, Denver, Colorado, le 7 août 1975.
Deux avions ont décollé juste avant le Continental. Les 2 pilotes ont reporté "cisaillement de vents durant et immédiatement après le décollage".

Continental 426 décolla avec la poussée maximum de décollage. Il entra rapidement dans une pluie dès la rotation ; après celle-ci l'avion monta avec une assiette de 14°. Soudain en moins de 10s il perdit 42 kts (22 m/s) en vitesse indiquée.
Le pilote prit alors 10° d'assiette et l'avion continua de descendre jusqu'au sol (Fig. 4).

La divergence du flux à la surface dans le microburst que Continental 426 a rencontré était estimée à 150 - 250 par heure (soit 0,04 à 0,07 par seconde). Si on suppose que cette amplitude de divergence s'étendait jusqu'à une altitude de 45 m au-dessus du sol, les vitesses du flux descendant à différentes hauteurs étaint :

1 à 2 kts à 15 m
2 à 4 kts à 30 m
3 à 6 kts à 45 m

La perte de portance à une assiette de 10° est de 2,5 % par kts. Il en résulte une perte maximum de 15 % de portance à 45 m à cause du flux descendant. Les 42 kts de perte de vitesse indiquée étaient très importants dans ce cas car ils pouvaient induire une perte de portance jusqu'à 55 %.

Comment peut-on prendre une décision, avant le décollage, de passer ou non dans un sévère cisaillement de vent. Heureusement, l'utilisation du radar peut donner la réponse à cette question. Les photographies radar prises par le National Weather Service (radar 10 cm) montrent des petits échos dispersés sur toute la zone de Denver. Le premier écho du microburst du Continental 426 a été photographié à 1606 MDT, 5 minutes avant l'accident. L'intensité maximale a été atteinte à 1612, soit 1 minute avant l'accident. Après l'écho s'est séparé en 2 parties, puis s'est évanoui. Il est difficile

d'identifier les échos de microburst par les radars qui ne sont pas Doppler.

Le second accident dont je parlerai est le "Royal Jordanian 600" à Doha, Qatar, en Mai 1976 en approche finale.

L'aéroport de Doha n'a qu'une piste 160 - 340°. A 0208 LST (temps local) le pilote voulait atterir face au Sud. La piste 16 était demandée et attribuée pour une approche visuelle. Alors que l'avion descendant vers cette piste, le vent passa de 90°/17 kts à 340°/6 kts. A ce moment le pilote n'avait pas encore vu la piste. Une procédure d'interruption d'approche fut engagée et une demande d'approche sur la piste 34 fut acceptée.

A 0235 LST après le dernier virage, le pilote vit la piste ; la clairance d'atterrissage fut donnée. Alors le vent changea à nouveau 180°/6 kts (ce qui correspond à un vent arrière sur la piste 34). La pluie était dense et la visibilité (à la Tour) inférieure à 1000 m. Avant d'atteindre la Hauteur de Décision, une 2e interruption d'approche fut initiée à 0237:19 LST à 90 m au-dessus du sol. Le pilote demanda alors une clairance pour Daran.

L'avion commença à monter avec une assiette de tangage de 12° et un variomètre de 1300 ft/mn (6,6 m/s). Pendant cette montée la vitesse indiquée chuta à 140 kts. A 750 ft (230 m) environ, au-dessus du sol, l'avion commença à descendre, il heurta le sol avec une vitesse verticale de 4200 ft/mn (21 m/s). Durant les 7 dernières secondes, la vitesse indiquée crut rapidement jusqu'à 170 kts tandis que l'avertisseur de proximité de sol donna une alarme continue depuis 11s avant l'impact.

L'analyse de l'auteur (Dr. Fujita) montre (Fig. 5) que l'avion a rencontré un vent debout qui s'est amplifié de 28 kts (151 à 179 kts). Il est probable que l'avion vola en-dessous du rouleau du vortex. Lorsque la 2e remise de gaz fut initiée à 0237:19, l'avion était dans la zone morte du flux descendant, et le pilote n'a pas réalisé qu'il était en train de pénétrer dans une zone de vent arrière du microburst. Lorsque l'avion vola en dehors du microburst, la vitesse indiquée ne pouvait plus assurer à l'avion un maintien d'altitude. Après avoir atteint son altitude maximale, l'avion perdit de l'altitude et s'écrasa à 0237 : 58 LST" (fin de citation).

Que conclure de ces 2 accidents ?

Ils résultent d'une situation imprévisible du champ de vitesse des masses d'air que l'avion a rencontré (gradients de vitesse très importants) ; à cause de l'inertie de l'avion sa vitesse indiquée subit ces gradients et l'avion peut attendre la vitesse de décrochage. Dans l'accident Continental 426 l'avion a perdu 42 kts de vitesse indiquée en moins de 10 s. En plus il se trouvait dans une colonne d'air descendant de 20 à 25 m/s, vitesse plus grande que la vitesse ascensionnelle maximum continue que l'avion peut prendre en air calme.

Lorsque ces masses d'air froid rencontrent le sol, un premier gigantesque vortex torique est engendré puis un second, un troisième etc ... C'est assimilable à un chaos non déterministe (ou chaos stochastique) ; le cerveau humain peut difficilement identifier une telle situation et, même s'il l'a correctement identifiée il a les plus grandes difficultés pour contrer les perturbations aléatoires qui varient rapidement et échapper sûrement de cette situation. Des modes spécifiques du P.A. existent et ont des performances acceptables [7]. Il est toutefois nécessaire de détecter à temps un tel phénomène. Ce peut être fait par des détecteurs placés à bord de l'avion (problème difficile, solution chère) ou en équipant l'aéroport de détecteurs de vitesse de vent (plusieurs centaines sont nécessaires sur l'aéroport) et par traitement de signal identifier le "downbrust" avec une grande probabilité de succès (mieux que 0.9) et un faible taux de fausse alarme.

C'est un problème de dynamique non linéaire très complexe car il est impossible d'obtenir un ensemble cohérent de données iso-datées sur un contour ou une surface.

A l'heure présente il y a beaucoup de recherches sur les types de détecteurs les mieux adaptés : lidars, radars, senseurs IR, senseurs acoustiques...

Il y a plusieurs façons de modéliser un cisaillement de vent (et un downburst). On utilise les équations de Navier-Stokes en 3-D, non stationnaires pour un fluide incompressible. Il est alors possible de mettre

---

[7] il est surprenant qu'un PA réagisse mieux qu'un pilote; ceci est partiellement dû au fait que l'action immédiate que le pilote doit faire est opposée au bon sens : l'avion est en descente et le pilote doit, en priorité ; mettre plein gaz afin d'accroître le plus vite possible l'énergie totale de l'avion. Le Pilote Automatique n'hésite pas !

en évidence la présence de gouttelettes, leur densité et parfois leur taille.

L'ONERA a étudié quelques modèles et la Fig. 6 donne les lignes de courant dans un plan axisymétrique à 2 instants 26 et 43 mn [5].

Le flux est situé dans un parallélépipède de 8 x 8 x 5 km (hauteur) ; la base du nuage était à 5 km. La longueur caractéristique est prise égale au rayon du nuage (1 km) la vitesse caractéristique est la vitesse axiale maximale à la base du nuage (0,02 km/s, le nombre de Reynolds es. 5.10^3).

La Fig. 6a montre la naissance de 2 vortex de même axe mais de signes opposés. La Fig. 6b montre clairement le développement de ces 2 vortex. Il existe une bonne corrélation avec les données expérimentales exposées dans l'ouvrage de Fujita [3] [4].

4. Comportement étrange de systèmes linéaires

La propriété fondamentale d'un système linéaire est le principe de superposition : si $s_1(t)$ est la réponse à une entrée $e_1(t)$ et $s_2(t)$ celle à $e_2(t)$ alors $\alpha\, e_1(t) + \beta e_2(t)$ donne pour réponse $\alpha s_1(t) + \beta s_2(t)$ - (α, β coefficients numériques) Un système tel que :

$$S(t) = \Sigma\, aj(t) \frac{d^j e_j}{d\ t^j}$$

satisfait une telle propriété.

Revenons maintenant sur le concept de stabilité en partant de la fonction de transfert d'un système, avec éventuellement une entrée "perturbation" et supposons d'abord que les coefficients des équations -donc de la fonction de transfert- soient constants.

Un tel système est stable si les pôles sont situés dans le demi plan de gauche (abscisses : amortissements, ordonnées : fréquences).

Stabilité signifie que si le système est temporairement, écarté d'un état stable, il reviendra à cet état après un temps plus ou moins long (degré de stabilité, stabilité asymptotique de Ljapounov). Si des pôles sont situés dans le demi plan de droite la sortie tend, théoriquement, vers l'infini, mais souvent des saturations apparaîtront et limiteront l'amplitude ou les oscillations.

Ce vieux concept de la stabilité -toujours valable- est trop loin de la réalité et du point de vue de l'utilisateur, la stabilité est normalement attachée au degré de corrélation qui existe entre l'entrée et la sortie.

Si les pôles sont prêts de l'axe imaginaire, la stabilité est faible et la réponse à un Dirac est une oscillation faiblement amortie (dans le cas où il n'y a pas, en plus, de perturbations). Si l'entrée varie continuellement, la sortie varie également mais la corrélation est pauvre.

Supposons maintenant que les coefficients varient dans le temps mais supposons qu'ils restent toujours dans le demi plan de gauche. Le système peut être considéré comme linéaire et stable. Supposons que tous les pôles sont complexes (s'il y a un pôle réel, à gauche, ce qui suit peut ne pas être vrai). Si le pôle de fréquence ω_i se déplace lentement dans le temps, lentement par rapport à $1/\omega_i$, par exemple, sinusoïdalement à la fréquence Ω_i telle que $\Omega_i << \omega_i$, alors le système se comporte comme une collection de systèmes à coefficients constants et la corrélation entrée-sortie n'est que très légèrement altérée. Si Ω_i est beaucoup plus grand que ω_i, alors la sortie comporte apparamment un "bruit" additionnel et la corrélation entrée-sortie n'est, là encore, que peu affectée.

Dans les 2 cas, on suppose que l'énergie contenue dans le signal d'entrée (spectre) dans $d\Omega_i$ autour de Ω_i est faible. C'est le cas usuel. Si Ω_i est proche de ω_i ou si le spectre du signal d'entrée contient une énergie suffisante au voisinage de Ω_i, alors la corrélation entrée-sortie peut disparaître complètement et la réponse à une entrée peut aparaître comme totalement décorrelée à celle-ci : c'est une sorte de chaos déterministe.

En fait cet exemple appelle 2 commentaires. D'abord, dans ce qui précède on fait l'hypothèse que le modèle du système existe et on raisonne sur ce modèle. On suppose donc qu'il n'y a pas d'incertitudes sur les coefficients à chaque instant (puisque ceux-ci varient dans le temps). La structure du système est alors parfaitement connue ; elle entre dans l'équation

générale $X = A\dot{X} + Bu$, équation dans laquelle les coefficients de la matrice A dépendent du temps. Mais comme il a été dit plus haut, dans toutes les applications les incertitudes sur les coefficients existent et l'hypothèse sur la façon dont varient les coefficients avec le temps s'estompe. Les concepts modernes de la Commande Automatique impliquent la robustesse, c'est-à-dire le choix de B de façon que les incertitudes sur A n'aient pas d'incidence sur le vecteur de sortie ($y = CX$) au-delà d'une certaine valeur (une partie de l'erreur, en général, erreur quadratrique moyenne, acceptable).

Ensuite, le concept de fonction de transfert ou de matrice de transfert (localisation des pôles) ne prévoit pas, a priori, de variation temporelle des positions des pôles ; la transformée de Laplace suppose que les coefficients de l'équation temporelle sont constants. Il n'est donc pas acceptable d'appliquer simultanément le concept de linéarité d'une équation (c'est-à-dire le concept de superposition) et le concept de stabilité à partir de la localisation des pôles, tout au moins lorsque les fréquences de mouvement des pôles sont voisines de la fréquence des pôles.

Les "systèmes paramétriques" -tel était le nom donné à ces systèmes linéaires à coefficients dépendant du temps- ne sont plus guère étudiés à ce jour ; lorsqu'ils l'étaient, voici quelques 20 années, le chaos n'était pas encore redécouvert. Il pourraît être intéressant de reprendre l'étude de ces systèmes dans l'optique de ce que l'on sait, aujourd'hui du chaos.

5. Le cerveau et le chaos déterministe [8]

Je voudrais mentionner ce thème bien qu'il soit fort éloigné de mes préoccupations quotidiennes.

Un système chaotique en état stationnaire est instable sur son attracteur ; il possède ainsi la propriété et les possibilités d'explorer l'espace des phases que l'on peut attendre pour les systèmes nerveux. L'idée selon laquelle la dynamique du cerveau, dans certains de ses aspects, pourraît être chaotique et de petites dimensions est acceptée ainsi que divers essais pour l'interprétation de signaux encephalographiques (EEG) en terme de chaos déterministe. On s'attend à trouver un attracteur étrange dans presque chaque signal a (fréquences 8 - 13 Hz).

Une difficulté majeure dans l'étude des EEG est la non-stationnarité du signal ; il doit être échantillonné en périodes courtes et de ce fait limite la dimension de l'attracteur. Peut-on conclure que cette non-stationnarité peut être interprêtée comme la preuve d'un caractère fugitif des attracteurs du cerveau ? Ou bien, en d'autres termes, les attracteurs sont spécifiques de la fonction exécutée par le cerveau à un instant donné (ou durant une courte période de temps).

6. Conclusions

Les considérations stochastiques dans l'ingénierie des systèmes ont été introduites par Norbert Wiener dans les années 1940 (souvenez-vous de son fameux livre "Cybernetics").

Les premières applications concernaient le comportement des systèmes en présence de perturbations stochastiques ; à la même époque des circuits linéaires prédicteurs ont été calculés et réalisés ; ils fonctionnaient bien pour des entrées aléatoires stationnaires. A peu près à la même époque, Claude Shanon introduisait la théorie de l'Information et la décennie 50 - 60 confirmait le bien fondé et l'intérêt de l'introduction des considérations stochastiques dans les activités de l'Ingénieur.

Plus tard, les ingénieurs ont demandé plus : les systèmes linéaires sont rares (mais souvenez-vous que souvent ils sont considérés comme une bonne approximation de systèmes non-linéaires) et la stationnarité d'un signal est rare, sauf cependant, dans certaines catégories de perturbations, par exemple, celles résultant de la

---

[8] d'après C.R. Académie des Sciences, Paris t. 311, Série II, p. 1037-1044, 1990 Roger Cerf et al. Parmi les références bibliographiques citées dans le CR je mentionne :

EN Lorentz, J. Atmosph. Sci. 20, 1963, p.130 - 141.
D. Ruelle and F. Takens, Commun. Math. Phys. 20, 1971, p. 167 - 192.
D. Ruelle, Proc. Roy. Soc. Lond. A, 427, 1990, p. 261 248
P. Grassberger et I. Procaccia, Physica, 9D, 1983, p. 189 - 208.
J. Theiler, Phys. Review A 34, 1986, p. 2427 - 2432.

nature granulaire de l'électricité [9]. Si le signal considéré n'est pas stationnaire, alors il ne peut pas être approché par des signaux stationnaires.

Maintenant les ingénieurs sont familiers avec les notions de fonction et processus aléatoires : les filtres de Kalman, qui connaissent de nombreuses variantes équipent les récepteurs GPS, les pilotes automatiques et tous les robots intelligents...

Cependant l'accroissement des capacités des calculateurs rendit l'ingénieur insatisfait. Il savait que les modèles qu'il utilisait étaient des approximations des systèmes réels, comme d'ailleurs le type de signaux qui entraient dans le système (entrées ou perturbations). Le concept de robustesse a été introduit voici quelques 20 années et de nouveaux algorithmes d'optimisation permettaient d'accepter quelques incertitudes sur les paramètres.

Puis le chaos arriva ou plutôt resurgit parce que, comme nous l'avons dit, il a été annoncé par Poincaré voici un peu plus de 100 ans.

C'est probablement la loi d'équilibre biologique d'une population d'êtres vivants qui a conduit les scientifiques par une étude minutieuse de cette simple équation :

$$X_{n+1} = \alpha X_n (1 - X_n)$$

(équation de Verkust) d'entrevoir toutes les conséquences sur le comportement des systèmes non linéaires [10].

A partir de tout ce bagage une théorie mieux structurée de la dynamique des systèmes non linéaires qui inclut la théorie du chaos a été élaborée et continue de l'être.

Les conférences qui vont suivre développeront les principaux aspects de ce nouveau chapitre en vue des applications dans le domaine de l'ingéniérie.

[9] aux bornes d'une résistance R, à la température T, la tension fluctue d'une façon stationnaire. Si ΔF est la bande passante dans laquelle le signal est observé, la valeur quadratique moyenne de la fluctuation de tension est $e^2 = 4kRT\Delta f$, k constante de Boltzman ($1{,}380.10^{-23}$ $J.K^{-1}$).

[10] l'équation de Verhust est bien commentée dans la référence [6] lorsque α varie de 0 à 3,56999 ...

Références

[1] La Corrélation. Académie des Science et Académie Nationale de l'Air et de l'Espace. International Symposium, Toulouse, Nov. 1991. Cepaduès Ed. Toulouse, ou ANAE 1, avenue Camille Flammarion, 31500 Toulouse.

[2] Stability in Aerospace Systems. Agard Report 789, Feb. 1993.

[3] "The downburst". Theodore Fujita, 1985 University of Chicago.

[4] "DFW Microburst". Theodore Fujita, 1986, University of Chicago.

[5] "Modélisation des cisaillements de vent" B. Cantaloube, Th. Lé, Nov. 1990. Rapport ONERA 12/3619 SYA.

[6] "Turbulent Miroir", John Briggs, F. David Peat, 1989 (Harper and Row).
"Un miroir turbulent", version française, 1991 (Interedition).

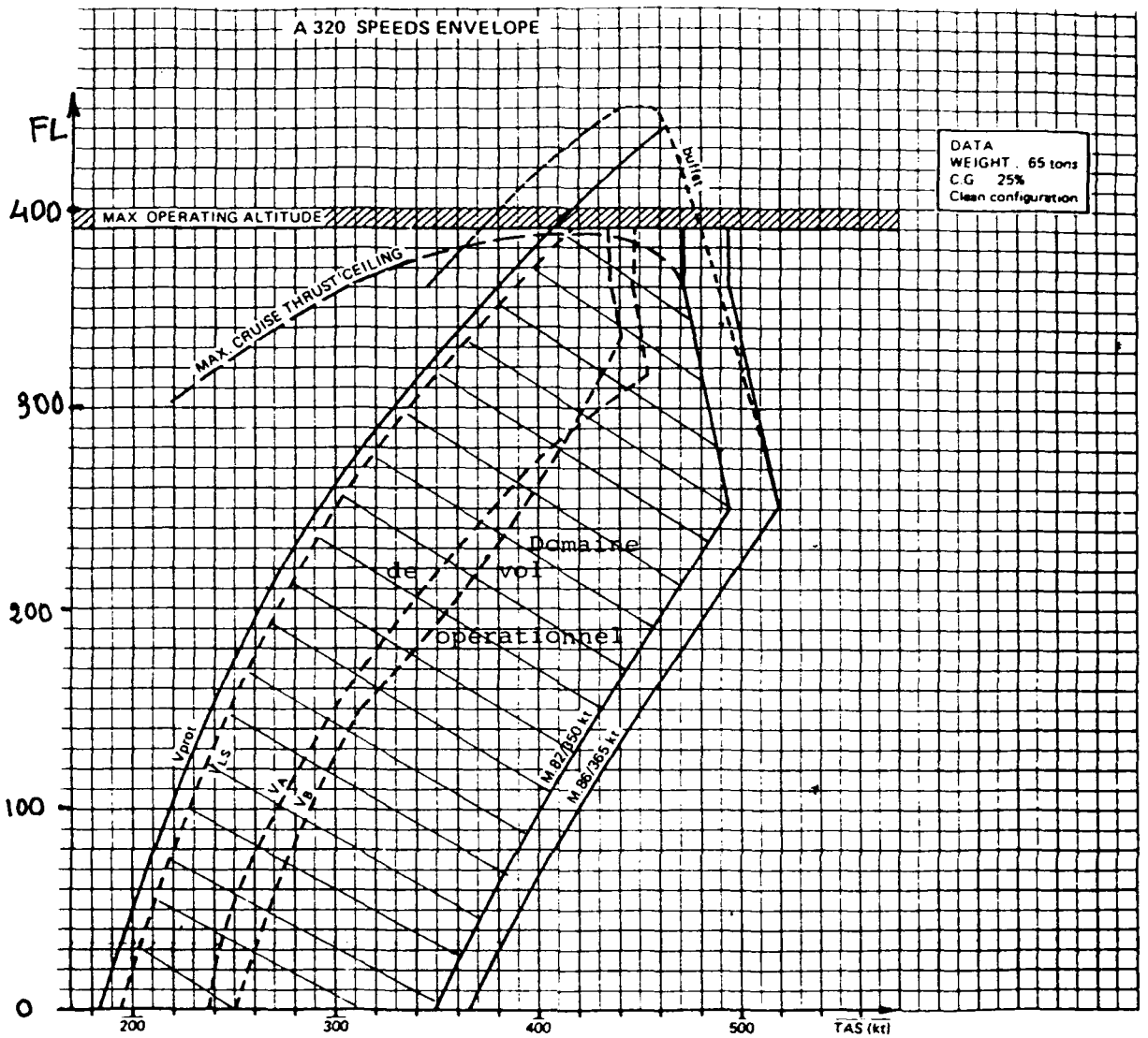

V_{LS} vitesse minimale acceptable

V_A vitesse maximale "de manœuvre" au facteur de charge maximum

V_B vitesse maximale en turbulence "sévère"

M 0,82/350 kt Mach et vitesse maximaux opérationnels

M 0,86/365 kt Mach et vitesse maximaux continus avec manche, en piqué maximum

V_{prot} vitesse minimale "protegée" correspondant à l'angle maximal d'incidence "protégé"

TAS True Air Speed vitesse aérodynamique vraie - par opposition avec IAS (Indicated Air Speed) ou CAS (Calibrated Air Speed) qui ne correspondent pas à la vitesse vraie

FL *Flight Level* :
Niveau de vol 3000 → 30 000 pieds

Domaine de Vol A 320

Les autres tableaux se trouvent dans la version anglaise.

Bifurcation Theory: Chaos and Patterns

P. Coullet
Institut Nonlinéaire de Nice
France
UMR CNRS 129

Abstract

These lectures are devoted to study the transition towards chaos and the bifurcations leading to patterns. The qualitative and universal aspects of these phenomena are emphasized.

1 Introduction

Natural systems provide a great variety of motions. Some are regular such the seasonal rhythms, wheras others are very complex and apparently random, such as ocean waves or the fluid motion behind an obstacle. H. Poincare, at the beginning of this century, discovered that apparently random phenomena could well be the consequence of simple deterministic dynamical systems [1]. More than 60 years afterwards physicists rediscovered Poincare theory and the science of chaos was born.

The theory of dynamical systems allows us to describe the changes that a deterministic system can suffer when some of its characteristic parameters are varied [2]. It describes these changes in a *qualitative* but universal way. In particular, it allows us to understand why similar phenomena arise in systems as different as a mechanical system or a biological one.

These lectures are divided into two parts. In the first part we study the transition towards chaos through the cascade of period doubling bifurcations. The second part is devoted to the phenomena of symmetry breaking and pattern formation.

2 Chaos

One of the most exciting experimental discoveries of the last 20 years is that simple hydrodynamical and chemical systems can show complex temporal behavior (see fig. (1)) which can be, in turn, reproduced by simple dynamical models [3] [4]. A powerful way to analyze an experimentally obtained complex time series $X(t)$ was proposed by F.Takens [5]. An arbitrary delay τ is introduced. The signals $X_0(t) = X(t)$, $X_1(t) = X(t-\tau)$, $X_2(t) = X(t-2\tau)$, ... up to

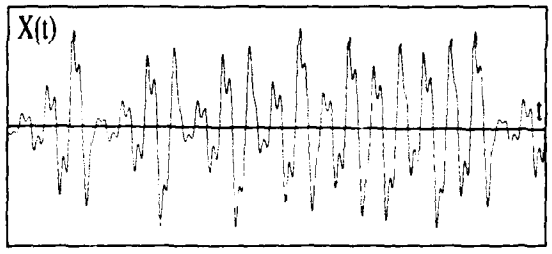

Figure 1: A typical experimental signal

$X_n(t) = X(t-n\tau)$ are then constructed with the help of the delay. The space generated by these variables is called the n-dimensional reconstructed phase space. The basic idea behind the Takens reconstruction is to reduce the complexity of the signal by trying to represent it in a finite dimensional phase space. Practically one considers the trajectory obtained by increasing the dimensionality n of the phase space. For each n the dimension ν of the reconstructed attractor is measured. The procedure stops when ν does not change anymore. A simple way to measure the dimension of the attractor was suggested by Procaccia and Grassberger [6]. The number of points N_r which falls in a small ball of radius r on the attractor is measured. When r goes to zero this quantity exhibits a scaling law from which the local dimension ν is extracted $N \sim r^{\nu}$. In the case of the signal presented in figure (1), the reconstruction with $n = 2$ leads to a phase portrait (see fig. (2)) which eventually fills a finite area of the plane. This suggests that the attractor's dimension is greater or equal to 2. The three dimensional reconstruction confirms that the dimension is actually in between 2 and 3. A cut of the attractor by a plane reveals the structure of the attractor (see figure (3)). This analysis shows that signals as complex as the one of figure (1) can be coded with a finite number of data points. Three in our case: $X(0)$, $X(\tau)$ and $X(2\tau)$. The data in figure (1) were not obtained from a real experiments but from the numerical solution of a differential equation

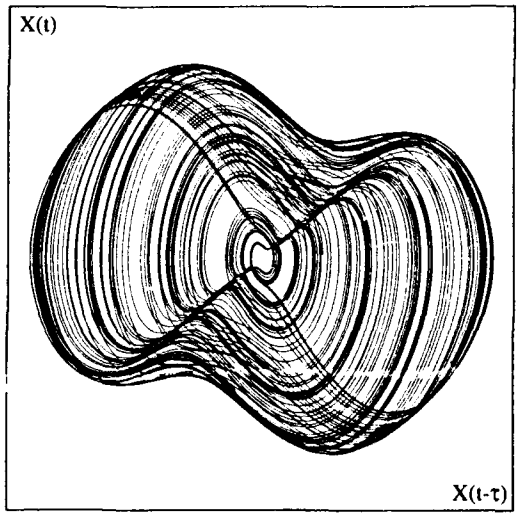

Figure 2: Two dimensional phase space reconstruction of the signal shown on figure (1)

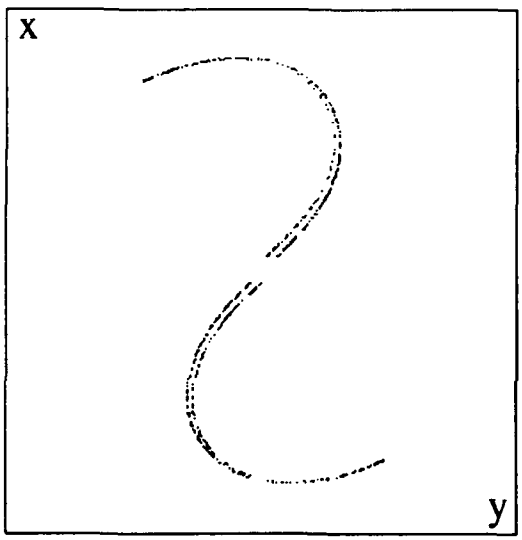

Figure 3: Poincare cut of the three dimensional reconstructed attractor.

whose phase space is actually three dimensional

$$\ddot{\Theta} + \nu\dot{\Theta} + (1 + f\Omega^2\cos(\Omega t))\sin\Theta = 0 \qquad (1)$$

This equation describes the motion of a pendulum in a periodically varying gravitational field. Equation (1) can be written as a set of three coupled first order equations

$$\begin{aligned} \dot{X}_0 &= X_1 \\ \dot{X}_1 &= -2\nu X_1 \\ &\quad -(1 + f\Omega^2\cos X_2)\sin X_0 \\ \dot{X}_2 &= \Omega \end{aligned} \qquad (2)$$

or

$$\dot{X} = F(X) \qquad (3)$$

where $X = (X_0, X_1, X_2)$ and the vector field F is given by

$$F = (X_1, -\nu X_1 + (1 - f\Omega^2\cos X_2)\sin X_0, \Omega)$$

The dynamical system given by equation (3) depends on parameters which control the transition from regular to irregular behavior. In what follows, we describe a numerical experiment where ν and Ω are kept fixed. The amplitude, f, of the periodic modulation of the gravitational field is increased from zero. The solution $X_0 = X_1 = 0, X_2 = \Omega t$ represents the rest state of the pendulum. In phase space, it corresponds to a limit cycle with a period $T = \frac{2\pi}{\Omega}$. The projection of this circle in the $X_0 - X_1$ plane is a point located at the origin. The stability of this solution is controlled by the Mathieu equation [7]. In the $(f - \Omega)$ plane the instability domains are located inside the resonance tongues. The signal of figure (1) has been obtained close to the strong resonance $\Omega \sim 2$. As f is increased, the attractor of equation (3) changes its dimension. For f small enough the rest state is stable. Above a critical value, f_0, it loses its stability (see figure (4)) and the pendulum oscillates. The corresponding orbit in the phase plane is still topologically a circle. The change of dynamical state that the pendulum undergoes when the amplitude of the modulation is varied is a typical example of bifurcation. One of the most useful results of the theory of bifurcation is the possibility of classifying the generic bifurcations which occurs in real experiments. When f is slightly above a second critical value, f_2, a new bifurcation transform the cyclic attractor into a knotted orbit (see fig. (5)). In this process the period of the solution doubles. This bifurcation provides the key mechanism for the transition towards chaos. A further increase in the amplitude of the forcing leads a complete cascade of such bifurcations. At each critical value f_n the orbit length doubles. At the n^{th} step a cut of the attractor consists of 2^n points. The sequence of the f_n is shown to converge geometrically

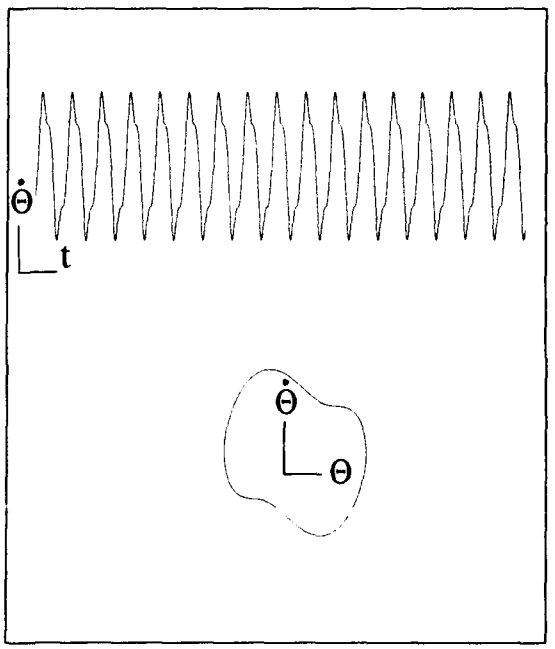

Figure 4: The parametric oscillation.

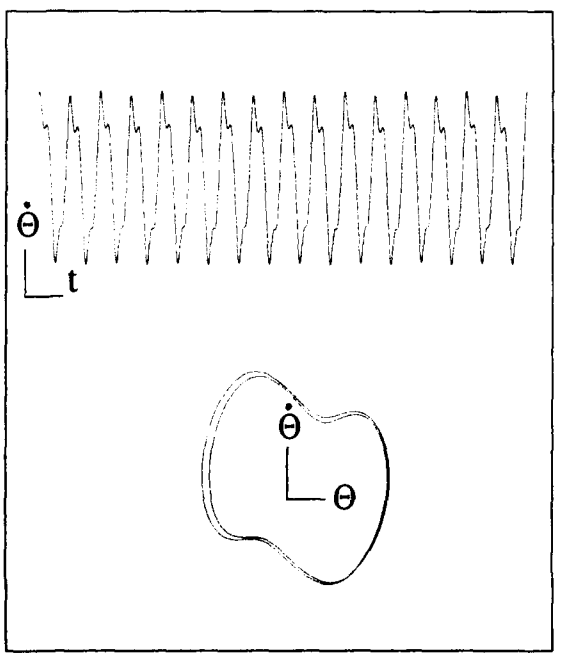

Figure 5: Period doubling bifurcation.

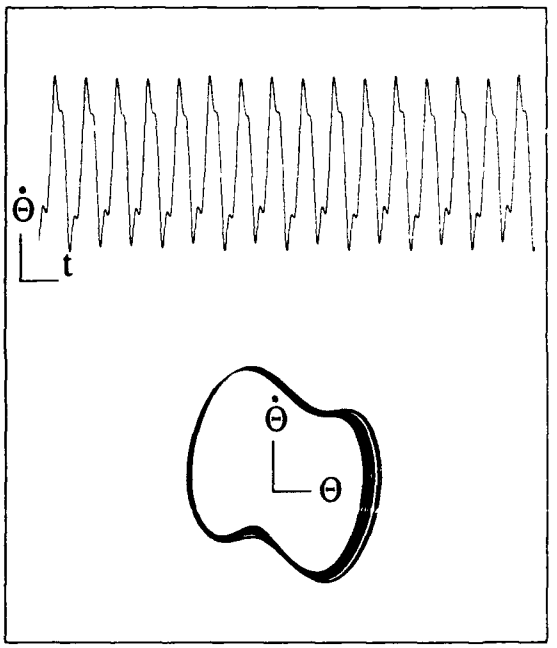

Figure 6: Slightly above f_∞.

to f_∞. The sequence of cuts suggests the existence of a Cantor set for this parameter value. Above this critical value the signal obtained (X_1, for example, as a function of time) exhibits weak irregularities (see figure (6)). The chaotic behaviors can be characterized by quantities which measures the amount of chaos. These are entropies and Lyapunov numbers [8]. They are rigorously defined rigorously in the framework of ergodic theory. Thoses very interesting aspects of dynamical systems are not covered in this lecture. We will instead focus our attention on the transition to chaos through a cascade of period doubling bifurcations. The cut of the flow by a plane (Poincare cut) defines a diffeomorphism of the plane into itself. The flow associated with equation (3) has the property to uniformly contract the volume in the phase space. The contraction is given by the divergence of the vector field

$$\frac{\partial \dot{X}_0}{\partial X_0} + \frac{\partial \dot{X}_1}{\partial X_1} + \frac{\partial \dot{X}_2}{\partial X_2} = -\nu$$

Obviously the Poincare map should then uniformly contracts the areas in the plane. Let us define the coordinates in a typical Poincare plane as x_0 and y_0. The Poincare map may be written as

$$\begin{aligned} x_0' &= f(x_0, y_0) \\ y_0' &= g(x_0, y_0) \end{aligned}$$

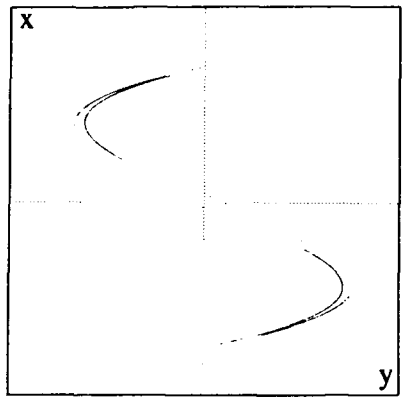

Figure 7: 10000 first iterates of (0,0) of the cubic Henon's map

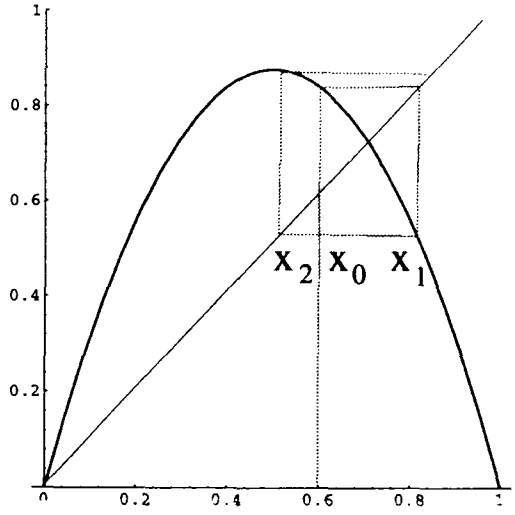

Figure 8: The logistic map

The simplest nonlinear diffeormorphism [9] of the plane which uniformly contract the areas can be written as

$$\begin{aligned} x_0' &= ax_0(1-x_0) - by_0 \\ y_0' &= x_0 \end{aligned} \tag{4}$$

At each iteration an arbitrary area in the plane is contracted by a constant factor given by the Jacobian of the transformation (4)

$$J = \frac{\partial x_0'}{\partial x_0}\frac{\partial y_0'}{\partial y_0} - \frac{\partial x_0'}{\partial y_0}\frac{\partial y_0'}{\partial x_0} = b$$

Numerical simulations of the mapping (4) for increasing values of a, for fixed b, reveal the existence of a cascade of period doubling bifurcations as the precursor of chaotic behavior. In the chaotic regime, the attractor of the cubic Henon's map ($ax_0(1-x_0) \rightarrow ax_0(1-x_0^2)$ in equation (4)) exhibits strong similarities to the Poincare map of the parametrically forced pendulum shown in the figure (3) (see figure (7)). The mechanism of the cascade of period doubling bifurcations and its relationship to nonlinearity can be understood in the limit where $b \rightarrow 0$. The Henon map (4), in this limit becomes a one-dimensional map (see figure (8)) known as the logistic map

$$x_0' = ax_0(1-x_0) \equiv \lambda_a(x) \tag{5}$$

As a increases from zero the following scenario is observed. For $0 < a < 1$ the iterates of all the initial conditions converge toward zero. For $1 < a < 3$ the iterates of all the initial condition except (0) and (1) converge towards a fixed point, a solution of

$$x^* = \lambda_a(x^*)$$

For $3 < a < 3.5$ almost all the initial conditions converge towards an alternate serie (x_-, x_+), solution of the equations

$$\begin{aligned} x_+ &= \lambda_a(x_-) \\ x_- &= \lambda_a(x_+) \end{aligned}$$

or

$$\begin{aligned} x_+ &= \lambda_a(\lambda_a(x_+)) = \lambda_a^{(2)}(x_+) \\ x_- &= \lambda_a(\lambda_a(x_-)) = \lambda_a^{(2)}(x_-) \end{aligned}$$

where $\lambda_a^{(2)}$ denotes the second iterate of λ_a. For $a_n < a < a_{n+1}$ almost all initial conditions converge towards a periodic cycle consisting of 2^n points $x_1, x_2, ..x_{2^n}$ such that

$$x_i = \lambda_a^{(2^n)}(x_i)$$

for all $i = 1, ..2^n$. The sequence of the a_n converge in a geometric fashion towards a limit value a_∞:

$$\lim_{n\rightarrow\infty} \frac{a_{n+1} - a_n}{a_{n+2} - a_{n+1}} = 4.669.. \equiv \delta \tag{6}$$

For $a > a_\infty$, chaotic behaviors is observed for a measurable set of parameter values (see fig. 9) . The mechanism of the cascade of period doubling bifurcations can be understood in the following way

- The first period doubling bifurcation is a simple consequence of the nonlinearity of the map. The stability of the fixed point x^* is controlled by the derivative of the map at this point. A small deviation, δx, around the fixed point becomes after one iteration

$$\delta x' = \left.\frac{\partial \lambda_a}{\partial x}\right|_{x^*} \delta x$$

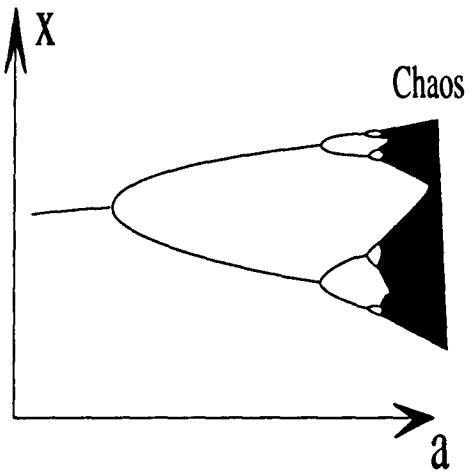

Figure 9: Sketch of the cascade of period doubling bifurcations

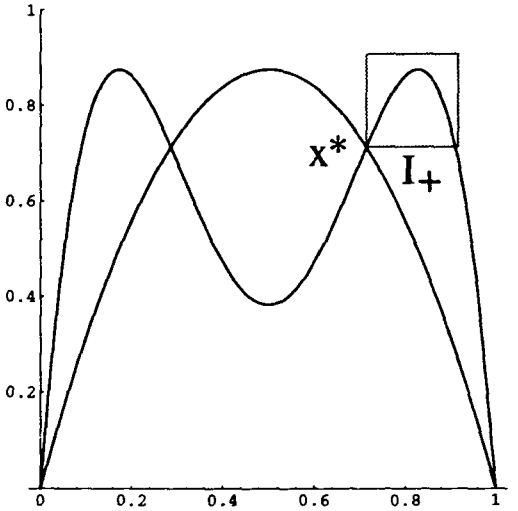

Figure 10: The logistic map and its second iterate

When r increases, the fixed point eventually reaches the region where the map has a negative slope. When $|\partial\lambda_a/\partial x|_{x^*}| \geq 1$, the fixed point x^* loses its stability. This occurs when $\partial\lambda_a/\partial x|_{x^*} = -1$, which defines a_1 in an unique way. Slightly above a_1, the iterates of almost all initial conditions converge toward a periodic cycle of period two, whose elements are fixed points of the second iterate of the map (see figure (10))

- The form of the graph of $\lambda_a^{(2)}$ allows us to understand the existence of a cascade of bifurcations. The restriction of $\lambda_a^{(2)}$ to the interval denoted I_+ in figure (10) is similar to $\lambda_a^{(2)}$ itself. When a is increased x_+ reaches the domain of $\lambda_a^{(2)}$ in I_+ where the slope $\partial\lambda_a^{(2)}/\partial x\Big|_{x^+}$ becomes smaller than -1. The periodic solution of period two becomes unstable for this parameter value. This simple idea is at the root of a theory proposed simultaneously by M. Feigenbaum [11] and P. Coullet and C. Tresser [12] [13] in order to analyze the cascade of period doubling bifurcations. We present here a crude calculation which illustrates this theory. The second iterate of the logistic map $\lambda_a^{(2)}$ is

$$\begin{aligned} x' &= (2-a)^2 x \\ &\quad -a(6-5a+r^2)x^2 \\ &\quad +a^2(4-3r)x^3 - r^3y^4 \end{aligned} \tag{7}$$

We have chosen the origin of the coordinates at the point $(x^*, \lambda_a(x^*))$. A truncation at the quadratic order and a scaling tranformation brings it into the form

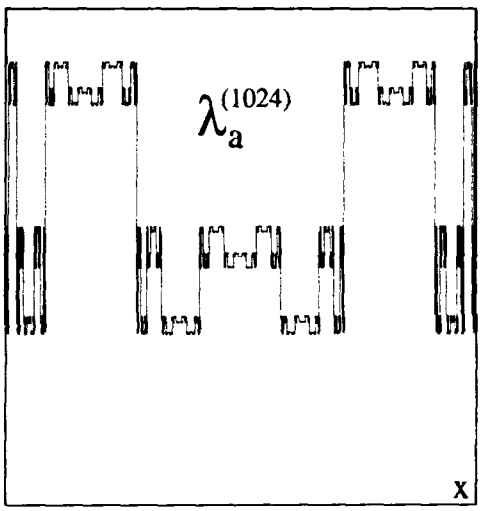

Figure 11: Self similarity of $\lambda_{a_\infty}^{(1024)}$

$$x' = a'x(1-x) \tag{8}$$

where $a' = (2-a)^2$.

This map is called the renormalization map. Up to a translation, a change of scales and a change of the parameter (renormalization), $\lambda_a^{(2)}$ is equivalent to λ_a. a' is called the renormalized parameter. The renormalization map has two fixed points $a = 1$ and $a = 4$. Let us consider only the fixed point with the positive slope ($a = 4$). We identify this value of a with a_∞. If our calculation was exact $\lambda_{a_\infty}^{(2)}$ would be exactly self-similar to λ_{a_∞} (see fig. (11)). When a is close enough to a_∞, $\lambda_{a_{\infty-\rho}}^{(2)}$ is almost equivalent to $\lambda_{a_{\infty-\delta\rho}}$, where δ is the slope of the renomalization map

at the fixed point a_∞. Thus a typical parameter range for the map λ_a is shrunk by a factor δ for its second iterate $\lambda_a^{(2)}$. In particular the domain of stability of the cycle of period $2^{(n+1)}$ is δ time smaller that the domain of stability of the cycle 2^n. One gets $\delta = 4$. The truncation is the only serious criticism of this analysis. This approximation introduces in particular a spurious fixed point $a = 1$. Our crude calculation can be transformed into a poweful and rigourous theory (renormalization group) [14] which allows one to prove the existence of a cascade of period doubling bifurcation and its universality. It is beyond the scope of this review paper to go into the details of this theory.

The main steps are the following:

1. Definition of a renormalization map as

$$\Psi(x) = h^{-1}\Phi(\Phi(h(x)))$$

where h is an affine transformation.

2. Computation of its fixed points

$$\Phi^*(x) = h^{-1}\Phi^*(\Phi^*(h(x)))$$

3. Computation of the spectrum at the fixed points

$$\Delta(x) = \left.\frac{D\Psi}{D\Phi}\right|_{\Phi^*}$$

The main results are the following:

1. Analytic maps have a denumerable set of fixed points.
2. One of the fixed points (unimodal map with a quadratic maximum) has a spectrum with only one eigenvalue $\delta = 4.669..$ whose modulus is greater than 1
3. Multidimensional perturbations of this fixed point, as for example the generalization of the Henon map, does not destroy the results (1) and (2).

These results explains why the cascade of period doubling bifurcation with its universal number $\delta = 4.66920160910210909..$ are actually observed in such a wide class of dynamical systems.

3 Patterns

The bifurcations provide the most obvious mathematical explanation for the changes which occur in a physical system when its parameters are varied [15]

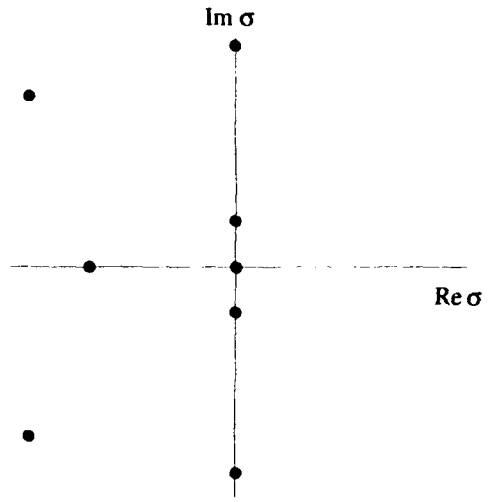

Figure 12: typical spectrum of $Df_\mu/DU|_{U^*}$ at a bifurcation point

[16]. Patterns which are frequently observed in natural systems can be understood as the result of a symmetry breaking bifurcation. Patterns break the basic symmetries of space and time: time translations, space translations, rotations and space inversion.

In the introduction to this chapter, we will summarize some of the simple tools of bifurcation theory. Let U^* be the fixed point associated with the flow of a finite dimensional vector field $F(U)$. Then

$$\partial_t U = F_\mu(U) \tag{9}$$

where $U = (U_1, U_2, ..U_n)$ and μ is a set of k parameters $\mu = (\mu_1, \mu_2, ..\mu_k)$. The fixed point U^* is such that $F_\mu(U^*)$. The topological type of the flow in the neighborhood of the fixed point U^* changes whenever an eigenvalue of the spectrum of the linearized vector field, $Df_\mu/DU|_{U^*}$, crosses the imaginary axis. These changes are called bifurcations. In many practical applications of bifurcation theory a stable fixed point loses its stability at the bifurcation point. In that case, the spectrum of $Df_\mu/DU|_{U^*}$ is completely contained in the right half of the complex plane except for a finite number of eigenvalues which sit, at the bifurcation, on the imaginary axis (see figure (12)). The main result of bifurcation theory is that, close to the bifurcation equation (9) can be reduced to a simpler one called its normal form [2] [15] [16]. This result is based on the central manifold theorem which asserts the existence of a local manifold which captures all the interesting phenomena occuring at the bifurcation. The topological change that the vector field close to the fixed point suffers at the bifurcation can be analyzed on this manifold only. It is the straightforward generalization of the linear space generated by the part of the spectrum

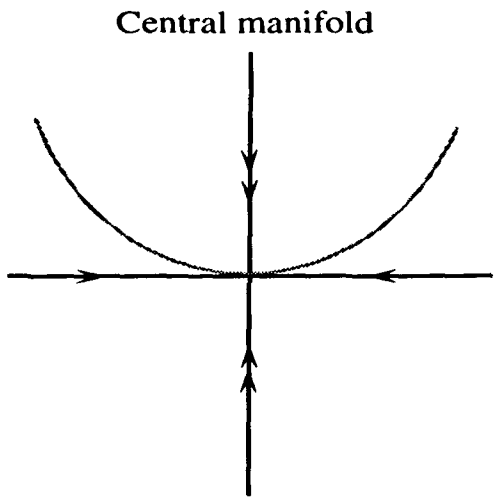

Figure 13: Sketch of the central manifold

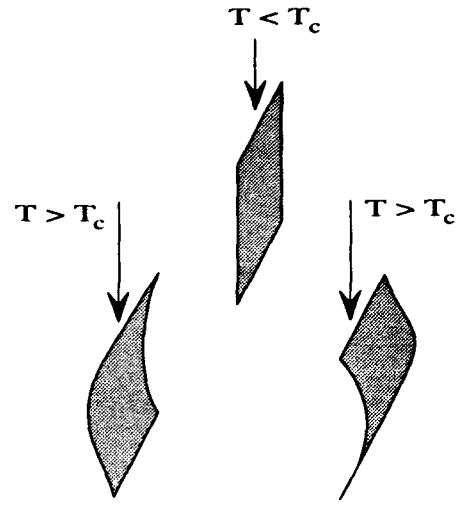

Figure 14: The buckling of a plate

of $Df_\mu/DU|_{U^*}$ which lies on the imaginary axis (see figure (13)). The restriction of equation (9) to this manifold using appropriate coordinates is the normal form. Bifurcations of a fixed point are easily classified. The generic (co-dimension one) bifurcations correspond either to the crossing of a single zero eigenvalue (stationary bifurcation) or a pair of complex eigenvalues (oscillatory or Hopf bifurcation) [15] [16] .

3.1 Symmetry breaking

Symmetry groups play an important role in the understanding of physical systems. The description of the crystalline structure by Bravais is probably the most famous success of this theory. The phenomenon of symmetry breaking was first fully appreciated by the French physicist P. Curie. Bifurcations in symmetric dynamical systems often lead to the symmetry broken phenomenon [17] [18]. The theory of phase changes by Landau can be interpreted in this framework. The buckling of a plate provides a simple example of a spontaneous symmetry breaking transition. A vertical tension is applied to a vertical elastic plate (see figure (14)). When the tension exceeds a critical value, the plate bends. The side on which the plate bends depends on the existence of small fluctuations when the tension passes its critical value. In a well controlled experiment there is as equal probability that the plate will bend to the left as to the right. Let us denote the amplitude of the bend by a real number, A. This quantity (the order parameter in Landau's terminology) should be one of the coordinates of the central manifold since the most obvious topological change associated with the bifurcation (the breaking of the left-right symmetry of the apparatus) is associated with it. The simplest case corresponds to a one dimensional central manifold parametrized by A only. The bifurcation equation (normal form) is thus a priori

$$\partial_t A = f(A) \tag{10}$$

where, in order to satisfy the symmetry of the physical system, $f(-A) = -f(A)$. Since at the threshold of the instability (bifurcation) A is small (at least for short times), A can be expanded in a Taylor series. The truncation of the normal form at the first nonlinear term can be written as

$$\partial_t A = f_1 A + f_3 A^3 \tag{11}$$

where f_1 is proportionnal to $T - T_c$, and T and T_c represents the tension and the critical tension respectively. The sign of f_3 is crucial. In the case of the buckling, f_3 is negative. In that case, the bifurcation is supercritical and the amplitude of the bend saturates to a finite value, $A^* = \sqrt{f1/(-f_3)}$. When $f_3 > 0$, the amplitude grows indefinitely in time. In that case, equation (11) is only valid for short times, when A is still small. The bifurcation of the buckling plate is known as the pitchfork bifurcation (see figure (15)) and the amplitude equation (normal form) is known as the Landau equation. From a purely mathematical point of view this bifurcation corresponds to the crossing of an eigenvalue through zero for a dynamical system which possesses reflection symmetry. Equation (11) can be obtained in a rigourous way from the equations of elasticity. Technically one can either use singular perturbation theories (Poincare-Lindsted and its generalization [7]) or normal form theories [2] [15] [19] [21]. Let us consider, as a simpler example of a pitchfork bifurcation, the behavior

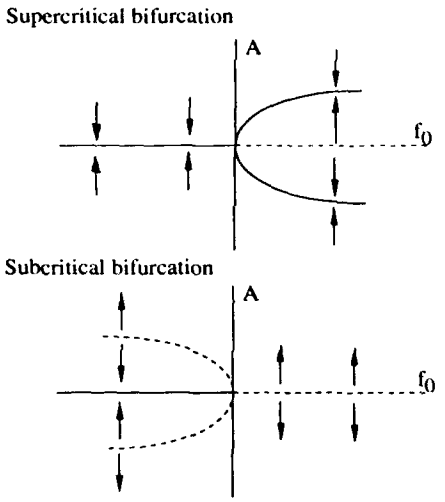

Figure 15: Diagram of a supercritical pitchfork bifurcation

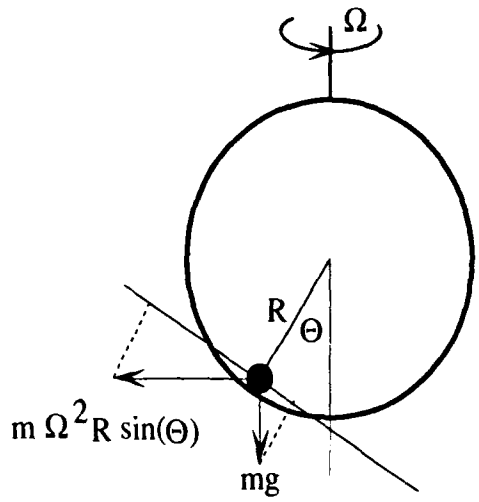

Figure 16: The conic pendulum

of a ball gliding in a hoop which is rotating around a vertical axis (also known as the problem of the conic pendulum, see figure (16)). The motion of the ball is described by the equation

$$\ddot{\Theta} + 2\nu\dot{\Theta} + \sin\theta - \Omega^2 \sin\Theta cos\Theta = 0 \qquad (12)$$

When the normalized velocity of the hoop Ω is greater than or equal to 1 the equilibrium position of the ball, $\dot{\Theta} = \Theta = 0$, becomes unstable. The ball moves towards a new equilibrium position. The bifurcation is again a pitchfork bifurcation. The ball can either reach a new position with a positive angle or with a negative and opposite angle. The bifurcation breaks the $\Theta \rightarrow -\Theta$ symmetry. Close to the bifurcation point, a straightforward calculation shows that the spectrum of the linear operator consists of a negative eigenvalue whose value is close to $-\nu$ and an eigenvalue close to zero. This suggests that the dynamics of the ball consists in a "fast" time relaxation (with a characteristic time $\tau \sim 1/\nu$) and a slow time variation. For times larger than the fast relaxation time, the dynamics of the ball is slow, and the amplitude of the motion is small. Since the amplitude $A \equiv \Theta$ is small and $\dot{A} << A$ equation (12) can be reduced to the Landau equation (11) with $f_1 = (\Omega^2 - 1)/2\nu$ and $f_3 = -1/4\nu$.

The third example of spontaneously broken symmetry we want to discuss is associated with the parametric forcing of a pendulum (see equation (1 of chapter (2)). We study here the case where the forcing occurs close to twice the natural frequency of the pendulum. In that case equation (1) becomes:

$$\ddot{X} + 2\nu\dot{X} + \epsilon\cos(2(1-\eta)t))\sin X = 0 \qquad (13)$$

where the detuning, η, measures the deviation from

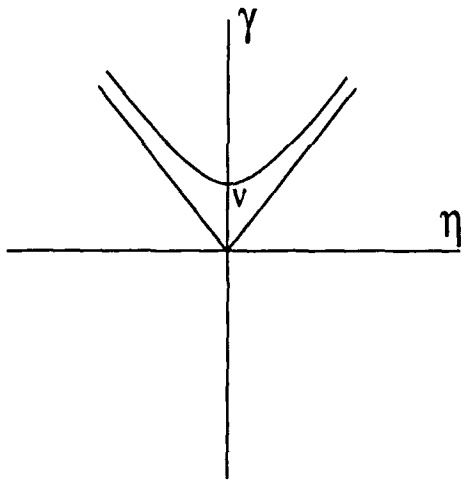

Figure 17: 1:2 parametric resonance

the exact resonance and $\epsilon = 4f(1-\eta)^2$. The instability sets in when the forcing, f, exceeds a critical value (see figure (17)). The oscillatory motion of the pendulum has a period which is then precisely half of the driven frequency. This bifurcation is actually a period doubling bifurcation. Close to the instability threshold, a solution of the equation is considered to be of the form

$$X = A(t)e^{i(1-\eta)t+i\phi} + c.c + harmonics \qquad (14)$$

where $A(t)$ is a real function which is assumed to be slowly varying in time. The differential equation to be satisfied by A can be obtained by using averaging techniques [2], since A does not vary much at the time scale of the oscillation. This equation is, a priori:

$$\partial_t A = f(A) \qquad (15)$$

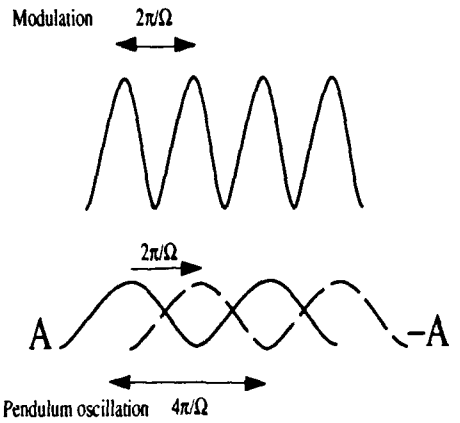

Figure 18: Symmetry breaking in the parametric excitation of a pendulum

Equation (13) is invariant under the transformation

$$t \to t + 2\pi/\Omega$$

where $\Omega = 2(1-\eta)$ is the actual period of the modulation of gravity. Let us apply this transformation to the solution given by expression (14)

$$\begin{aligned} X &= A(t+2\pi/\Omega)e^{i\pi}e^{i(1-\eta)t+i\phi}\ldots \qquad (16)\\ &\sim -A(t)e^{i(1-\eta)t+i\phi}+\ldots \end{aligned}$$

Since $X(t+2\pi/\Omega)$ is a solution of equation (13), $-A$ should be a solution of equation (15). This requirement implies that $f(A) = -f(-A)$. At the leading order, the equation to be satisfied by the amplitude is then the Landau equation (11). The parametric instability is a symmetry breaking bifurcation. Two possible oscillatory states can be observed as the result of the instability. They differ by a phase shift of π, i.e. a period of the external driving frequency (see figure (18)). It means that if one considers an assembly of such pendulums, statistically half of them will oscillate with a given amplitude and half of them with the opposite amplitude. Similar to the case of the buckling of the plate and the conic pendulum, the viscous damping , ν, is responsible for the reduction to a first order differential equation. When the damping becomes weaker, the phase of the oscillation becomes an active parameter. The solution of equation (13) is then considered to be of the form

$$X = A(t)e^{i(1-\eta)t} + c.c + harmonics \qquad (17)$$

where A is now a complex amplitude which contains informations on both the real amplitude and the phase of the oscillation. When the expression (17) is inserted into the equation (13), taking account that A is small and slowly varying, and that ν and f are also small quantities, one gets the amplitude equation (normal form) as a compatibility condition,

$$\partial_t A = (-\nu + i\eta)A - i\alpha|A|^2A + i\gamma\bar{A} \qquad (18)$$

where $\alpha = 1/4$, $\gamma = \epsilon/4$ and $\bar{A}$ denotes the complex conjugate of A. When the forcing goes to zero ($\gamma = 0$) equation (18) becomes invariant under the transformation $A \to Ae^{i\theta}$, where θ is an arbitrary phase. This equivariance property is a consequence of the translational invariance of the equation of the unforced pendulum. The term $\gamma\bar{A}$ in equation (18) represents the symmetry breaking induced by the forcing. It reduces the symmetry group under which (18) is invariant to the transformation $A \to -A$. The stability analysis of the pendulum at rest proceed as follow. Let us introduce the real and imaginary parts of the complex amplitude $A = X + iY$. The linear equations to be satisfied by X and Y are

$$\begin{aligned} \partial_t X &= -\nu X + (\gamma - \eta)Y \qquad (19)\\ \partial_t Y &= -\nu Y + (\gamma + \eta)X \qquad (20) \end{aligned}$$

Let $X = X_0e^{\sigma t}$ and $Y = Y_0e^{\sigma t}$. The equation for σ is

$$(\sigma + \nu)^2 = \gamma^2 - \eta^2$$

The eigenvalues are both real if $|\gamma| > |\eta|$ (frequency locking). The instability sets in inside the frequency locking tongue, when $\gamma^2 \geq \eta^2 + \nu^2$

At the instability threshold the eigenvalues are $\sigma = 0$ and $\sigma = -2\nu$. The marginal eigenmode is such that

$$\frac{Y_c}{X_c} = -\frac{\nu}{\gamma + \eta} \equiv \tan\phi$$

where X_c and Y_c are the components of the unstable mode and ϕ is the phase introduced in the solution given by expression (14). Near the threshold the equation (18) can be reduced to a simpler one that is first order in time. This equation for the real amplitude, A, of the marginal mode is none other that the Landau equation.

3.2 Pattern forming transitions

At all scales matter exhibits structures. Some patterns are very regular, such as for example the honeycomb-like convective cells observed in a well controlled experiment. Others are quite irregular, such as the hydrodynamical flow behind an obstacle at high Reynolds number. Patterns arise due to the spontaneous symmetry breaking of space-time symmetries. When a material fills an empty space it usually inherits its homogeneity properties. Most of the time patterns reflect the topology of the space

in which the physical system is embedded. In particular, patterns which are observed on a flat surface or a curved one are quite different. Hexagonal patterns can regularly fill a piece of plane, it is not the case one the sphere. The matter itself can influence the morphogenesis when it breaks the homogeneity of space. The molecule of a nematic liquid crystal, for example breaks the isotropy of space at the microscopic level. Patterns observed in such systems will have original features associated with the symmetry of the molecules. Mathematically, patterns are the solutions of partial differential equations. Before describing formal aspects of the theory of pattern formation, let us first discuss a very naive example of pattern formation.

The problem of the coupling of two pendulums allows one to introduce the basic mechanism of pattern formation. In this problem, space is simulated by two points, the two pendulums. The equations which describe the motion of the pendulums are

$$\ddot{\Theta}_1 + \sin\Theta_1 = \kappa(\Theta_2 - \Theta_1) \quad (21)$$
$$\ddot{\Theta}_2 + \sin\Theta_2 = \kappa(\Theta_1 - \Theta_2) \quad (22)$$

where κ, the torsion constant is assumed to be small. One of the invariance properties of equation (21) (1) $\leftrightarrow$ (2) reflects the homogeneity of the "space". Let us introduce the sum and the difference of the angle of the two pendulums $\Sigma = \Theta_1 + \Theta_2$ and $\Delta = \Theta_1 - \Theta_2$. Linearizing equation (21) around the rest state one obtains :

$$\ddot{\Sigma} + \Sigma = 0 \quad (23)$$
$$\ddot{\Delta} + (1+2\kappa)\Delta = 0 \quad (24)$$

The normal modes of this simple mechanical system are thus given by

- $\Delta \neq 0$ and $\Sigma = 0$ where the two pendulums oscillate with the same amplitude at the same frequency as a single pendulum.
- $\Delta \neq 0$ and $\Sigma = 0$ where the two frequency oscillate with opposite phase, at a higher frequency $\sqrt{1+2\kappa}$

The first normal mode does not break the (1) $\leftrightarrow$ (2) invariance while the second one does. We will say that the second mode of oscillation describes a pattern in its simplest form since this solution breaks the homogeneity of the "space". In order to understand a little more about the spontaneous appearance of patterns, let us consider the case where the two coupled pendulums are weakly damped and subjected to a small periodic variation of the gravitational field, close to resonance (1:2). The dynamics of such a system is described by the equations

$$\ddot{\Theta}_1 + 2\nu\dot{\Theta}_1 + (1+f\Omega^2\cos(\Omega t))\sin\Theta_1 = \kappa(\Theta_2 - \Theta_1) \quad (25)$$
$$\ddot{\Theta}_2 + 2\nu\dot{\Theta}_2 + (1+f\Omega^2\cos(\Omega t))\sin\Theta_2 = \kappa(\Theta_1 - \Theta_2) \quad (26)$$

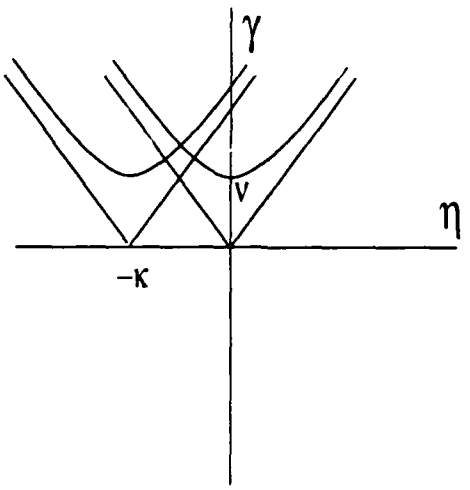

Figure 19: Stability diagram of the two coupled pendulums

where $\Omega = 2(1-\eta)$. Using the sum and the difference of the angles one get the linearized equations

$$\ddot{\Sigma} + 2\nu\dot{\Sigma} + (1+f\Omega^2\cos(\Omega t))\Sigma = 0 \quad (27)$$
$$\ddot{\Delta} + 2\nu\dot{\Delta} + (1+2\kappa)\Delta + f\Omega^2\cos(\Omega t)\Delta = 0 \quad (28)$$

We then look for solutions to these equations of the form

$$\Sigma = Ae^{i(1-\eta)t} + c.c + \cdots \quad (29)$$
$$\Delta = Be^{i(1-\eta)t} + c.c + \cdots \quad (30)$$

The (linear) bifurcations equations (normal form) reads

$$\partial_t A = -\nu A + i\eta A + i\gamma\bar{A} \quad (31)$$
$$\partial_t B = -\nu B + i(\eta+\kappa)B + i\gamma\bar{B} \quad (32)$$

The stability of the rest solution, $A = B = 0$, is straightforward: when the forcing frequency is close to the frequency of the structured mode, the instability leads to a state which breaks the homogeneity of the space (see figure (19)).

A more realistic example of pattern formation is obtained by coupling a large number of such identical pendulums. In the continuous limit the equation for the chain may be written as

$$\ddot{\Theta} + \nu\dot{\Theta} + (1+f\Omega^2\cos(\Omega t))\sin\Theta = c^2\Theta_{xx} \quad (33)$$

where c is a velocity which depends upon the torsion constant and the distance between pendulums. Space now appears explicitely through the second order derivative by respect to x. The homogeneity of space implies the invariance of the equation under the transformation $x \to x + a$ and $x \to -x$. The amplitude of the small oscillation of the chain A is now a function of time and position. It obeys the equation [22]

$$\partial_t A = (\mu + i\delta)A - i\alpha|A|^2 A + i\gamma\bar{A} - i\beta A_{xx} \quad (34)$$

where $\beta = c^2/2$. This equation can be obtained as usual by looking for a solution under the form

$$\theta = Ae^{i(1-\eta)t} + c.c + \cdots$$

When the parameters μ and γ vanish, the equation becomes the well known nonlinear Schoedinger equation [23]. In the case where $\alpha\beta > 0$, (this is the case of our chain of pendula), the homogeneous solution $A = A_0 e^{-i\alpha|A_0|^2 t}$ is unstable with respect to nonhomogeneous perturbations. This instability (self focusing) leads to the formation of solitary structures. In the presence of small forcing and dissipation, patterns can be observed depending upon the detuning parameter δ. The mechanism underlying the formation of patterns can be understood as before in the framework of the linear equations :

$$\partial_t A = (\mu + i\delta)A + i\gamma\bar{A} - i\beta A_{xx} \quad (35)$$

The invariance of this equation under time and space translation which reflects the isotropy of space allows one to look for solution under the form

$$A = A_k e^{\sigma t} e^{iqx}$$

The equation to be satisfied by σ is

$$\sigma^2 - 2\mu\sigma + \mu^2 - \gamma^2 + \eta_q^2 \quad (36)$$

where $\eta_q = \eta + \beta q^2$. Instability sets in when $\sigma_q = 0$. Depending on the forcing frequency (detuning) the instability can amplifly a wave number $q_0 = \sqrt{-\eta/\beta}$ (see figure 20). The wave number is selected by the dispersion relation of the waves that the unforced, undamped chain can sustain $\omega_q = \sqrt{1 + c^2 q^2}/2 \sim 1 + c^2 q^2/2 = 1 + \beta q^2$. The nonlinear analysis allows one to compute the amplitude of the pattern. Close to the pattern forming transition, a solution of equation (34) is looked for of the form

$$A = \mathcal{A}e^{iqx} + c.c + \cdots$$

The equation to be satisfied by $\mathcal{A}$ is a normal form which describes in a universal way the transition to one-dimensional modulated structure [24] [25].

$$\partial_t \mathcal{A} = \epsilon\mathcal{A} + f_{2,1}|\mathcal{A}|^2\mathcal{A} + D\mathcal{A}_{xx} \quad (37)$$

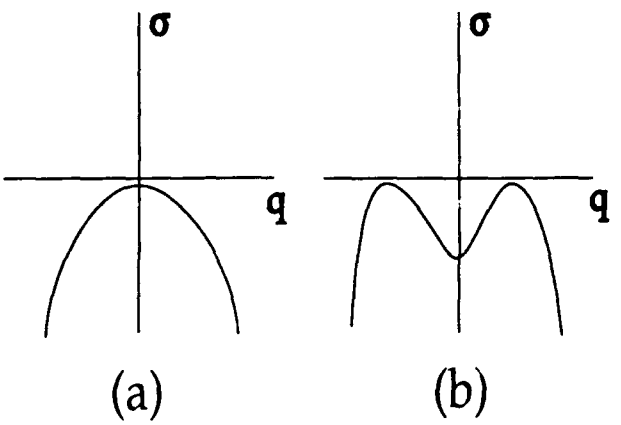

Figure 20: σ_q as a function of q. (a) the most unstable mode has a zero wavenumber (b) the most unstable mode breaks time translations.

where $\epsilon \sim \gamma_c - \gamma$. The equivariance property $\mathcal{A} \to \mathcal{A}e^{i\phi}$ is a direct consequence of the invariance of the physical system described by the equation (34) with respect to space translation. The invariance under space reflection $x \to -x$ implies that the coefficients of the amplitude equation (37) are real numbers. This simple example illustrates many of the features of a real pattern forming system. The Faraday experiment, [26] [27] [29] [28] in which a fluid is submitted to a periodic vertical acceleration, presents strong similarities with our chain of pendula. Above a critical amplitude of the acceleration, patterns form spontaneously at the surface of the fluid. The mechanism of the pattern formation in both cases is related to the dispersive nature of the waves that this kind of system can sustain.

Pattern formation is observed in a wide variety of physical, chemical and biological systems.

- From a purely mathematical point of view, patterns arise as the result of a symmetry breaking bifurcation. The broken symmetry is one of the symmetries imposed by the homogeneity of space and time. The functions $e^{i\vec{q}\cdot\vec{r}}e^{\sigma t}$ are the eigenfunctions of time and space translations. The rotational invariance of the physical space implies that $\sigma_{\vec{q}}$ is a function of the modulus of $\vec{q}$ only, $\sigma_{\vec{q}} = \sigma(q^2)$. The two elementary bifurcations correspond to the crossing of a real eigenvalue (stationary bifurcation) and the crossing of a pair of eigenvalues (Hopf bifurcation) respectively. In the case $\sigma = 0$ the instability does not break time translation. Two cases have to be considered. They depend on the form of σ as a function of q (see figure (20)). In the first case (see figure (20.a)) no breaking of symmetry occurs in the linear theory, while in

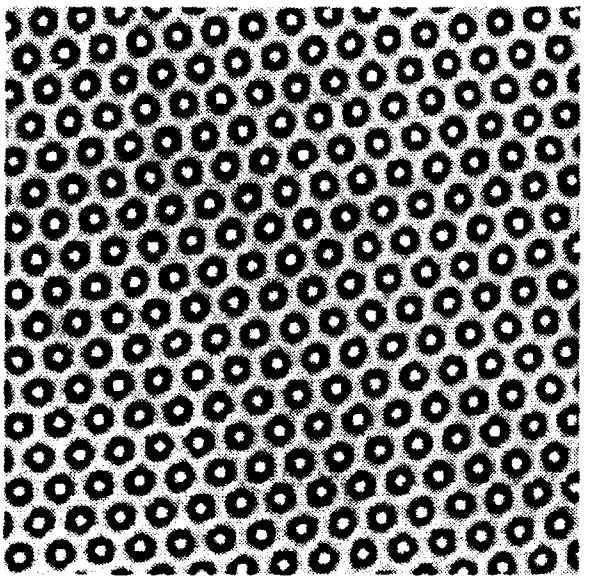

Figure 21: Hexagonal pattern in the two dimensional version of the complex Ginzburg-Landau equation.

the second case, the linear theory selects modes with a finite wave number q_0 (see figure (20.b)). The actual pattern arises as a nonlinear competition between various modes with different orientations. Patterns which only break space translations can be stripes, hexagons [30], squares and more exotic patterns, such as, for example quasi-periodic patterns (see figure (21)). In the case where $\sigma = \pm i\omega$, the instability breaks time translation at the onset. Two cases again have to be considered. They depends on the form of the real part of σ as a function of q (see figure (20) where σ is replaced by its real part). In the first case, no breaking of space translation occurs. It corresponds to homogeneous oscillations in space. In the second case, the instability selects a wavenumber. The corresponding pattern can either be a travelling wave or a standing wave, whatever its spatial strucure (stripes, hexagons, etc..). The selection arises as a nonlinear competition between right and left propagating travelling waves.

- From a physical point of view patterns appear as the result of an instability which selects a particular structured mode [31]. Each pattern forming transition has its own mechanism. In the case of the parametric excitation of a chain of pendula, the forcing which has a well defined frequency picks up a particular wavenumber because of the dispersive nature of the waves that this system can sustain. The Faraday experiment [27] falls into this class. In optics, [32] the transverse section of a coherent beam can exhibit structures which are related to diffraction. In fluid mechanics, the first appearance of a pattern is often associated with an intrinsic characteristic length. The Rayleigh-Benard instability [33], for example, leads to convective cells which have a typical size of the height of the container. In chemical and biological systems instabilities can lead to patterns only because the species involved have different diffusion coefficients. This mechanism is known as the Turing instability [34]. Turing patterns have been observed experimentally only very recently [35] [36].

Acknowledgment: Part of this work has been supported by the CNRS (GDR "Order and Chaos in matter") and the EEC ("Study of Topological Defects in Non-equilibrium Systems"). Some of the numerical simulations presented in this paper have been performed on the Connection Machine of the INRIA at Sophia-Antipolis.

References

[1] Poincare, H., "Methodes Nouvelles de la Mécanique Paris, France, Gauthier Villars, 1892.

[2] Arnold, V.I., "Geometrical Methods in the Theory of Differential Equations", Berlin, Springer-Verlag, 1977.

[3] Swinney, H.L. and Gollub, J.P., "Hydrodynamical and the transition to turbulence", in the serie "Topics 45, Berlin, Springer-Verlag, 1981.

[4] Iooss, G. and Stora, R., "Chaotic Behaviors of Systems", Les Houches, XXXVI, North Holland, 1983.

[5] Takens, F. "Detecting Strange Attractors in Dynamical systems and Turbulence", Eds Rand, D and Sringer-Verlag, 1981.

[6] Procaccia, I. and Grassberger, P., Phys. Lett. 50, 1983.

[7] Roseau, Vibration in Mechanical Systems", in the serie "Analytical Methods and Application", Berlin-Heidelberg-New-York, Sringer-Verlag, 1980.

[8] Eckmann J.P. and Ruelle, D., "Ergodic Theory of and Strange Attractors", Review of Modern Physics, 57, 1985.

[9] Henon, M. "A Two Dimensional Mapping with a Strange Attractor", Com. Math. Phys. 50, 1976.

[10] P.Berge, Y. Pomeau and C. Vidal, "Order within Chaos, Wiley, 1984.

[11] Feigenbaum, M.J., "Quantitative Universality for a Class of Nonlinear Transformation", J. Stat. Phys., 19, 1978.

[12] Coullet, P. and Tresser, C. "Iteration et Groupe de Renomalisation" Journal de Physique, Paris, C5, 1978.

[13] Tresser, C. et Coullet, P., "Iteration d'Endomorphisme et Groupe de Renormalisation C.R. Acad. Sci., Paris, A287, 1978.

[14] Sullivan,. D., "Bounds, Quadratic Differential and Centennial Publication, Vol. 2, Century", Providence, Am. Math. Soc, 1992.

[15] Guckenheimer, J. and Holmes, P. "Nonlinear oscillations, Dynamical systems and Bifurcations of Vector Fields", New-York, Springer, 1983.

[16] Iooss. G., and Joseph., D., "Elementary Stability and Bifurcation Theory", Berlin, Springer-Verlag, 1980.

[17] Golubitsky, M. and Schaeffer,. D. and Group Theory", Vol I, in the serie "Applied 51, New-York, Springer, 1985.

[18] Golubitsky, M., Stewart, I. and Schaeffer,. D. Mathematical Sciences", 6, New-York, Springer, 1988.

[19] Iooss, G. and Aldermeyer, "Topics in Bifurcation Theory and Applications", in the serie "Advanced Series in Nonlinear Dynamics", Vol 3, Word Scientific, 1992.

[20] Coullet, P. and Spiegel, E., "Amplitude Equations for Systems with Competing Instabilities", SIAM J. Appl. Math. 43, 1983.

[21] Elphick, C., Tirapegui, E., Brachet, M.E., Coullet, P. and Iooss, G., "A Simple Global Characterization for Normal Form of Singular Vector Fields", Physica D, 29, 1987.

[22] Coullet, P., Frisch, T. and Sonino, G., "Dispersion Induced Pattern Formation", Nice, France, INLN preprint, 1993.

[23] Zakharov, V.E., Ed, "Wave Collapses", Physica D 52,1991.

[24] Newell, A. C. "Enveloppe Equations", Lecture In Applied mathematics, 15, American Mathematical Society, Providence, R.I. 1974.

[25] Newell, A.A. and Withehead, J.A. "Finite Finite Amplitude Convection", J. Fluid Mech., 38, 1969.

[26] Faraday, M., "On the Form and States Assumed by Fluids in Contact with Vibrating Elastic Surfaces", Phil. Trans. , London, 52, 1831.

[27] Miles, J.W. "Nonlinear Faraday Resonance", J. Fluid Mech. 146, 1984.

[28] Douady, S. and Fauve, S., "Pattern Selection in the Instability", Eur. Phys. Lett., 6, 1988.

[29] Gollub, J.P. and Ramshankas, Spatio-temporal Chaos in Interfacial Waves", in "New Perspectives in Turbulence", Sirovitch Ed., New-York, Springer-Verlag,1991.

[30] Coullet, P. and Emilsson, K. "Strong Resonances of Spatially Distributed Oscillators:a Laboratory to Study Patterns and Defetcs", Physica D, 61, 1992.

[31] Walgraef, D., "Structures Spatiales Loin de l'Equilibre", Paris, Masson, 1988.

[32] Moloney, J. and Newell, A.C., "Nonlinear Optics", Addsison Welsey Reading M.A. 1992.

[33] Normand, C., Pomeau, Y., and Velarde, M. Instability:a Physicist Approach", Review of Modern 49, 1977.

[34] Turing, A.M., "The Chemical Basis of Morphogenesis", Phil. Trans. R. Soc., London, B237, 1952.

[35] Castets, V., Dulos, E., Boissonade, J. and De "Experimental Evidence of a Sustained Standing Turing-Type Chemical Pattern", P., Phys. Rev. Lett., 64, 1990.

[36] Ouyang, Q. and Swinney, H., "Transition from a State to Hexagoanl and Stripped Turing pattern", Nature, 352, 1991.

STABILITY ANALYSIS THROUGH BIFURCATION THEORY (1)

Ph. Guicheteau
ONERA
Boite Postale 72
92322 Chatillon CEDEX
France

1. ABSTRACT

This communication is the first part of the three papers which are presented by the author in the same AGARD Lecture Series (LS 191) [1,2]. It aims at the study of asymptotic solutions of non-linear differential equations depending on parameters. The first part of the communication is devoted to a brief presentation of the basis of Bifurcation Theory which is limited to the non-linear phenomena observed by the author when he has analysed high performance aircraft behaviour. In particular, complex bifurcations and chaotic motions are not treated in this paper. Numerical procedures developed to use results from Bifurcation Theory are presented. Then, some remarks are stated to establish a connection between asymptotic and quasi-stationary behaviour. Finally, a methodology dedicated to the analysis of non-linear systems is proposed.

2. RESUME

Cette communication est la première d'une série de trois présentées par l'auteur dans le cadre de la Lecture Series de l'AGARD (LS 191) [1, 2] dont l'objet est d'aborder l'étude des solutions asymptotiques des systèmes différentiels non linéaires dépendant de paramètres. La première partie de cette communication présente rapidement quelques fondements de la théorie des bifurcations en se limitant aux seuls phénomènes non-linéaires que l'auteur a rencontré au cours de l'étude du comportement des avions très manoeuvrants. En particulier les mouvements chaotiques ne sont pas traités ici. Ensuite, les procédures numériques utilisées pour mettre à profit les résultats provenant de la théorie des bifurcations sont passées en revue. Puis, quelques commentaires sont effectués en vue d'établir une liaison entre le comportement quasi-stationnaire d'un système et son comportement asymptotique. Enfin, une méthodologie d'études des systèmes non linéaires est proposée.

3. INTRODUCTION

In practical situations, non-linear dynamic systems are very frequently simplified or "linearised" at the beginning of their analysis. Unfortunately, such linearised equations do not give a full account of the observed phenomena and only some limited conclusions regarding stability may be reached. . Thus under certain conditions the normal behaviour of dynamic systems which is predictable on the basis of "linearised" theory suddenly gives way to "incomprehensible" behaviours when linearised analysis is no longer valid.

Nevertheless, a careful examination of the observed phenomena in connection with mathematical results on non-linear systems called Bifurcation Theory reveals that, in many cases, these surprising behaviours can be well understood.

This communication is the first part of the three papers which are presented by the author in the same AGARD Lecture Series (LS 191) [1,2].These communications aims at the presentation of non-linear flight dynamics phenomena occurring on high performance aircraft [2]. To achieve this, the first two papers are devoted to the presentation of some theoretical results concerning non-linear dynamic systems. In particular, taking into account the class of non-linear equations encountered in Flight Dynamics, this paper deals with the study of asymptotic solutions of non-linear autonomous differential equations depending on parameters.

Although, a great number of specialised book exists in the literature, the first part of the communication is devoted to a brief presentation of Bifurcation Theory basis. It is limited to the non-linear phenomena which have been observed by the author when he has analysed high performance aircraft behaviour (fixed points, periodic orbits). In particular, complex bifurcations and chaotic motions are not treated here.

As in most practical cases it is not possible to get analytical asymptotic solutions, the second part of the paper is related to the numerical procedures which have been developed to use results from Bifurcation Theory. The construction of equilibrium solutions by means of continuation process is discussed and a review of the available packages is presented.

From a theoretical point of view, parameter variations are assumed fixed an independent of time. When temporal parameter variations are not small, one can observed behaviours which are different from those initially predicted by means of Bifurcation Theory. The following part of the paper is dedicated to a discussion of the connection between asymptotic behaviour and quasi-stationary and/or transient behaviour. These last considerations are closely connected with the attracting basin computation problem which will be treated in the following paper [1].

At the end of the paper, the methodology which has been used to analyse non-linear systems behaviour, especially in Flight Dynamics, is proposed.

4. SOME SIMPLE EXAMPLES OF NON-LINEAR SYSTEMS

Let us consider a set of linear or "linearised" differential equations depending on parameters. It is well known that, for a given value of the parameter, there exists only one solution to the fixed point problem the stability of which is provided by an eigenvalue analysis. Even if the fixed point is unstable, there is only one asymptotic solution when time tends to infinity[1]. As it will be shown in the two following examples, the

[1]If one or several eigenvalues of the system have null real part, one can be noticed that it is possible to transform the initial system in a law dimensional one which exhibits only one asymptotic solution.

situation is more complex when the "linearisation" is not valid and/or when the system is non-linear.

4.1 Riemann-Hugoniot's catastrophe

Let consider the differential scalar equation:

$$\dot{x} = -\left(x^3 + ax + b\right)$$

where x represents the state of the system and (a,b) slowly varying parameters. This equation may be considered as describing the evolution of x in a gradient field the potential of which is defined by equations:

$$\dot{x} = -grad\left(\varphi(x)\right)$$

Consequently, a study on the extrema of $\varphi(x)$ provides information on the stability of the equilibrium states (figure 1).

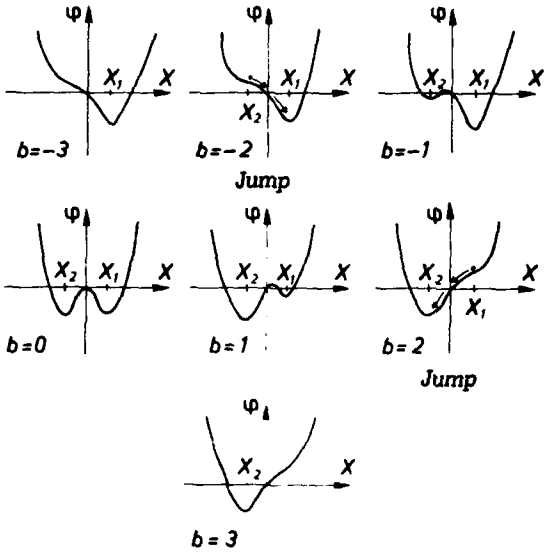

fig. 1 - Riemann-Hugoniot catastrophe: potential function.

$$\varphi(x) = \left(x^4/4\right) + \left(ax^2/2\right) + bx \quad \text{with} \quad a = -3$$

In the (x,a,b) space, the equilibrium manifold (M) is defined as the set of equilibrium points $(\dot{x} = 0)$ and (C) is its projection onto the (a,b) plane (figure 2).

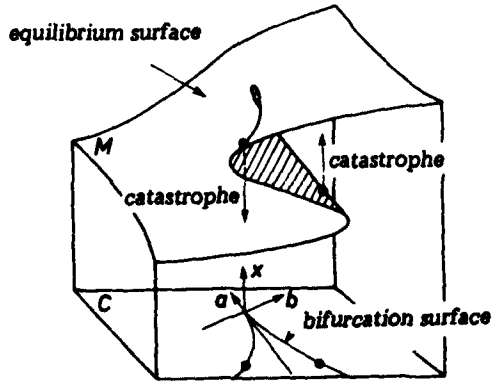

fig. 2 - Riemann-Hugoniot catastrophe: equilibrium manifold and bifurcation surface.

In this plane, (C) is the locus of points so that the equation (1) admits three solutions is within a curve in the form of a cusp

$$a^3/27 + b^2/4 = 0$$

This curve is called a bifurcation surface.

4.2 Hopf's bifurcation

Let consider a 2-dimensional system in polar coordinate (r,θ) with a parameter c :

$$\begin{cases} \dot{\theta} = -1 \\ \dot{r} = r\left(c - r^2\right) \end{cases}$$

where $r^2 = x_1^2 + x_2^2$ and $\theta = Arctg\left(x_2/x_1\right)$. For $c < 0$, only one stable equilibrium solution exists $(r = 0)$. For $c \geq 0$, solution $(r = 0)$ becomes unstable and a new stable solution appears $\left(r = \sqrt{c}\right)$. This latter corresponds to a limit cycle (periodic orbit) the radius of which increases as $\sqrt{c}$ (figure 3).

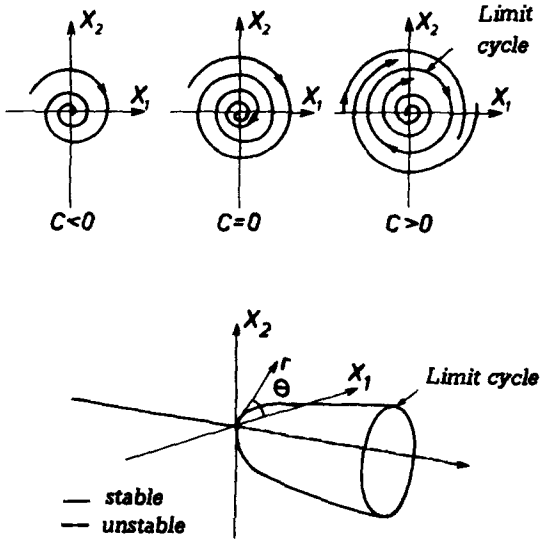

fig. 3 - Hopf's bifurcation. a) Equilibrium solutions as a function of c , b) return to steady state as a function of c .

5. FOUNDATIONS OF BIFURCATION THEORY

The mathematical basis of Bifurcation Theory can be found in a great number of specialised books [3, 4, 5]. Nevertheless, it appears to be essential to present a few aspects of this theory at the beginning of this communication in order to facilitate the understanding of the following chapters. It can be noticed that chaotic motions are not treated here.

5.1 Preliminaries

The present topic is devoted to the behaviour analysis of non-linear autonomous ordinary differential equations depending on parameters.

In the following, we will study system

$$\dot{x} = f(x,\mu) \qquad (1)$$

where x is an n-dimensional vector, μ is an m-dimensional parameter vector and $f: R^n \times R^m \rightarrow R^n$ are n non-linear continuous and differentiable relations.

The equilibrium states provide no information about the transient response of the non-linear system to a parameter variation. Nevertheless, the previous examples show that the computation of fixed points and/or periodic orbits and the characterisation of their stability are essential to analyse the asymptotic behaviour of non-linear equations. In order to achieve this, the Implicit Function Theorem, only for gradient type systems, and the center manifold Theorem which are stated below are two of the most important contributions to Bifurcation Theory.

Implicit Function Theorem: Let $f: R^n \times R^m \to R^n$ be a gradient type system satisfying, for some $\rho_1 > 0$ and $\rho_2 > 0$ sufficently small:

i) $f(x_0, \mu_0) = 0$,

ii) $f_x(x_0, \mu_0) = \left[\partial f(x_0, \mu_0)/\partial x\right]$ has a bounded inverse,

iii) $f(x, \mu)$ and $f_x(x, \mu)$ continuous for $|x - x_0| < \rho_1$ and $|\mu - \mu_0| < \rho_2$.

Then, there exists $x = x(\mu)$ for all $|\mu - \mu_0| < \rho_2$ such that:

a) $x(\mu_0) = x_0$,

b) $f(x(\mu), \mu) = 0$,

c) for $|\mu - \mu_0| < \rho_2$, there is no solution other than $x(\mu)$,

d) $x(\mu)$ is continuous.

This theorem allows conditions under which a non-linear gradient system of equations has a unique solution in a small region around a fixed point.

Many real non-linear autonomous dynamic systems are non gradient type. They can exhibit limit cycles (periodic orbits) when a pair of two conjugate imaginary eigenvalues crosses the imaginary axis under a variation of a parameter. To analyse this new situation one need to generalise the previous results to general system. This is achieved by the Center Manifold Theorem [6].

Center Manifold Theorem for flows: Let f be a C^r vector field on R^n vanishing at the origin $(f(0) = 0)$ and let A the Jacobian matrix at the origin $(A = Df(0))$. Divide the spectrum of A into three parts, $\sigma_s, \sigma_c, \sigma_u$ with

$$\operatorname{Re}\lambda \begin{cases} < 0 & \text{if } \lambda \in \sigma_s, \\ = 0 & \text{if } \lambda \in \sigma_c, \\ > 0 & \text{if } \lambda \in \sigma_u, \end{cases}$$

Let the generalised eigenspaces of σ_s, σ_c and σ_u be E^S, E^C and E^U, respectively. Then there exist C^r stable and unstable manifold W^S and W^U tangent to E^S and E^U at 0 and a C^{r-1} center manifold tangent to E^C at 0. The manifolds W^S, W^U and W^C are all invariant for the flow f. The stable and unstable manifolds are unique, but W^C need not be.

At the bifurcation point the center manifold theorem implies that the bifurcating system is locally topologically equivalent to

$$\begin{aligned} \dot{\tilde{x}} &= \tilde{f}(\tilde{x}) \\ \dot{\tilde{y}} &= -\tilde{y} \qquad \text{with } (\tilde{x}, \tilde{y}, \tilde{z}) \in W^c \times W^s \times W^u \\ \dot{\tilde{z}} &= \tilde{z} \end{aligned} \tag{2}$$

It can be noticed that the essential non-linearities of the original system are described completely by equation 1, and since bifurcations occur only in non-linear systems, the complete bifurcational behaviour can be studied by analysing only the reduced system (2).

From a practical (and partial) point of view, an interesting case occurs when the unstable manifold is empty. We assume that the linear part of the bifurcating system is in block diagonal form:

$$\begin{aligned} \dot{x} &= Bx + f(x, y) \\ \dot{y} &= Cy + g(x, y) \end{aligned} \tag{3}$$

where $(x, y) \in R^n \times R^m$, B and C are $n \times n$ and $n \times n$ matrices whose eigenvalues have, respectively, zero real parts and negative real parts, and f and g vanish, along with their first partial derivatives, at the origin. Then, if we introduce the center manifold in the y=0 space

$$W^c = \{(x, y) : y = h(x)\} \quad \text{with } h(0) = Dh(0) = 0$$

where $h: U \to R^m$ is defined on some neighbourhood $U \subset R^n$ of the origin (figure 4) and if we consider the projection of the vector field on $y = h(x)$ onto E^C one can estimates that

$$\dot{x} = Bx + f(x, h(x)) \tag{4}$$

is a good approximation of (2) restricted to W^C.

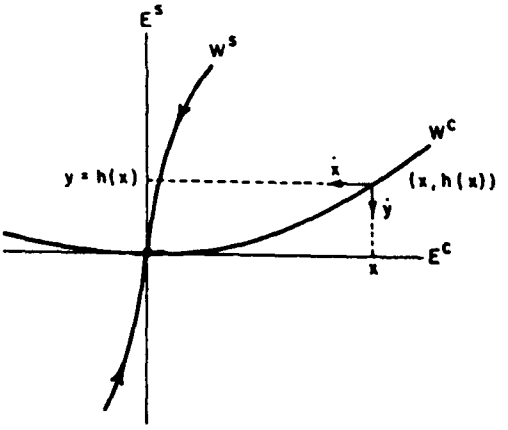

***fig. 4** - The center manifold and the projected vector field.*

From Henry [7]and Carr [8], it follows that $h(x)$ can be approximated arbitrary closely as a Taylor series at $x = 0$ and that the local asymptotic stability or unstability of the original systems is given by the stability properties of equation (4) which can be deduced from the original system by means of the classical projection method [9, 10].

Furthermore, let the original system (3) depends upon a k-vector of parameter (μ)

$$\begin{aligned} \dot{x} &= B_\mu x + f_\mu(x, y) \\ \dot{y} &= C_\mu y + g_\mu(x, y) \\ \dot{\mu} &= 0 \end{aligned}$$

where $(x,y) \in R^n \times R^m$ and $\mu \in R^k$. One can state that, at the origin, the parametrized system has an $n+k$ dimensional center manifold tangent to (x,μ) space, which may be approximated as the power series of the graph $h: R^n \times R^k \rightarrow R^m$. The invariance properties of center manifolds guarantee that any small solutions bifurcating from the origin must lie in any center manifold and thus we may follow the local evolution of bifurcating families of solutions in suspended family of center manifold.

5.2 Bifurcation of fixed points

When assumption ii) of the implicit function theorem does not hold, i. e. a real eigenvalue changes sign, the uniqueness assumptions c) no longer holds and branching solutions, starting from (x_0,μ_0) can appear. The most common situation occurs when the equilibrium curve exhibits a limit point (figure 5). At this point a real eigenvalue must change sign as the parameter is varied and the solution curve is unique.

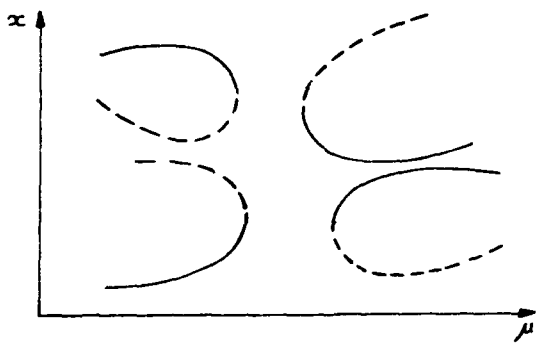

fig. 5 - Limit (regular turning) points;
—— stable solution, - - - - unstable solution.

In fact, considering one of the state variable as a new parameter and the ancient parameter as the missing state variable, it can be noticed that in most practical situations the following inequality is valid[2]:

$$\det\left[\frac{\partial f(x_1,\ldots,x_{i-1},\alpha,x_{i+1},\ldots,x_n)}{(x_1,\ldots,x_{i-1},\alpha,x_{i+1},\ldots,x_n)}\right] \neq 0$$

and the implicit function theorem works.

With the same restrictions than for limit points, the second case is related to double bifurcations points. They are irregular point, i. e. the implicit function theorem does not work, through which pass two and only two equilibrium branches with distinct tangent (figure 6). The stability of the bifurcating branches is given by the following theorem.

Theorem :The stability of such equilibrium curves must change at each regular turning point and at each singular point (which is not a turning point) and only at such points.

Schematically speaking, branching new solutions may occur, in principle in three ways. These situations are called transcritical, supercritical and subcritical bifurcation. Transcritical bifurcation occurs at a bifurcation point (e to h) while supercritical (b, d) and subcritical (a, c) appear at bifurcation-limit points.

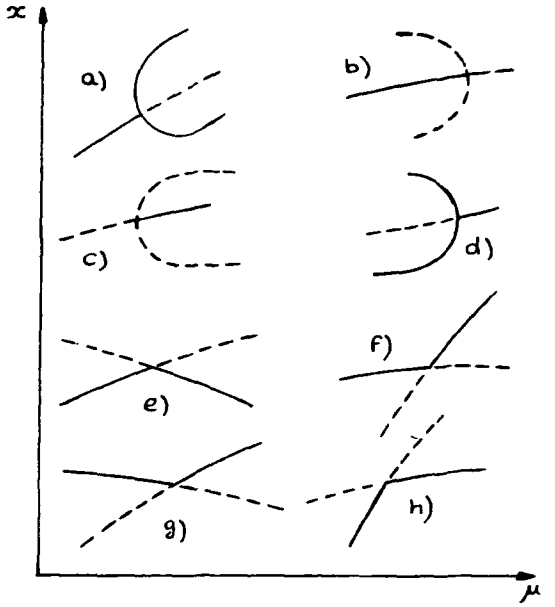

fig. 6 - Double bifurcation points- bifurcation points (a to d), bifurcation-limit (singular turning) points (e to h).
—— stable solution, - - - - unstable solution.

The previous figures are related to one dimensional systems. When the dimension of the system is greater than one, the following cases may be encountered (figure 7).

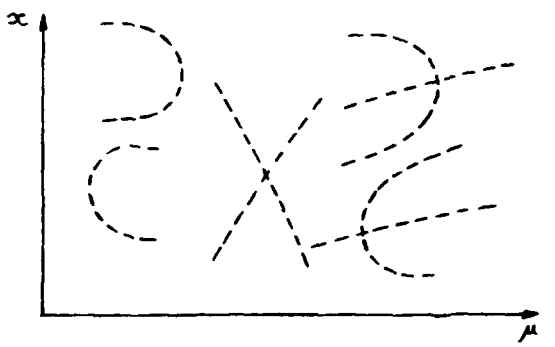

Fig. 7 - possible bifurcation cases when n is greater than 1
—— stable solution, - - - - unstable solution.

Coming back to double point bifurcations, it is of interest to mention that there can exist isolated solutions which may be generated by breaking these bifurcations points under another system parameter variation (different from μ). This problem is known as Imperfect or Perturbed Bifurcation Theory [3, 11].

In Flight Dynamics as in many physical problem, this situation can occur when the non-linear equations possess symmetry properties which are broken by one of the parameters. The following figure shows an illustration of this phenomenon in which the sign of the breaking bifurcation parameter determines the evolution of the initial stable branch beyond

---

[2]Let n=1 and (x^*,α^*) be a regular limit point of $f(x,\alpha)=0$.

Let consider the equation $\tilde{f}=[f(x,\alpha)]^2=0$ which has the same limit point. However, $\partial f/\partial x = 0$ at this point. Thus (x^*,α^*) is irregular for $\tilde{f}$.

the unperturbed bifurcation point and the location of new isolated solutions.

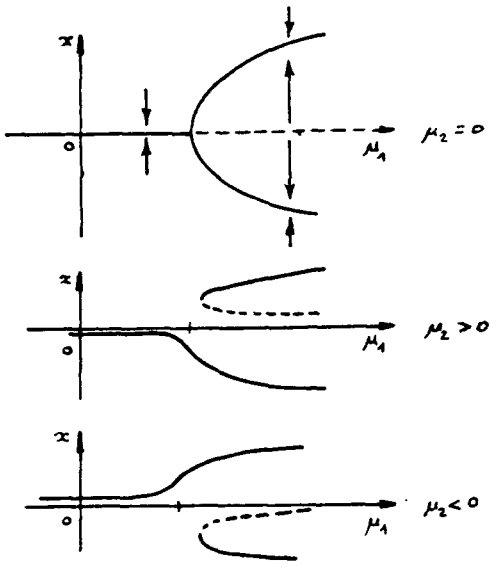

fig. 8 - Imperfect Bifurcation Theory - a) the symmetric problem, b) the asymmetric problem.

To conclude with real bifurcations, one must mention that there exist (rare) cases for which more than one real eigenvalue changes sign at the same equilibrium point. The case in which two eigenvalues vanish at the same point is called the Bogdanov-Takens bifurcation [12].

Coming back to gradient type or locally gradient type systems, it is necessary to mention that the theorem of Elementary Catastrophe proposed by Thom [13]. It classifies all bifurcational behaviour (catastrophes) of finite dimensional gradient systems for up to four parameters. The list of the seven catastrophes which corresponds to bifurcations of codimension ≤ 4 is in the following figure.

Name	Germ	Universal Unfolding	Codimension
(1) The fold	x^3	$x^3 + ux$	1
(2) The cusp (Riemann-Hugoniot)	x^4	$x^4 + ux^2 + vx$	2
(3) The swallow tail	x^5	$x^5 + ux^3 + vx^2 + wx$	3
(4) The butterfly	x^6	$x^6 + ux^4 + vx^3 + wx^2 + tx$	4
(5) The hyperbolic umbilic	$x^3 + y^3$	$x^3 + y^3 + wxy + ux + vy$	3
(6) The elliptic umbilic	$x^3 + 3xy^2$	$x^3 + 3xy^2 + w(x^2 + y^2) + ux + vy$	3
(7) The parabolic umbilic	$x^2y + y^4$	$x^2y + y^4 + wx^2 + ty^2 + ux + vy$	4

fig. 9- Classification of the seven elementary catastrophes.

Apart from this classification, one can notice that, for such a system, the Jacobian matrix describing its linearised approximation is symmetrical and therefore have only real eigenvalues. Moreover, for systems with less than six parameters, no more than two eigenvalues can vanish at the same equilibrium point. Therefore, through the center manifold theorem the complete bifurcational behaviour of these systems can be analysed by studying either a one or a two dimensional system. The exact form of the reduced system depends on the nature of the higher order terms in its Taylor series expansion. One can notice that the first example of § 4 in an illustration of the cusp catastrophe:

Finally, one has to consider the case when two conjugate imaginary eigenvalues cross the imaginary axis as one of the parameters varies while the other eigenvalues remain in the left half plane. Known as Hopf Bifurcation, this situation corresponds to the apparition of closed orbit in addition to the fixed point as stated by the next theorem.

Hopf Bifurcation Theorem: Suppose that the system $\dot{x} = f(x,\mu)$, $x \in R^n$ and $\mu \in R$ has an equilibrium point (x_0,μ_0) at which $f_x(x_0,\mu_0)$ has a simple pair of pure imaginary eigenvalue and no other eigenvalues with a zero real parts. Then, there is a smooth curve of equilibrium points $(x(\mu),\mu)$ with $x(\mu_0) = x_0$. The eigenvalues $\lambda(\mu), \bar{\lambda}(\mu)$ of $f_x(x_0,\mu_0)$ which are pure imaginary at $\mu = \mu_0$ $(\lambda(\mu), \bar{\lambda}(\mu) = \pm i\omega)$ vary smoothly with μ. If, moreover,

$$\left(\frac{d\left(\mathrm{Re}(\lambda(\mu))\right)}{d\mu}\right)_{\mu=\mu_0} = d \neq 0$$

then there is a unique three-dimensional center manifold passing through (x_0,μ_0) in $R^n \times R$ and a smooth system of coordinates (preserving the planes μ =const.) for which the Taylor expansion of degree 3 on the center manifold is given by

$$\dot{\tilde{x}}_1 = \left(d\mu + a\left(\tilde{x}_1^2 + \tilde{x}_2^2\right)\right)\tilde{x}_1 - \left(\omega + c\mu + b\left(\tilde{x}_1^2 + \tilde{x}_2^2\right)\right)\tilde{x}_2$$

$$\dot{\tilde{x}}_2 = \left(\omega + c\mu + b\left(\tilde{x}_1^2 + \tilde{x}_2^2\right)\right)\tilde{x}_2 + \left(d\mu + a\left(\tilde{x}_1^2 + \tilde{x}_2^2\right)\right)\tilde{x}_1$$

which is expressed in polar coordinates as

$$\dot{r} = \left(d\mu + ar^2\right)r \qquad (5)$$

$$\dot{\theta} = \left(\omega + c\mu + br^2\right)$$

If $a \neq 0$, there is a surface of periodic solutions in the center manifold which has quadratic tangency with the eigenspace $\lambda(\mu_0), \bar{\lambda}(\mu_0)$ agreeing to second order with the paraboloid $\mu = -ar^2/d$. If $a < 0$, the bifurcation is supercritical and these periodic solutions are stable limit cycles, while if $a > 0$, the bifurcation is subcritical and the periodic solutions are unstable limit cycle (figure 10).

For an observer, the system behaviour is very different in the two Hopf Bifurcation situations. Crossing a subcritical Hopf Bifurcation leads to a smooth divergence to a limit cycle with a small amplitude. Moreover, this divergence disappears if the parameter value comes back to its initial value. When the bifurcation is supercritical a sudden and violent divergence can be exhibited by the system. In the most simple cases, this situation may lead to a stable periodic orbit with a great amplitude. The return to the previous "quiet" situation can be problematic because of an hysterisis effect of the orbits to parameter variations which is very similar to the phenomenon observed in the Riemann-Hugoniot's catastrophe for fixed points (§ 4.1).

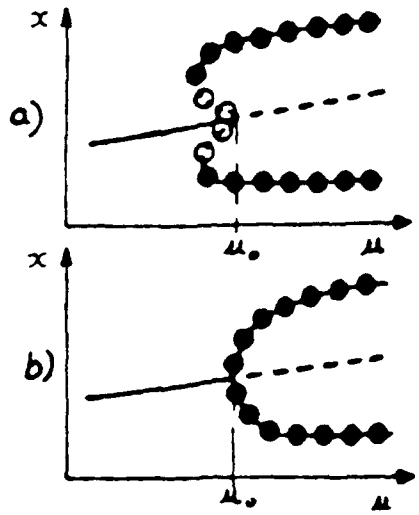

fig. 10- Hopf bifurcation. a) subcritical, b) supercritical

Coming back to (5), one can note that these equations are invariant under the symmetry $(r,\theta)\rightarrow(-r,-\theta)$. So, carrying the normal form of the Hopf bifurcation up to the fifth order and replacing the third order coefficients (a) by a variable parameter (μ_2), it is then possible to study the generalised Hopf bifurcation singularity with the radial part:

$$\dot{r} = a_3 r^3 + O(r^7)$$

by independently varying the coefficients μ_1 and μ_2 [3]. Apart from the standard Hopf bifurcation point, a second bifurcation set is the semi parabola:

$$\mu_2^2 = 4a_2\mu_1 \qquad with \quad \mu_2/a_2 < 0$$

on which a pair of closed orbits, one an attractor and the other a repeller, coalesce and vanish (figure 11).

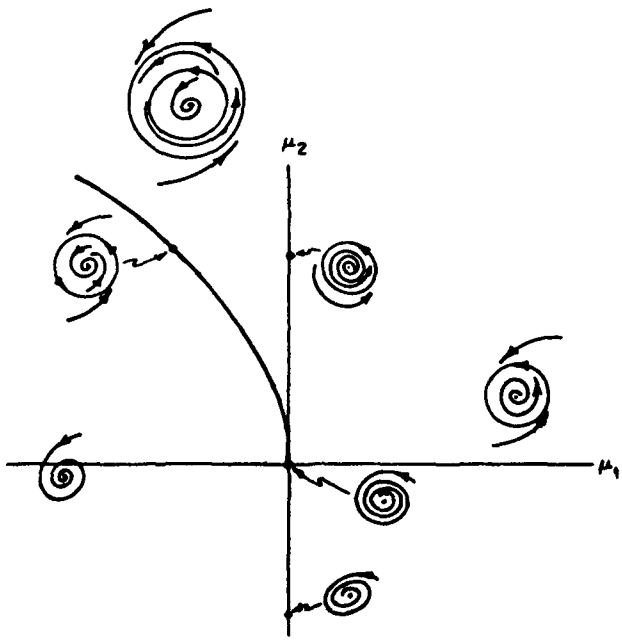

fig. 11 - The generalised Hopf bifurcation, $a_3 < 0$ case.

Although it seems to be very rare in Flight Dynamics, it is of interest to consider the case bifurcation point for which there are two conjugate pure eigenvalues in addition to a null real eigenvalue. This case is known as the Gavrilov-Guckenheimer bifurcation for which the normal form is given by the following equations in cylindrical polar coordinates:

$$\dot{r} = a_1 rz + a_2 r^3 + a_3 rz^2 + O(|r,z|^4)$$

$$\dot{z} = b_1 r^2 + b_2 z^2 + b_3 r^2 z + b_4 z^3 + O(|r,z|^4)$$

$$\dot{\theta} = \omega + O(|r,z|^2)$$

Considering the interaction between the Hopf bifurcation and the various real bifurcation point one can find additional bifurcations of periodic orbits from non trivial branches and additional bifurcations giving rise to three dimensional dynamics such as invariant tori [5, 14].

5.3 Stability of periodic solutions

There are two ways to determine the stability of closed orbit. The first is the classical Floquet Theory, the second comes from the use of Poincaré Maps. Although these two methods lead to the same results, the last one is a more geometrical approach.

Let γ be a periodic solution of some flow Φ_t in R^n arising from a non-linear vector field $f(x)$. Let $\Sigma \subset R^n$ be a local cross section of dimension n-1 to which the flow is everywhere transverse. Let p be the unique[3] point where γ intersects and let $U \subseteq \Sigma$ be a neighbourhood of p.

For a point $q \in U$, the Poincaré map or first return $P: U \rightarrow \Sigma$ is defined by

$$P(q) = \Phi_\tau(q)$$

where $\tau = \tau(q)$ is the time taken for the orbit $\Phi_t(q)$ to first return to Σ (figure 12). Generally, τ depends on q and need not to be equal to the period (T) of γ however $\tau \rightarrow T$ as $q \rightarrow p$.

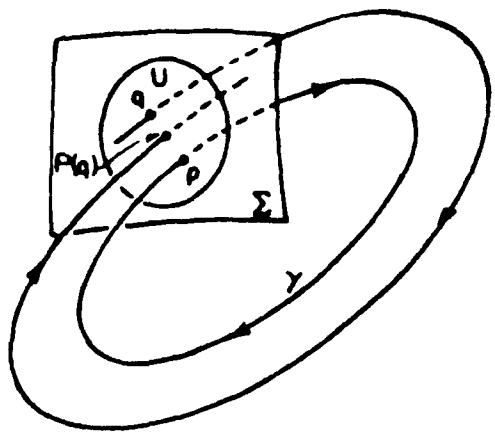

fig. 12 - The Poincaré map.

[3] If γ has multiple intersections with Σ, then shrink Σ until there is only one intersection.

It can be noticed that p is a fixed point for the map P and that the stability of p for P reflects the stability γ for the flow Φ_t. Moreover, considering P as a (n-1) discrete time system, stability or instability of the orbit is given by the situation of the (n-1) eigenvalues of the linearised map to the unit circle.

Coming back to Floquet Theory, the stability of γ is determined by the eigenvalues (Floquet multipliers) of the following matrix

$$H = \left[\frac{\partial \int_0^T f(x,\tau)d\tau}{\partial x} \right]$$

which is a representation of a particular fundamental solution matrix e^{TR}, where R is a $n \times n$ matrix, of the system. From a practical point of view, H can be obtained by generating a set of n linearly independent perturbed solutions of $f(x)$.

Considering the particular form of the fundamental solution matrix, it can be noticed that the multiplier associated with perturbations along γ is always unity while the module of the remaining $(n-1)$, if none are unity, determine the stability of the orbit.

Finally, one can noticed that the $(n-1 \times n-1)$ matrix of the previous linearised Poincaré map is also a representation of the fundamental solution matrix by suppressing all the elements coming from perturbations along γ.

5.4 Bifurcation from periodic orbit

The stability of periodic solutions may change with the variations of system parameters; one or two multipliers can move outside the unit circle.

The Bifurcation Theory for fixed point with eigenvalue 1 is completely analogous to the Bifurcation Theory for equilibria with eigenvalue 0. The typical case corresponds to a limit point along the dependence curve of periodic solutions on a parameter (figure 13). However, one may encounter more complicated behaviour of periodic solution branches in the neighbourhood of the bifurcation point when there is an inherent symmetry.

The second case occurs when one multiplier crosses through the unit circle at -1. This bifurcation do not have an analogue for equilibria. In the literature, this bifurcation is refereed as "Brunovsky bifurcation", "flip bifurcation", "period doubling bifurcation" or "subharmonic bifurcation". At this point, the originally stable periodic solution becomes unstable and a branch of periodic solutions with a two fold period branches off (figure 13).

Multipliers on the new branch are equal to the square of the original multipliers. With respect to the orientation of the parameter variation, the branching can be either supercritical or subcritical. If the original branch of periodic solution is unstable, the new branch will also be unstable. Moreover, the period doubling bifurcation often occurs repeatedly leading to complex orbit associated to very long period.

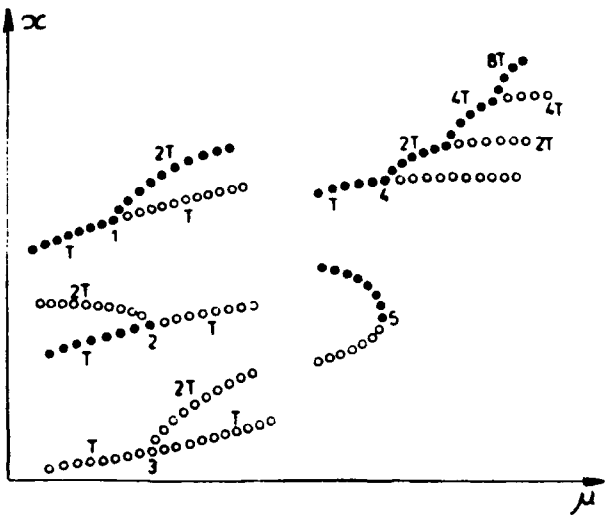

fig. 13 - limit point and period doubling bifurcation. ●●●● stable and 0000 unstable periodic orbits a) periodic limit orbit, b) supercritical -1 bifurcation, c) subcritical -1 bifurcation, d) -1 bifurcation from an unstable branch, e) repeated -1 bifurcations

The last type of bifurcation from the branch of periodic solutions occurs when two complex conjugate eigenvalues intersect the unit circle. At this point, the originally stable branch of periodic solutions becomes unstable and a stable or unstable torus may appear (figure 14).

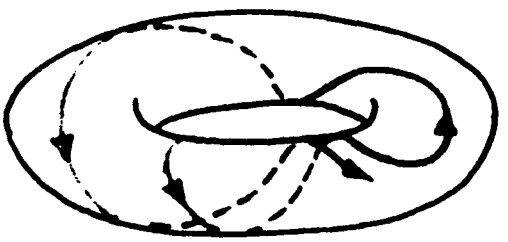

fig. 14 - "Complex" bifurcation.

Analogy with Hopf bifurcation suggests that orbits near the bifurcation will be present and will encircle the fixed point of the Poincaré map. As an individual orbit of a discrete mapping cannot fill an entire circle, the bifurcation structure is much more complicated than that which can be deduced from a search of periodic orbit. Indeed, there are flows near the bifurcation which have no periodic orbits near the bifurcating one but have quasi periodic orbits instead.

As for fixed point, one have to mention that there exist cases in which several eigenvalues cross the unit circle at the same parameter value. This leads to complex phenomena which will not presented in this paper. See [5].

6. NUMERICAL PROCEDURES

During the past ten or fifteen years many method have been suggested for the numerical solution of non-linear problems. This includes, in particular, the solution of parameter dependant non-linear equations by continuation techniques and the related methods for bifurcation and stability analysis. In an alphabetical order, and without claiming completeness, we list

some relevant available packages: ALCON [15], ASDOBI [16], AUTO [17], BIFPACK [18], BISTAB [19], CONEX [20], CONKUB [21], CONSOL [22], HOMPACK [23], LINLBF [24], PATH [25], PITCON [26], PLTMG [27], Some of these codes are in the nature of packages that deal with several aspects of the problem while others concentrate only on specific aspects. However all these codes are based on continuation methods.

6.1 Continuation methods [28]

Continuation methods are a direct result of the implicit function theorem which states that if the Jacobian of a non-linear system at a fixed point (x_0,μ_0) is non-singular, then there exist a unique curve of fixed points containing the known fixed point Although this result is only valid in a small region around the fixed point, the curve of fixed points can be extended by applying the implicit function theorem at a fixed point near the end of the curve known to exist through (x_0,μ_0).

When the Jacobian is singular, the continuation process fails and must be modified. The modification consists in taking the arc length of the solution curve (s) as a parameter to continue the equilibrium curve in the $(n+1)$ dimensional space as follows.

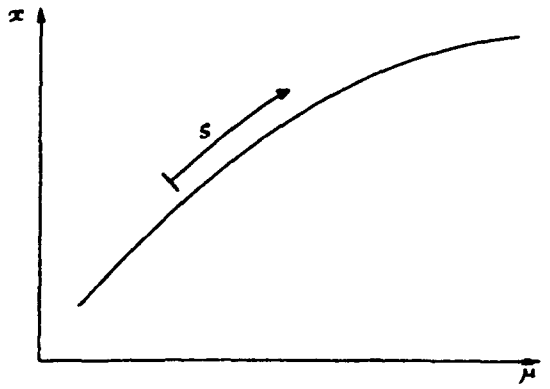

fig. 15 - Continuation principle.

Introducing the arc length with the following equation

$$\left(\frac{dx_1}{ds}\right)^2+\cdots+\left(\frac{dx_n}{ds}\right)^2+\left(\frac{d\alpha}{ds}\right)^2=1 \qquad (6)$$

and differenting () with respect to arc length, we obtain a system of n linear algebraic equations in n+1 unknowns:

$$\frac{df_i}{ds}=\sum_{j=1}^{n}\frac{\partial f_i}{\partial x_j}\frac{dx_j}{ds}+\frac{\partial f_i}{\partial \mu}\frac{d\mu}{ds}=0 \qquad (i=1,\cdots,n) \qquad (7)$$

Let us assume that the matrix is regular for certain values s and k. Then, the equation can be solved in the form

$$\frac{dx_i}{ds}=\beta_i\frac{dx_k}{ds}, \qquad i=1,2,\cdots,k-1,k+1,\cdots,n+1 \qquad (8)$$

in which the coefficients β_i can be carried out by means of Gauss elimination.

Now, if we introduce (8) in (6), we get the relation

$$\left(\frac{dx_k}{ds}\right)^2\left(1+\sum_{\substack{i=1\\ i\neq k}}^{n+1}\beta_i^2\right)=1.$$

in which the sign of the derivative dx_k/ds is given by the orientation of the parameter s along the curve. So, the other derivatives are computed from (8) and the system of differential equations (7) can be solved by any numerical technique for the integration of initial value problem.

As the errors of approximation accumulate during integration and the computed solution deviates from the correct solution, i., e., equilibrium curve, it is necessary to improve the accuracy of the obtained solution by means of Newton's method applied to (7) with a fixed value of x_k.

6.2 Remarks

It can be noticed that this continuation process allows the computation of the various bifurcation points. This is achieved by introducing additional "bifurcation functions" to the original system. As an example, a curve of limit points is determined by the solutions of the new system:

$$f(x,\mu_1,\mu_2)=0$$

$$\det\left[\frac{\partial f}{\partial x}\right]=0$$

The reader is invited to see [28] for other bifurcation functions.

Another interesting case is the computation of the periodic orbits envelope. Two different approaches are generally encountered. In the first, the periodic orbit is considered as the solution of a classical boundary value problem for partial equations. Rather than considering the entire orbit, the Poincaré map is used in the second. It leads to the computation of fixed point. The difference between these two approaches is the dimension of the resulting set of algebraic equations to be solved. It can be noticed that the second approach gives a low dimensional set of equations compared with the first one.

Finally, it can be noticed that continuation requires the evaluation of the system and the computation of partial derivatives which can be very time consuming. Thus, there is a need to improve performance of such codes in order to get almost interactive procedures even for high dimensional non-linear systems.

7. QUASI-STATIONARY AND TRANSIENT BEHAVIOUR

Up until now, it has been considered that the value of the parameter μ is fixed and independent of time. In many practical situations it is not the case and the system exhibits quasi-stationary behaviours and transient motions; the difference between these two evolutions is the value of parameter change over time. If it is slow in comparison to changes of states variables, quasi-stationary behaviour is observable. There are at least two situations to be considered:

a) movement along a stable branch,
b) movement through bifurcation points.

In the first situation, Douglas and al [29] shows that if the system has a stable manifold and fixed points corresponding to constant inputs, then an initial state close to this manifold and a slowly varying input signal, in an average, sense produce a trajectory that remains close to the manifold.

The second situations leads to different behaviour regarding the nature of the bifurcation point encountered. As an illustration, the following figure shows possible situations.

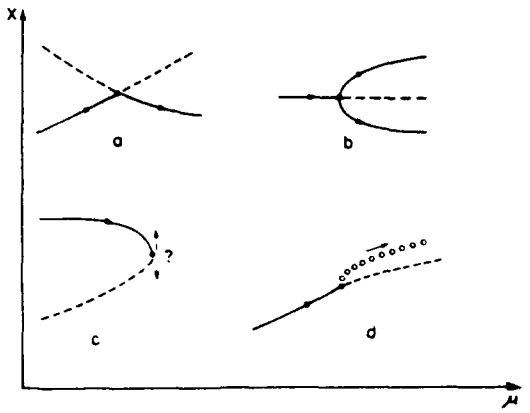

fig 16 - Examples of possible crossing f bifurcation and limit points during quasi-stationary behaviour.

Case a) corresponds to a simple bifurcation point. A solution continues after the bifurcation point along a stable branch. In case b), where the bifurcation is also a limit point, the branch on which the solution continues is chosen at random. In real problems, the problem has to be formulated statistically; the character of distribution of fluctuations of state variables determines the probability of the choice of individual branches of solutions. Case c) is a very interesting one because after crossing the limit point the system evolves into the closest stable state, i., e., a state in whose domain of attraction the limit point belongs. This new notion will be treated in [1]. The last case (d) corresponds to the Hopf bifurcation. Generally the apparition of the stable periodic orbit seems to be delayed and the low amplitude solution around the bifurcation point is unobservable [30].

8 METHODOLOGY

In many real problem as in Flight Dynamics, one has to deal with high dimensional sets of equations in which the parameter cannot always be considered as independent of time. Then it is necessary to set up a methodology to investigate non-linear behaviours.

The first step is to compute all the steady solutions of the system and their associated stability. As this step is generally time consuming the computations are limited to the field of interest. Nevertheless one must be very careful because, the number of steady solutions for a given parameter in generally not known.

The second step consists in making graphic representations of the results in appropriate subspaces especially if the dimension of the system is greater then 3. This step requires versatile graphic codes and a good experience of the system under consideration. Sometimes this step shows that equilibrium branches miss.

The third step is concerned with the prediction of the system behaviour when a bifurcation point is encountered. To achieved this, the computation of the attracting domain of the stable steady states and, once more, the experience of the engineer are very useful to investigate the various possibilities.

Experience acquired by the processing of a large number of case is extremely valuable for correctly predicting the system behaviour. Thanks to this experience, it is not always necessary to check the predictions by means of numerical simulations . But for the difficult cases and if there is any doubt, the last step of the methodology consists in performing only a few numerical simulations before testing the predictions on the real system.

CONCLUSION

This paper is the first part of the three communications which are presented in the Agard Lectures Series (LS 191) which are devoted to a presentation of non-linear phenomena observed on high performance combat aircraft. More generally we are concerned with the asymptotic behaviour of non-linear differential equations depending on parameters.

After introducing the reader to non-linear dynamics by means of simple example, the main part of this paper is related to a brief presentation of Bifurcation Theory for ordinary differential equations. This presentation has been limited to the lonely non-linear phenomena encountered by the author in the Flight Dynamics domain. Nevertheless basic theorems, bifurcation of fixed points and periodic orbits have been described.

In order to compute the bifurcational behaviours, the basis of numerical procedures have been discussed and a list (not exhaustive) of available numerical code have been given to the reader. Then, a methodology which has been set up to investigate the behaviour of high performance aircraft is proposed.

In many real problem, the parameter are fixed and independent of time. It may follow transient motions or/and quasi-stationary behaviours. In spite of the difficulty of this problem which is connected to the computation of the attracting domain of stable steady state treated in the next paper [1], some typical examples are given in the last part of the paper.

REFERENCES

1. Guicheteau, P., "Stability analysis through Bifurcation theory (2)", AGARD LS191, 1993.

2. Guicheteau, P., "Non-linear Flight Dynamics", AGARD LS191, 1993.

3. Ioos, G., and Joseph, D., D, "Elementary Stability and Bifurcation Theory", Springer Verlag, 1981.

4. Marsden, J., E., and Mc Cracken, M., "The Hopf Bifurcation and its Applications", Springer Verlag, 1976.

5. Guckenheimer, J., and Holmes, P., "Nonlinear Oscillations, Dynamical systems and Bifurcations of Vector Fields", Springer Verlag, 1983.

6. Kelley, A., "The stable, center stable, center, center unstable and unstable manifolds", *in* J. Diff. Eqns., Vol 3, 1967.

7. Henry, D., "Geometric Theory of Semilinear Parabolic Equations", Springer Lectures Notes in Mathematics, Vol 840, Springer Verlag, 1981.

8. Carr, J., "Applications of Center Manifold Theory", Springer Verlag, 1981.

9. Cochran, J., E. and Ho, C., S., "Stability of aircraft motion in critical cases", J. of aircraft, 1983.

10. Guicheteau, P., "Etude du comportement transitoire d'un avion au voisinage de points de bifurcations" *in* "Unsteady Aerodynamics - Fundementals and Application to Aircraft Dynamics", AGARD CP 386, 1985.

11. Keener, J., P., and Keller, H., B., "Perturbed Bifurcation Theory", Arch. Rational Mech. Anal., Vol. 50, 1973.

12. Bogdanov, R., I., "Funct. Anal. Appl., vol. 9, 1975..

13. Thom, R., "Stabilité structurelle et morphogénèse", Ediscience, Paris, 1972.

14. Langford, W., F., "A review of interactions of Hopf and steady state bifurcations" *in* "Nonlinear Dynamics and Turbulence", Pitman Advanced Publishing Program, 1983.

15. Deuflhard, P., Fiedler, B. and Kunkel, P., "Efficient numerical path following beyond critical points", SIAM J. Num. Anal., Vol 24, 1987.

16. Guicheteau, P., "Notice d'utilisation du code ASDOBI", Pre-print ONERA, 1992.

17. Doedel, E. and Kernevez, J., P., "AUTO: Software for continuation and bifurcation problems in ordinary differential equations", California Institute of Technology, Pasadena, 1986.

18. Seydel, R., "BIFPACK: a program package for continuation, bifurcation and stability analysis", University at Würzburg, 1989.

19. Wood, E., F., Kempf, J., A. and Mehra, R., K., "BISTAB: A portable bifurcation and stability analysis package", Appl. Math. Comp., Vol 15, 1984.

20. Rosendorf, P., Orsag, J., Schreiber, I. and Marek, M., "Interactive system for studies in non-linear dynamics" *in* Continuation and bifurcations: numerical techniques and applications, NATO ASI Series, Vlo 313, Kluwer Academic Publishers, 1990.

21. Meija, R., "CONKUB: A conversational path-following for systems of non-linear equations", J. of Comp. Physics, Vol. 63, 1986.

22. Morgan, A., "Solving polynomial systems using continuation", Prentice Hall, Englewood, 1987.

23. Watson, L., T., Billups, S., C. and Morgan A., "HOMEPACK: A suite of codes for globally convergent homotopy algorithms", ACM transactions on Math. Software, Vol 13, 1987.

24. Khibnik, A., I., "LINLBF: A program for continuation and bifurcation analysis of equilibria up to codimension three" *in* Continuation and bifurcations: numerical techniques and applications, NATO ASI Series, Vol. 313, Kluwer Academic Publishers, 1990.

25. Kass-Petersen, C., "PATH: Users's guide", University at Leeds, Centre for non-linear studies, 1987.

26. Rheinboldt, W., C. and Buckardt, J., "A locally parametrized continuation process", ACM on Transactions of Math. Software, Vol. 9, 1983.

27. Bank, R., E., "PLTMG User's guide - Edition 5.0", University of California, La Jolla, 1988.

28. Kubicek, M. and Marek, M., "Computational Methods in Bifurcation Theory and Dissipative structures", Springer Verlag, New York, 1983.

29. Douglas, A., L. and Rugh, W., J., "On a stability theorem for non-linear systems with slowly varying inputs", IEEE trans. on Auto. Control, Vol. 35, N° 7, 1990.

30. Neishtadt, A., I., "Persistence of stability loss for differential equations", Differential'ne Uravneniya, Vol. 23,1987.

STABILITY ANALYSIS THROUGH BIFURCATION THEORY (2)

Ph. Guicheteau
ONERA
Boite Postale 72
92322 Chatillon CEDEX
France

1. ABSTRACT

This communication follows [1] which was presented in the same Agard Lecture Series (LS 191). In the previous communication, some theoretical foundations of Bifurcation Theory have been recalled and a methodology aiming at a systematic prediction of the behaviour of non-linear differential equations has been presented. This communication mentions some problems which are connected with the introduction of control laws in order to stabilise an unstable dynamic system and presents a brief state of the art related to the determination of the attracting region of a stable equilibrium point.

2. RESUME

Cette communication est la suite de [1], présentée dans le même cadre de la Lecture Series 191 de l'Agard, dans laquelle des bases de la théorie de bifurcations des systèmes différentiels non linéaires ont été rappelées et une méthodologie visant à prédire le comportement des systèmes dynamiques a été présentée. Cette communication évoque quelques problèmes liés à l'utilisation de lois de commande pour stabiliser des systèmes instables en boucle ouverte et fait une revue des méthodes employées pour déterminer la région d'attraction d'un point d'équilibre stable d'un système différentiel non linéaire.

3. INTRODUCTION

It is now well known that Bifurcation Theory can be of help for the prediction of the asymptotic behaviour of non-linear differential equations depending on parameter [1]. Efficient numerical procedures are now available and a number of previous studies have demonstrated that Bifurcation Analysis can be used to predict complex phenomena.

In practical situations non-linearities are numerous either in the dynamic system or in its control laws. Rather than detailing non-linear control theory, the first purpose of this communication is to show that, without invoking complex phenomena, it can be very instructive to introduce Bifurcation Analysis while designing control laws in order to exhibit basic non-linear effects without performing extensive numerical simulations.

Some objectives of control laws are to stabilise unstable systems and/or to increase their robustnesses under system modifications and under perturbations. The robustness of a stable steady state is closely related to its attracting region.

The other purpose of this communication is to present a review of the methods employed to compute the attracting basin of a stable equilibrium state. Starting with the stability theory proposed by Liapounov, the review describes the different fields of research actually investigated to compute either the stability region or its boundary for low and high dimensional non-linear dynamic systems.

4. SOME REMARKS ABOUT CONTROL PROBLEM

As opposed to many theoretical approaches, practical control laws are generally non-linear because of their formulation or the use of non-linear elements. Then, it is interesting to investigate if the methodology proposed in [1] can help the designer to design "good" control laws from a stability point of view. More precisely, one must answer the following question: can "stabilising" control laws introduce new bifurcations while they are used to "stabilise" the open loop system?

Without invoking Bifurcation Theory, these control problems are studied and, fortunately, "good" solutions have been found in many particular cases. An amount of results is already available in the literature (see [2] among others).

In this chapter, we are concerned with an autonomous dynamic system:

$$\dot{x}(t) = f(x(t), u(t)) \qquad (1)$$

where x and u denote state and control vectors respectively. f and x are n-dimensional vectors, u is m-dimensional vector and $f(x(t), u(t))$ are non-linear functions satisfying Lipschitz conditions.

As opposite to [1] in which u does not usually depend on x and t, here we assume that u depends on the state variables in the following way:

$$u(t) = g(x(t), p) \qquad (2)$$

where p are new control parameters and $g(x(t), p)$ are non-linear functions satisfying Lipschitz conditions.

From the definition of the control vector (2), it follows that every equilibrium point of the open loop system (1) is also an equilibrium point of the closed loop system and vice versa. However, the stability of the closed loop solutions can differ from the stability of the open loop solutions and new complex asymptotic solutions may appear.

In order to precise these phenomena, let us consider two cases:

a) a linear control law applied to a non-linear system,
b) a non-linear control law applied to a linear system.

4.1 Linear control law [3]

The non-linear dynamic system described motion equations of an F-15 fighter mathematical model. The control law is a linear 3-axis control augmentation system (CAS) for a given angle of attack:

$$u = kx$$

where k is a gain matrix. This control law has been designed, among other, to delay and suppress wing rock at angle of attack greater than 20°.

When lateral control deflection are at neutral and considering gains as new parameters in the continuation process described in [1], it is possible to investigate their influence on Hopf bifurcation at zero sideslip angle (figure 1) and to show that this influence is not linear. Further more, beyond a particular value of the gain (k_i), the stable equilibrium domain decreases.

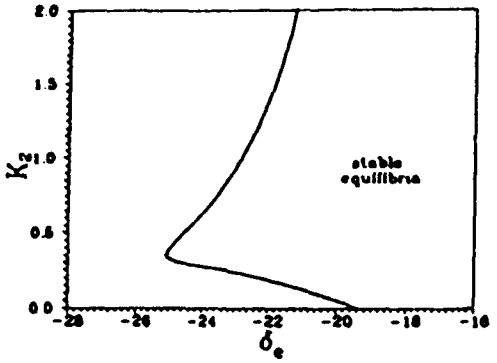

fig. 1 - Evolution of the limit of stability of the Dutch roll mode as a function of elevator deflection and control gain.

Beyond the new stability limit for the controlled aircraft, one can see the influence of the gains on the existence and on the stability of periodic orbits which are considered as wing rock (figure 2) thus helping to understand aircraft behaviour.

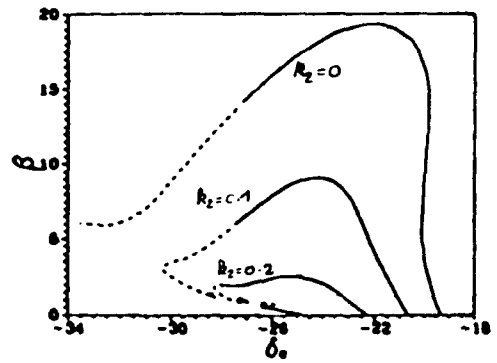

fig . 2 - Maximum amplitude of periodic orbits as a function of elevator deflection and control gain.

4.2 Non-linear control laws

In practical situations, non-linearities are numerous in control laws. They can be introduce by the designer to solve specific control problem (non-linear behaviour for a linear system, "linearisation" of a non-linear systems, ...). They appear also because non-linear elements are present (saturation, stop, hysterisis, ...). In spite of the numerous previous works in which Bifurcation Theory is used to solve control problems [4,5,6,7], the following example shows that the methodology proposed in [1] can be used to predict the robustness of the controlled system under perturbations.

Let an unstable second order linear differential equation be stabilised by a control law which depends on a non-linear element as it is described on figure 3.

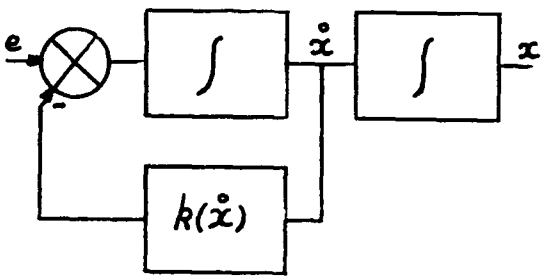

fig . 3 - Controlled unstable second order dynamic system.

A linearised analysis of the closed loop system

$$\ddot{x}+\left(2\zeta_0\omega_0+\frac{\partial k(\dot{x})}{\partial \dot{x}}\right)\dot{x}+\omega_0^2 x=e$$

shows the influence of the gain on the stability of the asymptotic solution. When $(\partial k(\dot{x})/\partial \dot{x})$ goes from zero to the adopted value k^* for the closed loop system, it crosses a value k^c for which the steady state admits two conjugate pure imaginary eigenvalues.

From a non-linear point of view, one can say that there is a Hopf bifurcation in k^c. Moreover, let $k(\dot{x})$ a non-linear gain in the following form:

$$k(\dot{x})=\frac{2}{\pi}k(\dot{x})_{lim}\,arctg\frac{k\pi\dot{x}}{2k(\dot{x})_{lim}}$$

i. e. the feedback is almost linear $(k(\dot{x})\cong k)$ in the vicinity of the equilibrium points and is saturated $(k(\dot{x})\cong k(\dot{x})_{lim})$ when $\dot{x}$ tends to infinity. Then, one can easily show that the Hopf bifurcation is sub critical. Thus, when k is greater than k^c, periodic orbits surround the stabilised equilibrium points. These orbits can exist even for the adopted gains value k^* (figure 4).

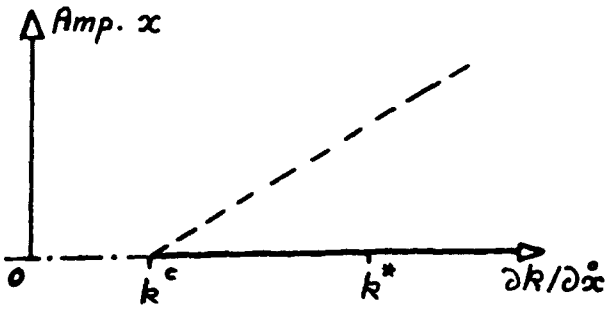

fig. 4 - Amplitude of the steady solutions as a function of the non-linear control gain.
—— stable, - - - - unstable, --*- oscillatory unstable.*

In this 2-dimensional case, the unstable periodic orbit envelope visualises the boundary of the attracting region of the controlled system. As an example, if the amplitude of a perturbation is greater then the amplitude of the periodic orbit, the controlled system exhibits a divergence.

Applied to a typical combat aircraft with unstable lateral modes which is stabilised by a saturated feedback on angular rates and stops on lateral control deflections, computation of the unstable orbit surrounding the stabilised equilibrium point gives a first insight to the "robustness" of the control law. As the dimension of the system is greater than two, the unstable periodic orbit is only one element of the attracting region boundary(figure 5).

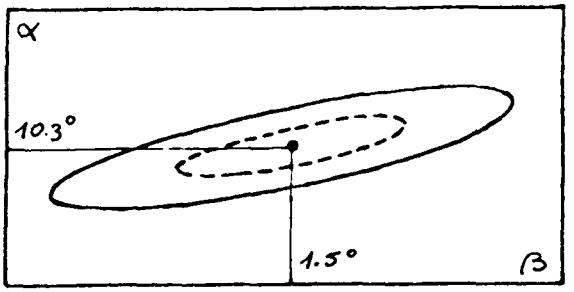

fig. 5 - Fixed point and periodic orbits for a stabilised typical combat aircraft.
* *fixed point,* —— *stable orbit,* - - - - *unstable orbit.*

In this example, stops on control deflections generate a stable periodic orbit which surrounds the unstable limit cycle and limits the divergence of the motion. The unstable limit cycle belongs to the attracting region boundary of stable periodic orbit.

5. ATTRACTING BASIN

A stable equilibrium state of a non-linear dynamic system is surrounded by a stability region. The determination of this region is of great interest for dynamics and engineers. It allows to define the limit of validity of linearised approximations for the original non-linear equations, to better understand the global behaviour of the system and to determine the maximum values of the perturbations for which the perturbed system returns to the initial stable state.

The aim of this chapter is to present several methods which are used today in order to give an answer to the attracting basin computation problem for sets of ordinary non-linear differential equations.

5.1 Preliminaries

The systems under consideration are of the general form:

$$\dot{x}(t) = f(x(t)) \qquad (3)$$

where f and x are n-dimensional vectors and where $f(x(t))$ are non-linear functions satisfying Lipschitz conditions.

It exhibits, at least, a steady state x^*

$$dx^*(t)/dt = 0 \qquad t > t_0$$

or a periodic orbit $\Phi^*(t)$ defined by

$$\dot{\Phi}^*(t) = f(\Phi^*(t))$$

where

$$\Phi^*(t+\tau) = \Phi^*(t) \qquad \tau = NT$$

where N is a positive integer.

Considering periodic orbit and without loss of generality, we can assume that $x^* = 0$ and $t_0 = 0$ and notice that by sustituting $\xi = x - \Phi^*(t)$ in (3), the study of periodic solutions for time invariant system is transformed in the study of periodic systems (Poincaré map).

The domain of attraction (attracting basin, region of asymptotic stability) of a steady state or of a periodic orbit is defined as the set of all initial conditions $x_0(t_0)$ that tend respectively to x^* or to $\Phi^*(t)$ when time tends to infinity.

Numerous methods have been proposed in the literature for estimating the region of asymptotic stability. They may be roughly divided in several classes according to the following figure.

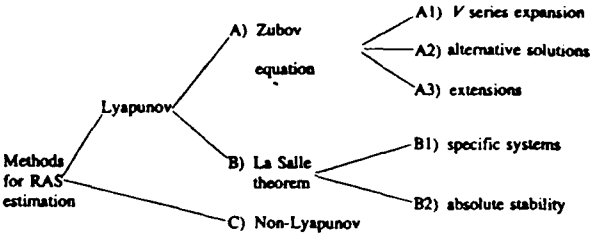

fig. 6 - Classification of the methods for the estimation of the domain of attraction.

Nevertheless, the distinction between these different classes is less obvious in modern methods because they use generally joint approaches.

5.2 Stability in the sense of Liapounov [8]

To characterise the stability of an equilibrium point of non-linear differential equations, two well-known methods are due to Liapounov.

5.2.1 First method

In the vicinity of an equilibrium point x^*, the non-linear differential equation (3) is rewritten under the following form

$$\dot{y} = Ay + R(y), \qquad y = x - x^* \qquad (4)$$

where A is the jacobian matrix of f in x^* and $R(y)$ are non-linear functions which satisfies two conditions:

$$R(0) = 0$$

$$\forall \varepsilon \geq 0, \exists \eta \geq 0 : \|Y\| \leq \eta \Rightarrow \|R(y)\| \leq \varepsilon \|Y\|$$

The first method gives stability conditions for x^* in (3) using stability results from (4).

Poincaré-Liapounov's theorem: If all the eigenvalues of the jacobian matrix (A) have a strictly negative real part, then x^* is an asymptotic stable steady state for (3). If, at least, one eigenvalue of the jacobian matrix (A) have a strictly positve real part, then x^* is an unstable steady state for (3).

5.2.2 Second method

This second method is based on the relation between generalised energy functions around the equilibrium points and their stability. These functions are called Liapounov functions. They can be define for autonomous and non-autonomous systems.

Lemma 1: a function V(x) is said to be positive definite within an open $\Omega \subseteq R^n, x \in \Omega$ if:
a) V and its partial derivatives are continuous in Ω,
b) V(x) = 0 for x = 0,
c) V(x) > 0 for $x \neq 0$.

For an autonomous system, a Liapounov function is a definite positive function in the vicinity of x such that its time derivative is negative or null along the trajectory defined by (3).

Lemma 2: A non-autonomous function W(x,t), is said to be positive definite inside an open $\Omega \subseteq R^n, x \in \Omega$ if:
a) W and its first partial derivatives are continuous in Ω for all $t \geq 0$,
b) W(0,t) = 0, for all $t \geq 0$,
c) there exists an autonomous positive definite function V(x) such that $W(x,t) \geq V(x), \quad \forall x \in \Omega, \forall t \geq 0$.

Then, an non-autonomous positive definite function W(x,t) is a Liapounov function in Ω if

$$W(x,t) \geq V(x), \quad \forall x \in \Omega, \forall t \geq 0$$

Theorem: The solution x = 0 of (3) is stable if a Liapounov function exists in the vicinity of the origin. It is asymptotically stable if, in addition, $(-\dot{V}(x))$ is also positive definite.

5.3 Liapounov methods
The methods using Liapounov functions are derived from the results obtained by Liapounov in [8]. Two approaches have been developed using either results from Zubov or an extension of Liapounov's theorems due to La Salle.

5.3.1 Zubov 's methods [9, 10]
All the following methods are derived from a theorem proposed by Zubov.

Theorem: Let us consider an equilibrium point x inside a region $A \subset R^n$. A is an attracting region for (3) if and only if there exists functions V(x) and $\Phi(x)$ such that:

a) V(x) is a continuous function in A and $\Phi(x)$ is a continuous function in R^n,
b)

$$\forall x \in A, \quad \|x\| \neq 0, \quad -1 < V(x) < 0$$
$$\forall x \in R^n, \quad \|x\| \neq 0, \quad \Phi(x) > 0$$

c)

$$\forall \gamma_2 > 0, \quad \exists (\gamma_1, \alpha_1) \in R^+ \quad \text{such that} \quad V(x) < -\gamma_1 \text{ for } \|x\| \geq \gamma_2$$
$$\text{and} \quad \Phi(x) > \alpha_1 \text{ for } \|x\| \geq \gamma_2$$

d) $V(x) \to 0$ and $\Phi(x) \to 0$ when $\|x\| \to 0$
e) if y is on the boundary of A, $y \neq 0$, (O is an equilibrium point), then $\lim_{x \to y} V(x) = -1$,

f) $$\frac{dV}{dt} = \Phi(x) \cdot (1 + V(x)) \cdot \sqrt{1 + \sum_{i=1}^{i=n} f_i^2}$$

If the origin is asymptotically stable, Zubov equations

$$\dot{V}(x) = [\nabla V(x)]^T \cdot f(x) = \Phi(x) \cdot (1 + V(x)) \cdot \sqrt{1 + \sum_{i=1}^{i=n} f_i^2}$$

admit only one solution for all x belonging to A and satisfying V(0)=0. Moreover, this solution verifies Zubov conditions for all $\Phi(x)$ such that $\int_0^{\bar{}} \Phi(x)dx < \infty$, for $\|x\|$ sufficently small.

Following Zubov theorem, V(x)=-1 is the boundary of the attracting region. Unfortunately, this last equation never admits a closed form solution and, therefore, different approximations have been proposed in order to estimate the attracting region.

Referring to the hypothesis of the Poincaré-Liapounov theorem, Zubov assumed that the system is written as

$$\dot{x} = Ax + R(x)$$

where A is a constant matrix having negative real part eigenvalues and R(x) admits a Taylor expansion. In this case, the solution of Zubov equation may be expressed in a form of the series

$$V(x) = V_2(x) + V_3(x) + \cdots + V_m(x) + \cdots$$

where $V_m(x)$ is a homogeneous function of mth degree.

Moreover, Zubov established the following properties

a) $V_2(x)$ is negative definite,
b) the serie converges in the vicinity of the origin,
c) $V(x)$ is analytically continuous along the trajectory starting from the origin and ending to the boundary (∂A) of the attracting region,
d) for every approximation $(\hat{V})$ of $V(x)$ truncated at the term of degree m, the boundary of the attracting region lies between the surfaces

$$\hat{V}(x) = \min_{\hat{V}=0} \hat{V}; \quad \hat{V}(x) = \max_{\hat{V}=0} \hat{V}$$

It can be noticed that the computation of the terms V_1, V_2, ... V_m is made by solving sequantially equations linear in their coefficients derived by substitution in

$$\dot{V}(x) = [\nabla V(x)]^T \cdot f(x) = -\Phi(x) \cdot (1 - V(x))$$

From a theoretical point of view, Zubov method provides the true attracting region when m tends to infinity but the convergence is not uniform. From a practical point of view, it can be remarked that the choice of the function Φ affects the domain of convergence of $V(x)$ and influences the shape of the surface $\hat{V} = cte$.

Drawbacks of these methods appear to be the assumption of analyticity of the system, the numerical computation, the arbitrariness of Φ and the non-uniform convergence of the procedures. On the other hand, an analytical estimate of the true region of stability is obtained.

Based on Zubov equations other methods have been proposed in the literature. Several authors express the solution in the form of Lie series by means of differential geometry concepts. The last class of method consists in using the following equation

$$\dot{V}(x) = -\frac{\Psi(x)}{\beta(x) \cdot V(x)}$$

as a generalised Zubov equation where the functions Ψ and β must satisfy suitable equations.

5.3.2 La Salle method [11,12]

The largest class of methods for the estimation of the attracting region refers to an extension of Liapounov theory due to La Salle and Lefschetz which applies to continuous and discrete systems respectively.

Theorem 1. Let $V(x)$: $R^n \to R$ be a continuously differentiable function. Let Ω_l designate the region where $V(x) < l$. Assume that Ω_l is bounded and that within Ω_l:

i) $V(x) > 0$ for $x \neq 0$,

ii) $V(x) < 0$ along the trajectory of the system, for all $x \neq 0$ in Ω_l.

Then

a) $x = 0$ is asymptotically stable,

b) every trajectory of the system in Ω_l tends to $x = 0$ as $t \to \infty$

Theorem 2. Let $V(x)$: $R^n \to R$ be a continuously differentiable function. Let Ω_l designate the region where $V(x) < l$. Assume that Ω_l is bounded and that within Ω_l:

i) $V(x) > 0$ for $x \neq 0$,

ii) $\delta V(x) = V(x(m+1)) - V(x(m)) < 0$ along the trajectory of the discrete system.

Then

a) $x = 0$ is asymptotically stable,

b) every trajectory of the discrete system in Ω_l tends to $x = 0$ as $m \to \infty$

These theorems imply that every solution which starts within Ω_l must remain in it. Also, if one adopts the level curves of $V(x)$ as the measure of distance from the origin, every trajectory that starts within Ω_l converges to the origin monotonically.

This approach has a more limited objective than the Zubov one but it is still based on the construction of a suitable Liapounov functions. It can be decomposed in two groups of methods.

The first group of methods may be applied to low dimensional non-linear systems with an exactly defined structure. In this field, all the classical procedures (graphical or numerical) have been applied to construct Liapounov functions:

a) Luré Liapounov functions [13,14, 15],
b) variable gradient procedures [16, 17],
c) Krasowskii results [18].

Generally these methods lead to conservative results. For higher dimensional systems, several optimisation approaches have been used to modify an inital Liapounov function in order to enlarge the volume of the attracting region [19].

The second group of method is related to the application of the concept of absolute stability in the frequency domain as proposed by Popov criterion, choosing a suitable Liapounov function holding for a whole class of non-linear systems defined by a sector condition in the sense of Aizerman. Then, the results obtained with this approach are specific of a type of non-linear system but they are more general than the previous one. Nevertheless, they are also too conservative.

5.4 Non-Liapounov methods

Nowadays, to compute the attracting region, there are essentially two methods which do not use explicitly Liapounov functions.

5.4.1 Trajectory reversing method

This method is known as trajectory reversing method or backward mapping. It is based on La Salle extension of the Liapounov stability theory. It provides an iterative procedure for obtaining the global attracting region for multidimensional systems, both time-invariant and time varying without conditions on the topological nature of the asymptotically stable point under study.

Following theorem 1 of §5.3.2, let C_0 the boundary of Ω_l. Let $\{t_j\}$, $j = 0, \pm 1, \pm 2, \ldots$ denote a sequence of time instants, where $t_j > t_k$ for $j > k$, $t_j > 0$ for $j > 0$ and $t_j < t_k$ for $j < 0$. Let C_j denote the map of the points on C_0 along the trajectories of the system at time $t = t_j$. Then

$$C_j \subset C_k \quad \text{for} \quad j > k,\ j, k = \pm 1, \pm 2, \ldots$$

provided that the measure of distance of a point to the origin is given by the value of the function V at this point.

A curve C_j is obtained by integration of the dynamic equations of (1) from $t = 0$ to $t = t_j$. For $j > 0$, the integration is done forward in time, while for $j < 0$ the integration is backward in time.

Then, if $C_{-\infty}$ denotes the map of the curve C_0 as $t \to -\infty$, due to the uniqueness of the solution of the equation (1), $C_{-\infty}$ is the domain of attraction of the origin.

The last remaining problem is the construction of an initial estimation of the attracting region bounded by the curve C_0. A solution to this problem follows from Liapounov results.

Suppose that f(x) in (3) is continuously differentiable and suppose that its jacobian matrix A has eigenvalues with negative real part. Then, noting that there exists a unique positive definite solution P to the matrix equation

$$PA + A^T P = -Q$$

for every positive definite matrix Q, Liapounov indirect method states that $V = x^T P x$ is a Liapounov function of (1) close to the origin. Moreover, assuming an Euclidian norm, it can be stated that:

$$x^T P x < \rho_{min} x^T x = \rho_{min} r^2$$

where ρ_{min} is the minimum eigenvalue of P. Hence a curve C_0 defined as

$$C_0 : x^T P x = \rho_{min} r^2$$

is a suitable inital estimate boundary of the attraction domain.

Based on the previous considerations, numerical procedures have been set up and applied on low dimensional continuous time systems [20,21].

Example 1: The Van der Pol's equation:

$$\dot{x}_1 = x_2$$

$$\dot{x}_2 = x_1 - \mu(1 - x_1^2)x_2$$

where μ is a parameter. For $\mu > 0$, the origin is asymptotically stable and the attracting region is bounded by an unstable periodic orbit. Considering $\mu = 1$, and starting with r = 0.5 in C_0, the evolution of the successive estimations of the attracting region is shown in the next figure.

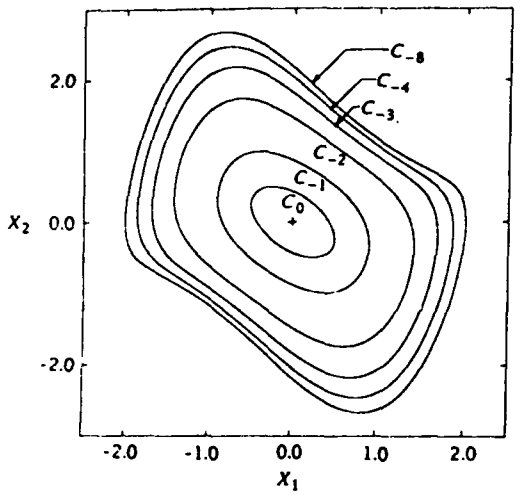

fig. 7 - Evolution of the domain of attraction of the origin for the Van der Pol's equation for the case $\mu = 1$. C_{-8} is the total domain of attraction.

It can be noticed that the backward image C_{-8} is indistinguishable from the exact domain of attraction of the origin.

Using theorem 2 of §4.3.2, the previous procedure may be extended to systems with periodic coefficients described by difference equations. The existence of the inital curve C_0 derives from unique and positive definite solution P of the discrete version of Liapounov's equation

$$H^T P H - P = -Q$$

where $H = [\partial F / \partial x]_{x=0}$ has eigenvalues with modulus less than one for any given Q.

Example 2: Parametrically excited pendulum

The motion of a pendulum whose support is harmonically excited in the vertical direction is given by the following differential equation with periodically varying coefficients:

$$\dot{x}_1 = x_2$$

$$\dot{x}_2 = -\mu x_2 - (\delta - \varepsilon \sin 2t)\sin x_1$$

where μ, δ and ε are systems parameters. This system possesses two equilibrium solutions $x_1 = (0,0)$ and $x_2 = (\pm\pi, 0)$ as well as numerous periodic solutions of various period. Considering the case $\mu = 0.02, \delta = 0.1$ and $\varepsilon = 1.5$ for which the origin is stable, the evolution of estimates of the attracting region surrounding the origin is shown on the next figure with $h = \pi$ and C_0 at t =0.

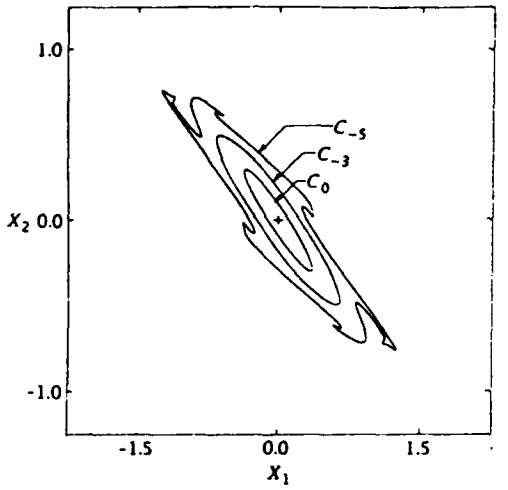

fig. 8 - Evolution of the domain of attraction of the origin for the parametrically excited pendulum for the case

$\mu = 0.02, \delta = 0.1$ and $\varepsilon = 1.5$.

The trajectory methods are attractive because of their generality and simple theoritical framework. However, their computational efficiency is generally poor and only low dimensional systems have been treated with them.

To reduce the computational effort, (n-1) facets can be used to approximate the basin boundary of an nth order system [22]. Starting from a local quadratic Liapounov function around the stable equilibrium point under study, a small convex polytope[1] is generated. Then, the vertices of this initial polytope are integrated backward in time to generate the vertices of a non-convex polytope approximation of the basin boundary. Thus, the real image approximates the attracting region as backwards integration time approaches infinity.

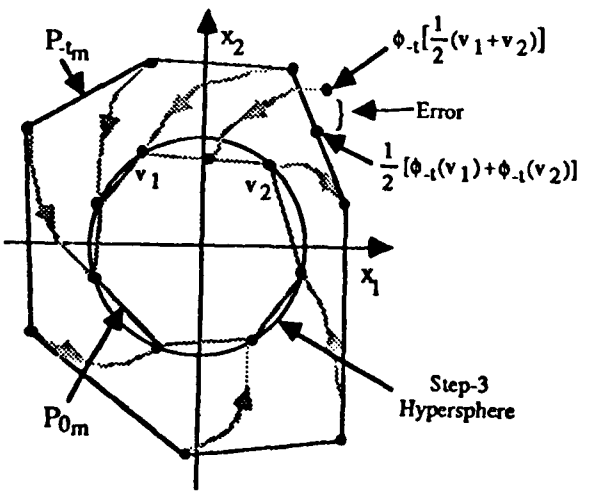

fig. 9 - An inital convex polytope and its backwards integration approximation.

[1] A polytope is a finite, flat slide solid in any high dimensional space.

As the system is a non-linear one, a test is applied to check whether the new non-convex polytope is a good approximation of the image of the original convex polytope. Adaptative facet refinement is used to correct any accuracy of the image approximation (figure 9).

The vertices of P_{-im} are derived by following the flow (half tone curves with arrows) backwards from the vertices of P_{0m}. The non-linearity test for facet $[v_1, v_2]$ is illustrated in the upper right-hand corner. The point generated by following the flow backwards in time from the center of the P_{0m} facet should be close to the center of the corresponding P_{-im} facet. As it is not close, a new vertex will get added to the hypersphere between v_1 and v_2 to generate the new polytope P_{0m+1}.

Recently, this method has been applied to construct the attracting region of an unstable aircraft lateral directional model with feedback stabilisation and control saturation [22].

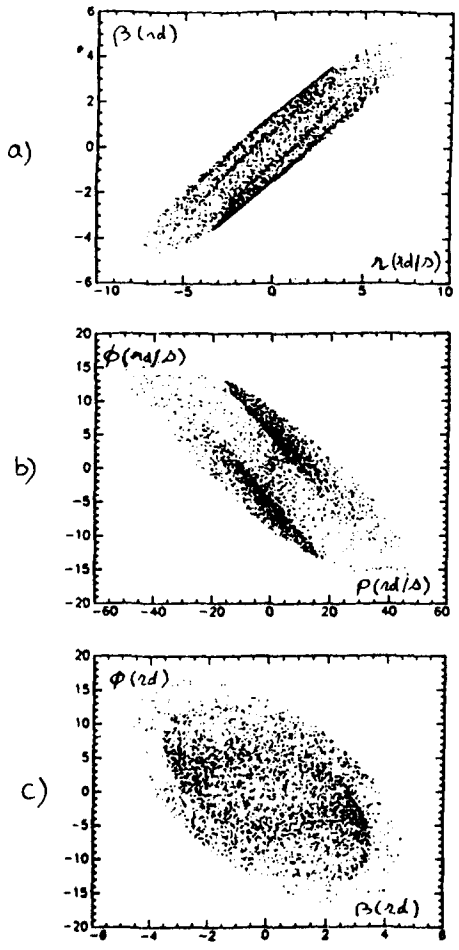

fig. 10 - Vertices of a polytope approximation of the basin boundary (t=1 sec) for the lateral/directional aircraft; a) sideslip angle vs. yaw rate, b) roll angle vs. roll rate, c) roll angle vs. sideslip angle.

Due to a linear representation of aircraft motion equations the state values are not realistic. However, this example shows that a great number of vertices are still required for accurate approximation. More generally, extension to higher dimensional cases is limited actually by the rapid growth of the (facet number)/(vertex number) ratio with the growth of state space dimension.

Apart from these numerical procedures, one must mention the method proposed by Genesio [23] because he uses a very simple trajectory method in connection with topological considerations which have been recalled in the two following theorems.

Theorem 1: The boundary of the region of stability is formed by whole trajectories.

As a consequence, excluding the trivial case n = 1, the following conclusions may be drawn:

a) n = 2. If the region of asymptotic stability is bounded, its boundary is formed by either a periodic orbit or a phase polygon (with unstable equilibrium points) or a closed curve of critical points.
b) n > 2. If the region of asymptotic stability is bounded, there exist constraints on the number of equilibrium points and precisely the following holds.

Theorem 2: Given an odd system ($n \neq 5$) without degenerate[2] equilibrium points, a necessary condition for the region of stability to be bounded with a smooth boundary is that at least two other equilibrium points exist apart from the origin, an even number of which must lie on the boundary.

For even order systems, the necessary condition for the region of asymptotic stability boundedness is much weaker, since the sum of the indexes of the equilibrium points on the boundary is equal to 0.

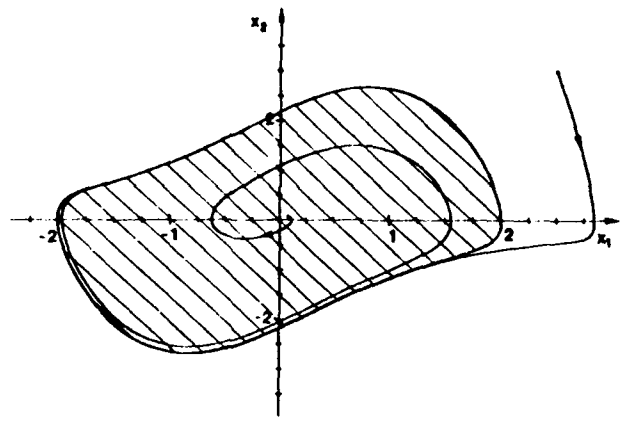

fig. 11 - Estimation of the domain of attraction of the origin for the van der Pol's equation.

Rather than describing successive approximations of the attracting region, Genesio used only a limited number of starting points from an inital estimate of the attracting basin in connection with the knowledge of all the equilibrium states for the given system.

[2]Degenerate equilibrium points are considered those for which some of the eigenvalues of the linearised system are zero or pure complex in pairs.

Coming back to the Van der Pol oscillator, the region of asymptotic stability is obtained performing only one backward integration from inside or from outside the periodic orbit (figure 11).

Although this method is only efficient and applicable to low order systems, use of topological considerations leads to the following differential geometry method.

5.4.2 Differential geometry method [24]

This method gives a complete characterisation of the stability boundary for a fairly large class of non-linear autonomous dynamic systems satisfying two generic properties plus one additional condition that every trajectory on the stability boundary approaches one of the equilibrium states (fixed points or/and periodic orbit) as the time t tends to infinity. Then, it is shown that the stability boundary of this class on non-linear systems consists of the union of the stable manifolds of all equilibrium states on the stability boundary.

To present the theoritical basis of this theory, one need to introduce some definitions.

An equilibrium point $(\hat{x})$ of (3) is said to be hyperbolic if, in local coordinate, none of the eigenvalues of the jacobian matrix $J_x f$ at x has zero real part. For this equilibrium point we can decompose the tangent space T_x uniquely as a direct sum of two subspaces E^S+E^U such that each subspace is invariant under the linear operator $J_x f$. The eigenvalues of $J_x f$ restricted to E^S have a negative real part. The eigenvalues of $J_x f$ restricted to E^U have a positive real part. The stable and unstable manifolds $W^s(\hat{x})$, $W^u(\hat{x})$ are defined as follows:

$$W^s(\hat{x}) = \{x \in M : \Phi_t(x) \to \hat{x} \text{ as } t \to \infty\}$$

$$W^u(\hat{x}) = \{x \in M : \Phi_t(x) \to \hat{x} \text{ as } t \to -\infty\}$$

A periodic orbit (γ), i. e. an image of a non-constant periodic solution of (1) is said to be hyperbolic if all the eigenvalues of the transition matrix have modulus not equal to one (one must be always 1) [3]. The stable and unstable manifolds of a hyperbolic periodic orbit are defined as follows :

$$W^s(\gamma) = \{x \in M : \Phi_t(x) \to \gamma \text{ as } t \to \infty\}$$

$$W^u(\gamma) = \{x \in M : \Phi_t(x) \to \gamma \text{ as } t \to -\infty\}$$

Obviously, one can notice that these manifolds are invariant sets, i. e. every trajectory starting inside remains inside. In the following, an equilibrium point or a periodic orbit of the vector field f is said to be a critical element.

To further characterise the stability boundary, the idea of transversality is introduced. First we say that a map $g: M \to N$ is an immersion at x if the derivative map $df_x : T_x(M) \to T_{f(x)}(N)$ is injective, where $T_x(M)$ and $T_{f(x)}(N)$ are the tangent spaces of M and N at points $x \in M$ and $f(x) \in N$, respectively. Then, if A, B are injectively immersed manifolds in M, they satisfy the transversality condition if either at every point of intersection $x \in A \cap B$, the tangent spaces of A and B span the tangent space of M at x or they do not intersect at all. An important feature of a hyperbolic equilibrium point $\hat{x}$ is that its stable and unstable manifolds intersect transversaly at $\hat{x}$. Furthemore, the transversal intersection persists under pertubation of the dynamic system.

The following theorem characterises a critical state being on the stability boundary of the region of stability.

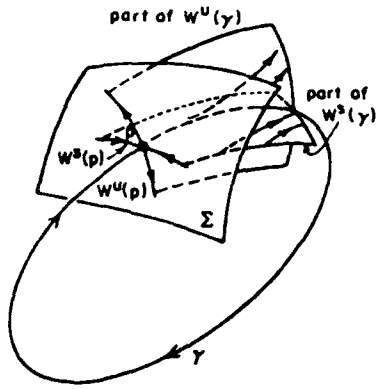

fig. 12 - Stable and unstable manifolds of a hyperbolic periodic orbit.

Theorem : Let A be the stability region of a stable equilibrium point. Let $\hat{r}$ be a critical element. Assume the following:

i) All the critical elements on the stability boundary (∂A) are hyperbolic,
ii) The stable and unstable manifolds of critical elements on ∂A satisfy the transversality condition,
iii) Every trajectory on ∂A approaches one of the critical elements as $t \to \infty$.
Then,

a) $\hat{r}$ is on the stability boundary ∂A if and only if $W^u(\hat{r}) \subseteq A = \emptyset$,

b) $\hat{r}$ is on the stability boundary ∂A if and only if $W^s(\hat{r}) \subseteq \partial A$.

The hypotheses of this theorem are very important and must be checked carefully. For an example, we can observe that the transversality condition does not hold for homoclinic and

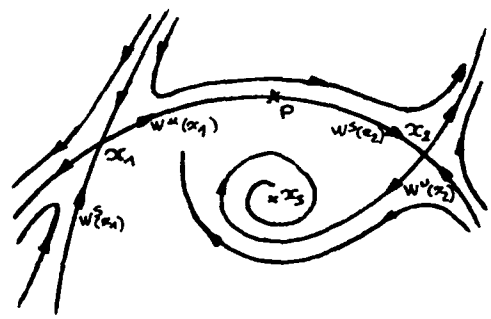

fig. 13 - The transversality condition is not verified; $p \in W^u(x_1) \cap W^s(x_2)$

heteroclinic orbit as it can be seen on the figure 13 because the intersection of the unstable manifold of x_1 and the stable

manifold of x_1 is a portion of manifold whose tangent space has dimension 1.
In the next example (figure 14), the unstable manifold of x_1 does not intersect with the stability region and a part of the stable manifold of x_1 is not on the stability boundary.

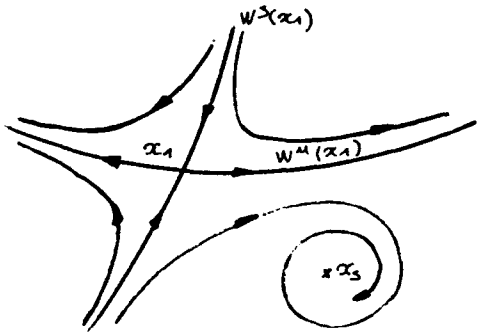

fig. 14 *- The transversality condition is not verified;* $W^u(x_1) \cap A = \varnothing$

The following theorems characterise the stability boundary.

Theorem : Let (3) be a dynamic system whose vector field satisfies the following assumptions:

i) All the critical elements on the stability boundary are hyperbolic,
ii) The stable and unstable manifolds of critical elements on the stability boundary satisfy the transversality conditions,
iii) Every trajectory on the stability boundary approaches one of the critical elements as $t \to \infty$,

Let x_i, i=1,2, ... be the equilibrium points and γ_j, j=1, 2, ..., be the periodic orbit on the stability boundary ∂A of a stable equilibrium point, then

$$\partial A = \bigcup_i W^s(x_i) \bigcup_j W^s(\gamma_j)$$

Now, the next theorem gives an insight on the structure of equilibrium points on the stability boundary.

Theorem : Let (3) be a non-linear dynamic system which contains two or more stable equilibrium points and satisfies the following assumptions

i) All the critical elements on the stability boundary (∂A) are hyperbolic,
ii) The stable and unstable manifolds of critical elements on ∂A satisfy the transversality condition,
iii) Every trajectory on ∂A approaches one of the critical elements as $t \to \infty$.

Then, the stability boundary must contain at least one equilibrium point having an eigenvalue with a positive real part. If, furthermore, the stability region is bounded, then ∂A must contain at least one equilibrium point having an eigenvalue with a positive real part and one source.

The contrapositive of the theorem gives a sufficient condition for the stability region to be unbounded.

Corollary : For the non-linear dynamic system (3), if it satisfies the assumptions of the previous theorem and if $\partial A(x_s)$ contains no source, then the stability region $A(x_s)$ is unbounded.

With all these results, a numerical procedure can be set up to determine the stability boundary by means of the construction of the stable manifolds of all the critical elements which belong to it [23, 24].

As an example, after computing the two stable equilibrium points, (0., 0., 0.) and (-7.45, -7.45, -7.45), and the unstable equilibrium point (-2.45, -2.45, -2.45) of the following system:

$$\dot{x} = -x + y$$
$$\dot{y} = 0.1x + 2y - x^2 - 0.1x^3$$
$$\dot{z} = -y + z$$

the procedure allows to compute the stability boundary of the attracting domain of the stable equilibrium points as the stable manifold of the unstable equilibrium point. A partial view of it is shown in figure 15.

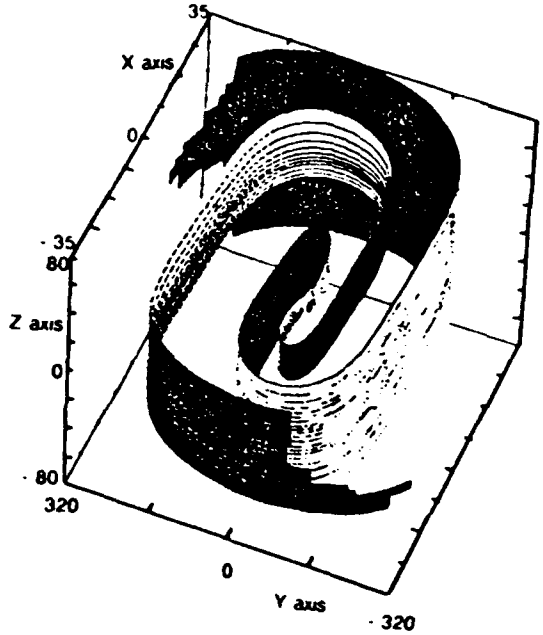

fig. 15 *- Partial view of the boundary of the domain of stability.*

For higher dimensional system, graphic representation of the boundary is difficult. Nevertheless, its projection in particular subspaces furnishes useful informations. The next figure

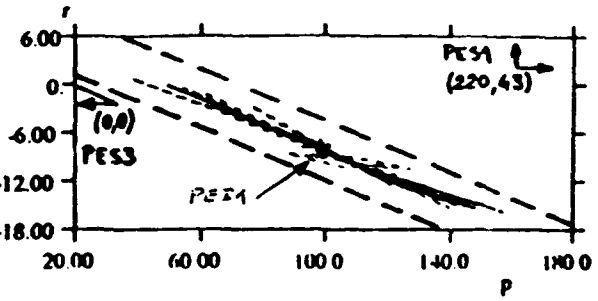

fig. 16 *- Projection in the (p,r) plane of the boundary of the domain of stability. PES1 and PES2 are stable equilibrium points while PEI1 is an unstable one.*

shows partial view of the stability boundary between two stable equilibrium points of a set of five non-linear equations describing aircraft motion at low angle of attack under inertia coupling conditions.

It should be noticed that this result seems to be complementary to those obtained by the construction of the attracting domain in §4.3.2.

6. CONCLUSION

This communication follows [1] which is presented in the same Agard Lecture Series (LS 191). In the previous communication, some theoretical foundations of Bifurcation Theory have been recalled and a methodology aiming at a systematic prediction of the behaviour of non-linear differential equations has been presented.

The first part of the communication is related to the examination of several problems which are connected with the introduction of control laws in order to stabilise an unstable dynamic system. From a stability point of view and under implicit assumptions on the controlled system (continuous time, continuous non-linearities, ...) it has been shown that Bifuraction Theory can help the designer to predict system behaviour and to compute a "good" control laws. Although promising results are available in the literature, some efforts remain to be done to take into account practical discrete systems. These control problems are closely connected with the attracting region of a stable steady state.

The second part of the communication is related to determination of the attracting region of a stable equilibrium point of non-linear dynamic systems. Many works have been done in this field. They are mainly based on Liapounov's stability theory and the extensions due to Zubov and La Salle. More recently, introducing topological considerations, trajectory reversing methods have been developed and numerous computational procedures have been proposed. These procedures are appropriate on low dimensional dynamic system. However, there is a need for improving them for higher dimension. Due to the difficulty to work with high dimensional systems, a limited part of attracting basin is generally computed. Is it sufficent? Are we interested by the entire domain of attraction? It seems that a lot of work is needed to give practical answers to this problem [27].

REFERENCES

1. Guicheteau, P., "Stability analysis through Bifurcation theory (1)", AGARD LS191, 1993.

2. Isidori, A., "Nonlinear Control Systems - An Introduction", Springer-Verlag, 1989.

3. Planeaux, J., B., and al, "Bifurcation Analysis of a Model Fighter Aircraft with Control Augmentation", AIAA-90-2836.

4. Casti, J., L., "Bifurcations, Catastrophes and optimal control", IEEE Trans. on automatic control, vol. AC 25, n° 5, 1980.

5. Hirai, K., I., and Ushio, T., "Catastrophic Jump Phenomena in a Nonlinear Control System", IEEE Trans. on automatic control, vol. AC 26, n° 2, 1981.

6. Holmes, P., "Bifurcation and chaos in a simple feedback control system", IEEE WP5-4:00, 1983.

7. Mitobe, K. and Adachi, N., "Hopf bifurcation in an adaptative d. c. servo system", Int. J. Control, Vol 54, n° 4,1991.

8. Liapounov, A., M., "The general Problem of the stability of Motion", Princeton University Press, Princeton, New Jersey, 1949.

9. Béliard, O., "Détermination du domaine d'attraction des états d'équilibre stables d'un système différentiel non linéaire autonome", Mémoire pour le Mastère de techniques aéronautiques et spatiales.

10. Zubov, V., I., "Methods of A. M. Liapounov and their applications", Nordhoff, Groningen, 1964.

11. La Salle, J., P., "Some extensions of Liapounov second method", IEE Trans. Circuits Theory, Vol CT-7, 1960.

12. La Salle, J., P., and Lefschetz, S., "Stability by Liapounov's Direct Method with Applications", Academic Press, New York, 1961.

13. Szergo, G., P., "A contribution to Liapounov's second method: Nonlinear systems" *in* International Symposium in Nonlinear Differential equations and Nonlinear mechanics, Academic Press, New York, 1963.

14. Schultz, D., G., "The generalisation of Liapounvov functions" *in* Advances in Control Systems, Academic Press, New York, 1965.

15. Hewit, J., R., and Storey, C., "Numerical application of Szergo's method for constructing Liapounov functions", IEEE Trans. on automatic control, vol. AC 14, 1969.

16. Schultz, D., G., and Gibson, J., E., "The variable gradient method for denerating Liapounov function", AIEE Trans. Appl. Ind, Vol 81, 1962.

17. Hang, C., C., and Chang, J., A., "An Algorithm for constructing Liapounov functions based on the variable gradient method", IEEE Trans. on automatic control, vol. AC 15, 1970.

18. Berger, A., J., and Lapidus, L., "Stability of high dimensional nonlinear systems using Krasovski's theorem", AIChE J., Vol 15, 1969.

19. Michel, A., N., and al, "Stability analysis of complex dynamical systems. Some computational methods", Circ. Syst. Signal Processing, Vol 1, 1982.

20. Guttalu, R., S., and Flashner, H., "A numerical method for computing domains of attraction for dynamical systems", *in* Int. J. Num. Met. in Eng, Vol 26, 1988.

21. Guttalu, R., S., and Flashner, H., "A computational approach for studying domains of attraction for non-linear systems", *in* Int. J. Non-linear Mechanics, Vol 23, 1988.

22. Piaski, M., L., and Luh, Y., P., "Nonconvex polytope approximation of attracting basin boundaries for non-linear systems", AIAA-90-3512-CP, 1990.

23. Genesio, R., and al, "On the estimation of Asymptotic stability regions: State on the art and New proposal", IEEE Trans. on automatic control, vol. AC 30, n° 1, 1985.

24. Chiang, H., D., and al, "Stability regions of non-linear autonomous dynamical systems", IEEE Trans. on automatic control, vol. AC 33, 1988.

25. Guicheteau, P., "Domaine d'attraction d'un point d'équilibre" *in* Mécanique du vol aux grandes incidences, RT ONERA n° 47/5148 SY, 1990.

26. Guicheteau, P., "Analyse non linéaire et dynamique du vol", Worshop AGARD/GCP, 1992.

27. Skowronski, J., M. and Guttalu, R., S., "Real-time attractors" *in* Dynamic and stability of systems, Vol 5, n° 4, 1990.

NON-LINEAR FLIGHT DYNAMICS

Ph. Guicheteau
ONERA
Boite Postale 72
92322 Chatillon CEDEX
France

1. ABSTRACT

In Flight Dynamics, aircraft motion is described by a set of non-linear differential equations, depending on parameters, associating the state vector (angle of attack, sideslip angle, speed, angular rates, ...) with the control vector (motivators, ...) through flight dynamics equations, aerodynamic model and flight control system. This communication presents some works which aim at improving the knowledge and the prediction of aircraft behaviour in particular flight phases for which classical linearised analysis of non-linear differential equations is insufficient or not valid.

2. RESUME

En dynamique du vol, le mouvement d'un avion est décrit par un ensemble d'équations différentielles non linéaires, dépendant de paramètres, liant les variables d'état (incidence, dérapage, vitesse, vitesses angulaires, ...) et les variables de commandes (gouvernes, ...) par l'intermédiaire des équations de la mécanique du vol, du modèle aérodynamique et du système de contrôle du vol. La communication évoque les travaux réalisés en France et à l'Etranger en vue d'améliorer la compréhension et de prédire avec précision le comportement de l'avion dans des situations de vol particulières pour lesquelles l'analyse linéarisée habituelle des équations différentielles non linéaire est insuffisante ou inadaptée.

3. NOMENCLATURE

C_X, C_Y, C_Z : dimensionless body axes force coefficients

C_l, C_m, C_n : dimensionless rolling, pitching and yawing moment coefficients

X^A, Y^A, Z^A : body axes aerodynamic forces

L^A, M^A, N^A : body axes aerodynamic moments

F_X, F_Y, F_Z : body axes thrust components

L^t, M^t, N^t : body axes thrust moments

p, q, r : roll, pitch and yaw rates

u, v, w : body axes components of aircraft velocity

α : angle of attack

β : sideslip angle

$\delta_l, \delta_m, \delta_n$: aileron, elevator and rudder deflections

δ_y : lateral offset of the center of gravity

Θ, Φ : pitch and roll angles

g : gravitational acceleration

m : aircraft mass

A, B, C : moments of inertia for X, Y and Z axes

E : product of inertia for X and Z axes

4. INTRODUCTION

For many years, study of losses of control and spins of combat aircraft has been a very important field of research. In spite of the efforts made, an analysis of such phenomena is still difficult due to their complexity, their apparently random character and the small amount of knowledge available in the field of high angle of attack aerodynamics.

Nevertheless, a careful examination of the many results obtained from flight tests on very different aircraft reveals an astonishing degree of similarity in behaviours which is difficult to attribute to hazard. Further, the study of analytical losses of control or spins showed that it was possible, given an adequate model, to obtain satisfactory matching between computational and either vertical wind tunnel or flight tests results. Thus it seems that control losses and spins are closely related to the differential system used in simulation.

In Flight Dynamics, aircraft motion is described by a set of non-linear differential equations, depending on parameters, associating the state vector (angle of attack, sideslip angle, speed, ...) with the control vector (motivators) through flight dynamics equations, aerodynamic model and flight control system.

Since the beginning of the aviation era, analytical non-linear methods on simplified sets of equations have been used to try to explain several phenomena occurring in Flight Dynamics. Independently of the interest of these approaches to analyse dangerous Flight Dynamics phenomena, the simplified assumptions used in these calculus often reduce the quality and the precision of the results.

This communication aims at the presentation of recent results obtained in Flight Dynamics with a global stability analysis methodology making use of Bifurcation Theory for non-linear differential ordinary equations depending on parameters when linearized analysis is insufficient or not valid.

The first part is related to the early works about non-linear phenomena using analytical techniques on reduced set of equations.

Using two typical aircraft models, the second part of this presentation is related to the application of Bifurcation Theory to basic, but very simple and well-known, non-linear phenomena such as, for example, spiral mode, auto-rotational rolling and Dutch Roll instability.

The aim of the third part of this paper is to present the results obtained when the previously mentioned theory is applied to a real combat aircraft, i.e. the German-French Alpha-Jet from Dassault Aviation. The study is specifically dedicated to oscillatory motions and to sensitivity analysis of departures and spin predictions to a given set of parameters.

After a brief description of the aircraft model, the oscillatory flight cases such as "agitated" spins are studied by means of learning the stability characteristics of periodic orbits related to oscillatory unstable equilibrium points. Complex oscillatory modes are pointed out. The synthesis of all these results shows the existence of two very different spin modes for some given control deflections. It illustrates too that the lack of a realistic non-linear model may lead to great difficulties for flight analysis when the motion is quasi-periodic or chaotic. Comparisons between predictions and flight tests at the French flight tests center are shown. Analysis of the sensitivity of predictions to some model parameters modifications is also presented. The first sensitivity analysis deals with the influence of lateral offset of the center of gravity on normal spin recovery. The second one deals with the influence of gyroscopic torques induced by engine rotors.

Finally, the interest of this methodology is discussed in the conclusion.

5. SIMPLIFIED NONLINEAR ANALYSIS OF AIRCRAFT BEHAVIOUR

The prediction and the analysis of control losses and spins of aircraft are old problems. However, with the lack of computers capabilities, the former works are related to the application of exact or approximate analytical methods on simplified non-linear equations.

Among the others, one can notice the work done by Phillips [1] about inertial coupling at low angle of attack. In this problem, the difficulty consists in taking into account the gyroscopic torques in the equations of motion. Neglecting gravity effects and simplifying the force equations, he has exhibited stability criteria which are still used today [2]. More recently, Hacker and Oprisiu revisited the validity domain of these criteria [3].

At moderate angle of attack, losses of control are more generally connected with aerodynamic non-linearities. They are related to the loss of stability of longitudinal and/or lateral modes [4]. A lot papers are concerned with Dutch Roll instability [5,6] for which aerodynamic non-linearities are expressed as Taylor series.

At high angle of attack, quiet spin has been easily identified as an equilibrium state of the complete set of motion equations providing adequate aerodynamic model is available [7]. These studies have shown that spin is a vertical helicoïdal motion in which lift and drag balance weight and centrifugal force. However, in spite of the development of numerical tools and the similarity between Euler-Poinsot motion and spin of modern combat aircraft. agitated spin was always considered as an hazardous phenomena [8].

The study of Schy and Hannah [9,10] can be considered as one of the last works which can be related to a simplified treatment of control losses. They have shown the possibility of multiple equilibrium solutions for a simplified set of flight equations; several of them are stable. It can be said that these latest works have been the basis of the global methodology used in this communication.

6. BASIC NON-LINEAR PHENOMENA

The study of Flight Dynamics is generally based on a linearized analysis of the motion equations. There is no doubt that this approach is well suited for learning. However, this limited point of view cannot show the genesis of loss of stability and cannot explain more complex phenomena.

Based on simple examples and others more complex, it is proposed to show the contribution of the global methodology to the prediction of the behaviour of a natural aircraft for which motivators are considered as parameters.

6.1 Motion equation and non-linearities classification

The adopted system of equations represents a six degree of freedom motion of a rigid aircraft. Since, there will be found:

a. three momentum equations, assuming $D = F = 0$

$$A\dot{p} - E\dot{r} + (C-B)qr - Epq = L^A + L^F$$

$$B\dot{q} + (A-C)rp + E\left(p^2 - r^2\right) = M^A + M^F$$

$$C\dot{r} - E\dot{p} + (B-A)pq + Erq = N^A + N^F$$

b. three force equations

$$m(\dot{u} + qw - rv) = X^A + F_x - mg\sin\Theta$$

$$m(\dot{v} + ru - pw) = Y^A + F_y + mg\cos\Theta\sin\Phi$$

$$m(\dot{w} + pv - qu) = Z^A + F_z + mg\cos\Theta\cos\Phi$$

c. two kinematic equations. Euler's kinematic equation for heading angle is not taken into account

$$\dot{\Phi} = p + \tan\Theta(q\sin\Phi + r\cos\Phi)$$

$$\dot{\Theta} = q\cos\Phi - r\sin\Phi$$

The many non-linearities of this system can be classified into two groups.

The first one includes those which are intrinsic to the system and which are due to the motion equations of a solid in space (trigonometric lines and gyroscopic momentum).

The second one includes those from the aerodynamic model. In this category, distinction should be made between curvature non-linearities of coefficients ($C_Z(\alpha)$, $C_l(\beta)$, etc..) and coupling non-linearities such as certain coefficients which connect longitudinal and lateral variables ($C_m(\beta)$, $C_l(\alpha)$, etc..).

Such a distinction is not immediately obvious but is justified by experience. The first group leads to sudden jumps in aircraft motion for a smooth variation of the control deflections whereas the second induces more or less steady oscillations.

6.2 Aircraft models

These former applications of Bifurcation Theory are performed on two typical combat aircraft aerodynamic models.

Model A is a linear aerodynamic model with coefficients independent of the angle of attack. It is used for the simplified auto-rotational rolling example.

Model B describes the aerodynamic model of a fictive aircraft with high wing and tail unit. It is nevertheless

realistic since it results from a synthesis of numerous wind tunnel tests. It is a non-linear aerodynamic model without hysterisis. The validity of which is extended to angles of attack from $-10°$ to $+90°$ and sideslip angle from $-40°$ to $+40°$ (figure 1). It is used for spiral mode example and for Dutch roll instability.

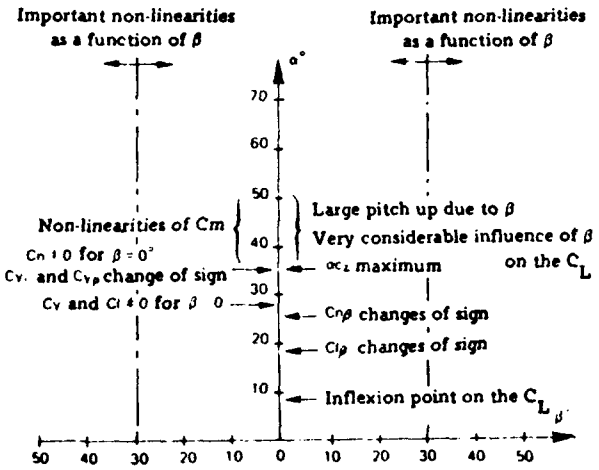

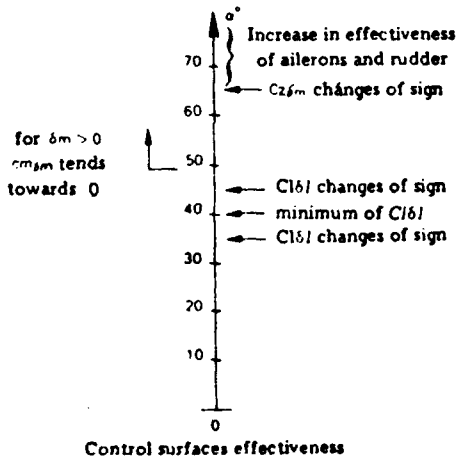

fig . 1 - Recapitulative diagram for the principal non-linearities of model B.

The formulation of model B has been adapted to the requirements of flight mechanics numerical computations. Each of six global coefficients: $C_l, C_m, C_n, C_X, C_Y, C_Z$, is expressed independently as a function of the influencing parameters: α, β, p, q, r, control surfaces. Thus the non-linearities and aerodynamic coupling are expressed by means of a Taylor series expansion around reference values (steady state) defined as follows:

$$\alpha = \bar{\alpha}, \quad \beta = 0, \quad p = q = r = 0 \quad \delta_l = \delta_m = \delta_n = 0$$

6.3 Spiral instability

This slow motion occurs at low angle of attack when the aerodynamic model is symmetrical. Then inertial coupling is negligible and the aerodynamic model is almost linear. Only gravity and pitch angle have an effect on the stability of the motion at zero sideslip angle.

When lateral control deflections are at neutral, the equilibrium surface of the system shows that spiral instability coincide with the existence of a fork bifurcation on the lateral variables of the system [11,12]. Moreover, it shows the stable steady states which can be reached by the system when the instability is encountered

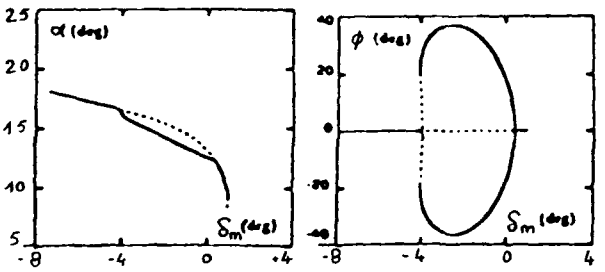

fig. 2 - Spiral bifurcation; a) (α, δ_m) plane, b) (Φ, δ_m) plane. ——— stable fixed points, - - - - unstable fixed points

Starting from an equilibrium condition at an angle of attack of 13° and a slightly nose up attitude, we encounter the instability for an elevator deflection value of -0.5°. It corresponds approximately to the appearance of spiral instability foreseen by traditional criteria. Stability returns at about $\delta_m = -4.°$ (figure 2).

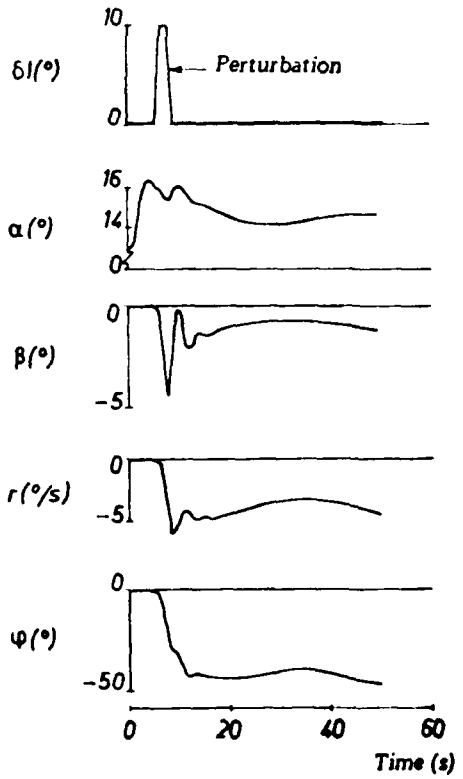

fig. 3 - Simulation of spiral instability.

Between these two limits of stability, the aircraft is unstable in straight level flight and, in response to a lateral disturbance, it tends towards a turning down flight, the characteristics of which are determined by the stable equilibrium branches located between the two limits of stability at zero sideslip angle (figure 3).

By comparison to the classical linearized flight mechanics, this methodology is able to predict the system behaviour beyond the limit of stability. It gives also an idea on the non-linearities which are responsible of the instability. Thus, considering the essential non-linearities it is possible to analyse the aircraft behaviour by reducing the motion equations to a scalar one:

$$\dot{\Phi} = (A\sin\Theta + B\cos\Theta\cos\Phi)\sin\Phi + (C_{\delta l}\delta l + C_n\delta n)\cos\Phi + D_{\delta l}\delta l + D_n\delta n$$

in which A, B, C, D, are coefficients which depend on the aerodynamic characteristics. In particular, B is the classical stability criteria for the linearized motion equations when $\Theta = 0$.

This scalar equation describes the evolution of variable Φ in a gradient field. The potential function (V) is defined by the following equation:

$$\dot{\Phi} = -grad(V(\Phi))$$

In spite of its simplicity, this formulation synthesises aircraft behaviour in the vicinity of the spiral instability. Moreover, it exhibits that spiral bifurcation can appear in the (δ_l, δ_n) plane even if level flight at zero sideslip angle is stable $(\delta_l = \delta_n = 0)$, (figure 4).

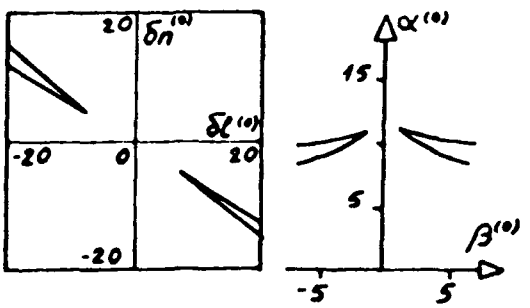

fig. 4 - Spiral bifurcation; a) (δ_l, δ_n) plane, b) (α, β) plane.

6.4 Auto-rotational rolling [12]

This phenomena is known for a very long time and its study has been recently revisited by Schy [9,10], Mehra [13], and others [14 to 17].

Experiments and previous computations have shown that auto-rotational rolling occurs at low angle, that speed varies only a little and that the influence of gravity is negligible. Thus, the complete set of equations of motion is simplified as follows:

i) the aircraft aerodynamic model is model A,
ii) the drag equation is absent (constant speed),
iii) the terms including quantity g/V are assumed to be always small and constant.

This last assumption has the advantage of decoupling the two kinematic equations, i. e. aircraft motion is not constrained to be about a vertical axis. Furthermore, considering also that pitch rate and yaw rate are much more smaller than roll rate, it is still possible to transform the initial problem in the study of a polynomial non-linear scalar equation relating yaw rate and control deflections:

$$\dot{p} = f_6(\delta_m)p^5 + \left(f_{5_{\delta l}}\delta l + f_{5_{\delta n}}\delta n\right)p^4 + f_4(\delta_m)p^3 + \left(f_{3_{\delta l}}\delta l + f_{3_{\delta n}}\delta n\right)p^2 + f_2(\delta_m)p + \left(f_{1_{\delta l}}\delta l + f_{1_{\delta n}}\delta n\right)$$

which, by a change of variable:

$$x = p + (f_5/f_4)$$

comes back to the differential equation:

$$\dot{x} = x^5 + dx^3 + cx^2 + bx + a$$

Thus, we demonstrate the canonical form of a singularity $R^4 \to R^1$ which is called "butterfly catastrophe" a study of which gives bifurcation points which can result in jumps for certain values of parameters (a,b,c,d). For our example, an illustration of the bifurcation surface is given in the figure 5.

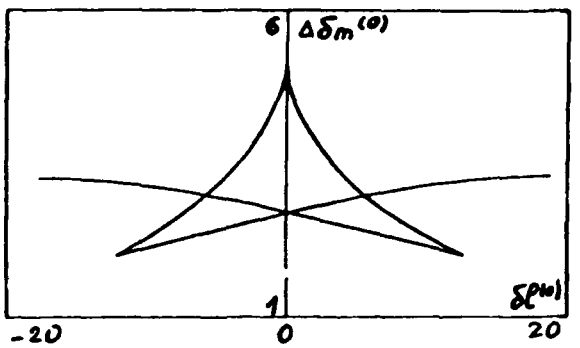

fig. 5 - Bifurcation surface in the (δ_l, δ_m) plane, rudder at neutral.

For a pitch down elevator angle from the trim position $(\Delta\delta_m = \delta_m - \delta_{m\,trim})$, corresponding to the selected angle of attack $(\alpha = 5°)$ with the lateral control surfaces at neutral, there are five possible equilibrium states identified by A1 to A5 on figure 6, and not only one as predicted by the linear approximation. States A1, A3 and A5 are stable; A2 and A4 are unstable.

Beginning from steady state A3, progressive ailerons deflection which correspond to a small right hand roll, performed at slightly negative load factor, displace the operating point to A'3 and then causes it to "jump" towards A'1. Precisely, the roll rate responds at the very beginning more or less linearly (that is to say intuitively) to the pilot's input and then it suddenly "jumps" to a level which is excessively high in relation to the control deflection. Generally the pilot immediately decides to return the ailerons to neutral while the elevator remains in a pitch down deflection. It can be noticed that this action will be more or less without effect, and remains so even if he deflects the ailerons in the opposite direction.

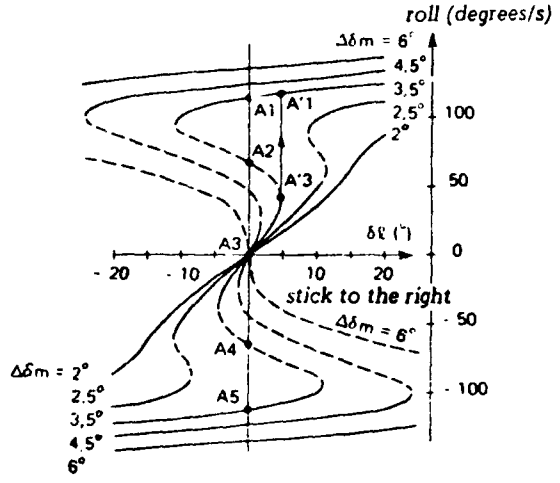

fig. 6 - Evolution of equilibrium roll rate as a function of ailerons deflections.

These two phenomena appear clearly in the following simulation which has been performed with complete equations (figure 7).

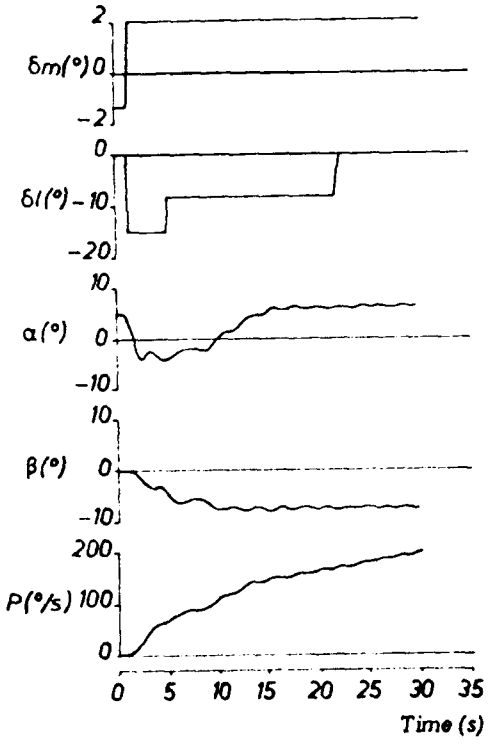

fig.7 - Simulation of auto-rotational rolling conditions.

Taking account of gravity effects, this simulation leads to the following remarks:

a) gravity effects result in an oscillation of the state variables around a mean value and,
b) cause the aircraft to dive and accelerate. It follows that the roll rate does not stabilise at the predicted value. More generally, it is observed that it is possible to rewrite the system under study using the reduced variable $p^* = pl/V$. We then verify that, in spite of the increase of the aircraft speed and the roll rate, the value of p^* is perfectly stabilised at the value anticipated by the equilibrium computations.

$$\delta\ell = 0.5\,(\delta\ell_D - \delta\ell_G)$$

$$\delta m_o = \delta m \text{ trim at } \alpha_o = 5°$$

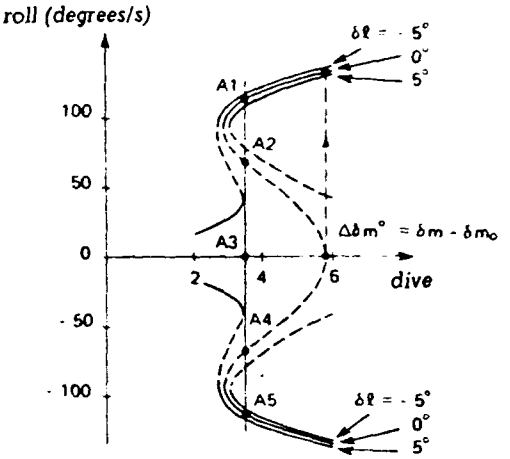

fig. 8 - Auto-rotational rolling, elevator influence.

Similarly, a pitch down elevator action can result in a spontaneous jump from A3 type equilibrium to A1 type (figure 8).

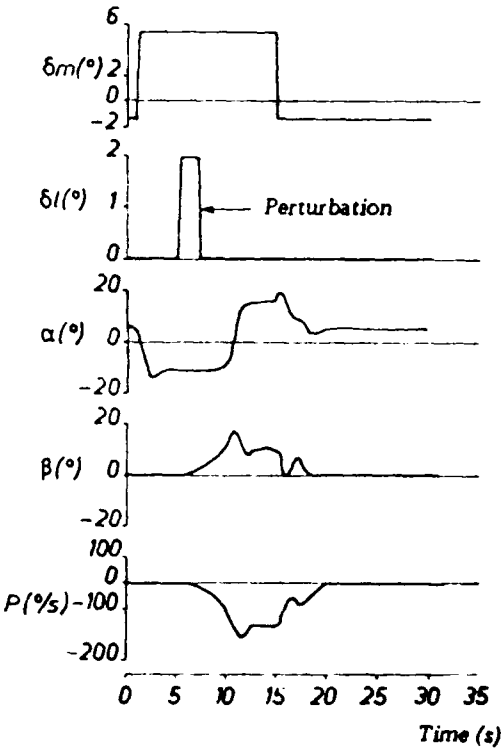

fig. 9 - Simulation of auto-rotational rolling conditions with a pitch down elevator action.

Finally, after an examination of the equilibrium curves, it can be observed that, beginning from point A1, ailerons at neutral, it is possible to return to the initial state without roll rate. This can be achieved by another jump obtained by returning the elevator to its trim position (figure 9).

Regarding the influence of aerodynamic coefficients, it can be noticed that, in spite of the differences between model A and model B, the equilibrium surfaces are very similar (figure 10).

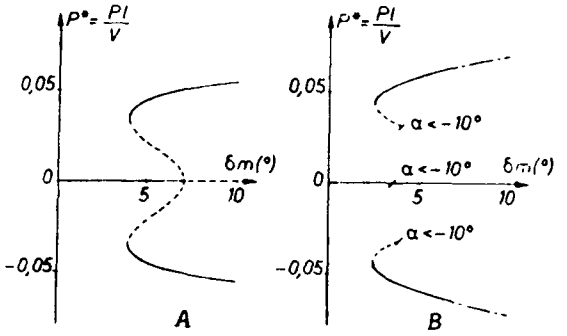

fig. 10 - Auto-rotational rolling. Comparison between model A and model B.
——— stable, - - - - - unstable, --*-*-* oscillatory unstable*

From a practical point of view, it can be said that this type of loss of control can be reached in spin recovery (figure 11).

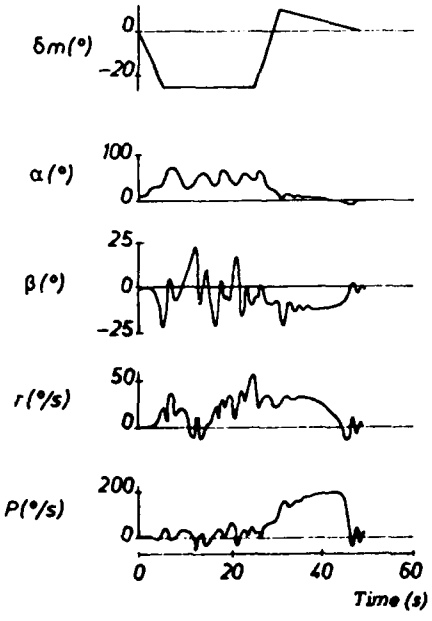

fig. 11 - Spin recovery by auto-rotational rolling.

In addition to aircraft behaviour analysis, computation of equilibrium surfaces and bifurcation points provides valuable information on the appropriate method to be used in order to avoid jumps. In the present case, computation of the bifurcation surface in the (δ_l,δ_n) plane for a given deflection of the elevator shows that there is a region free of bifurcation (figure 12).

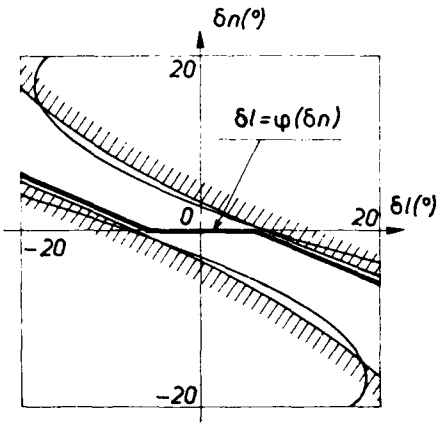

fig. 12 - Auto-rotational rolling. Influence of the control law in the (δ_l,δ_n) plane.

It follows that if the system is constrained to remain in this previously mentioned region, the aircraft will have a quasi-linear behaviour in response to pitch and roll control. In practice, such a system is an aileron-rudder coupling (ARI) which is used on many aircraft. Although it does not modify the pattern of the bifurcation curves which is intrinsic to the aircraft, it does modify their occurrence; the possible equilibria are no longer the same, and are not so varied, as is shown in figure 13. In simulation, the jump disapears.

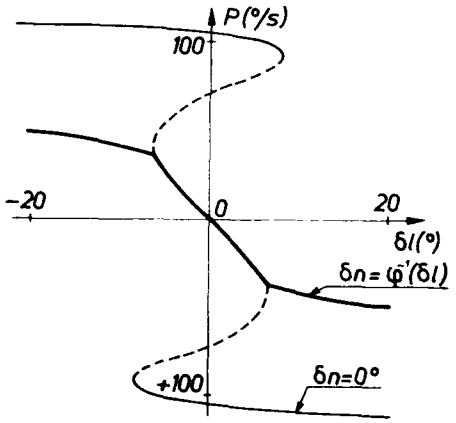

fig. 13 - Auto-rotational rolling. Influence of the control law on the roll rate.

6.5 Dutch roll instability

This pheromena is very well reported in the literature (See [5], [6] and [18] among the others!). It is now considered that the instability is connected to a Hopf bifurcation point which is approximated by classical theoretical and experimental Handling Quality criteria ($Cn_\beta dyn$, Kalviste, ...).

In this case, the first point of interest of Bifurcation Theory and especially the projection method is to characterise the Hopf bifurcation (subcritical or supercritical) [19] in order to get an indication about the amplitude of the periodic motion beyond the limit of stability. The second point of interest is the computation periodic orbits envelope without usual simplified assumptions (figure 14) in order to investigate

secondary bifurcations which can induce the apparition of wing rock or spins

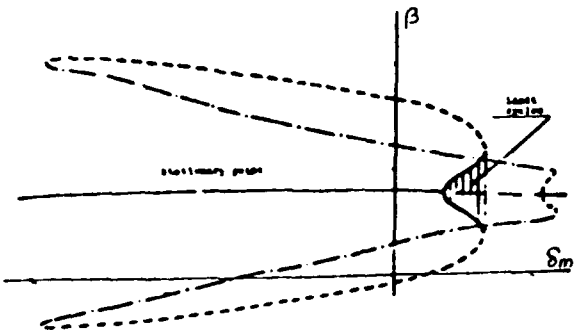

fig. 14 - Dutch Roll instability and periodic orbits envelope.

6.6 More complex phenomena

In the previous paragraphs, it has been shown that Bifurcation Theory is a powerful tool to give a better understanding of several classical non-linear Flight Dynamics phenomena for which a linearized approach is not adapted. This last paragraph presents more complex phenomena which are also encountered on combat aircraft.

Computation of periodic orbits envelope and their bifurcations for different aircraft shows that agitated behaviour can be also analysed by means of Bifurcation Theory.

The most current bifurcation is periodic limit orbit as it is exhibited on the previous figure.

When a pair of two conjugate imaginary eigenvalues crosses the unit circle, the stable orbit becomes unstable and the motion lies on a toroïdal surface surrounding the newly unstable orbit (figure 15).

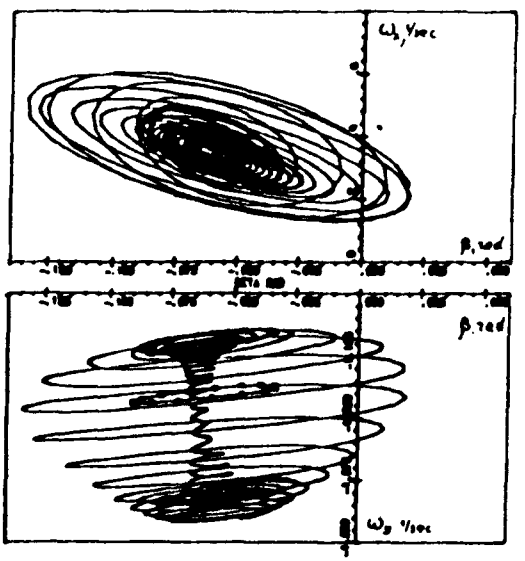

*fig. 15 - Motion on a torus [21] - * - * - * - * oscillatory unstable orbit.*

In this particular case [15], the motion seems to be a superposition of two periodic motions with very different period ($T_1 \approx 4s$ et $T_2 \approx 120s$). Then it could result in some difficulties to analyse such a phenomena from flight tests because the running time is generally less than the larger period.

The second illustration is related to flip bifurcation which can considerably modify the appearance of spin behaviour under small perturbations on controls [20] (figure 16).

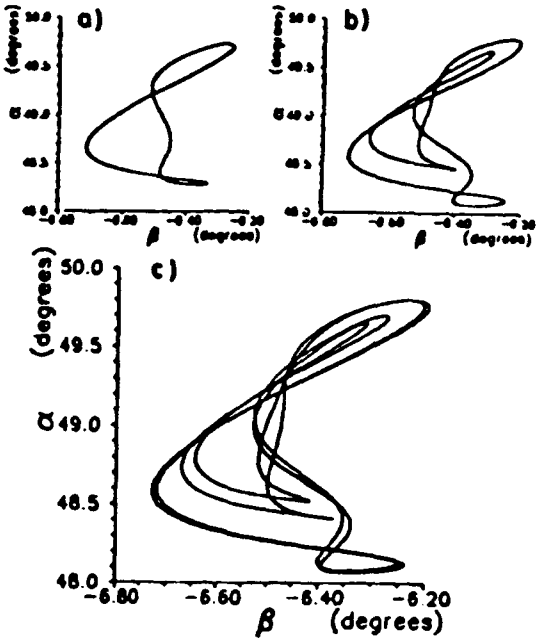

fig. 16 - Period doubling bifurcation. a) $\delta_m = -18.784°$, *b)* $\delta_m = -18.971°$, *c)* $\delta_m = -19.002°$.

Finally, when all the equilibrium states are unstable excepted one which is weakly stable, very long transient motions can appear [20]. Sometimes, these motions seem to be complex and/or chaotic (figure 17).

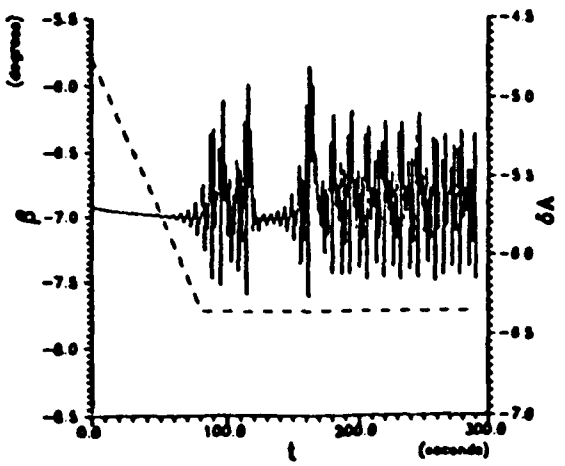

fig. 17 - Transient chaotic oscillations [21].

7. APPLICATION TO A REAL COMBAT AIRCRAFT [21]

Alpha-Jet is a tandem two seat German-French aircraft for close support and battlefield reconnaissance. With narrow strake on each side of nose, it is also an advanced jet trainer.

Considering its great ability to safely demonstrate numerous and various high angle of attack behaviours and for flight tests correlation, the training version was chosen to investigate the interest of the methodology.

7.1 Aircraft Model

Each of six global coefficients $C_l, C_m, C_n, C_X, C_Y, C_Z$, is expressed independantly as a function of flight and control parameters.

General expression of coefficients is in form

$$C_i = C_{i\,stat} + C_{i\,unstat}$$

Coefficients $C_{i\,stat}$ represent stationary aerodynamic effects. They expresse the influence of sideslip, angle of attack, control deflections and angular rates.

$C_{i\,unstat}$ terms take into account unsteady effects. They are expressed as a transfert function.

All these terms have been measured on a rotary balance in the vertical wind tunnel at ONERA/IMFL and tabulated over a wide state and control domain,

$$0 \le \alpha \le 180°$$

$$-90° \le \beta \le 90°$$

$$-600°/s \le \Omega \le 600°/s$$

In order to prevent continuation problem and fictive localized deformations of equilibrium surfaces, aerodynamic coefficients are usually smoothed to ensure continuity and derivability conditions for the resulting non-linear dynamic system.

In our application, no preliminary smoothing was done. Coefficients are evaluated by linear interpolation of the tabulated data. The following results will illustrate the robustness of our continuation algorithm.

The adopted non-linear differential equations consists of:

a) a set of motion equations (6 DOF),
b) four additional equations according to the Laplace formulation of unsteady aerodynamic influence on C_l, C_m, C_n, C_Z.

7.2 Spins

The results presented here are related to control losses, spin and spin recovery. In order to simplify the interpretation of computations, only typical cases will be shown. More precisely, inverted spin and spin recovery using low negative angles of attack are not considered.

Starting from a straight level flight at low angle of attack, when the pilot moves the elevator for a full nose up attitude $(\delta_m = -20°)$, we can observed that multiple steady states appear at high angle of attack when both aileron and rudder deflection varies. The projection of the equilibrium surface

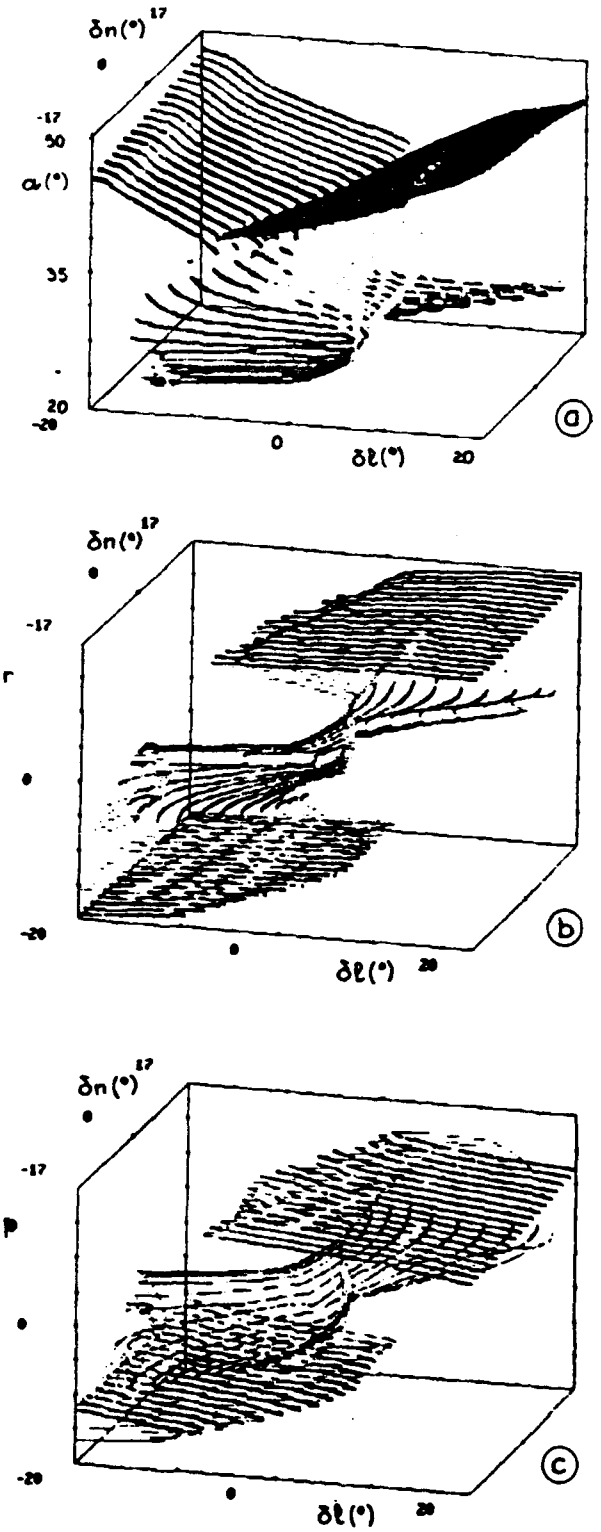

fig. 18 - Equilibrium surface projection in characteristic sub-spaces: (a) $(\alpha, \delta_l, \delta_n)$; (b) (r, δ_l, δ_n); (c) (p, δ_l, δ_n). black stable, grey oscillatory unstable, little grey unstable divergent

in three characteristic sub-spaces $(\alpha,\delta_l,\delta_n)$, (r,δ_l,δ_n) and (p,δ_l,δ_n) allows easily to identify the domains of spins and rolling motions (figure 18).

It should be observed that this surface is not symmetric. This is due to non symmetrical aerodynamic data for symmetrical aileron and rudder deflections at high angle of attack.

As it can be seen on the previous figure, stability is very different from a point to another. More precisely, it seems that left spins, related to negative δ_l, are much more unstable than right spins. Perhaps this low degree of stability can explain pilot's difficulties to demonstrate left steady spins on Alpha-Jet. The third type of steady states encountered on this surface corresponds to an important roll motion at moderate angle of attack. In flight, this kind of motion occurs mainly when pilots fail spin entry or fail the transition from one spin on one side to another spin on the other side.

In order to precise these motions, let us consider the equilibrium curve corresponding to full rudder deflection $(\delta_n = 17°)$ (figure 19).

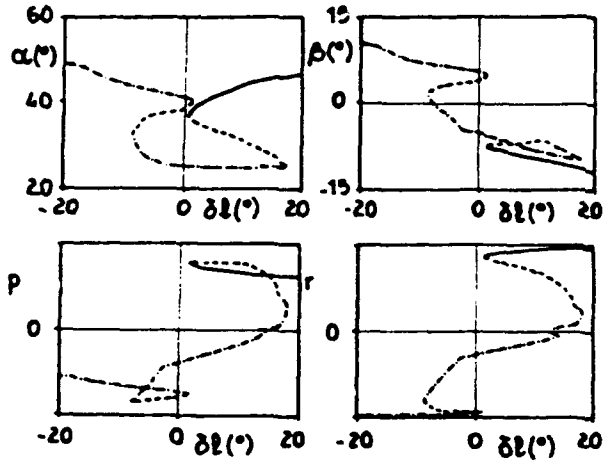

fig. 19 - Equilibrium curve for $\delta_n = 17°$.
--- stable, - - unstable divergent
-.- oscillatory unstable.

It can be observed that right spin is stable while left spin is always oscillatory unstable excepted for a few positive aileron deflections. In the vicinity of this last equilibrium branch (δ_l negative), there exist several periodic orbits when aileron deflection decreases from $\delta_l = -0.2°$ to $\delta_l = -20°$. (figure 20).

Two distinct branches can be observed. On the first one, the limit points are numerous. Between $\delta_l = -0.308°$ to $\delta_l = -7°$, two convergent series of flip periodic bifurcations determine a region in which an Alpha-Jet can exhibit a chaotic behaviour. In our case, on the contrary with typical chaotic behaviours exhibited by well known particular differential equations, there are only little differences in amplitude between the different orbits of period T, 2T, etc.

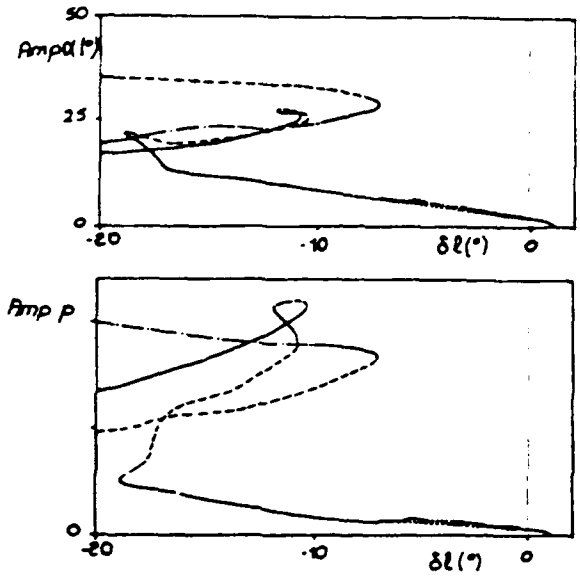

fig. 20 - Envelope of periodic orbits when δ_l *varies for* $\delta_l = -20°$ *and* $\delta_n = -17°$.

Then, it seems that this behaviour will be very difficult to observe and to characterise in flight. Finally, the most important phenomena on this branch of the envelope is the rapid variation of orbits amplitude when δ_l is less than -10°. This could explain the sensibility of spin agitations versus aileron which is well known by pilots.

On another branch of the periodic envelope, between $\delta_l = -3.5°$ and $\delta_l = -7.5°$, there exist oscillatory unstable orbits with great amplitude. (figure 20). Around them, the motion takes place on a toroïdal surface if it is stable. Nevertheless, the existence, for same values of δ_l, of an invariant torus and a stable orbit can lead to non similar flight behaviours. These different behaviours depend on the initial state and of the history of control deflections during the manoeuvre.

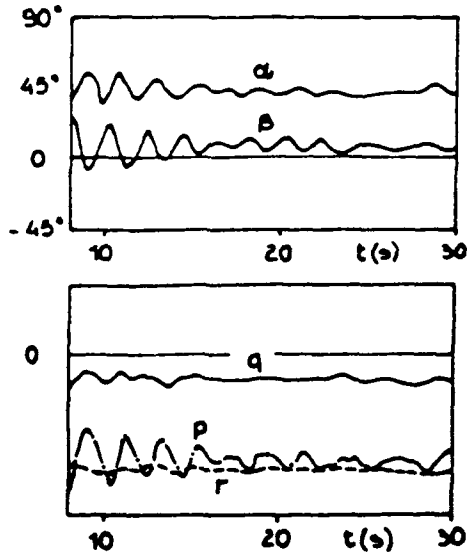

fig. 21 - Quiet left spin for $\delta_l = -4°$.

All these phenomena can be demonstrated in flight. In order to make correlations between predictions and flight, flight tests have been done at the French Flight Test Center in Istres. The results which are going to be presented in the following have been obtained at the end of 1988 and analysed with standard flight test techniques at ONERA/IMFL in Lille during 1989.

For full elevator and rudder deflections $(\delta_m = -20°, \delta_n = 17°)$ quiet left spin is obtained for $\delta_l = -4°$. (figure 21).

For an aileron deflection in the vicinity of $\delta_l = -5°$, chaotic motion was not demonstrated. This result is due to the short duration of spin tests and to the absence of great differences between the orbits in presence as it was previously mentionned.

When aileron deflection is close to -10°, Alpha-Jet can exhibit three very different motions due to the existence of two stable orbits and a stable invariant torus. (figures 22 to 24).

Another very interesting behaviour is what happens when pilots fail left spin entry. In this case, an oscillatory motion at a moderate angle of attack appears. (figure 25). It corresponds to orbits which surround the lower oscillatory unstable equilibrium branch of figure 19.

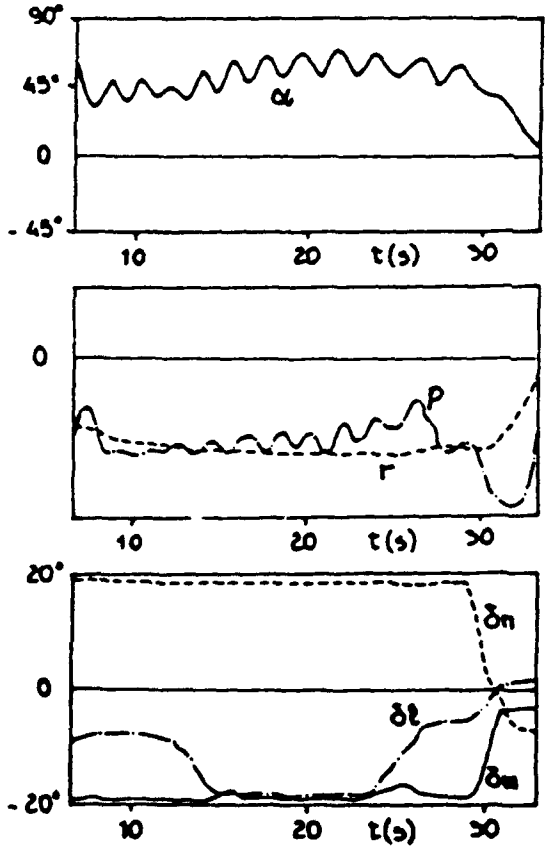

fig. 22- Quiet left spin for δ_l moving from -20° to 0°.

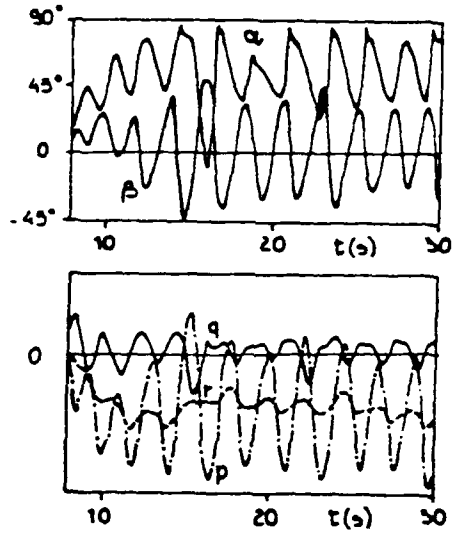

fig. 23 - Regular agitated spin for $\delta_l = -10°$.

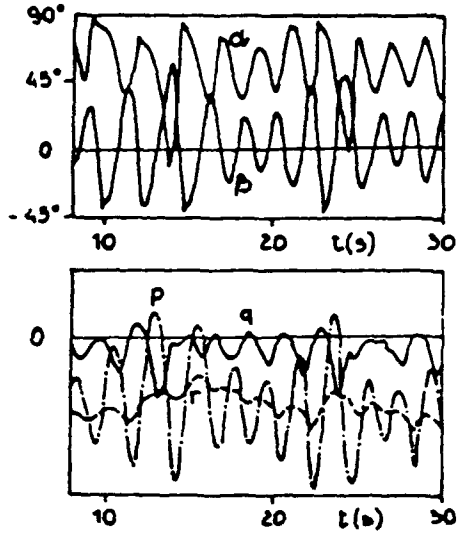

fig. 24 - Motion on a toroidal surface for $\delta_l = -10°$.

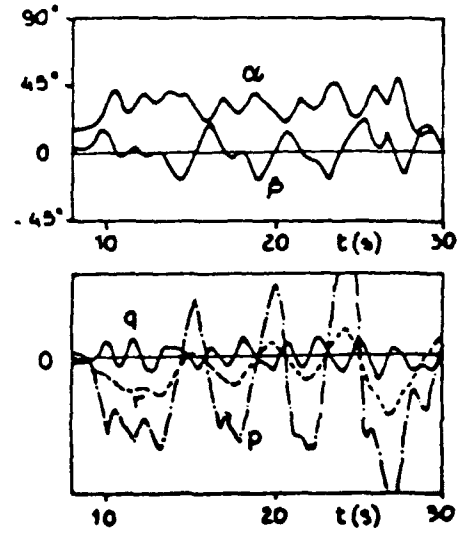

fig. 25 - Unsuccessful spin entry.

Starting with the previous quiet left spin for $\delta_l = -4°$ and reversing rudder deflection, another quiet spin can be observed for a rather unusual combination of lateral control deflections. (figure 26). However, there is a very good agreement with the stable equilibrium branch obtained for $\delta_n = -17°$ and negative aileron deflections. (figure 18).

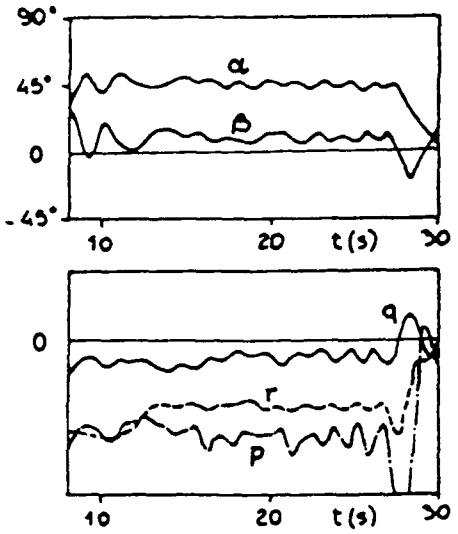

fig. 26 - Quiet left spin for $\delta_n = -17°$ and negative aileron deflection.

Coming back to full positive rudder deflection, quiet spin turns into flat spin when pilots push on the stick according to equilibrium states computations for different elevator deflections. (figure 27 and figure 28).

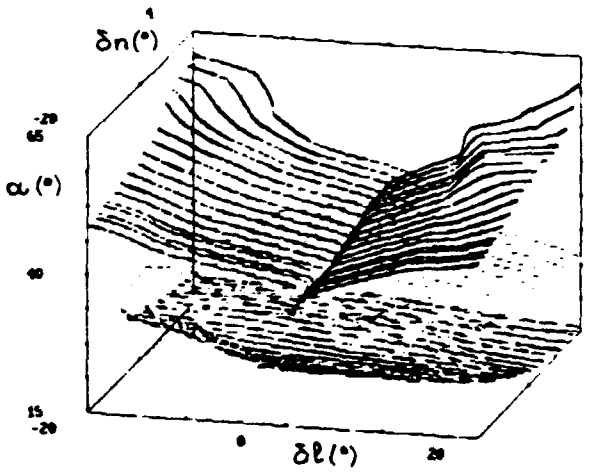

fig. 27 - Equilibrium surface for $\delta_m = 4°$ in the $(\alpha, \delta_l, \delta_n)$ space. black stable, grey oscillatory unstable, little grey unstable divergent.

As it can be seen on the following figure, for example, spin recovery is always satisfactory achieved by putting lateral control deflections at neutral, after a transient small positive aileron deflection, and pushing on the stick in order to decrease elevator deflection.

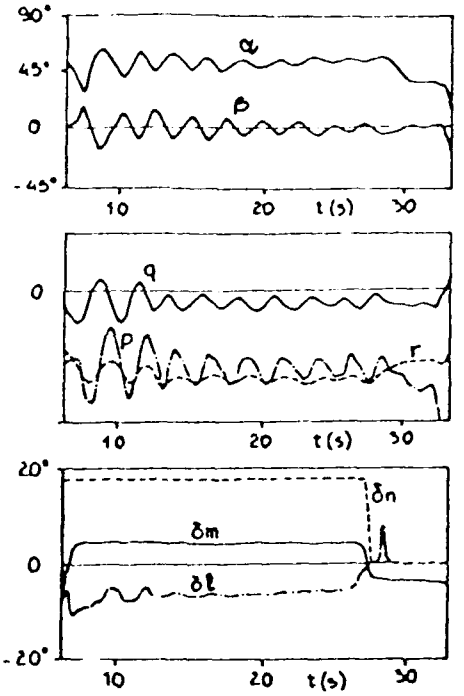

fig. 28 - Flat spin for $\delta_m = 4°$.

7.3 Influence of a lateral offset of the cg

During previous flight tests on Alpha-Jet and spin tests in the vertical wind tunnel at ONERA/IMFL, it has been found that spin is very sensitive to a lateral offset of the center of gravity.

In the following, we will show that Bifurcation Theory is also able to study this influence of the position of the cg on spin recovery.

It is assumed that the lateral offset of the cg is only similar to a shift (δ_y) of the cg outside the symmetry plane, along the Y body axis. Then, only moments due to exterior forces are modified. Rudder at neutral and for a positive value of elevator deflection, spin recovery from left spin is achieved through a limit point for $\delta_l < 4°$. Due the stabilising effect of positive δ_y on left spin and when δ_y increases, the limit point moves in the (δ_l, δ_y) plane in a such way that spin recovery may be less easy to obtain. (figure 29).

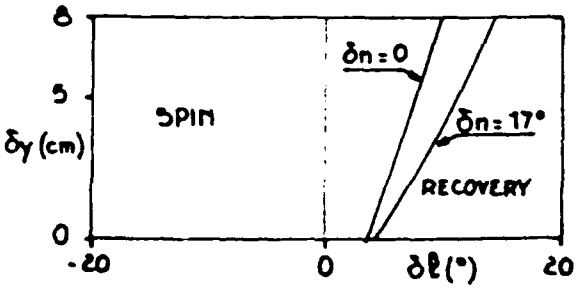

fig. 29 - Influence of lateral offset of the cg on left spin recovery in the (δ_l, δ_y) plane.

7.4 Influence of gyroscopic torques due to engines

Rotor speed effects appear in the momentum motion equation :

$$\frac{d\sigma}{dt} = M$$

with $\sigma = \sigma_{fixed\ part} + \sigma_{rotor(s)}$

and $\sigma_{rotor(s)} = \sum (I_{rotor}\Omega_{rotor})$

In the following, we will consider constant rotor speed. Then, these effects are easier to take into account. It is similar to introduce additional moments in the previous motion equations which have the same effect that taking into account cross coupling aerodynamic coefficients due to angular rates

Considering inertia characteristics and rotor speed of LARZAC engines which are used on Alpha-Jet, it seems that these additional terms are non negligible damping terms.

Equilibrium computations show no significant influence of this effect excepted only few localised deformations of equilibrium surfaces.

In simulation, when only one stable equilibrium exists, no difference can be seen with or without rotor effects. However, when several stable equilibrium states are in presence, the influence of rotor speed is more important. In certain cases, it can lead to very different final states for the same control deflections. (figure 30).

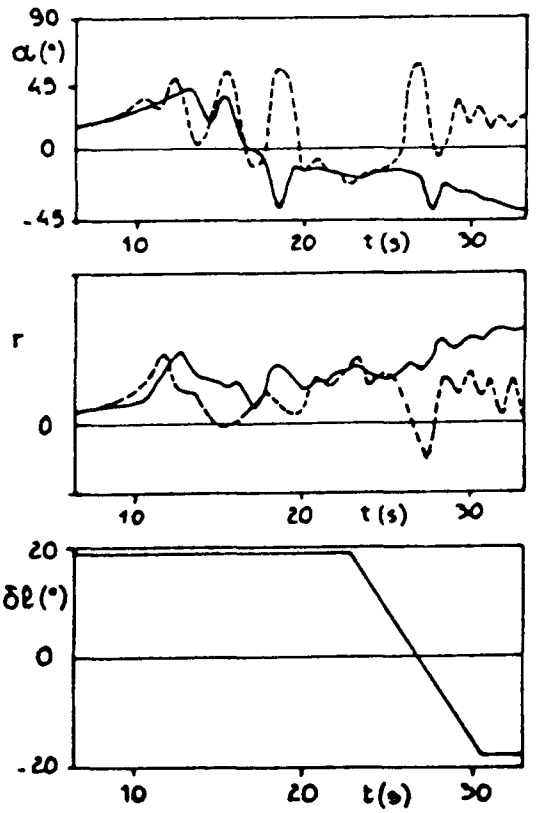

fig. 30 - Influence of engines rotor gyroscopic torque on final state. -------- without - - - - with gyros. torques

This difference cannot be explained by a possible instability of one equilibrium state. This phenomena is more surely related to the stabilising effect of rotor speed during the transient motion which is closely related to the time history of control deflections. Then, it can be said that, if no significant effect is found on equilibrium state, gyroscopic torques due to rotor speed have to be taken into account, in simulation, in order to increase the reality of spin entry.

8. CONCLUSION

At high angle of attack flight, fighter aircraft behaviour is so complex that it is very difficult to predict it exhaustively. Usually, this flight domain is investigated by means of systematic or Monte Carlo numerical simulations before the first flight and by means of extensive and expensive flight tests.

However, in spite of these tedious efforts, it remains that an analysis of such phenomena is still very delicate due to their complexity and their apparently random character.

Thanks to Bifurcation Theory and to computers capabilities, a methodology and a software to investigate asymptotic behaviour of non-linear differential equations depending on parameters have been developed. This methodology has been used to study high angle of attack behaviours of an Alpha-Jet aircraft.

After predicting aircraft behaviours by means equilibrium surfaces and periodic orbits envelopes, flight tests have been performed. Thanks to flight test pilots, to which it has been asked to perform rather unusual flight tests, very good correlations with results predicted by the theory have been obtained.

The results presented in this paper show the interest of the informations provided by this methodology. However, one cannot forget that the quality of predictions is directly connected with the quality of the aerodynamic data base of the aircraft model.

Then, considering all these results, it can be said that this technique has a great potentiality and is appropriate to investigate aircraft behaviours, using only wind tunnel data.

At a further step, it can also be used to investigate non-linear behaviours induced by non-linear elements in flight control systems. In this field, it seems very interesting to complete the analysis by the determination of the region of asymptotic stability of a stable equilibrium point in order to quantify control laws robustness.

Finally, for a complete understanding of non-linear systems behaviour, transient motion have also to be studied in order to understand the immediate behaviour and the influence of speed variation of controls on the motion.

Independently of these future studies, it can be noticed that steady behaviours are of great interest because if asymptotic states are not always achieved by a limited number of simulations and flight tests, they exist and probably will happen, at least one time, during aircraft life.

In the future, due to its ability to deal with non-linear differential equations, this methodology would be successfully applied to other highly non-linear systems like,

just for example, high performance missiles, helicopters or submarines.

ACKNOWLEDGEMENTS

A part of the results presented here have been carried out under STPA (Services Techniques des Programmes Aéronatiques) contract. It was done in connection with Dassault Aviation for the aircraft, and with the Flight Test Center in Istres and ONERA/IMFL for the realisation and the analysis of flight tests.

From predictions to flight tests, they provide the opportunity to investigate the interest of the methodology developed at ONERA. I would like to thank them all for their supporting advices.

REFERENCES

1. Phillips, W.H., "Effect of steady Rolling on Longitudinal and Directional Stability", NASA TND-1627, 1948.

2. Pinsker, W.J.G., " Critical Flight Conditions and Loads Resulting from Inertia Cross-coupling and Aerodynamic Stability Deficiences", ARC-TR-CP-404, 1958.

3. Hacker, T. et Oprisiu, C., "A discussion of the roll-coupling problem" *dans* "Progress in Aerospace sciences", Vol n° 15, Pergamon Press, 1974.

4. Kalviste, Y et Eller, B., "Coupled Static and Dynamic Stability Parameters", AIAA-89-3362, 1989.

5. Ross, J.A. et Beecham, L.J., "An approximate analysis of the nonlinear lateral motion of a slender aircraft (HP115) at low speed", ARC R&M 3674, 1971.

6. Padfield, G.D., "The application of Perturbation Methods to Nonlinear Problems in Flight Mechanics", PhD Thesis, Cransfield Institute of Technology, 1979.

7. Adams, W.M., "SPINEQ: A Program for Determining Aircraft Equilibrium Spin Characteristics Including Stability", NASA TM 78759, 1978.

8. Laburthe, C., "Une nouvelle analyse de la vrille basée sur l'expérience française sur les avions de combat" *dans* "Stall/Spin Problems of Military Aircraft", AGARD CP 199, Papier n° 15A, 1975.

9. Schy, A.A. et Hannah, M.E., "Prediction of Jump Phenomena in Roll-Coupling Manoeuvers of Airplane", J. of Aircraft, Vol. 14, avril 1977.

10. Schy, A.A., Young, J.W. et Johnson, K.G., "Pseudo-state Analysis of Nonlinear Aircraft Manoeuvers", NASA TP 1758,1980.

11. Jahnke, C.C., "Application of Dynamical Systems Theory to Nonlinear Aircraft Dynamics", Thesis, Engineering and Applied Sciences, CALTECH, 1990.

12. Guicheteau, p., "Application de la théorie des bifurcations à l'étude des pertes de contrôle sur avion de combat" *dans* "Combat Aircraft Manoeuvrability", AGARD CP 319, Papier 17, 1981.

13. Mehra, R.K., Carrol, J.V. et Kessel, W.C., "Global Stability and Control Analysis of Aircraft at High Angle of Attack", Technical Report, ONR CR215-248-1, 1978.

14. Hawkins, C.A., "Application of Bifurcation and Catastrophe Theories to Near Stall Flight Mechanics", AFIT/CR/NR 86-54T, 1985.

15. Zagaynov, G.I. et Goman, M.G., "Bifurcation Analysis of critical Aircraft Flight Regimes, ICAS-80-4.2.1, 1984.

16. Gonzales Blazquez, A.L., "Mathematical Modelleing for Analysis of Nonlinear Aircraft Dynamics", Computers and Structures, Vol 37, N° 2, 1990.

17. Lowenberg, M.H., "Bifurcation Methods-A Practical Methodology for Implementation by Flight Dynamicists", ICAS-90-5.10R, 1990.

18. Gao, H., Wang, Z.J. et Zhang, S.G., "A study of wing rock", ICAS-90-5.10.3, 1990.

19. Guicheteau, P., "Etude du comportement transitoire d'un avion au voisinage d'un point de bifurcation" *dans* "Unsteady Aerodynamics - Fundamentals and Applications to Aircraft Dynamics", AGARD CP 386, Papier S10, 1986.

20. Planeaux, J.B. et Barth, T.J., "High Angle of Attack Dynamic Behaviour of a Model of High Performance Fighter Aircraft", AIAA-88-4368,1988.

21. Guicheteau, P., "Bifurcation Theory in Flight Dynamics - An Application to a Real Combat Aircraft, ICAS-90-5.10.4, 1990.

INTRODUCTION TO

QUANTITATIVE FEEDBACK THEORY (QFT) TECHNIQUE

Constantine H. Houpis
Air Force Institute Of Technology
Wright-Patterson AFB, Ohio, 45433, USA

I -- INTRODUCTION

I-1 -- Quantitative Feedback Theory -- QFT has achieved the status[9] as a powerful design technique for the achievement of assigned performance tolerances over specified ranges of plant parameter uncertainties without and with control effector failures. It is a frequency domain design technique utilizing the Nichols chart (NC) to achieve a desired robust design over the specified region of plant parameter uncertainty. An introduction to QFT analog and discrete design techniques is presented for both multiple-input single-output (MISO)[1,5,13] and multiple-input multiple-output (MIMO)[3-4,6-7,10-12] control systems. QFT CAD packages are readily available to expedite the design process. The purposes of these lectures are: (1) to provide a basic understanding of QFT, (2) to provide the minimum amount of mathematics necessary to achieve this understanding, (3) to discuss the basic design steps, and (4) to present 2 practical examples.

I-2 -- Why Feedback? -- For the answer to the question of "Why do you need QFT?" consider the following system.

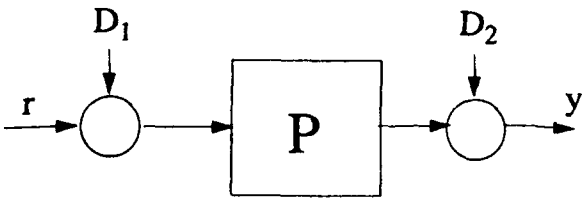

Fig. 1. An open-loop system (basic plant)

The plant P responds to the input r(t) with the output y(t) in the face of disturbances $d_1(t)$ and $d_2(t)$. If it is desired to achieve a specified system transfer function T(s) [= Y(s)/R(s)] then it is necessary to insert a prefilter, whose transfer function is T(s)/P(s), as shown in Fig. 2.

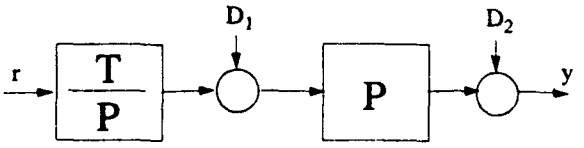

Fig. 2 A compensated open-loop system

This compensated system produces the desired output as long as the plant does not change and there are no disturbances. This type of system is sensitive to changes in the plant (or uncertainty in the plant), and the disturbances are reflected directly into the output. Thus, it is necessary to feed back the information in the output in order to reduce the output sensitivity to parameter variation and attenuate the effect of disturbances on the plant output.

In designing a control system, it is desired to utilize a technique that:

a. Addresses all known plant variations up front.

b. Incorporates information on the desired output tolerances.

c. Maintains reasonably low loop gain (reduce the "cost of feedback").

Item c is important in order to avoid the problems associated with sensor noise amplification, saturation, and high frequency uncertainties.

I-3 -- What Can QFT Do -- Assume the characteristics of a plant, that is to be controlled over a specified region of operation, vary. This plant parameter uncertainty may be described by the Bode plots of Fig. 3. This figure represents the range of variation of plant magnitude (dB) and phase over a specified frequency range. The bounds of this variation, for this example, can be described by 6 LTI plant transfer functions. By the application of QFT a single compensator and a prefilter may be designed to achieve a robust design.

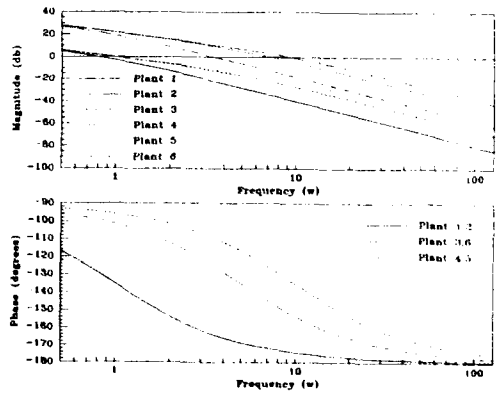

Fig. 3 Bode plots of 6 LTI plants: the range of parameter uncertainty.

I-4 -- Benefits of QFT -- The benefits of QFT may be summarized as follows:

a. The result is a robust design which is insensitive to plant variation.

b. There is one design for the full envelope (no need to verify plants inside templates).

c. Any design limitations are apparent up front.

d. There is less development time for a

full envelope design.

e. One can determine achievable specifications early in the design process.

f. One can redesign for changes in the specifications quickly.

g. Structure of compensator (controller) is determined up front.

II. The MISO Analog Control System[1]

II-1 -- Introduction -- As shown in Sec IV-2, an mxm feedback control system can be represented by an equivalent m^2 MISO feedback control systems shown in Fig. 4. Thus this and the next section present an introduction to the QFT technique by considering only a MISO system.

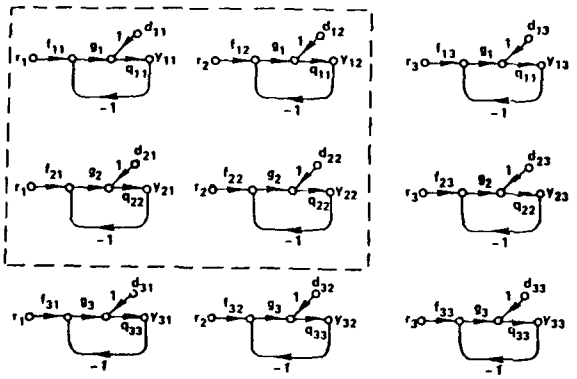

Fig. 4 m^2 MISO equivalent of a 3x3 MIMO feedback control system.

II-2 -- MISO System -- The MISO QFT design technique is presented in terms of the minimum-phase (m.p.) LTI MISO system of Fig. 5. The control ratios for tracking (D = 0) and for disturbance rejection (R = 0) are, respectively,

$$T_R = \frac{F(s)G(s)P(s)}{1 + G(s)P(s)} = \frac{F(s)L(s)}{1 + L(s)} \qquad (1)$$

$$T_D = \frac{P(s)}{1 + G(s)P(s)} = \frac{P(s)}{1 + L(s)} \qquad (2)$$

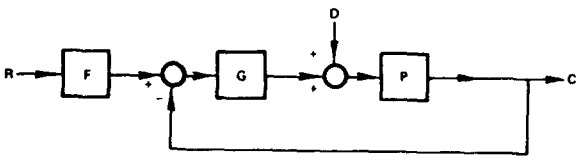

Fig. 5 A MISO plant

The design objective is to design the F(s) and G(s) so the specified robust design is achieved for the given region of plant parameter uncertainty. The design procedure to accomplish this objective is as follows:

Step 1: Synthesize the desired tracking model.
Step 2: Synthesize the desired disturbance model.
Step 3: Specify the J LTI plant models that define the boundary of the region of plant parameter uncertainty.
Step 4: Obtain plant templates, at specified frequencies, that pictorially described the region of plant parameter uncertainty on the NC.
Step 5: Select the nominal plant transfer function $P_o(s)$.
Step 6: Determine the stability contour (U-contour) on the NC.
Steps 7-9: Determine the disturbance, tracking, and optimal bounds on the NC.
Step 10: Synthesize the nominal loop function $L_o(s) = G(s)P_o(s)$ that satisfies all bounds and the stability contour.
Step 11: Based upon Steps 1 through 10 synthesize the prefilter F(s).
Step 12: Simulate the system to obtain the time response data for all J plants.

The following sections illustrate this design procedure.

II-3 -- Synthesize Tracking Models -- The tracking thumbprint specifications, based upon satisfying some or all of the step forcing function figures of merit for underdamped (M_p, t_p, t_s, t_r, K_m) and overdamped (t_s, t_r, K_m) responses, respectively, for a simple-second system, are depicted in Fig. 6(a). The Bode plots corresponding to the time responses $y(t)_U$ [Eq. (3)] and $y(t)_L$ [Eq. (4)] in Fig. 6(b) represent the upper bound B_U and lower bound B_L, respectively, of the thumbprint specifications; i.e., an acceptable response y(t) must lie between these bounds. Note that for the m.p. plants, only the tolerance on $|T_R(j\omega_i)|$ need be satisfied for a satisfactory design. For nonminimum-phase (n.m.p.) plants, tolerances on $\angle T_R(j\omega_i)$ must also be specified and satisfied in the design process.[4,5] It is desirable to synthesize the tracking control ratios

$$T_{R_U} = \frac{(\omega_n^2/a)(s + a)}{s^2 + 2\zeta\omega_n s + \omega_n^2} \qquad (3)$$

$$T_{R_L} = \frac{K}{(s - \sigma_1)(s - \sigma_2)(s - \sigma_3)} \qquad (4)$$

corresponding to the upper and lower bounds T_{RU} and T_{RL}, respectively, so that $\delta_R(j\omega_i)$ increases as ω_i increases above the 0 dB crossing frequency of T_{RU}. This characteristic of δ_R, which determines the tracking bounds $B_R(j\omega_i)$, simplifies the process of synthesizing $L_o(s) = G(s)P_o(s)$. The achievement of the desired performance specification is based upon the frequency bandwidth BW, $0 < \omega \leq \omega_h$, which is determined by the intersection of the -12 dB line and the B_U curve in Fig. 6(b).

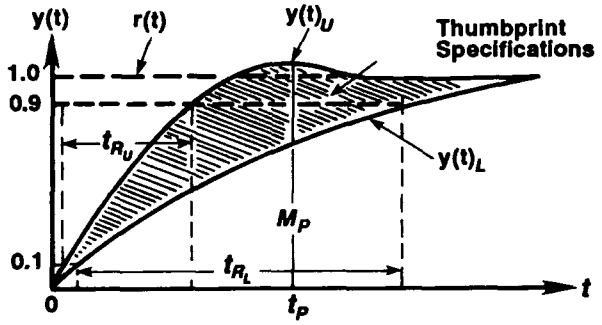

(a) Thumbprint specifications

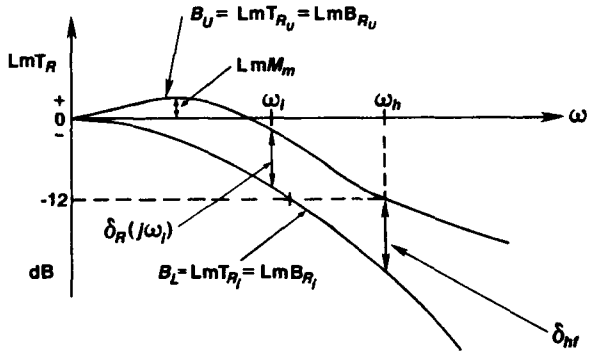

(b) Bode plots of T_R

Fig. 6 Desired response specifications

II-4 -- Disturbance Model -- The simplest disturbance control ratio model specification is $|T_D(j\omega)| = |Y(j\omega)/D(j\omega)| \leq \alpha_p$ a constant [maximum magnitude of the output based on a unit step disturbance input (d_1 of Fig.1)]. Thus the frequency domain disturbance specification is Lm $T_D(j\omega) \leq$ Lm α_p over the specified BW. Thus the disturbance specification is represented by only an upper bound on the NC over the BW.

II-5 -- J LTI Plant Models -- The simple plant, for illustrative purposes, is

$$P_j(s) = \frac{Ka}{s(s+a)} = \frac{K'}{s(s+a)} \qquad (5)$$

where $K' = Ka$, $K \in \{1,10\}$ and $a \in \{1,10\}$. The region of plant parameter uncertainty is illustrated by Fig. 7. This region is described by J LTI plants, where $j = 1,2, \ldots J$, which lie on the region's boundary. That is, the points 1, 2, 3, 4, 5, & 6 are utilized to obtain 6 LTI plant models that adequately define the region of plant parameter uncertainty.

II-6 -- Plant Templates of $P_j(s)$, $\Im P(j\omega_i)$ -- With L = GP, Eq. (1) yields

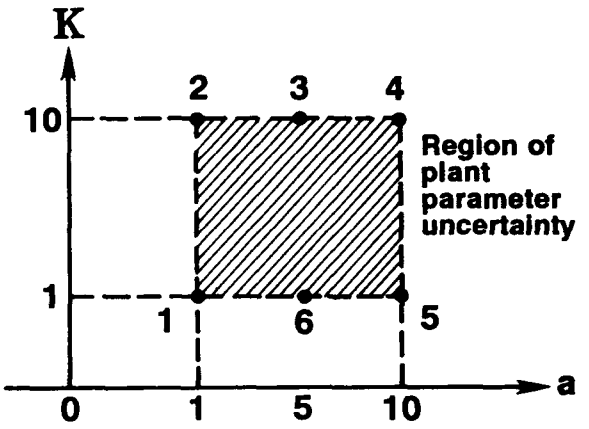

Fig. 7 Region of plant uncertainty

$$Lm\ T_R = Lm\ F - Lm\left[\frac{L}{1+L}\right] \qquad (6)$$

The change in T_R due to the uncertainty in P, since F is LTI, is

$$\Delta(Lm\ T_R) = Lm\ T_R - Lm\ F = Lm\left[\frac{L}{1+L}\right] \qquad (7)$$

By a proper design of $L = L_o$ and F, this change in T_R is restricted so that the actual value of Lm T_R always lies between B_U and B_L of Fig. 6. The first step in synthesizing an L_o is to make NC templates which characterize the variation of the plant uncertainty (see Fig. 8), as described by the J LTI functions, for various values of ω_i over the BW. The plant template boundary can be obtained by mapping the boundary of the plant parameter uncertainty region, Lm $\mathbf{P}_j(j\omega_i)$ vs $\angle\mathbf{P}_j(j\omega_i)$, as shown on the NC in Fig. 8. A curve is drawn through the points 1, 2, 3, 4, 5, and 6. The shaded area, labeled $\Im P(j1)$, may be represented by a plastic template. Templates for other values of ω_i are obtained in a similar manner. A characteristic of these templates is: starting from a low value of ω_i, they widen (angular width becomes larger) for increasing values of ω_i then as ω_i takes on larger values and approaches infinity they become narrower and eventually approach a staight line of height V dB [see Eq. (9)].

II-7 -- Nominal Plant -- While any plant case can be chosen it is an accepted practice to select, whenever possible, a plant whose NC point is always at the lower left corner for all frequencies for which the templates are obtained.

II-8 -- U-Contour (Stability bound) -- The frequency domain specifications on system performance [Fig. 6(b)] identify a minimum damping ratio ζ for the dominant roots of the closed-loop system which becomes a bound on the value of $M_p = M_m$. On the NC this bound on $M_m = M_L$ [Figs. 6(b) and 9] establishes a region that can not be penetrated by the templates and by the

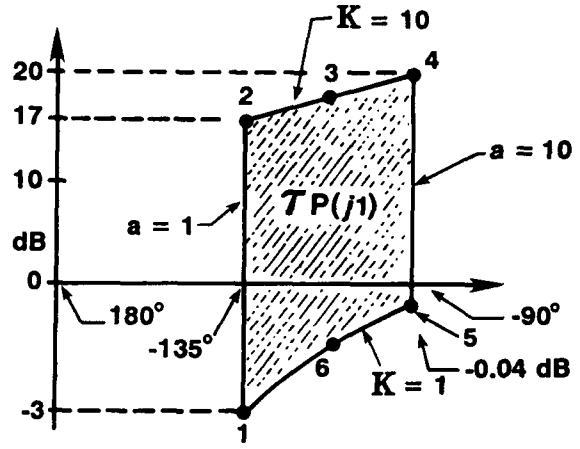

Fig. 8 The template $\mathcal{T}\mathbf{P}(j1)$

$\mathbf{L}(j\omega)$ plot for all ω. This region's boundary is referred to as the universal high-frequency boundary (UHFB) or stability bound (U-contour) because this becomes the dominating constraint on $\mathbf{L}(j\omega)$. Thus, the top portion (efa) of the M_L contour becomes part of the U-contour. For a large problem class, as $\omega \to \infty$, the limiting value of the plant transfer function approaches

$$\lim_{\omega \to \infty} [P(j\omega)] = \frac{K}{\omega^{\lambda}} \qquad (8)$$

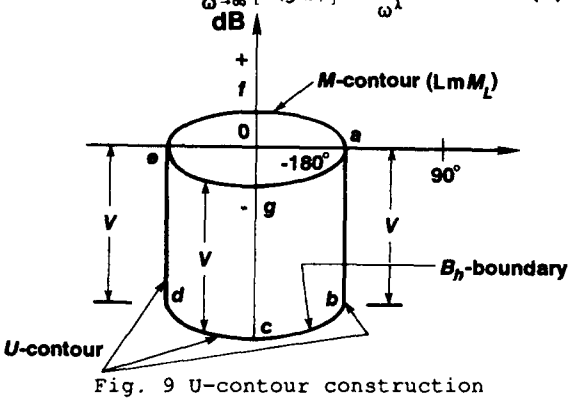

Fig. 9 U-contour construction

where λ represents the excess of poles over zeros of P(s). The plant template, for this problem class, approaches a vertical line of length equal to

$$\Delta \triangleq \lim_{(\omega \to \infty)} [Lm\ P_{max} - Lm\ P_{min}] \qquad (9)$$
$$= Lm\ K_{max} - Lm\ K_{min} = V \ \ dB$$

If the nominal plant is chosen at $K = K_{min}$, then the constraint M_L gives a boundary which approaches the U-contour abcdefa of Fig. 9.

II-9 -- Optimal Bounds $\mathbf{B}_o(j\omega)$ on $\mathbf{L}_o(j\omega)$ -- The determination of the tracking $\mathbf{B}_R(j\omega_i)$ and the disturbance $\mathbf{B}_D(j\omega_i)$ bounds are required in order to yield the optimal bounds $\mathbf{B}_o(j\omega_i)$ on $\mathbf{L}_o(j\omega_i)$.

II-9.1 -- Tracking Bounds -- The solution for $\mathbf{B}_R(j\omega_i)$ requires that the condition

(actual) $\Delta T_R(j\omega_i) \leq \delta_R(j\omega_i)$ dB (Fig. 6))

must be satisfied. Thus it is necessary to determine the resulting constraint, or bound $\mathbf{B}_R(j\omega_i)$, on $\mathbf{L}(j\omega_i)$. The procedure is to pick a nominal plant $P_o(s)$ and to derive NC tracking bounds, at specified ω_i values and by use of templates or a CAD package, on the resulting nominal function $L_o(s) = G(s)P_o(s)$. That is, along a NC phase angle grid line move the nominal point on the template $\mathcal{T}\mathbf{P}(j\omega_i)$ up or down, without rotating the template, until it is tangent to two M-contours whose difference in M values is essentially equal to δ_R. When this condition has been achieved the location of the nominal point on the template becomes a point on the tracking bound $\mathbf{B}_R(j\omega_i)$ on the NC. This procedure is repeated on sufficient NC angle grid lines to provide enough points to draw $\mathbf{B}_R(j\omega_i)$ and for all values of frequency for which templates have been obtained.

II-9.2 -- Disturbance Bounds -- The general procedure for determining disturbance bounds for the MISO control system of Fig. 5 is outlined as follows (for details see Ref. 2). From Eq. (2) the following equation is obtained:

$$T_D = \frac{P_o}{\frac{P_o}{P} + L_o} = \frac{P_o}{W} \qquad (10)$$

where $\mathbf{W} = (\mathbf{P}_o/\mathbf{P}) + \mathbf{L}_o$. From Eq. (10), setting $Lm\ \mathbf{T}_D = \delta_D = Lm\ \alpha_p$, the following relationship is obtained:

$$Lm\ \mathbf{W} = Lm\ \mathbf{P}_o - \delta_D \qquad (11)$$

For each value of ω_i for which the NC templates are obtained the magnitude of $|\mathbf{W}(j\omega_i)|$ is obtained from Eq. (11). This magnitude in conjuction with the equation $\mathbf{W}(j\omega_i) = [\mathbf{P}_o(j\omega_i)/\mathbf{P}(j\omega_i)]$ are utilized to obtain a graphical solution for $\mathbf{B}_D(j\omega_i)$ as shown in Fig. 10[1]. In this figure the template is plotted in rectangular or polar coordinates.

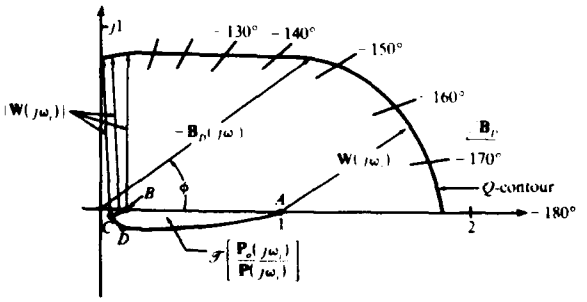

Fig. 10 Graphical evaluation of $\mathbf{B}_D(j\omega_i)$

II-9.3 -- Optimal Bounds -- For the case shown in Fig. 11 $\mathbf{B}_o(j\omega_i)$ is composed of those portions of each respective bound $\mathbf{B}_R(j\omega_i)$ and $\mathbf{B}_D(j\omega_i)$ that have the largest dB values. The synthesized $\mathbf{L}_o(j\omega_i)$ must lie on or just above these bound $\mathbf{B}_o(j\omega_i)$.

II-10 -- Synthesizing (or Loop Shaping) $L_o(s)$ and $F(s)$ -- The shaping of $\mathbf{L}_o(j\omega)$ is shown by the dashed curve in Fig. 11. A

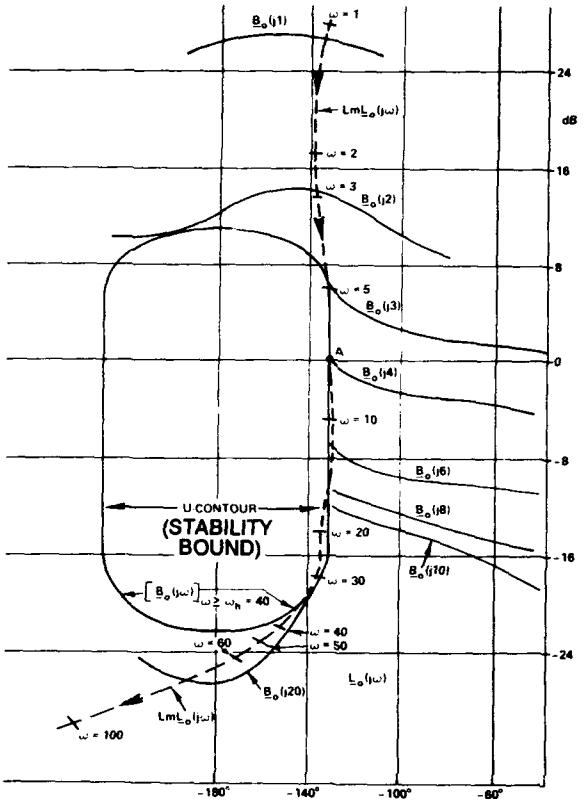

Fig. 11 Bounds $\mathbf{B}_o(j\omega_i)$ and loop shaping

point such as Lm $\mathbf{L}_o(j2)$ must be on or above $\mathbf{B}_o(j2)$. Further, in order to satisfy the specifications, $\mathbf{L}_o(j\omega)$ cannot violate the U-contour. In this example a reasonable $\mathbf{L}_o(j\omega)$ closely follows the U-contour up to ω = 40 r/s and must stay below it above ω = 40 as shown in Fig 11. It also must be a Type 1 function (one pole at the origin). Synthesizing a rational function $L_o(s)$ which satisfies the above specification involves building up the function

$$\mathbf{L}_o(j\omega) = \mathbf{L}_{ok}(j\omega) = \mathbf{P}_o(j\omega)\prod_{k=0}^{W}[K_k G_k(j\omega)] \qquad (12)$$

where for k = 0, $\mathbf{G}_o$ = 1∠0°, and K = $\prod_{k=0}K_k$. In order to minimize the order of the compensator a starting point for building up the loop transmission function is to initially assume that $\mathbf{L}_{oo}(j\omega) = \mathbf{P}_o(j\omega)$ as indicated in Eq. (12). $\mathbf{L}_o(j\omega)$ is built up term-by-term or by a CAD loop shaping routine,[8] in order (1) that the point $\mathbf{L}_o(j\omega_i)$ lies on or above the corresponding optimal bound $\mathbf{B}_o(j\omega_i)$ and (2) to stay just outside the U-contour in the NC of Fig. 11. The design of a proper $L_o(s)$ guarantees only that the variation in $|\mathbf{T}_R(j\omega_i)|$ is less than or equal to that allowed, i.e., $\delta_R(j\omega_i)$. The purpose of the prefilter F(s) is to position Lm $[\mathbf{T}(j\omega)]$ within the frequency domain specifications, i.e., that it always lies between B_U and B_L [Fig. 6(b)] for all J plants. The method for determining F(s) is discussed in the next section. Once a satisfactory $L_o(s)$ is achieved then the compensator is given by $G(s) = L_o(s)/P_o(s)$. Note that for this example $\mathbf{L}_o(j\omega)$ slightly intersects the U-contour at frequencies above ω_h. Because of the inherent over-design feature of the QFT technique, as a first trial design, no effort is made to fine tune the synthesis of $L_o(s)$. If the simulation results are not satisfactory then a fine tuning can be made. The available CAD packages simplify and expedite this fine tuning.

II-11 -- Prefilter Design[1,2,4,5] -- Design of a proper $L_o(s)$ guarantees only that the variation in $|\mathbf{T}_R(j\omega)|$ is less than or equal to that allowed, i.e., Lm $\mathbf{T}_R(j\omega)_{max}$ - Lm $\mathbf{T}_R(j\omega)_{min} \leq \delta_R(j\omega)$. The purpose of the prefilter F(s) is to position

$$Lm\,\mathbf{T}(j\omega) = Lm\,\frac{\mathbf{L}(j\omega)}{1+\mathbf{L}(j\omega)} \qquad (13)$$

within the frequency domain specifications. A method for determining the bounds on F(s) is as follows:

Step 1: Place the nominal point of the ω_i plant template on the $\mathbf{L}_o(j\omega_i)$ point on the $\mathbf{L}_o(j\omega)$ curve on the NC (see Fig. 12).

Step 2: Traversing the template, determine the maximum Lm T_{max} and the minimum Lm T_{min} values of Eq. (13) are obtained from the M-contours.

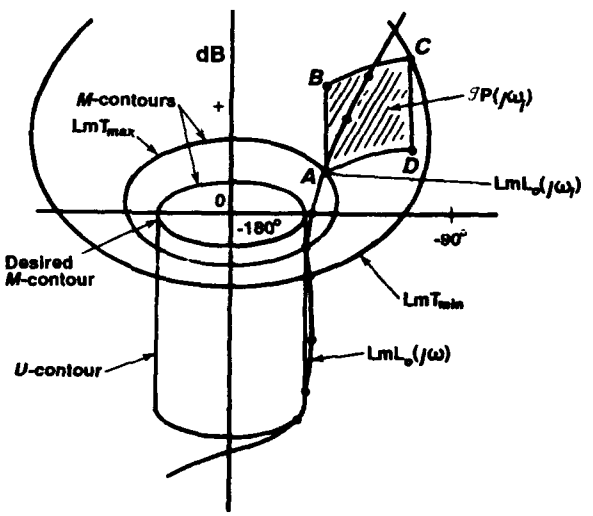

Fig. 12 Prefilter determination

Step 3: Based upon obtaining sufficient data points within the desired BW, for various values of ω_i, and in conjunction with the data used to obtain Fig. 6(b) the plots of Fig. 13 are obtained.

Step 4: Utilizing Fig. 13, the straight-

line Bode technique and the condition

$$\lim_{s \to 0} F(s) = 1 \qquad (14)$$

for a step forcing function, an F(s) is synthesized that lies within the upper and lower plots in Fig. 13.

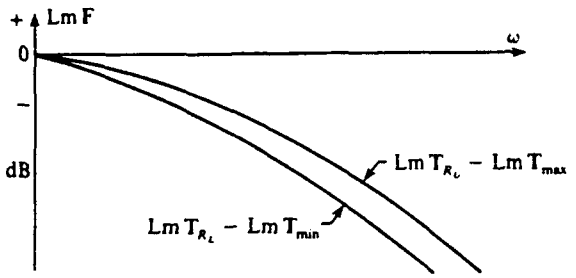

Fig. 13 Frequency bour ds on F(s)

II-12 -- Simulation -- The goodness of the synthesized $L_o(s)$ and F(s) is determined by simulating the QFT designed control system for all J plants. CAD packages, discussed in Sec. II-13, are available that expedite this simulation phase of the complete design process.

II-13 -- MISO QFT CAD Packages -- The first useable MISO QFT CAD package was developed in 1986 for the analog design (see App. A) and in 1991 for the discrete design (see App. B) at the Air Force Institute of Technology (AFIT). This CAD package has been a catalyst in assisting the newcomer to QFT to understand the fundamentals of this powerful design technique.

II-13.1 -- MISO QFT CAD -- The AFIT package is called "ICECAP/QFT" which is designed for the VAX. Those desiring a copy of this package can contact: Professor Gary B. Lamont, AFIT/ENG, Wright-Patterson AFB, OH 45433. Currently Professor Lamont is developing a PC version of this package. These packages have been designed as an "educational tool."

II-13.2 -- MISO QFT PC CAD -- Dr. Oded Yaniv, Tel-Aviv University, Israel, has a MISO QFT PC CAD package for both analog and discrete system design. This package can be purchased from Dr. Yaniv.

III. The MISO Discrete Control System[13]

III-1 -- Introduction -- The bilinear transformation, z-domain to the w'-domain and vice-versa, is utilized in order to accomplish the QFT design for both MISO and MIMO sampled-data (discrete) control system design in the w'-domain. This transformation enables the use of the MISO QFT analog design technique to be readily used, with minor exceptions, to perform the QFT design for the controller G(w'). If the w'-domain simulations satisfy the desired performance specification then by use of the bilinear transformation the z-domain controller G(z) is obtained. With this controller a discrete-time simulation is obtained to verify the goodness of the design. The QFT technique requires the determination of the minimum sampling frequency $(\omega_s)_{min}$ bandwidth that is needed for a satisfactory design.[13,14] The larger the plant uncertainty and the narrower the system performance tolerances are, the larger must be the value of $(\omega_s)_{min}$. Henceforth, the prime is omitted from w' thus whenever the symbol w is used it is be interpreted as w'.

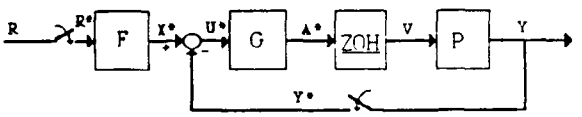

Fig. 14 A MISO sampled-data control system

III-2 -- The MISO Sampled-data Control System -- Figure 14 represents the MISO discrete control, having plant uncertainty, that is to be designed by the QFT technique. The equations that describe this system are as follows:

$$P_z(z) = G_{zo}P(z) = (1 - z^{-1})\mathbf{Z}\left[\frac{P(s)}{s}\right] = (1 - z^{-1})P_e(z) \qquad (15)$$

$$L(z) = G_{zo}P(z)G_1(z), \quad P_e \equiv \frac{P(s)}{s}, \quad P_e(z) = \mathbf{Z}\left[\frac{P(s)}{s}\right] = \mathbf{Z}[P_e] \qquad (16)$$

$$D(s) = \frac{1}{s}, \quad P_e(s) = P(s)D(s), \quad P_e(z) = \mathbf{Z}[P(s)D(s)] = PD(z) \qquad (17)$$

$$T_R = \frac{F(z)L(z)}{1 + L(z)} \qquad Y_D = \frac{PD(z)}{1 + L(z)} \qquad (18)$$

$$Y(z) = \left[\frac{L(z)F(z)}{1 + L(z)}\right]R(z) + \frac{PD(z)}{1 + L(z)} = Y_R(z) + Y_D(z) = T_R(z)R(z) + Y_D(z) \qquad (19)$$

III-3 w'-Domain -- The pertinent s-, z-, and w-plane relationships are:

$$\alpha^2 = \left(\frac{\sigma T}{2}\right)^2 \ll 2, \qquad \frac{\omega T}{2} \leq 0.297 \qquad (20)$$

$$s = \sigma + j\omega \qquad (a)$$

$$w = u + jv = \left(\frac{2}{T}\right)\left[\frac{z - 1}{z + 1}\right] \qquad (b) \qquad (21)$$

$$z = \frac{Tw + 2}{-Tw + 2} \qquad (a)$$

$$v = \left(\frac{2}{T}\right)\tan\left(\frac{\omega T}{2}\right) = \left(\frac{\pi}{\omega_s}\right)\tan\left(\frac{\omega\pi}{\omega_s}\right) \quad (b) \qquad (22)$$

$$\omega_s = 2\pi/T, \qquad \boldsymbol{z} = e^{\sigma T}\angle\omega T = |\boldsymbol{z}|\angle\omega T \qquad (23)$$

III-4 -- Assumptions -- For this paper the following assumptions are assumed:

a. Minimum-phase (mp) stable plants
b. The analogue desired models, Eqs (3) and (4), yield the desired time response characteristics for the discrete-time system.
c. The sampling time T is small enough so that over the BW, $0 < \omega \leq \omega_b$, Eq. (23) is valid permitting the approximation $s \approx w$ and in-turn

$$T_R(w) \approx [T_R(s)]_{s=w} \qquad (24)$$

Both the upper and lower bound w-domain tracking models are obtained in this manner. The disturbance specification is the same as for the analog case.

III-5 -- Nonminimum Phase $L_o(w)$ -- It is important to note that in the w domain any practical L(w) is nonminimum phase (nmp) containing a zero at 2/T (the sampling zero). This result is due to the fact that any practical L(z) has an excess of at least one pole over zeros. Thus, the design technique for a stable uncertain plant is modified[14] to incorporate the all-pass filter (apf)

$$A(w) = \frac{w - \frac{2}{T}}{w + \frac{2}{T}} \qquad A'(w) = \left[\frac{\frac{2}{T} - w}{\frac{2}{T} + w}\right] \qquad (25)$$

as follows: let the nominal loop transmission be defined as:

$$L_o \equiv L_{mo}(w)A(w) = L_{mo}(w)A'(w) \qquad (26)$$

From Eq. (26) it is seen that

$$\angle\boldsymbol{L}_{mo}(jv) = \angle\boldsymbol{L}_o(jv) - \angle\boldsymbol{A}'(jv) \qquad (27)$$

where

$$-\angle\boldsymbol{A}'(jv) = 2\tan^{-1}\frac{vT}{2} > 0 \qquad (28)$$

An analysis of Eqs. (26) through (28) reveals that the bounds $\mathbf{B}_i'(jv_i)$ on $\mathbf{L}_o(jv)$ become the bounds $\mathbf{B}_{mo}(jv_i)$ on $\mathbf{L}_{mo}(jv)$ by shifting, over the desired BW, $\mathbf{B}_i'(jv_i)$ positively (to the right on the NC) by the angle $\angle\mathbf{A}'(jv_i)$, as shown in Fig. 15. The U-contour ($\mathbf{B}_i'$) must also be shifted to the right by the same amount, at the specified frequencies v_i, to obtain the shifted U-contour $\mathbf{B}_{hi}(jv_i)$. The contour $\mathbf{B}_{hi}'$ is shifted to the right until it reaches the vertical line $\angle\mathbf{L}_{mo}(jv_K) = 0°$. The value of v_K, which is function of ω_s and the phase margin angle as shown in Fig. 15,[13] is given by

$$2\tan^{-1}\left(\frac{v_K T}{2}\right) = 180° - \gamma \qquad (29)$$

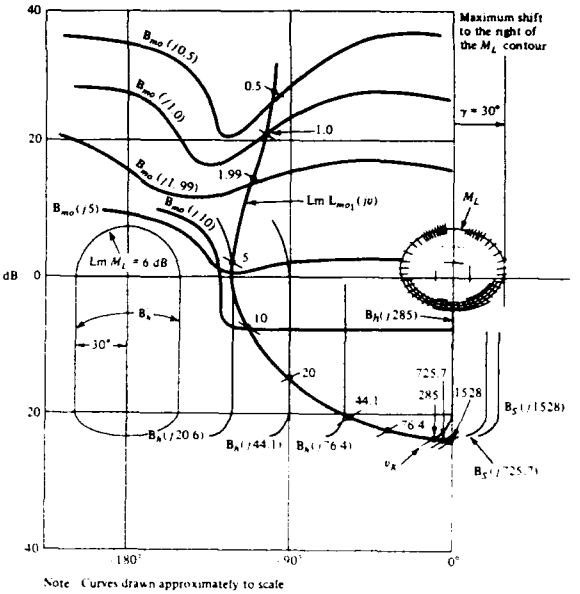

Fig. 15 The shifted bounds on the NC

It should be mentioned that loop shaping or synthesizing $L_o(w)$ can be done directly without the use of an apf.

III-6 -- Plant Templates $\mathfrak{Z}\mathbf{P}(jv_i)$ -- The plant templates in the w-domain have the same characteristic as those for the analog case (see Sec. II-4) for the frequency range $0 < \omega_i \leq \omega_s/2$ (see Fig. 16(a). In the frequency range $\omega_s/2 < \omega_i < \infty$ the w-domain templates widen once again and then eventually approach a vertical line [see Fig. 16(b)].

III-7 -- Synthesizing $L_{mo}(w)$ -- The frequency spectrum is divided into four regions for the purpose of synthesizing an $\mathbf{L}_{mo}(w)$ that will satisfy the system performance specifications for the plant having plant parameter uncertainty. These four regions are:

Region 1: For the frequency range where Eq. (23) is satisfied use the analog templates; i.e. $\mathfrak{Z}\mathbf{P}(j\omega_i) = \mathfrak{Z}\mathbf{P}(jv_i)$. The w-domain tracking, disturbance and optimal bounds and the U-contour are essentially the same as those for the analog system. The templates are used to obtain these bounds on the NC in the same manner as for the analog system.

Region 2: For the frequency range $v_{0.25} < v_i < v_k$, where $\omega_i \leq 0.25\omega_s$, use the w-domain templates. These templates are used to obtain all 3 types of bounds, in the same manner as for the analog system, in this region and the corresponding $\mathbf{B}'_h(jv_i)$ contours are also obtained.

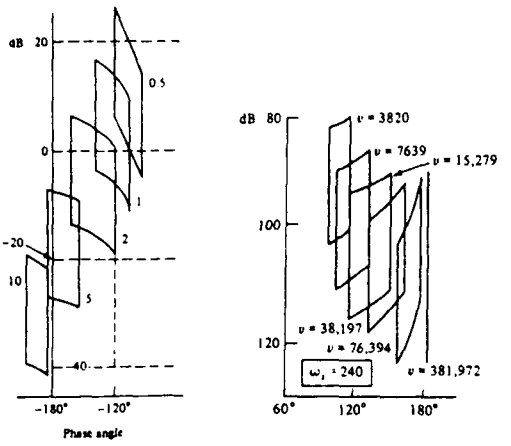

(a) (b)

Fig. 16 w-domain plant templates

Region 3: For the frequency range $v_h < v_i \leq v_K$, for the specified value of ω_s, only the B'_h-contours are plotted.

Region 4: For the frequency range $v_h > v_K$ use the w-domain templates. Since the templates $\mathfrak{I}\mathbf{P}_e(jv_i)$ broaden out again for $v_i > v_K$ (see Fig.16) it is necessary to obtain the more stringent (stability) bounds $\mathbf{B}_S$ shown in Fig. 17. The templates are used only to determine the stability bounds B_S.

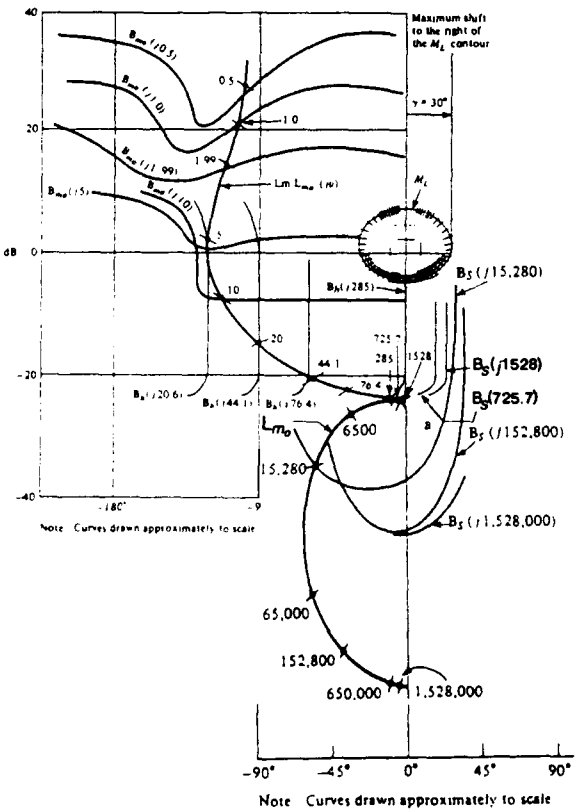

Fig. 17 A satisfactory design: $L_{mo}(jv)$ at $\omega_s = 240$.

The synthesis of $L_{mo}(w)$ involves the synthesizing the following function:

$$\boldsymbol{L}_{mo}(jv) = \boldsymbol{P}_{eo}(jv) \prod_{k=0}^{w} [K_k G_k(jv)] \qquad (30)$$

where the nominal plant $P_{eo}(w)$ is the plant from the J plants that has the smallest dB value and the largest (most negative) phase lag characteristic. The final synthesized $L_{mo}(w)$ function must be one that satisfies the following conditions:

1. In Regions 1 and 2 the point on the NC that represents the dB value and phase angle of $\mathbf{L}_{mo}(jv_i)$ must be such that it lies on or above the corresponding $\mathbf{B}_{mo}(jv_i)$ bound (see Fig. 15).

2. The values of Eq. (30) for the frequency range of Region 3 must lie to the right or just below the corresponding $\mathbf{B}'_h$-contour (see Fig. 15).

3. The value of Eq. (30) for the frequency range of Region 4 must lie below the $\mathbf{B}_S$ contour for negative phase angles on the NC (see condition 4).

4. In utilizing the bilinear transformation of Eq. (22a), the w-domain transfer functions are all equal order over equal order.

5. The Nyquist stability criterion dictates that the $\mathbf{L}_{mo}(jv)$ plot is on the "right side" or the "bottom right side" of the $\mathbf{B}_h(jv_i)$-contours for the frequency range of $0 \leq v_i \leq v_K$. It has been shown that:[3]

(a) $\mathbf{L}_{mo}(jv)$ must reach the <u>right-hand bottom</u> of $\mathbf{B}_h(jv_K)$, i.e., approximately point K in Fig. 17, at a value of $v \leq v_K$, and

(b) $\angle \mathbf{L}_{mo}(jv_K) < 0°$ in order that there exists a practical L_{mo} which satisfies the bounds $\mathbf{B}(jv)$ and provides the required stability.

6. For the situation where one or more of the J LTI plants, that represent the uncertain plant parameter characteristics, represent unstable plants and one of these unstable plants is selected as the nominal plant, <u>then the apf to be used in the QFT design must include all right-hand-plane (rhp) zeros of</u> P_{eo}. This situation is not discussed in this paper. Note: for experienced QFT designers $L_o(v)$ can be synthesized without the use of apf. This approach is not covered in this paper.

The synthesized $L_{mo}(w)$, obtained following the guidelines of this section, is shown in Fig. 17.

<u>III-8 -- Prefilter Design</u> -- The procedure for synthesizing F(w) is the same as for the analog case (see Sec. II-11) over the frequency range $0 < v_i \leq v_h$. In order to

satisfy condition 4 of Sec. III-7, a nondominating zero or zeros ("far-left" in the w-plane) are inserted so that the final synthesized F(w) is equal order over equal order.

III-9 -- w-Domain Simulation -- The goodness of the synthesized $L_{mo}(w)$ [or $L_o(w)$] and F(w) is determined by first simulating the QFT w-domain designed control system for all J plants in the w-domain (an "analog" time domain simulation). See Sec. II-13 for CAD packages that expedite this simulation.

III-10 -- z-Domain -- The test of the goodness of the w-domain QFT designed system is a discrete-time domain simulation of the system in Fig. 14. To accomplish this simulation, the w-domain transfer functions G(w) and F(w) are transformed to the z-domain by use of the bilinear transformation of Eq. (21b). This transformation is utilized since the degree of the numerator and denominator polynomials of these functions are equal and the controller and prefilter do not contain a zero-order-hold device.

III-10.1 -- Comparison of the Controller's w- and z-Domain Bode Plots -- Depending on the value of the sampling time T, warping may be sufficient to alter the loop shaping characteristics of the controller when it is transformed from the w- to the z-domain. For the warping effect to be minimal the Bode plots of the w- and z-domain controllers must essentially lie on top of one another within the frequency range $0 < \omega \leq [(2/3)(\omega_s/2)]$. If the warping is negligible then a discrete-time simulation can proceed. If not, a smaller value of T needs to be selected.

III-10.2 -- Accuracy -- The available CAD package determines the degree of accuracy of the calculations and simulations. The smaller the value of T the greater the degree of accuracy that is required to be maintained. The accuracy is enhanced by simulating G(z) and F(z) as a set of g and f cascaded transfer functions, respectively; that is

$$G(z) = G_1(z)G_2(z) \cdots G_g(z)$$
$$F(z) = F_1(z)F_2(z) \cdots F_f(z) \qquad (31)$$

III-10.3 -- Analysis of Characteristic Equation $Q_j(z)$ -- Depending on the value of T and the plant parameter uncertainty, the pole-zero configuration in the vicinity of the -1 + j0 point in the z-plane for one or more of the J LTI plants can result in an unstable discrete-time response. Thus before proceeding with a discrete-time domain simulation an analysis of the characteristic equation $Q_j(z)$ for all J LTI plants must be made. If an unstable system exists an analysis of $Q_j(z)$ and the corresponding root-locus may reveal that a slight relocation of one or more controller pole in the vicinity of the -1 + j0 point toward the origin may ensure a stable system for all J plants and maintain the desired loop shaping characteristic of G(z).

III-10.4 -- Simulation and CAD Packages -- With the design checks of Secs. III-10.1 through III-10.3 satisfied then a discrete-time simulation is performed to verify that the desired performance specifications are achieved. To enhance the MISO QFT discrete control system design procedure that is presented in this chapter the CAD flowchart of Sec. II-13.1 is shown in App. B.

IV -- MIMO Systems[2-12]

IV-1 -- Introduction -- Figure 18 represents an mxm MIMO closed-loop system in which **F**, **G**, and **P** are each m x m matrices, and $\mathcal{P} = \{\mathbf{P}\}$ is a set of J matrices due to plant parameter uncertainty. There are m^2 closed-loop system transfer functions (transmissions) t_{ij} contained within its system transmission matrix, i.e., $\mathbf{T} = \{t_{ij}\}$ relating the outputs y_i to the inputs r_j, e.g., $y_i = t_{ij}r_j$. These relationship hold for both the s- and w-domain analysis of a MIMO system. In a quantitative problem statement there are tolerance bounds on each t_{ij}, giving a

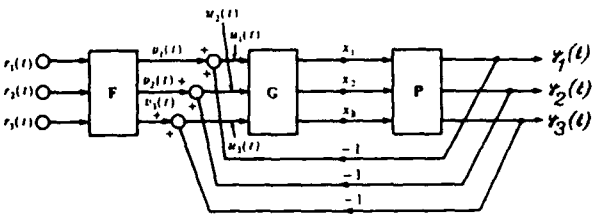

Fig. 18 A 3x3 MIMO feedback control system.

set of m^2 acceptable regions τ_{ij} which are to be specified in the design, thus $t_{ij} \in \tau_{ij}$ and $\mathfrak{T} = \{\tau_{ij}\}$. From Fig. 18 the system control ratio relating **r** to **y** is:

$$\boldsymbol{T} = [\boldsymbol{I} + \boldsymbol{PG}]^{-1}\boldsymbol{PGF} \qquad (32)$$

The t_{ij} expressions derived from this expression are very complex and not suitable for analysis. The QFT design procedure systematizes and simplifies the manner of achieving a satisfactory system design for the entire range of plant uncertainty. In order to readily apply the QFT technique another mathematical system description is presented in the next section. The material presented in this chapter pertains to both the s- and w-domain analysis of MIMO systems.

IV-2 -- Derivation of m^2 MISO System Equivalents -- The **G**, **F**, **P** and $\mathbf{P}^{-1}$ matrices are defined as follows:

$$\boldsymbol{G} = \begin{bmatrix} g_1 & 0 & \cdots & 0 \\ 0 & g_2 & \cdots & 0 \\ \vdots & \vdots & \vdots & \vdots \\ 0 & 0 & \cdots & g_m \end{bmatrix} \qquad \boldsymbol{F} = \begin{bmatrix} f_{11} & f_{12} & \cdots & f_{1m} \\ f_{21} & f_{22} & \cdots & f_{2m} \\ \vdots & \vdots & \vdots & \vdots \\ f_{m1} & f_{m2} & \cdots & f_{mm} \end{bmatrix} \tag{33}$$

$$\boldsymbol{P} = \begin{bmatrix} p_{11} & p_{12} & \cdots & p_{1m} \\ p_{21} & p_{22} & \cdots & p_{2m} \\ \vdots & \vdots & \vdots & \vdots \\ p_{m1} & p_{m2} & \cdots & p_{mm} \end{bmatrix} \qquad \boldsymbol{P}^{-1} = \begin{bmatrix} p_{11}^{*} & p_{12}^{*} & \cdots & p_{1m}^{*} \\ p_{21}^{*} & p_{22}^{*} & \cdots & p_{2m}^{*} \\ \vdots & \vdots & \vdots & \vdots \\ p_{m1}^{*} & p_{m2}^{*} & \cdots & p_{mm}^{*} \end{bmatrix} \tag{34}$$

Although only a diagonal **G** matrix is considered, the use of a nondiagonal **G** matrix may allow the designer more design flexiblity.[2] The m^2 effective plant transfer functions are based upon defining:

$$q_{ij} \equiv \frac{1}{p_{ij}^{*}} = \frac{\det \boldsymbol{P}}{adj \boldsymbol{P}_{ij}} \tag{35}$$

There is a requirement that det**P** be mp. The **Q** matrix is then formed as:

$$\boldsymbol{Q} = \begin{bmatrix} q_{11} & q_{12} & \cdots & q_{1m} \\ q_{21} & q_{22} & \cdots & q_{2m} \\ \vdots & \vdots & \vdots & \vdots \\ q_{m1} & q_{m2} & \cdots & q_{mm} \end{bmatrix} = \begin{bmatrix} \frac{1}{p_{11}^{*}} & \frac{1}{p_{12}^{*}} & \cdots & \frac{1}{p_{1m}^{*}} \\ \frac{1}{p_{21}^{*}} & \frac{1}{p_{22}^{*}} & \cdots & \frac{1}{p_{2m}^{*}} \\ \vdots & \vdots & \vdots & \vdots \\ \frac{1}{p_{m1}^{*}} & \frac{1}{p_{m2}^{*}} & \cdots & \frac{1}{p_{mm}^{*}} \end{bmatrix} \tag{36}$$

The matrix $\boldsymbol{P}^{-1}$ is partitioned to the form:

$$\boldsymbol{P}^{-1} = [\, p_{ij}^{*}] = [\frac{1}{q_{ij}}] = \boldsymbol{\Lambda} + \boldsymbol{B} \tag{37}$$

where Λ is the diagonal part and **B** is the balance of $\boldsymbol{P}^{-1}$; thus $\lambda_{ij} = 1/q_{ii} = p_{ii}^{*}$, $b_{ii} = 0$, and $b_{ij} = 1/q_{ij} = p_{ij}^{*}$ for $i \neq j$. Premultipling Eq. (32) by [**I** + **PG**] yields:

$$[\boldsymbol{I} + \boldsymbol{PG}]\boldsymbol{T} = \boldsymbol{PGF} \;\rightarrow\; [\boldsymbol{P}^{-1} + \boldsymbol{G}]\boldsymbol{T} = \boldsymbol{GF} \tag{38}$$

where **P** is nonsingular. Using Eq. (37) with **G** diagonal, Eq. (38) can be rearranged to the form:

$$\boldsymbol{T} = [\boldsymbol{\Lambda} + \boldsymbol{G}]^{-1}[\boldsymbol{GF} - \boldsymbol{BT}] \tag{39}$$

Equation (39) is used to define the desired fixed point mapping where each of the m^2 matrix elements on the right side of this equation can be interpreted as a MISO problem. Proof of the fact that design of each MISO system yields a satisfactory MIMO design is based on the Schauder fixed point theorm.[7] This theorem is described by defining a mapping

$$\boldsymbol{Y}(\boldsymbol{T}) = [\boldsymbol{\Lambda} + \boldsymbol{G}]^{-1}[\boldsymbol{GF} - \boldsymbol{BT}] \tag{40}$$

where each member of **T** is from the acceptable set $\mathfrak{Z}$. If this mapping has a fixed point, i.e., $\mathbf{T} \in \mathfrak{Z}$ such that $\mathbf{Y(T)} = \mathbf{T}$, then this **T** is a solution of Eq. (39). For a 3×3 case, for a unit impulse input, Eq. (40) yields the output:

$$y_{11} = \frac{q_{11}}{1 + g_1 q_{11}}\left[g_1 f_{11} - \left(\frac{t_{21}}{q_{12}} + \frac{t_{31}}{q_{13}}\right)\right] \tag{41}$$

Based upon the derivation of all the y_{ij} expressions from Eq. (40) yields the four effective MISO loops (in the boxed area), in Fig. 4, resulting from a 2×2 system and the nine effective MISO loops resulting from a 3×3 system.[4] The control ratios for the desired tracking inputs r_i by the corresponding outputs y_i for each feedback loop of Eq. (40) have the form

$$y_{ii} = w_{ii}(v_{ij} + d_{ij}) \tag{42}$$

where $w_{ii} = q_{ii}/(1 + g_i q_{ii})$ and $v_{ij} = g_i f_{ij}$. The interaction between the loops has the form

$$d_{ij} = -\sum_{k \neq i}\left[\frac{t_{kj}}{q_{ik}}\right] \quad k = 1,2,2, \ldots, m \tag{43}$$

and appears as a "disturbance" input in each of the feedback loops. Thus Eq. (42) represents the control ratio of the ith MISO system. The transfer function $w_{ii}v_{ij}$ relates the "desired" ith output to the jth input r_j and the transfer function $w_{ii}d_{ij}$ relates the ith output to the jth "disturbance" input d_{ij}. The outputs given in Eq. (42) can thus be expressed as

$$y_{ij} = (y_{ij})_{r_i} + (y_{ij})_{d_{ij}} = y_{r_i} + y_{d_{ij}} \tag{44}$$

or, based on a unit impulse input,

$$t_{ij} = t_{r_{ij}} + t_{d_{ij}} \tag{45}$$

where

$$t_{r_{ij}} = y_{r_i} = w_{ii}v_{ij} \qquad t_{d_{ij}} = y_{d_{ij}} = w_{ii}d_{ij} \tag{46}$$

and where now the upper bound, in the low-frequency range ($0 < \omega \leq \omega_h$), is expressed as b_{ij}'. Thus

$$\tau_{d_{ij}} = b_{ij} - b_{ij}' \tag{47}$$

represents the maximum portion of b_{ij} allocated toward disturbance rejection and b_{ij}' represents the upper bound for the tracking portion, respectively, of t_{ij}. For each MISO system there is a disturbance input which is a function of all the other loop outputs. The object of the design is to have each loop track its desired input while minimizing the outputs due to the disturbance inputs.

In each of the 9 structures of Fig. 4 it is necessary that the control ratio t_{ij} must be a member of the acceptable $t_{ij} \in \tau_{ij}$. All the g_i and f_{ij} must be chosen to ensure that this condition is satisfied, thus constituting 9 MISO design problems.

If all of these MISO problems are solved, there exists a fixed point, and then y_{ij} on the left side of Eq. (40) may be replaced by t_{ij} and all the elements of **T** on the right side by t_{kj}. This means that there exists 9 t_{ij} and t_{kj}, each in its acceptable set, which is a solution to Fig. 18. If each element is 1:1, then this solution must be unique. A more formal and detailed treatment is given in Ref. 7.

IV-3 -- Tracking and Disturbance Specifications -- The presentation for the remaining portion of this chapter and the next is based upon not only a diagonal **G** matrix but also for a diagonal **F** matrix. Thus, in Fig. 4 the t_{ij} terms, for $i \neq j$, represent disturbance responses due to the cross-coupling effect whereas the t_{ij} terms, for $i = j$, [see Eq. (45)] is composed of a desired tracking term t_r and of an unwanted or disturbance term t_d. Therefore the desired tracking specifications for the diagonal MISO systems of Fig. 4 contain an upper and lower bounds as shown in Fig. 6. The disturbance specification for all MISO loops is given by only an upper bound. These performance specifications are shown in Fig. 19 for a 2x2 (in the boxed area) and for a 3x3 MIMO feedback control system.

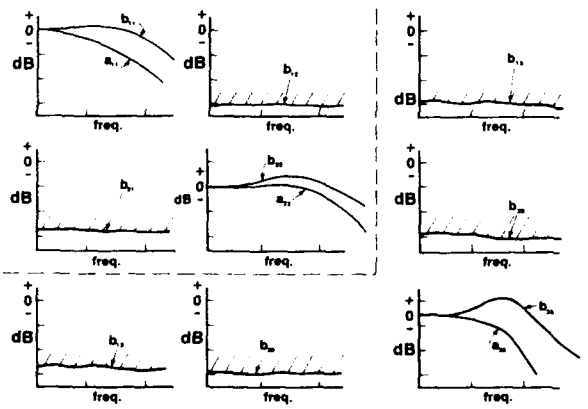

Fig. 19 Tracking and disturbance specifications for a 2x2 (in boxed area) and for a 3x3 MIMO system.

IV-3.1 -- Tracking Specifications -- Based upon the analysis of Eqs. (45) through (47), the specifications for the t_{ii} responses shown in Fig. 19 need to be modified as shown in Fig. 20. As shown in this figure a portion of $\delta_R(j\omega_i)$ (see Fig. 6) has been allocated[2-7] for the disturbance specification. Thus, based upon this modification, given an uncertain plant $\mathbf{P} = \{\mathbf{P}_j\}$ (j = 1,2, ... , J) and the BW ω_h above which output sensitivity is ignored it is desired to synthesize **G** and **F** such that for all $\mathbf{P} \in \mathbf{P}$

$$a'_{ii} \leq |t_{ii}(j\omega)| \leq b'_{ii} \quad \text{for} \quad \omega \leq \omega_h \tag{48}$$

A finite ω_h is recommended because in strictly proper systems, feedback is not effective in the high frequency range.

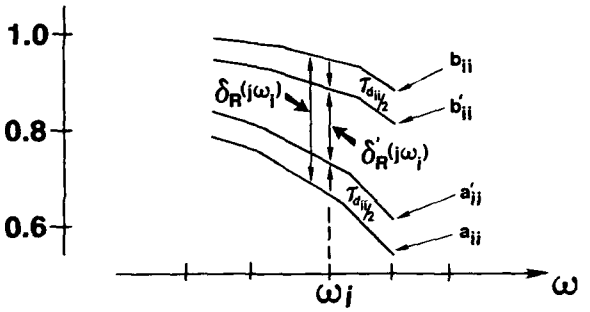

Fig. 20 Allocation for disturbance and tracking specifications for the t_{ii} responses.

IV-3.2 -- Disturbance Specification -- Based upon the previous discussion the disturbance specification, an upper bound, is expressed as

$$|t_{d_{ik}}| \leq |b_{ij}| \tag{49}$$

Thus the synthesis of **G** must satisfy both Eqs (48) and (49).

IV-4 -- Determination of Tracking, Disturbance, & Optimal Bounds -- The remaining portion of the MIMO QFT approach is confined to a 2x2 system. The reader can refer to the references for higher order systems (m > 2). From Eq. (39) the following equations are obtained:

$$t_{11} = \frac{L_1 f_{11} + d_{11} q_{11}}{1 + L_1} \tag{50}$$

$$\text{where } d_{11} = -\frac{t_{21}}{q_{12}}, \quad L_1 = q_{11} g_1$$

$$t_{12} = \frac{d_{12} q_{11}}{1 + L_1} \tag{51}$$

$$\text{where } d_{12} = -\frac{t_{22}}{q_{12}}, \quad f_{12} = 0$$

$$t_{21} = \frac{d_{21} q_{22}}{1 + L_2}$$

$$\text{where } d_{21} = -\frac{t_{11}}{q_{21}}, \quad L_2 = q_{22} g_2, \tag{52}$$

$$t_{22} = \frac{L_2 f_{22} + d_{22} q_{22}}{1 + L_2} \tag{53}$$

$$\text{where } d_{22} = -\frac{t_{12}}{q_{21}}$$

Equations (50) and (51) correspond to the MISO systems for the first row of loops in Fig. 4 and Eqs. (52) and (53) correspond to the MISO loops for the second row.

IV-4.1 -- Tracking Bounds -- The tracking bounds for the ii MISO system is determined in the same manner as for the MISO system of of PART II (see Sec. II-9.1). By use of the templates for the ii loop

plant the value of $\delta_R'(j\omega_i)$, shown in Fig. 20, is used to satisfy the constraint of Eq. (48).

IV-4.2 -- Disturbance Bounds -- From Eqs. (50) and (52), considering only the first row of MISO loops in Fig. 4, the following disturbance transfer functions are obtained:

$$|t_{d_{11}}| = \left|\frac{d_{11}q_{11}}{1 + L_1}\right| \le \tau_{d_{ij}} \equiv \tau_{d_{11}} \quad (Fig.20) \tag{54}$$

$$|t_{d_{12}}| = \left|\frac{d_{12}q_{11}}{1 + L_1}\right| \le b_{ij} \equiv b_{12} \quad (Fig.19) \tag{55}$$

By substituting for d_{11} and d_{12} into Eqs. (54) and (55), respectively, and replacing t_{21} and t_{22} by their respective upper bound values b_{21} and b_{22}, and rearranging these equations yield:

$$\left|\frac{1}{1 + L_1}\right| = \le \left|\frac{q_{12}}{q_{11}}\right| \frac{\tau_{d_{11}}}{b_{21}} \le M_{m_{11}} \tag{56}$$

$$\left|\frac{1}{1 + L_1}\right| \le \left|\frac{q_{12}}{q_{11}}\right| \frac{b_{12}}{b_{22}} = M_{m_{12}} \tag{57}$$

Substituting into these equations $L_1 = 1/l_1$ yields:

$$\left|\frac{l_1}{1 + l_1}\right| \le M_{m_{11}} \quad \cdots \quad \left|\frac{l_1}{1 + l_1}\right| \le M_{m_{12}} \tag{58}$$

By analyzing these equations, for each of the J plants, over the desired BW the maximum value that M_m that each of these equations can have, for each value of ω_i (or v_i), is readily determined by use of a CAD package. Thus, since $L_1 = 1/l_1$, the reciprocal of these values yield the value of the corresponding M-contours or disturbance bounds, for $\omega = \omega_i$ (or v_i), on the NC.

IV-4.3 -- Optimal Bounds -- The points on the optimal bound, for a given value of frequency and for a given row of MISO loops of Fig. 4, are determined by selecting the largest dB value, for a given NC phase angle, from all the tracking and disturbance bounds for these loops at this frequency. The MIMO QFT CAD package (Sec. IV-7) is designed to perform this determination of the optimal bounds.

IV-5 -- QFT Methods of Designing MIMO Systems -- There are two methods of achieving a QFT MIMO design. Method 1 involves synthesizing the loop transmission function L_i and the prefilter f_{ii} independent of the previous synthesized loop transmission functions and prefilters. Method 2 substitutes the synthesized g_i and f_{ii} of the first (or prior) MISO loop(s) that is (are) designed into the equations that described the remaining loops to be designed. For both methods it is necessary to make the decision as to the order that the L_i functions are to be synthesized. Generally the loops are chosen on the basis of the phase margin frequency ω_ϕ requirements. That is, the loop having the smallest value of ω_ϕ is chosen as the first loop to be designed, the loop having the next smallest value of ω_ϕ is selected as the second loop to be designed, etc. This is an important requirement especially for Method 2.

IV-5.1 -- Method 1 -- Method 1 involves overdesign (worst case scenario), i.e., in getting the M_m values of Eqs. (56) and (57), for the 2x2 case, the maximum magnitude that q_{12} and the minimum magnitude that q_{11} can have, for each value of ω_i, over the entire J LTI plants are utilized. This method requires that the diagonal dominance condition[2-7] be met. If this condition is not satisfied then Method 2 needs to be utilized.

IV-5.2 -- Method 2 -- Once the order in which the loops are to be designed and designated accordingly (loop 1, loop 2, etc) then the compensator g_1 and the prefilter f_{11} are synthsized. These are now known LTI functions which are utilized to define the loop 2 effective plant transfer function. That is, substitute Eq. (50) into Eq. (52) and then rearrange the result to obtain a new expression for t_{12} in terms of g_1 and f_{11} as follows:

$$t_{21} = -\left[\frac{\dfrac{f_{11}L_1q_{22_e}}{q_{21}(1 + L_1)}}{1 + g_2q_{22_e}}\right] \tag{59}$$

where the effective loop 2 transfer function is:

$$q_{22_e} = \frac{q_{22}(1 + L_1)}{(1 + L_1 - \gamma_{12})} \quad where \quad \gamma_{12} = \frac{q_{11}q_{22}}{q_{12}q_{21}} \tag{60}$$

Repeating a similar procedure the expression for t_{22} is:

$$t_{22} = \frac{f_{22}g_2q_{22_e}}{1 + g_2q_{22_e}} \tag{61}$$

Remember that a diagonal prefilter matrix has been specified. Note that Eqs. (59) through (61) involve the known f_{11} and g_1 which reduces the overdesign of loop 2.

IV-6 -- Synthesizing the Loop Transmission and Prefilter Functions -- Once the optimal bound has been determined for each L_i loop then the synthesis procedures for deter- mining the loop transmission and prefilter functions are the same as for the MISO analog and discrete systems as discussed in Chapters II and III, respectively.

IV-7 -- Overview of the MIMO/QFT CAD Package -- The MIMO/QFT CAD package, implemented using Mathematica, is capable of carrying a discrete or analog MIMO QFT design problem from problem setup through the design process to a frequency domain analysis of the compensated MIMO system. For analog control problems, the design process is performed in the s-plane, while for the discrete control problems the plants are discretized and the design process is performed either in the w-plane using the direct design approach or in the s-plane using the pseudo-continuous design approach (PCT). A flowchart of the package is given in App C.

The package automates the many design steps of the QFT control technique. For problem setup, the J plant models may be loaded directly in state space form from a MATRIXx *fsave* file or may be defined in transfer function form at the console. In addition, sensor dynamics, actuator dynamics, and all problem specifications are defined using a menu driven data entry process.

The QFT design process then begins with the selection of the weighting matrix $\mathbf{W}$ and sensor gain matrix $\mathbf{W}_{SENS}$ for squaring non-square plants (m x ℓ matrix $\mathbf{P}$) to achieve an effective mxm plant matrix $\mathbf{P}_{e\iota}$ for $\iota = 1, 2, \ldots, J$. The CAD software allows the designer to apply the Binet-Cauchy theorem to select, where possible, a weighting matrix which results in the formation of a mininum-phase $\det\mathbf{P}_e$.

The design process then continues with formation of the square effective plants $P_{e\iota}$ for $\iota = 1, 2, \ldots, J$. The polynomial matrix inverse is then performed on the square effective plants $\mathbf{P}_{e\iota}$ to form the equivalent plant matrices $\mathbf{Q}_\iota$ for $\iota = 1, 2, \ldots, J$. The designer may then perform automatic cancellation of nearly equal pole-zero pairs after specifying a measure of how closely the pole-zero pairs must match. Once the $\mathbf{Q}_\iota$ matricies are available, the compensators g_i and prefilter f_{ii} elements of the mxm diagonal $\mathbf{G}$ and $\mathbf{F}$ may be designed based on the equivalent mxm set of MISO loops which represent the more difficult MIMO control problem. For a discrete design the steps, as discussed, are identical except now $\mathbf{P}_{e\iota}$ and $\mathbf{Q}_\iota$ are in the w-domain.

For each channel, or feedback loop, a compensator g_i and a prefilter f_{ii} are designed to satisfy the specifications for row i of the mxm set of MISO loops associated with that channel. First, a set of templates are generated for a user-selected set of template frequencies and a nominal template point is selected. Next, the designer selects the set of bounds to be used during loop shaping on the NC. All selected stability, tracking, disturbance, gamma, and composite bounds are then automatically generated by the CAD package based on problem specifications. The bounds are then used for loop shaping of $L_{io} = g_i q_{iio}$ on the NC. Loop shaping is performed by adding and modifying poles and zeros and by adjusting the gain of g_i until the bounds on the NC are satisfied.

Once a satisfactory compensator g_i has been designed, the prefilter f_{ii} is designed. The CAD program automatically generates a set of prefilter bounds which must be satisfied by the nominal closed loop transmission $f_{ii}L_{io}/(1+L_{io})$ on the Bode plot. The prefilter is designed by adding and modifying poles and zeros and by adjusting the gain of f_{ii} until the prefilter bounds on the Bode plot are satisfied.

Once the compensator g_i and prefilter f_{ii} have been designed for the first row of the MISO loops chosen for the initial designed loop L_{io}, the improved method may be applied. When the designer applies the improved method, a new set of equivalent plants are generated for use in designing the remaining compensators and prefilters.

Once all compensators and prefilters are designed, a frequency-domain analysis of the completed design may be performed. For a stability analysis, the CAD program allows all open loop transmissions to be plotted along with the M_L contour on the NC. If no open loop transmissions violate the M_L contour, the desired stability margin has been achieved for that channel. For a performance analysis, the CAD program allows an mxm array of Bode plots to be generated, each illustrating the set of J possible transmissions for the true MIMO closed loop system along with the frequency domain performance bounds. If no performance bounds are violated, then the performance specifications (tracking and disturbance) are met in the frequency domain.

For the final step in design validation, the completed design may be exported to MATRIXx or Matlab for time-domain simulation. For a discrete design, the compensators g_i and prefilters f_{ii} are first transformed into the z-domain. The transient response of the closed loop system is then evaluated.

V -- QFT APPLICATIONS

V-1 -- Introduction -- Two MIMO QFT examples are presented to illustrate the power of this design technique. The first example is for a 2x2 analog flight control system whereas the second example is for a 3x3 discrete flight control system.

V-2 -- Analog QFT Design -- The successful validation of the MIMO/QFT CAD[15] package, based on Arnold's design problem[16] was a major landmark in the CAD software development effort. This validation illustrated the increased accuracy and efficiency achieved by the CAD package, and the straightforward method for designing an

analog MIMO control system. The specifications[16] require a robust analog design for the AFTI/F-16 which provides stability and meets time domain performance requirements for the specified 4 flight conditions (Table V-1) and the 6 aircraft failure modes (Table V-2). Table V-3 lists the resulting set of 24 plant cases which incorporate these flight conditions and failure modes. For stability a 45° phase margin is required for each of the two feedback loops. Frequency domain performance specifications, when met, result in the desired closed loop system performance in the time domain. The frequency domain specifications are shown as dashed lines on the Bode plots of Fig. 24.

Flight Condition	Aircraft Parameters	
	Mach	Altitude
1	0.2	30
2	0.6	30,000
3	0.9	20,000
4	1.6	30,000

Table V-1 Flight conditions

Failure Mode	Failure Condition
1	Healthy aircraft
2	One horizontal tail fails
3	One flaperon fails
4	One horizontal tail and one flaperon fail, same side
5	One horizontal tail and one flaperon fail, opposite sides
6	Both flaperons fail

Table V-2 Arnold's failure modes

Failure Mode	Flight Condition			
	1	2	3	4
1	#1	#7	#13	#19
2	#2	#8	#14	#20
3	#3	#9	#15	#21
4	#4	#10	#16	#22
5	#5	#11	#17	#23
6	#6	#12	#18	#24

Table V-3 Plant models for Arnold's design

The specifications, the plant models[16] for the 24 cases, and the weighting matrix are entered into the CAD package. The automated features accessed through the designer interface of the CAD package resulted in the synthesized loop transmission function $L_{2_o}(s)$ shown along with associated bounds on the NC in Fig. 21. In this design, a trade-off exists between performance and bandwidth and in synthesizing $L_{2_o}(s)$. In this example, the designer chooses to accept the consequences of violating the disturbance bound for ω = 2 r/s. $L_{1_o}(s)$ was synthesized in a similar manner. With $L_{1_o}(s)$ and $L_{2_o}(s)$ synthesized, the CAD package's automated features expedite the design of the prefilters $f_{11}(s)$ and $f_{22}(s)$.

The CAD package validation routines are now tested. First, a stability analysis;

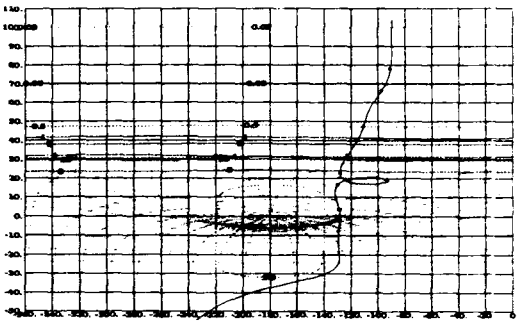

Fig. 21 Channel 2 nominal loop with bounds on NC

for example, the $L_{2_i}(s)$ are plotted for the i = 1, ... , 24 possible open loop transmissions along with the M_L contour on the NC shown in Fig. 22. None of the 24 open loop transmissions violate the M_L contour, in accordance with the fact that the nominal loop transmission $L_{2_o}(s)$ satisfied all stability bounds. For the second step in the design validation process the 2x2 array of Bode plots shown in Fig. 24 is generated showing on each plot the 24 possible closed loop transmissions from an input to an output of the completed system. The consequence of violating the channel 2 disturbance bound for ω = 2 r/s is seen where the closed loop transmissions violate b_{21}, denoted by dashed line, beginning at ω = 2 r/s. Violation of performance bounds during loop shaping may result in violation of the performance specifications for the closed loop system.

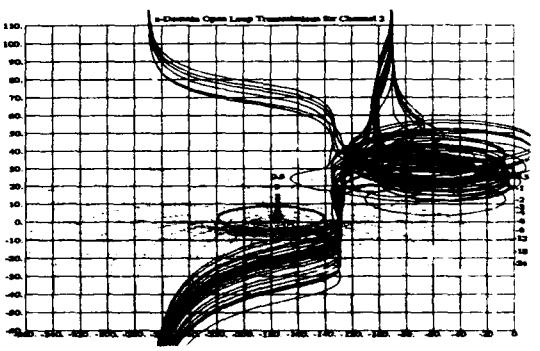

Fig. 22 Open loop transmissions on NC

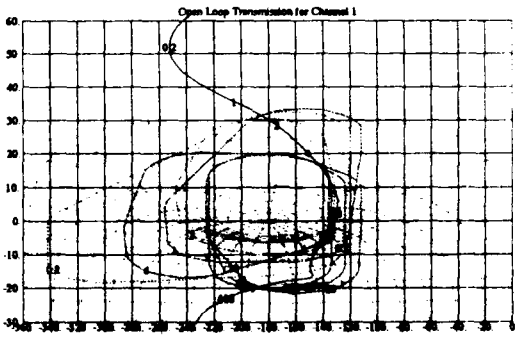

Fig. 23 Channel 1 nominal with bounds on NC

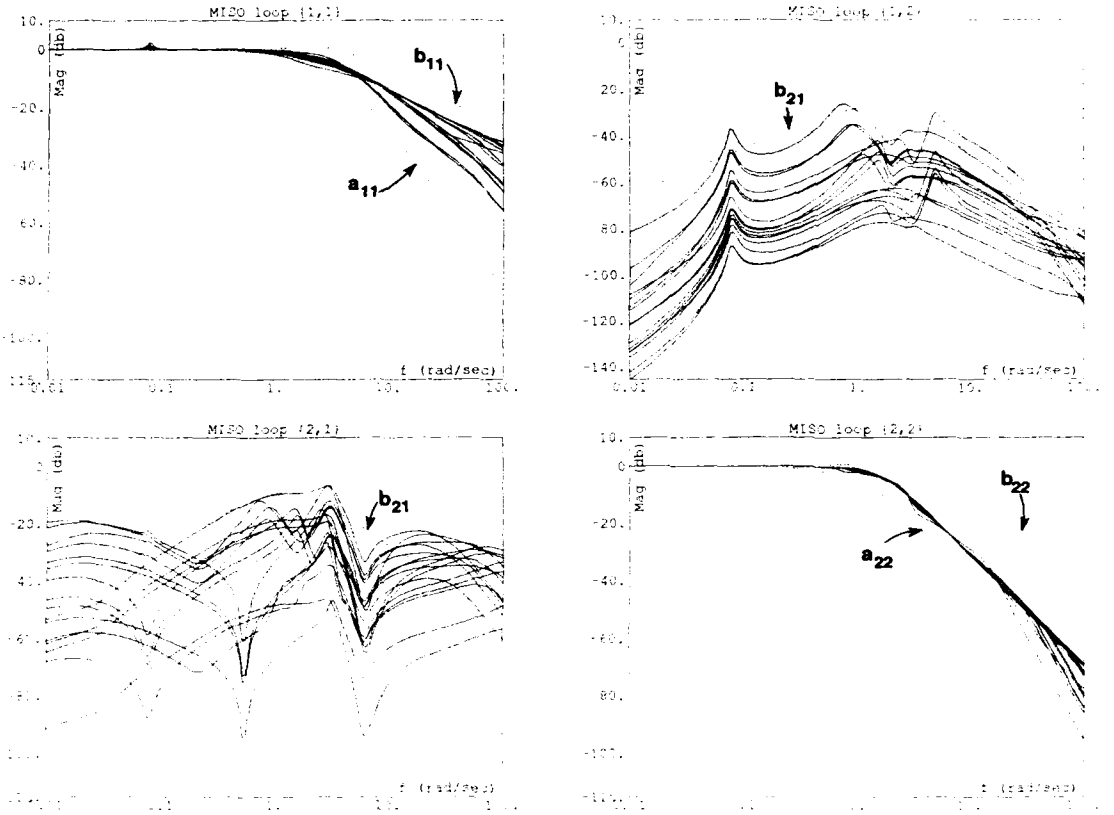

Fig. 24 Closed loop transmissions for an analog system

As seen in Fig. 24 a robust design has been achieved for this 2x2 MIMO analog flight control system. The time domain results, although not drawn, meet all specifications.

V-3 -- Discrete QFT Design -- The specifications for the digital control design require a digital controller be designed for the AFTI/F-16 which provides the required robustness with respect to stability and satisfying the time domain performance requirements for any of 4 flight conditions (Table V-1) and 9 failure modes (Table V-4). For stability, a 45° phase margin is required for each of the three feedback loops. Frequency domain performance specifications are shown as dashed lines on the Bode plots of Fig. 27.

Failure Mode	Failure Condition
1	Healthy aircraft
2	One horizontal tail fails
3	One flaperon fails
4	Rudder fails
5	Canards fail
6	One horizontal tail and one flaperon fail, same side
7	One horizontal tail and one flaperon fail, opposite sides
8	Both flaperons fail
9	Both flaperons and canards fail

Table V-4 Schneider's failure modes

The design process begins by entering the specifications, the plant models[17], for the 36 cases (see Table V-5), and the weighting matrix into the CAD package. Because of the nature of the failure cases and being a digital design, loop shaping for all three loops was difficult with respect to satisfying all bounds (tracking, disturbance, and stability bounds). For loops 2 and 3 the M_L stability bounds were satisfied. However, all stability bounds could not be satisfied during the design of loop 1.

Failure Mode	Flight Condition			
	1	2	3	4
1	#1	#10	#19	#28
2	#2	#11	#20	#29
3	#3	#12	#21	#30
4	#4	#13	#22	#31
5	#5	#14	#23	#32
6	#6	#15	#24	#33
7	#7	#16	#25	#34
8	#8	#17	#26	#35
9	#9	#18	#27	#36

Table V-5 Plant models for Schneider's design

The loop $L_{1_o}(w)$ was shaped to minimize violation of the stability bounds while maintaining the low frequency gain as large as possible to achieve the best possible performance. The final loop $L_{1_o}(w)$ was in violation of the stability bounds for ω = 2, 20, and 40 r/s and the

high frequency stability bound for ω = 400 r/s. A stability analysis is then performed to evaluate the consequences of the stability bound violations, by plotting the open loop transmissions $L_{1i}(w)$ for all i = 1, 2, ... , 36 plant cases along with the M_L contour, as shown in Fig. 25. The actual phase margin

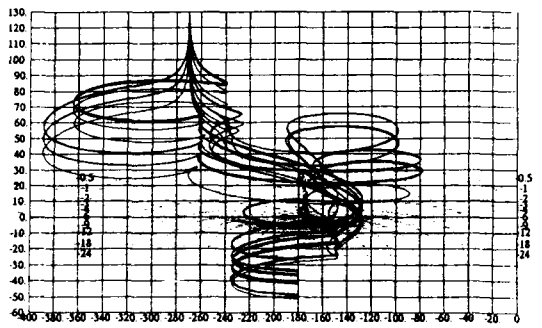

Fig. 25 Lm $L_{1i}(jw)$ plots for 36 cases and M_L-contour

is thereby determined to be γ = 20° rather then the desired 45°. The shortfall is a consequence of the degree of phase and magnitude uncertainty among the 36 plant cases. Plant case 33 (FC 4, FM 6) was responsible for the largest contribution in plant uncertainty, as shown in Fig. 25. The designer will have to accept whatever level of performance is achieved for channel 1 since stability is the most critical requirement.

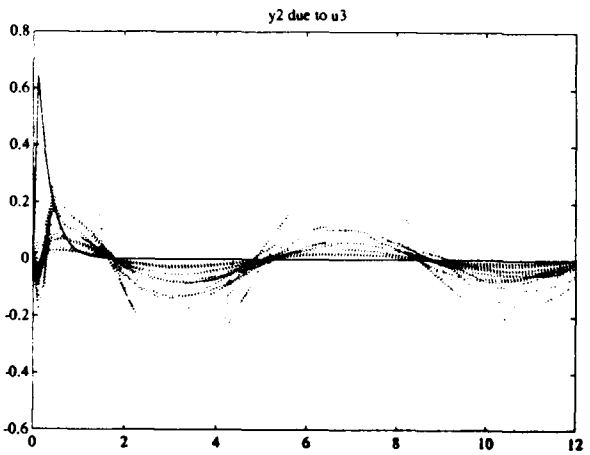

Fig. 26 $y_{23i}(t)$ responses to unit step input for input 3

For the design of $g_2(w)$ for channel 2 (the Roll channel) and $g_3(w)$ for channel 3 (the Yaw channel) the stability margins of γ = 45° were achieved while adding as much low frequency gain as possible to satisfy the performance bounds. The disturbance bounds for channel 2 and the tracking bounds for channel 3 proved to be impossible to satisfy while maintaining the desired stability margin. The design of the prefilter $f_{22}(w)$ for channel 2 was straightforward, as for channel 1. For the design of $f_{33}(w)$, the prefilter bounds were satisfied up to the frequency at which they cross (the frequency at which the tracking bounds were violated).

The 3x3 array of Bode plots shown in Fig. 27 illustrates on each plot the 36 possible closed loop transmissions from an input to an output of the completed system. The consequence of violating tracking or disturbance bounds is seen where the closed loop transmissions violate frequency domain performance specifications, denoted by dashed lines. Note the violation of the upper bound b_{23} on the third bode plot of the second row. The violation translates into a larger-than-desired response in roll when a yaw command is applied to the channel 3 input. The resulting set of 36 possible step responses of output 2 due to a unit step of input 3, shown in Fig. 26, illustrates the consequences of violating b_{23} in the time domain. Note for $r_1(t) = r_2(t) = 0$ and $r_3(t) = u_{-1}(t)$ that

$$y_2(t) = y_{21}(t) + y_{22}(t) + y_{32}(t) = y_{23}(t) \quad (62)$$

For plant case #33 the most extreme violation of b_{23} occurs, resulting in a step response much larger than for any of the other responses. For all other plant cases and for all other transmissions the peak step disturbance responses are below the maximum specified peak value (that is, $|y_{ij}| \leq |y_{ij}|_{max}$ for $i \neq j$). The tracking responses of channels 1 and 2 (that is, y_{ii} for i = 1, 2) fell tightly within the performance bounds a_{ii} and b_{ii}, while the responses y_{33} for channel 3 fell outside a_{33} and b_{33} but did not exceed the maximum allowable peak value. The larger than desired settling time for y_{33} is accepted as a tradeoff for achieving the desired stability margin.

This design of the digital control problem illustrates the results obtainable using an automated QFT CAD package. Despite the difficulty and large scale of the MIMO problem, the MIMO/QFT CAD package provides a straightforward method for design of a robust digital controller while providing insight into each stage of the QFT design process.

V-4 -- Dual Flight Control System Senario -- For a flight control system where battle dammage is of concern, a possible dual flight control system is as follows: a control system designed by QFT in combination with an adaptive control system. The QFT controller is designed to maintain a stable aircraft under certain battle dammage senarios while giving the adaptive control system time to identify the battle dammage and adjust its controller to improve the flying qualities as much as possible, as illustrated in Fig. 28.

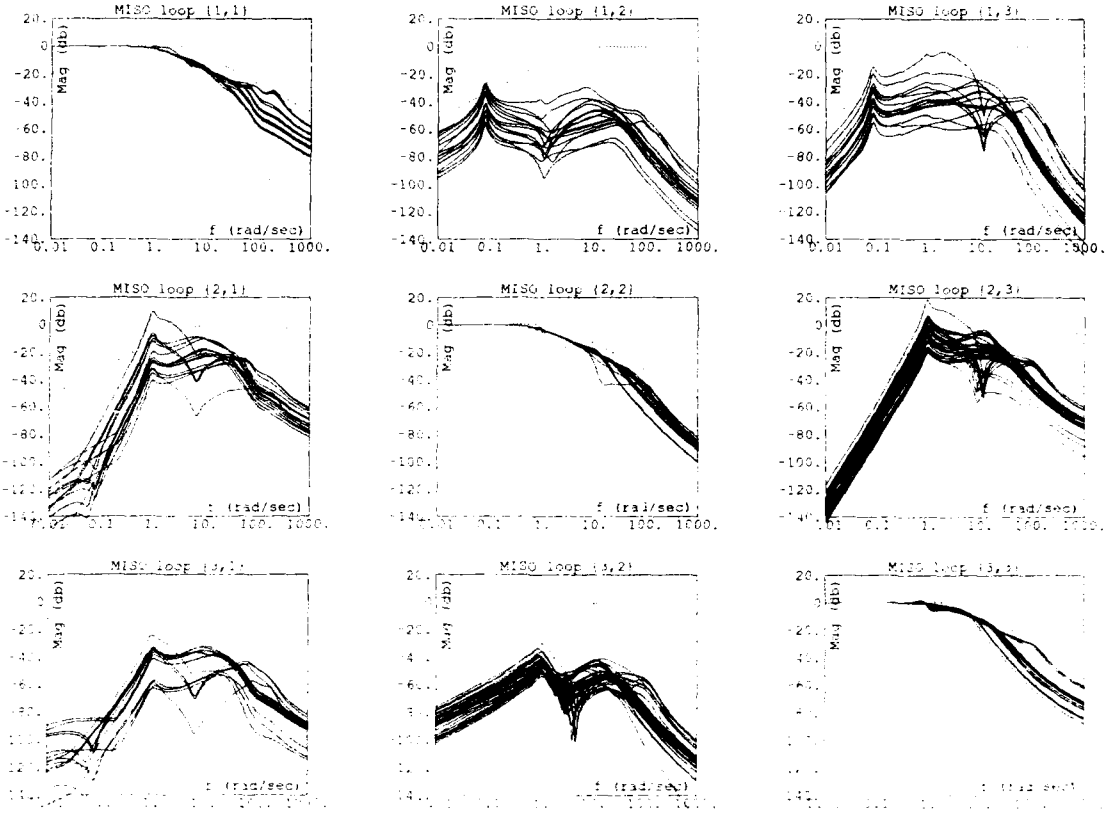

Fig. 27 Closed loop transmissions for a digital system

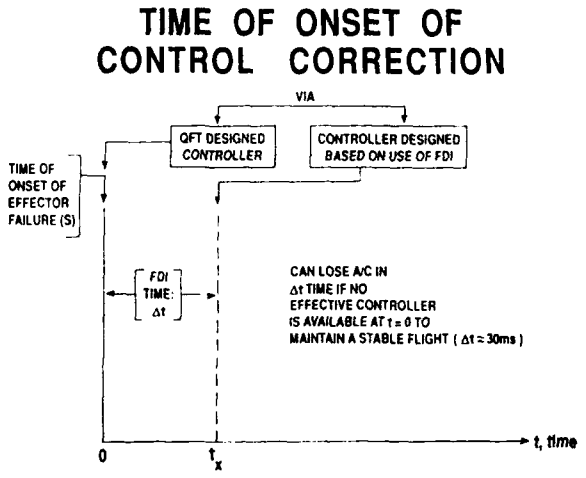

Fig. 28 A dual flight control system scenario

REFERENCES

1. D'Azzo, J. J., and C. H. Houpis: "Linear Control System Analysis and Design," McGraw-Hill, NY, 3rd Ed., '88.

2. Houpis, C. H.: "Quantitative Feedback Theory (QFT): Technique for Designing Multivariable Control Systems," AFWAL-TR-86-3107, AF Wright Aeronautical Laboratories, Wright-Patterson AFB, OH, '87. (Available from Defense; Technical Information Center, Cameron Station, Alexandria, VA 22314, document No. AD-A176883.)

3. Horowitz, I. M. and M. Sidi: "Synthesis of Feedback Systems with Large Plant Ignorance for Prescribed Time Domain Tolerances," Int. J. of Control, vol. 16, pp 287-309, '72.

4. Horowitz, I. M., and C. Loecher: "Design of a 3x3 Multivariable Feedback System with Large Plant Uncertainty, "Int. J. Control, vol. 33, pp. 677-699, '81.

5. Horowitz, I. M.: "Optimum Loop Transfer Function in Single-Loop Minimum Phase Feedback Systems," Int. J. Control, vol 22, pp. 97-113, '73.

6. Horowitz, I. M.: "Synthesis of Feedback Systems with Non-Linear Time Uncertain Plants to Satisfy Quantitative Performance Specifications," IEEE Proc., vol. 64, pp. 123-130, '76.

7. Horowitz, I. M.: "Quantitative Synthesis of Uncertain Multiple-Input Multiple-Output Feedback Systems," Int. J. Control, vol. 30, pp. 81-106, '79.

8. Thompson, D. F. and O. D. I. Nwokah, "Optimal Loop Synthesis in Quantitative Feedback Theory," Proceed. of the American

Control Conference, San Diego, CA, pp. 626-631, '90.

9. Houpis, C. H. and P. R. Chandler, Editors: "Quantitative Feedback Theory Symposium Proceedings," WL-TR-92-3063, Wright Laboratories, Wright-Patterson AFB, OH, '92.

10. Betzold, R. W.: "Multiple-Input Multiple-Output Flight Control Design with Highly Uncertain Parameters, Application to the C-135 Aircraft," M.S. Thesis, AFIT/GE/EE(83D-11), School of Engineering, Air Force Inst. of Technology, '83.

11. Arnold, P. B., I. M. Horowitz, and C. H. Houpis: "YF-16CCV Flight Control System Reconfiguration Design Using Quantitative Feedback Theory," Proceedings of the National Aerospace and Electronics Conference (NAECON), vol. 1. pp. 578-585, '85.

12. Migyanko, B. S., "Design of Integrated Flight/Propulsion Control Laws of a STOL Aircaft During Approach and Landing Using Quantitative Feedback Theory," M.S. Thesis, AFIT/GE/ENG/86D-33, School of Engineering, Air Force Inst. of Technolgy, '86.

13. Houpis, C. H. and G. Lamont: "Digital Control Systems: Theory, Hardware, Software," McGraw-Hill, NY, 2nd Ed., '92.

14. Horowitz, I. M. and Y. K. Liao: "Quantitative Feedback Design for Sampled-Data System," Int. J. Control, vol. 44,, pp. 665-675, '86.

15. Sating, R. R., I. M. Horowitz, and C. H. Houpis: "Development of a MIMO QFT CAD Package (Version 2)," Air Force Inst. of Technolgy, Wright-Patterson AFB, Ohio 45433, USA, submitted for presentation at the 1993 American Control Conference.

16. Arnold, P. B., "Flight Control System Reconfiguration Using Quantitative Feedback Theory," M.S. Thesis, AFIT/GE/ENG/-84D-15, School of Engineering, Air Force Inst. of Technology, '84.

17. Schneider, D. L., "QFT Digital Flight Control Design as Applied to the AFTI/F-16," M.S. Thesis, AFIT/GE/ENG/86D-4, School of Engineering, Air Force Inst. of Technolgy, '86.

APPENDIX A

CAD flowchart for MISO analog QFT design

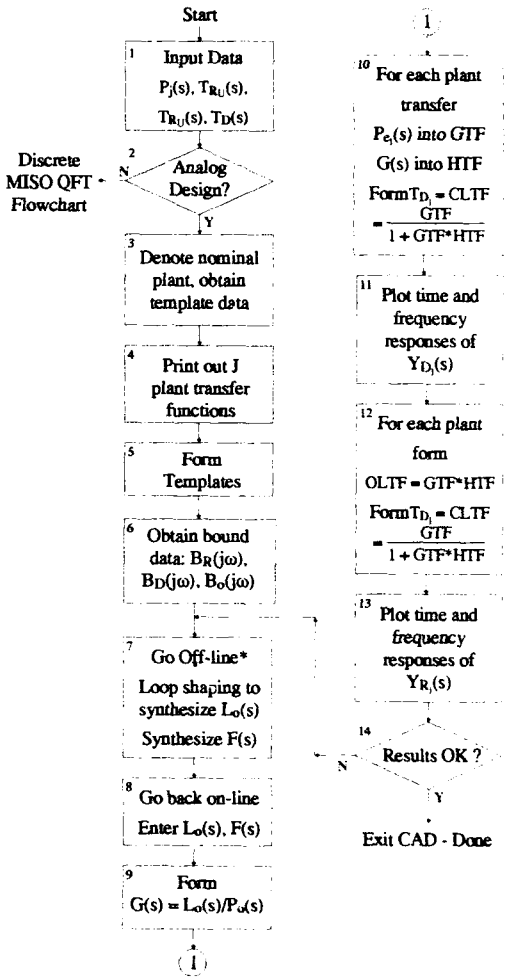

* Yaniv's package can do loop shaping interactively, on line.

APPENDIX B

CAD flowchart for MISO discrete QFT design

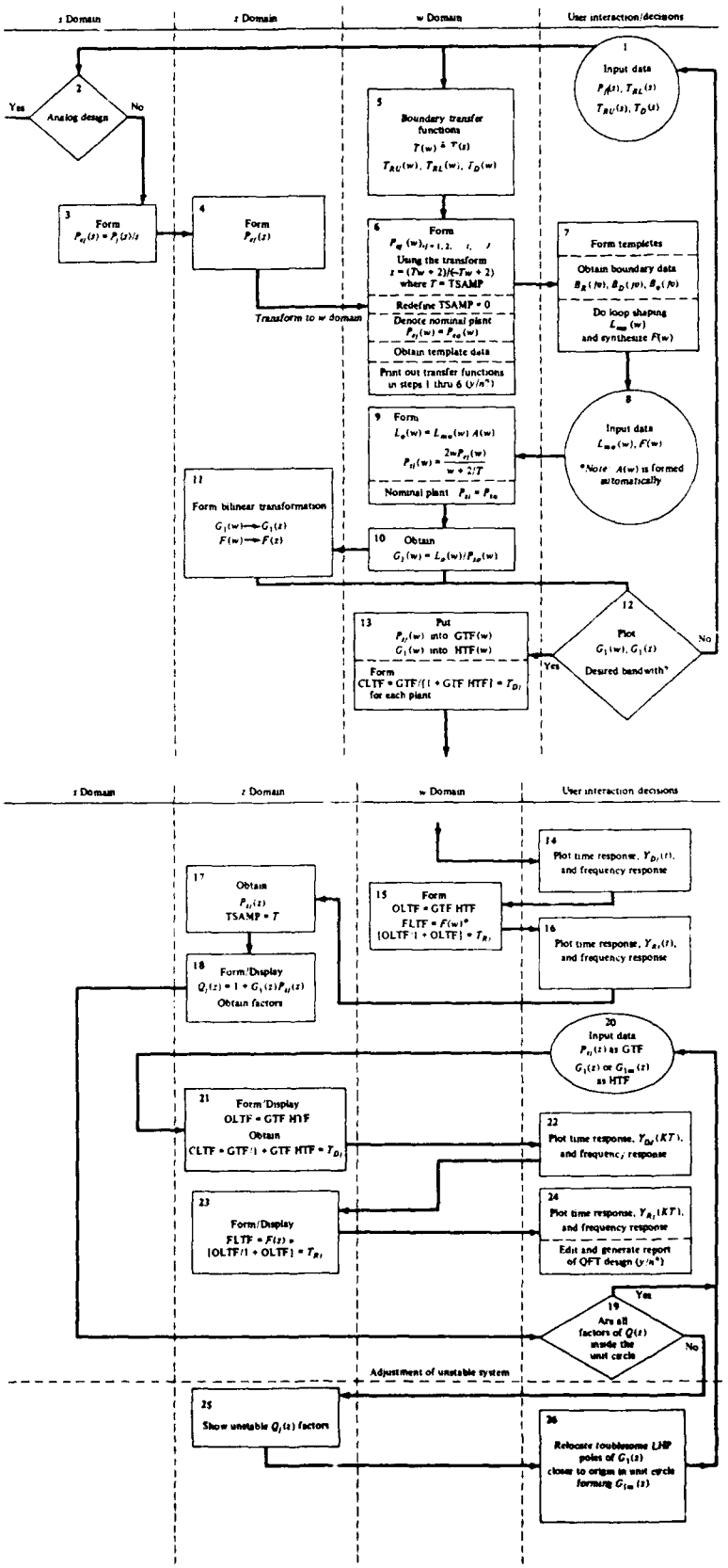

APPENDIX C

MIMO/QFT CAD flowchart for analog and discrete control systems

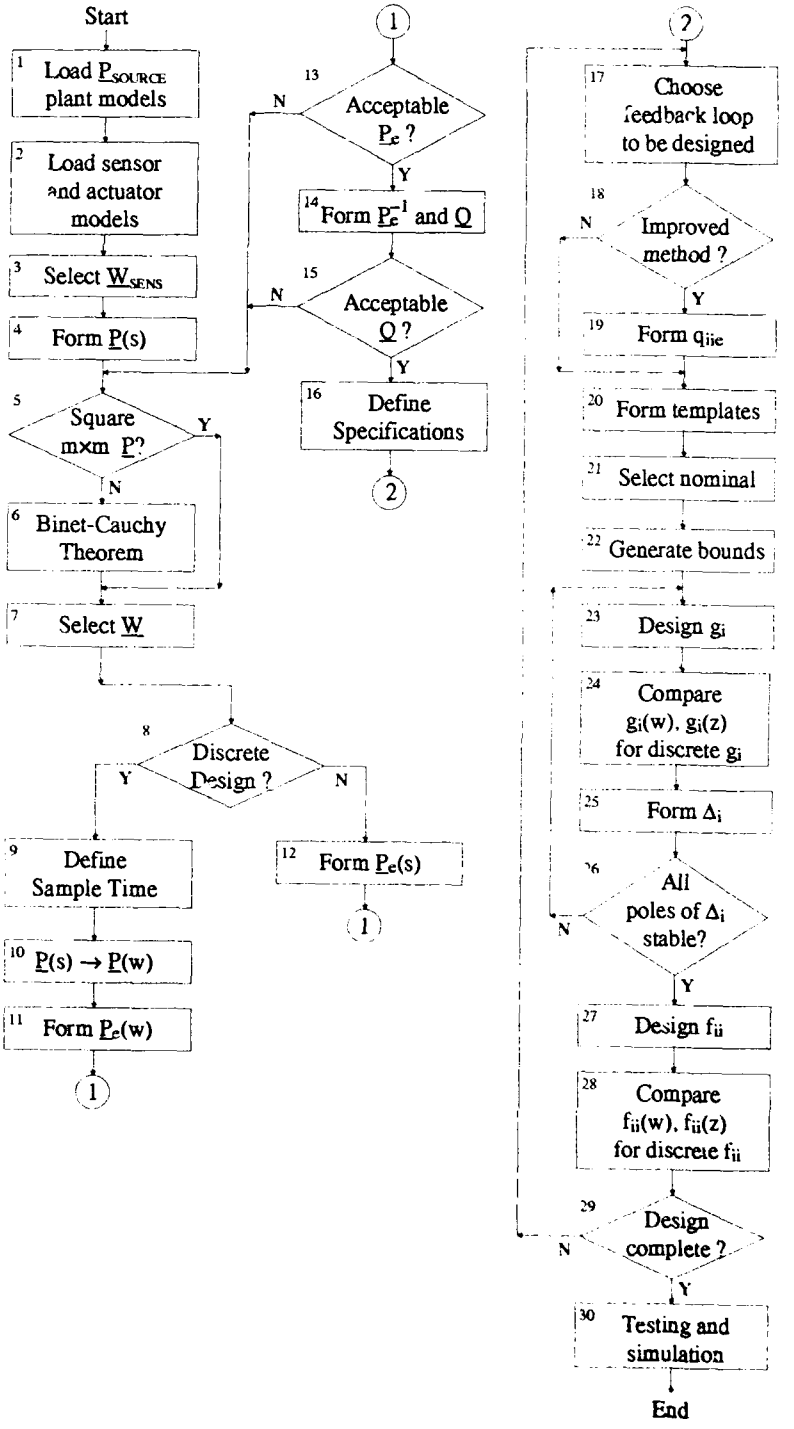

BIBLIOGRAPHY

This Bibliography was prepared by the Centre de Documentation de l'Armement (CEDOCAR), 00460 Armées, Paris, France in support of the Lecture Series.

NO - C9209-1340K-001
ET - Harmonic balance methods for the analysis of chaotic dynamics in nonlinear systems
AU - GENESIO R.; TESI A.
AF - Dipartimento di Sistemi e Inf., Firenze Univ., Italy
DT - Journal paper
TC - Theoretical mathematical
LA - ENG
PO - IT
JT - Automatica (UK); Automatica
SO - VOL. 28; NO. 3; PP. 531-48; 28 Ref.; DP. May 1992
CD - ATCAA9
SN - 0005-1098
CTN - 0005-1098/92/$5.00+0.00
AB - Considers the problem of determining the conditions under which a nonlinear dynamical system can give rise to a chaotic behaviour. On the basis of the harmonic balance principle, which is widely used in the frequency analysis of nonlinear control systems, two practical methods are presented for predicting the existence and the location of chaotic motions. This is formulated as a function of the system parameters, when the system structure is fixed by rather general input-output or state equation models. Several examples of application are presented to show the rather straightforward computations involved in the proposed methods, the kind of results which can be obtained and, due to the heuristic approach to the problem, their corresponding approximation
CC - C1340K; C1120; C1310
DE - chaos; control system analysis; describing functions; dynamics; harmonic analysis; nonlinear control systems
IT - harmonic analysis; input output equation models; control system analysis; chaotic dynamics; nonlinear dynamical system; harmonic balance principle; nonlinear control systems; state equation models; heuristic approach

NO - B9208-1160-007; C9208-1340K-011
ET - Bifurcation phenomena of a distributed parameter system with a nonlinear element having negative resistance
AU - NAKANO H.; OKAZAKI H. O.
AF - Dept. of Mech. Eng., Shonan Inst. of Technol., Fujisawa, Japan
DT - Journal paper
TC - Theoretical mathematical
LA - ENG
PO - JP
JT - IEICE Trans. Fundam. Electron. Commun. Comput. Sci. (Japan); IEICE Transactions on Fundamentals of Electronics, Communications and Computer Sciences
SO - VOL. E75-A; NO. 3; PP. 339-46; 7 Ref.; DP. March 1992
SN - 0916-8508
AB - Dynamic behavior of a distributed parameter system described by the one-dimensional wave equation with a nonlinear boundary condition is examined in detail using a graphical method proposed by Witt on a digital computer. The bifurcation diagram, homoclinic orbit and one-dimensional map are obtained and examined. Results using an analog simulator are introduced and compared with that of the graphical method. The discrepancy between these results is considered, and from the comparison among the bifurcation diagrams obtained by the graphical method, it is noted that the energy dissipation in the system considerably restrains the chaotic state in the bifurcation process
CC - B1160; C1340K
DE - chaos; distributed parameter systems; negative resistance; nonlinear systems
IT - distributed parameter system; nonlinear element; negative resistance; one dimensional wave equation; nonlinear boundary condition; graphical method; bifurcation diagram; homoclinic orbit; one dimensional map; analog simulator; chaotic state

NO - C9206-1340K-011
ET - Nonlinear control theory and chaotic dynamical systems
CT - Proceedings of the IEEE 1991 National Aerospace and Electronics Conference NAECON 1991 (Cat. No.90CH3007-2)
LC - Dayton, OH, USA
DC - 20-24 May 1991
AU - JONES J.
AF - Air Force Inst. of Technol., Wright-Patterson AFB, Dayton, OH, USA
SP - IEEE
DT - Conference paper
TC - Theoretical mathematical
LA - ENG
PO - US
ED - IEEE; New York, NY, USA
SO - NP. 3 vol. xviii+1345; PP. 571-6 vol.2; 0 Ref.; DP. 1991
BN - 0-7803-0085-8
AB - The author treats the role of multiparameters in the existence of solutions of highly coupled nonlinear dynamical systems and numerical computation of solutions. An attempt is made to develop methods applicable to control of highly coupled nonlinear dynamical systems containing multiparameters which may have a chaotic behavior. Due to the loss of components of a nonlinear dynamical system it may have a chaotic solution instead of a stable controllable observable solution. The basic mathematics involved in such nonlinear multiparameter systems is treated so as to make sufficient changes in the system without losing the system completely as far as applications are concerned. This requires the development of time-dependent multiple objective numerical algorithms involving time to acomplish various desired maneuvers results obtained can be used to establish feedback control laws for nonlinear dynamical systems of a specified form
CC - C1340K; C1340B; C1310
DE - chaos; control system synthesis; multivariable control systems; nonlinear control systems
IT - chaotic dynamical systems; highly coupled nonlinear dynamical systems; numerical computation; nonlinear multiparameter systems; time dependent multiple objective numerical algorithms; feedback control laws

NO - C9206-1340K-009
ET - Local prediction of chaotic time series
CT - Proceedings of the 33rd Midwest Symposium on Circuits and Systems (Cat. No.90CH2819-1)
LC - Calgary, Alta., Canada
DC - 12-14 Aug. 1990
AU - GIONA M.; CIMAGALLI V.; MORGAVI G.; PERRONE A.; JOHNSTON R. H.(Ed.)
AUS - NOWROUZIAN B.(Ed.); TURNER L. E.(Ed.)
AF - Rome Univ., Italy
SP - IEEE
DT - Conference paper
TC - Theoretical mathematical
LA - ENG
PO - IT
ED - IEEE; New York, NY, USA
SO - NP. 2 vol. 1205; PP. 894-7 vol.2; 13 Ref.; DP. 1991
BN - 0-7803-0081-5
CTN - CH2819-1/90/0000-0894$01.00
AB - Consideration is given to two different methods for chaotic signal local forecasting: a local interpolation and functional reconstruction. A brief review is presented of the mathematical framework on nonstatistical forecasting. An outline of some main techniques for chaotic signal characterization is furnished
CC - C1340K; C1310
DE - chaos; nonlinear systems
IT - chaotic time series; chaotic signal local forecasting; local interpolation; functional reconstruction; mathematical framework; nonstatistical forecasting; chaotic signal characterization

NO - C9206-1340J-005
ET - Analysis and reduction of an infinite dimensional chaotic system
CT - Proceedings of the 33rd Midwest Symposium on Circuits and Systems (Cat. No.90CH2819-1)
LC - Calgary, Alta., Canada
DC - 12-14 Aug. 1990
AU - HARTLEY T. T.; KILLORY H.; DE ABREU GARCIA J. A.; ABU KHAMSEH N.; JOHNSTON R. H.(Ed.)
AUS - NOWROUZIAN B.(Ed.); TURNER L. E.(Ed.)
AF - Coll. of Eng., Akron Univ., OH, USA
SP - IEEE
DT - Conference paper
TC - Theoretical mathematical
LA - ENG
PO - US
ED - IEEE; New York, NY, USA
SO - NP. 2 vol. 1205; PP. 889-93 vol.2; 14 Ref.; DP. 1991
BN - 0-7803-0081-5
CTN - CH2819-1/90/0000-0889$01.00
AB - A singularly perturbed nonlinear time delay system is considered. It is shown that as the system becomes more singular, it evolves through a series of bifurcations into chaotic behavior. Describing functions are used to predict when the initial bifurcations occur. Based on the attractor dimension, reduced-order finite-dimensional models are obtained that qualitatively reproduce the system dynamics
CC - C1340J; C1310; C1340K
DE - chaos; delays; describing functions; multidimensional systems; nonlinear systems
IT - analysis; nonlinear dynamics; model reduction; describing functions; reduction; infinite dimensional chaotic system; singularly perturbed nonlinear time delay system; bifurcations; chaotic behavior; initial bifurcations; attractor dimension; reduced order finite dimensional models

NO - C91056445
ET - Chaos prediction in nonlinear feedback systems
AU - GENESIO R.; TESI A.
AF - Dipartimento di Sistemi e Inf., Firenze Univ., Italy
DT - Journal paper
TC - Theoretical mathematical
LA - ENG
PO - IT
JT - IEE Proc. D, Control Theory Appl. (UK); IEE Proceedings D (Control Theory and Applications)
SO - VOL. 138; NO. 4; PP. 313-20; 29 Ref.; DP. July 1991
CD - IPDAD9
SN - 0143-7054
CTN - 0143-7054/91/$3.00+0.00
AB - Investigates the chaotic behaviour of nonlinear feedback systems. A heuristic model of this phenomenon is proposed and applied. Conditions for the existence and the location of chaotic motions are derived in terms of simple relations among the parameters of the system. Two examples show the application of the method and its approximation is discussed
CC - C1340K; C1310
DE - chaos; feedback; nonlinear control systems
IT - nonlinear feedback systems; chaotic behaviour; heuristic model; chaotic motions

NO - B91060515; C9105169?
ET - Chaotic phenomena in power systems
CT - International Conference on Control '91 (Conf. Publ. No.332)
LC - Edinburgh, UK
DC - 25-28 March 1991
AU - LAI L. L.; JIANG Z. Y.; JIANG R. H.
AF - City Univ., London, UK
DT - Conference paper
TC - Theoretical mathematical
LA - ENG
PO - GB
ED - IEE; London, UK
SO - NP. 2 vol. xxvi+1282; PP. 910-14 vol.2; 18 Ref.; DP. 1991
BN - 0-85296-509-5
AB - The authors outline some fundamental concepts of chaos theory and show how they may be applied to power systems. They apply nonlinear control theory and Melnikov's method to study the conditions under which chaotic phenomena could occur in such a power system. The analytical results demonstrate that complex nonlinear phenomena such as subharmonics and chaos can arise in a simple nonlinear system. Certain mode interactions may arise when a simple zero of a nonlinear autonomous system occurs at a certain critical combination of the parameters and as a result interesting phenomena could occur
CC - B8110; C3340H; C1340K
DE - chaos; nonlinear control systems; power systems
IT - power systems; chaos; nonlinear control theory; Melnikov s method; complex nonlinear phenomena; subharmonics; mode interactions; simple zero

NO - C90050517
ET - Designing autonomous relay systems with chaotic motion
CT - Proceedings of the 28th IEEE Conference on Decision and Control (Cat. No.89CH2642-7)
LC - Tampa, FL, USA
DC - 13-15 Dec. 1989
AU - AMRANI D.; ATHERTON D. P.
AF - Sch. of Eng. & Appl. Sci., Sussex Univ., Brighton, UK
SP - IEEE
DT - Conference paper
TC - Theoretical mathematical
LA - ENG
PO - GB
ED - IEEE; New York, NY, USA
SO - NP. 3 vol. 2747; PP. 512-17 vol.1; 6 Ref.; DP. 1989
CTN - CH2642-7/89/0000-0512$01.00
AB - An investigation has been conducted, using simulation, of the existence of chaotic motion in several relay feedback systems. Particular emphasis has been placed on determining when chaotic motion might exist from a knowledge of the unstable limit cycles predicted by the Tsypkin method, the largest amplitude unstable limit cycle being approximately sinusoidal. It is shown that this sinusoidal limit cycle can be calculated quite accurately by the describing function method, and it is found essentially to bound the region of chaotic motion. The chaotic motion gives the appearance of jumps between two or more of the unstable limit cycles found within the region. These unstable limit cycles exhibit two or more oscillations per half period, or spirals if viewed on a phase plane, and their peak amplitudes can be predicted approximately from consideration of the relay switching levels and the DC gain of the linear transfer function
CC - C1340K; C1310; C1320; C1120
DE - chaos; control system synthesis; describing functions; feedback; limit cycles; relay control
IT - control system synthesis; autonomous relay systems; chaotic motion; unstable limit cycles; Tsypkin method; describing function method; relay switching levels; DC gain; linear transfer function

NO - C90050508
ET - Chaos and fractals from nonlinear control process
AU - ARATANI T.
DT - Journal paper
TC - Theoretical mathematical
LA - JAP
PO - ZZ
JT - Syst. Control Inf. (Japan); Systems, Control and Information
SO - VOL. 34; NO. 2; PP. 98-105; 27 Ref.; DP. Feb. 1990
CD - SSEJE3
SN - 0916-1600
AB - The following topics are discussed: chaos, fractals, control systems, computer graphics and system nonlinearities
CC - C1340K; C6130B
DE - BASIC listings; chaos; engineering graphics; fractals; nonlinear control systems
IT - nonlinear systems; fractals; nonlinear control process; chaos; control systems; computer graphics; system nonlinearities

NO - A89084211; C89046697
ET - Adaptive control of chaotic systems
AU - HUBLER A.
AF - Inst. fur Theor. Phys. und Syrergetik, Stuttgart Univ., West Germany
DT - Journal paper
TC - Theoretical mathematical
LA - ENG
PO - DE
JT - Helv. Phys. Acta (Switzerland); Helvetica Physica Acta
SO - VOL. 62; NO. 2-3; PP. 343-6; 8 Ref.; DP. 1989
CD - HPACAK
SN - 0018-0238
CTN - 0018-0238/89/030343-04$1.50+0.20/0
AB - In order to describe the chaotic dynamics of a nonlinear system, a discrete map is reconstructed from the time series of an experimental system. The parameters of the map may depend on time. The map is a model for the dynamics of the experimental system. This model can be used in order to control the dynamics of the experimental system with small external perturbations, e.g. in order to get a special periodic dynamics or a special type of chaos. The author argues that modelling and controlling can be done simultaneously
CC - A0545; C1340E; C1340K
DE - adaptive control; chaos; nonlinear control systems
IT - adaptive control; simultaneous modelling control; chaotic systems; chaotic dynamics; nonlinear system; discrete map; time series; small external perturbations; special periodic dynamics

NO - C89037184
ET - Application of stochastic control techniques to chaotic nonlinear systems
AU - FOWLER T. B.
AF - Mitre Corp., McLean, VA, USA
DT - Journal paper
TC - Theoretical mathematical
LA - ENG
PO - US
JT - IEEE Trans. Autom. Control (USA); IEEE Transactions on Automatic Control
SO - VOL. 34; NO. 2; PP. 201-5; 29 Ref.; DP. Feb. 1989
CD - IETAA9
SN - 0018-9286
CTN - 0018-9286/89/0200-0201$01.00
AB - A control algorithm based on stochastic control techniques is devised for chaotic nonlinear systems. The algorithm uses a state estimator based on the Kalman filter, and yields performance improvements in at least some regions of state space with respect to that obtainable by use of a controller utilizing only the conditional mean of the system state vector. The method is applied to two typical chaotic nonlinear systems (the Henon-Heiles system and the Lorenz system), and their behavior with control is explored numerically
CC - C1340K; C1340G; C1220
DE - chaos; Kalman filters; nonlinear control systems; state estimation; stochastic systems
IT - state estimation; chaotic systems; stochastic control; nonlinear systems; Kalman filter; Henon Heiles system; Lorenz system

NO - C-92-F03981
FT - Action concertée de transfert DRET Les systèmes non linéaires Tome III Commande des systèmes non linéaires.
AU - MOUYON P.; DESCUSSE J.; LEVINE J.; NORMAND CYROT D.; FOSSARD A. J.
AF - CERT/DERA Toulouse (FR); ENSM Nantes (FR); ENSMP/CAI Fontainebleau (FR); LSS/ESE (FR); CERT/DERA (FR)
CS - DGA AFCET Groupe Non Linéaire (FR)
DT - Rapport
LA - FRE
PO - FR
NU - GNL1992
SO - 360 p; nb Réf.; nb Fig.; DP. 1992/03
CTR - DRET8834222004707501
LO - 05; M1363-8/7
AB - Commande au premier ordre des systèmes non linéaires par P MOUYON (pp 9-60 p). Linéarisation entrées-sorties par difféomorphismes et bouclage par J.DESCUSSE (pp 63-123). Linéarisation entrées-états par difféomorphismes et bouclage par J.LEVINE (pp 127-176 p).Linéarisation entrées-sorties et découplage par retour d'état : 1) réacteur chimique de neutralisation ; 2) commande en position des systèmes électropneumatiques par E. RICHARD, S.SCAVARDA, D.THOMASSET (pp 179-263). Optimisation approchée en boucle fermée des systèmes non linéaires par la méthodologie des perturbations singulières par A.J.FOSSARD, J.FOISNEAU, T.HUN HUYNG (pp 267-358).
AN - INFO/VU
CC - 12 01; 14 02
DE - SYSTEME NON LINEAIRE*; LINEARISATION*; FORME CANONIQUE; SYSTEME BOUCLE; COMMANDE NUMERIQUE; SYSTEME COMMANDE; DIFFEOMORPHISME

NO - C-92-F03980
FT - Action concertée de transfert DRET Les systèmes non linéaires Tome II Stabilisation des systèmes non linéaires : quelques approches.
AU - LEVINE J.; BORNE P.; MEIZEL D.; BURGAT C.; TARBOURIECH S.
AF - ENSMP/CAI Fontainebleau (FR); LAII/IDN Villeneuve d'Ascq (FR); UTC/HEUDIASYC Compiégne (FR); LAAS/CNRS Toulouse (FR); LAAS/CNRS Toulouse (FR)
CS - DGA-DRET Groupe Non Linéaire (FR)
DT - Rapport
LA - FRE
PO - FR
NU - GNL1992
SO - 320 p; nb Réf.; nb Fig.; DP. 1992/03
CTR - DRET8834222004707501
LO - 05; M1363-8/7
AB - Comportements asymptotiques des systèmes non commandés par J.LEVINE (50 p) .Stabilité, stabilisation, régulation Approche par les normes vectorielles par P.BORNE, J.P.RICHARD, N.E.RADHY.(68 p). Stabilisation robuste des systèmes à dynamique perturbée par D.MEIZEL (29 p).Stabilité et commande des systèmes linéaires avec saturations par C.BURGAT & S.TARBOURIECH (132 p).
AN - INFO/VU
CC - 12 01
DE - SYSTEME NON LINEAIRE*; STABILITE SYSTEME*; SYSTEME COMMANDE*; COMPORTEMENT ASYMPTOTIQUE; ROBUSTESSE; SYSTEME DYNAMIQUE; SATURATION; REGULATION; COURS ENSEIGNEMENT
CLI - SYSTEME A DYNAMIQUE PERTURBEE; SYSTEME INSTATIONNAIRE

NO - C-92-F03979
FT - Action concertée de transfet DRET : Les systèmes non linéaires Tome I Modèlisation Estimation.
AU - DAUPHIN TANGUY G.; WALTER E.; LOTTIN J.; SCAVARDA S.; BORNARD G.
AF - LAII/IDN Villeneuve d'Ascq (FR); LSS/ESE Gif sur Yvette (FR); LAMII Université de Savoie Annecy (FR); LAI/INSA Lyon (FR); LAG/INPG Grenoble (FR)
CS - DGA AFCET Groupe Non Linéaire (FR)
DT - Rapport
LA - FRE
PO - FR
NU - GNL1992
SO - 200 P; nb Réf.; nb Fig.; DP. 1992/03
CTR - DRET8834222004707501
LO - 05; M1363-8/7
AB - Modèlisation des systèmes physiques par Bond-graphs (graphes de liaisons) par G. DAUPHIN TANGUY & S. SCAVARDA (75p). Identifiabilités et non linéarités : modèlisation et estimation paramètrique, méthodes de test pour les modèles linéaires et non linéaires par rapport aux entrées, lien avec la planification d'expérience par E. WALTER & L. PRONZATO (41p) Identification et réalisation par modèles à état affine PAR J.LOTTIN & D.THOMASSET (40p).Observabilité et observateurs par G. BORNARD, F.CELLE & GILLES G.(40p).
AN - INFO/VU
CC - 12 01
DE - MODELISATION*; SYSTEME NON LINEAIRE*; GRAPHE LIEN*; IDENTIFICATION PARAMETRE*; SYSTEME MULTIDIMENSIONNEL; OBSERVABILITE; PROGICIEL; COURS ENSEIGNEMENT
CLI - SYSTEME ETAT AFFINE; OBSERVATEUR DE KALMAN

NO - C-92-010947
FT - Les réseaux neuronaux artificiels.
CT - Second International Conference on Artificial Neural Networks.
LC - Bournemouth International Centre (GB)
DC - 1991/11/18-1991/11/20
AU - FALLSIDE F.
CS - IEE (GB)
DT - Congrès
LA - ENG
PO - GB
ED - IEE.
SO - NO. 349; 383 p.; nb R f.; nb Fig.; nb Tabl.; DP. 1991
BN - 0-85296-531-1
SN - 0537-9989
LO - 05; ME131-3/349
AB - Les sujets de ces actes de conférences sont les suivants : 1-La théorie (Bartin : une structure neuronale qui apprend à prendre des décisions de risque minimum Bayesien, réseaux neuronaux à correction aval par des algorithmes génétiques), 2-Les implémentations (modélisation de circuits CMOS analogiques pour apprentissage, une conception rapide et nouvelle pour des réseaux multi-couches pouvant être montés en cascade), 3-Les images (identification et poursuite temps réel pour objets multiples dans un environnement bruité, un réseau neuronal basé sur un système de reconnaissance de couleur, réseaux neuronaux pour la reconstruction d'images), 4-Les applications en ingénierie (reconnaissance d'image à détecteurs rayon gamma sensibles à la position, réseaux neuronaux pour des diagnostics électroniques), 5-Les systèmes dynamiques (structures temporelles à apprentissage par rétropropagation continue), 6-Commandes et robotique (systèmes non linéaires utilisant les réseaux neuronaux, commandes intelligentes pour véhicules autonomes utilisant des réseaux neuronaux à mémoires associatives adaptatives temps réel), 7-Systèmes basés sur des règles, 8-Parole et langage naturel (algorithmes rapides pour trouver des caractéristiques invariantes à partir d'un réseau neuronal reconnaissant les mots, apprentissage algébrique dans les réseaux neuronaux syntaxiques), 9-Les applications médicales (surveillance des électrocardiogrammes avec des réseaux neuronaux), 10-La reconnaissance de caractères (texte calligraphique, caractères écrits à la main), 11-Reconnaissance de cibles, traitement de parole, problème de satisfaction de contraintes, composition musicale, recherche visuelle de codes postaux.
AN - INFO/SN
CC - 09 02
DE - RESEAU NEURONAL*; DECISION PROBABILISTE; APPRENTISSAGE; ALGORITHME; CMOS; STRUCTURE MULTICOUCHE; TEMPS REEL; POURSUITE; RECONNAISSANCE IMAGE; RECONSTRUCTION IMAGE; DETECTEUR POSITION; SYSTEME NON LINEAIRE; ROBOTIQUE; RECONNAISSANCE PAROLE; LANGAGE NATUREL; ELECTROCARDIOGRAMME; ELECTROENCEPHALOGRAPHIE; RECONNAISSANCE CARACTERE; RECONNAISSANCE CIBLE; SYSTEME EXPERT; METHODE MOINDRE CARRE

NO - C-92-010148
FT - Contrôle robuste décentralisé pour systèmes incertains à grande échelle : une conception basée sur la limite d'incertitude.
ET - Decentralized robust control for large-scale uncertain systems : a design based on the bound of uncertainty.
AU - CHEN Y. H.
AF - Georgia Inst. of Technol., Atlanta (US)
DT - Publication en série
LA - ENG
PO - US
JT - JOURNAL of DYNAMICS SYSTEMS, MEASUREMENT and CONTROL (Transaction of the "ASME") - (Série G.) (US).
SO - VOL. 114; NO. 1; pp. 1-9; 28 Réf.; 4 Fig.; DP. 1992/03
CD - JDSMAA
SN - 0022-0434
LO - 05; P 0470
AB - Etude d'une classe de systèmes linéaires incertains à grande échelle, l'incertitude étant variable dans le temps. On ne suppose aucune information déterministe ou stochastique à priori, excepté sa limite possible. Proposition d'un contrôle robuste décentralisé pour chaque sous-système. La caractéristique saillante de la conception réside dans le fait qu'elle décompose l'incertitude interne et l'interconnexion. Ceci permet d'incorporer la propriété structurelle de l'incertitude dans la conception. En outre, proposition d'une version adaptive du contrôle décentralisé.
AN - INFO/LV
CC - 12 01
DE - INCERTITUDE*; SYSTEME LINEAIRE*; CONTROLE THEORIE*; ETUDE THEORIQUE, STABILISATION; STABILITE SYSTEME

NO - C-92-F03292
FT - Structures dissipatives. Chaos et turbulence.
AU - MANNEVILLE P.
AF - CNRS, Saclay (FR)
DT - Ouvrage
LA - FRE
PO - FR
ED - CEA, Saclay.
SO - 417 p.; 196 Réf.; 142 Fig.; 1 Tabl.; DP. 1991/05
LO - 20; 92-62 STCAN/BIB
AB - Analyse de la stabilité des structures dissipatives qui apparaissent dans les milieux continus macroscopiques, et de la naissance du chaos dans les structures. Aboutissement d'enseignements donnés en troisième cycle à l'université de Paris VI et à l'Ecole de Physique de la matière condensée de BEG-ROHG, l'ouvrage constitue une monographie didactique qui introduit le lecteur à la complexité des processus non linéaires.
AN - STCAN/LV
CC - 20 13; 20 04
DE - STRUCTURE DISSIPATIVE*; CHAOS*; TURBULENCE*; SYSTEME NON LINEAIRE; CONVECTION THERMIQUE; INSTABILITE THERMIQUE; SYSTEME DYNAMIQUE; COPBIB

NO - C-92-F02127
FT - Optimisation approchée, en boucle fermée, des systèmes non linéaires, par la méthodologie des perturbations singulières.
AU - FOSSARD A. J.; FOISNEAU J.
AF - ONERA, Toulouse (FR); ONERA, Toulouse (FR)
CS - ONERA CERT Toulouse
DT - Rapport
LA - FRE
PO - FR
NU - ONERA/CERT/DERA N° 6/7709
SO - 113 p.; 20 Réf. ; Nb Fig.; DP. 1991/08; No de la fiche programme : T 233 B
CTR - DRET 88.34 [illegible]
LO - 05; M 5085-6/7709
AB - Le rapport comprend deux parties. 1 -On rappelle certaines notions de base sur les systèmes à échelles de temps multiples (formes standard et non standard, theorème de Tihonov...). 2 -On mesure l'intérêt que peut avoir, dans le cas des systèmes à échelles multiples, un traitement des problèmes d'optimisation, dans une optique de perturbations singulières, spécialement dans la recherche d'une solution en boucle fermée. Un certain nombre d'exemples, dans le domaine de l'optimisation de trajectoire, mettent en évidence d'une manière concrète cet intérêt.
AN - INFO/CD
CC - 12 01; 14 02
DE - SINGULARITE MATHEMATIQUE*;SYSTEME BOUCLE FERMEE*;SYSTEME NON LINEAIRE; ECHELLE TEMPS;OPTIMISATION SYSTEME;OPTIMALISATION TRAJECTOIRE
CLI - PERTURBATION SINGULIERE; THEOREME TIHONOV

NO - C-92-004230
FT - Contrôle glissant des systèmes non linéaires à entrée à multivariables et à sortie à multivariables.
ET - Sliding control of MIMO nonlinear systems.
CT - Actes de la première conférence européenne d'automatique Proceedings of the first european control conference -ECC 91-.
LC - Grenoble (FR)
DC - 1991/07/02-1991/07/05
AU - FOSSEN T. I.
AF - Instit of technol, Trondheim (NO)
CS - Groupement de recherche automatique -CNRS- (FR)
DT - Memoire Congres
LA - ENG
PO - NO
ED - Hermes, Paris (FR)
SO - VOL 2; pp. 1855-1860; 8 Ref.; 3 Fig.; DP. 1991
BN - 2-866-01281-X
LO - 05; M 6153-1/1991 vol 2
AB - On discute ce contrôle pour des systèmes à phase minimale. On insiste sur les conditions de stabilité en rapport avec les erreurs du modèle. La stabilité asymptotique globale est garantie par l'application du lemme de Barbalat semblable à celui de Lyapunov. On applique la loi du contrôle à un simulateur d'un réacteur de polymérisation.
AN - INFO/CD
CC - 14 02; 07 04
DE - SYSTEME MULTIVARIABLE*; POLYMERISATION*; SYSTEME NON LINEAIRE; ERREUR; STABILITE SYSTEME; COMPORTEMENT ASYMPTOTIQUE; LYAPOUNOV METHODE; RETROACTION; ROBUSTESSE

NO - C-92-003527
FT - Résultats récents sur la stabilisation adaptative des systèmes de dimensions infinies.
ET - Recent results on adaptive stabilization of infinite dimensional systems.
CT - Actes de la première conférence européenne d'automatique. Proceedings of the first european control conference - ECC 91 -
LC - Grenoble (FR)
DC - 1991/07/02-1991/07/05
AU - LOGEMANN H.; MARTENSSON B.
AF - Univ. of Bremen (DE); Univ. of Bremen (DE)
CS - Groupement de recherche automatique - CNRS - (FR)
DT - Memoire Congres
LA - ENG
PO - DE
ED - Hermès, Paris (FR)
SO - VOL 3; pp. 2067-2071; 31 Ref.; 1 Fig.; DP. 1991
BN - 2-866-01282-8
LO - 05; M 6153-I/1991 Vol 3
AB - L'auteur a montré, précédemment, que, pour stabiliser un système linéaire inconnu, invariant dans le temps, de dimensions finies, il était suffisant de connaître l'ordre de chaque contrôleur de stabilisation. Ici, on généralise ce résultat aux systèmes à dimensions infinies. On donne quelques résultats disponibles sur la stabilisation adaptative de ces systèmes.
AN - INFO/CD
CC - 12 01
DE - ESTIMATION PARAMETRE*; SYSTEME STABILISATION; SYSTEME ADAPTATIF; SYSTEME LINEAIRE; ALGORITHME; ESPACE HILBERT; SYSTEME A PARAMETRE REPARTI; COMMANDE ADAPTATIVE; ROBUSTESSE

NO - C-92-003125
FT - Structures à grande échelle en physique non linéaire.
ET - Large scale structures in nonlinear physics.
CT - Proceedings of the workshop "Large scale structures in nonlinear physics".
LC - Villefranche sur Mer (FR)
DC - 1991/01/13-1991/01/18
AU - FOUNIERS J. O.; SULEM P. L.
AF - Observation Côte d'Azur, Nice (FR); Observation Côte d'Azur, Nice (FR)
DT - Memoire Congres
LA - ENG
PO - FR
JT - Lecture notes in Physics (DE)
ED - Springer Verlag (DE)
SO - VOL 392; 353 p.; nb Ref.; nb Fig.; nb Tabl.; DP. 1991
CD - LNPHA4
BN - 3540548998; 038754899-8
LO - 05; 8490-392
AB - La conférence étudie les états cohérents, les modèles convectifs et turbulents, les cascades inverses, les interfaces et les phénomènes coopératifs dans les fluides et les plasmas, l'implémentation des concepts de la mécanique statistique à la physique des particules et à la matière nucléaire. Elle insiste sur certains phénomènes comme la prédictabilité qui interviennent dans les caractéristiques macroscopiques, même dans les processus dynamiques à faible échelle : structure homoclinique, théorie KAM, stabilité de Lyapunov. Un exposé est consacré aux nouvelles techniques perturbatives des champs classiques non linéaires et quantiques. On présente de nouveaux résultats relatifs à l'analyse des objets hiérarchiquement organisés.
AN - INFO/CD
CC - 20 05; 20 08
DE - MECANIQUE FLUIDE*; PHYSIQUE PARTICULE*; SYSTEME NON LINEAIRE; EFFET COHERENCE; CONVECTION; TURBULENCE; STRUCTURE CASCADE; MECANIQUE STATISTIQUE; SYSTEME DYNAMIQUE; LYAPOUNOV METHODE

NO - C-92-001150
FT - Réponse stationnaire exacte des systèmes dynamiques non linéaires hamiltoniens multi-dimensionnels avec excitations externes et paramétriques.
ET - Exact stationary response of multi-dimensional non-linear hamiltonian dynamical systems under parametric and external stochastic excitations.
AU - SOIZE C.
AF - ONERA (FR)
DT - Publication en serie
LA - ENG
PO - FR
JT - ONERA Tirés à Part (FR)
SO - NO 1991-185; pp. 1-24; 39 Ref.; DP. 1991
CD - ONTPAD
LO - 05; M 147-9/91-185
AB - On étudie une grande catégorie de systèmes dynamiques non linéaires hamiltoniens avec excitations externes et paramétriques aléatoires. Les excitations aléatoires sont modélisées par un bruit blanc gaussien. La partie conservative est une formulation hamiltonienne pour les systèmes dynamiques non linéaires indépendants du temps. La partie non conservative comporte trois termes : un terme d'amortissement linéaire ou non linéaire, une excitation externe aléatoire qui est le terme non homogène, et un terme d'excitation paramétrique aléatoire. La stabilité du système et l'existence d'une réponse stationnaire asymptotique sont étudiées car l'excitation paramétrique aléatoire a des variations des caractéristiques dynamiques avec le temps. La fonction de densité de probabilité en régime établi est construite comme solution de l'équation de Fokker-Planck. La fonction caractéristique et la matrice de croissance de la réponse stationnaire sont calculées explicitement. Plusieurs exemples montrent clairement les effets des non linéarités et de l'excitation paramétrique aléatoire pour des systèmes multi-dimensionnels.
AN - INFO/PA
CC - 12 01; 14 02
DE - SYSTEME DYNAMIQUE*; REPONSE*; STABILITE SYSTEME; ETUDE THEORIQUE; EQUATION FOKKER PLANCK; EXCITATION STOCHASTIQUE; SYSTEME MULTIVARIABLE; SYSTEME NON LINEAIRE; HAMILTONIEN

NO - C-91-013059
FT - Examen de plusieurs aspects de la conception de contrôleurs flous.
ET - A review of some aspects on designing fuzzy controllers.
CT - Knowledge-based system applications for guidance and control.
LC - Madrid, ES
DC - 1990/09/18-1990/09/21
AU - TRILLAS E.; DELGADO M.; VERDEGAY J. L.; VILA M. A.
AF - Ministère de Défense, Madrid, ES; Faculté des Sciences, Grenade, ES; Faculté des Sciences, Grenade, ES; Faculté des Sciences, Grenade, ES
DT - Memoire Congres
LA - ENG
PO - ES
JT - AGARD Conference Proceedings (FR)
ED - AGARD (neuilly-sur-Seine)
SO - VOL CP474; pp. 31.1-31.12; 23 Ref.; 2 Fig.; 1 Tabl.; DP. 1990/04
CD - AGCPAV
BN - 9-283-50610-3
LO - 02; AGARD-CP-474
AB - Description des fondements les contrôleurs flous et des différents moyens de les mettre en oeuvre. Etude du management de l'information, c'est-à-dire des voies utilisées pour réaliser les inférences à partir des connaissances des spécialistes (en général, la règle de base de déduction du calcul des prédicats). Analyse des fonctions d'implication possibles et des conséquences de leur utilisation.
AN - INFO/CR
CC - 09 05; 13 08
DE - SYSTEME COMMANDE NON LINEAIRE*; CONTROLE PROCESSUS*; PROCESSUS INDUSTRIEL; COMMANDE AUTOMATIQUE MACHINE; SYSTEME EXPERT; FONCTION FLOUE; REGLE INFERENCE; BASE DONNEE DEDUCTIVE

NO - C-91-002328
FT - Modélisation des systèmes non linéaires à l'aide de modèles de calcul de la moyenne mobile autorégressifs non linéaires (NARMAX).
ET - Modeling nonlinear systems by using nonlinear autoregressive moving average models (NARMAX).
CT - IEEE-ICASSP-1990-International conference on acoustics, speech, and signal processing- Vol 5 : Spectral estimation-Underwater signal processing.
LC - Albuquerque (US)
DC - 1990/04/03-1990/04/06
AU - SEIDEL D. K.; DAVIES P.
AF - Purdue Univ, West Lafayette (US); Purdue Univ, West Lafayette (US)
DT - Memoire Congres
LA - ENG
PO - US
ED - IEEE New York (US)
SO - NO 90CH2847-2; pp. 2559-2562; 9 Ref.; 4 Fig.; 2 Tabl.; DP. 1990
LO - 05; Me 349-98/1990 Vol 5
AB - Ces modèles sont des extensions des modèles ARMA.Ils peuvent servir à simuler la réponse échantillonnée des systèmes non linéaires. Ce sont souvent des modèles compacts, adaptés aux applications de contrôle et de conception. En établissant des relations entre ces modèles digitaux de données d'entrée-sortie et les modèles physiques des systèmes, on peut générer des estimations de paramètres physiques d'un système. Ici, on décrit le comportement de deux oscillateurs couplés non linéaires par un système d'équations non linéaires couplées. On applique une technique de représentation à ces équations pour générer des modèles NARMAX qui relient l'entrée échantillonnée à la réponse échantillonnée des systèmes non linéaires.
AN - INFO/CD
CC - 09 03; 12 01
DE - Traitement signal*; Moyenne mobile*; Système non linéaire; Système donnée échantillonnée; Donnée digitale; Estimation paramètre; Equation non linéaire; Modèle autorégressif*; Signal échantillonné*; Modèle ARMA

NO - C-90-011266
FT - Dynamique chaotique des systèmes non linéaires.
ET - Chaotic dynamics of nonlinear systems.
AU - RASBAND S. N.
AF - BRIGHAN Youry Univ. Provo (UJ)
DT - Ouvrage
LA - ENG
PO - ZZ
ED - John Wiley and sons New York
SO - 230 p.; nbres Ref.; DP. 1990
BN - 0-471-63418-2
LO - 05; 13859/6A
AB - Distributions à une dimension. Théorie de l'universalité. Dimension fractale. Dynamique différentielle. Exemples non-linéaires avec chaos. Distribution à deux dimensions. Dynamique conservative. Mesure du chaos. Complexité et chaos.
AN - INFO/VU
CC - 12 01; 14 02
DE - Géométrie différentielle*; Système non linéaire*; Objet fractal*; Chaos*; Dynamique système; Théorie bifu cation; Distribution multidimensionnelle

NO - C-90-F01880
FT - Contrôlabilité exacte, perturbations et stabilisation de systèmes distribués.
AU - LIONS J. L.
AF - Collège de France (FR)
DT - Ouvrage
LA - FRE
PO - FR
ED - Masson, Paris
SO - NO RMA 8 et 9; 536 et 272 p.; nb Ref.; Collection recherches mathématiques appliquées; DP. 1988
BN - 2225814775; 2-225814740
LO - 20; 90-68-1.2 STCAN/BIB
AB - Cet ouvrage présente la méthode HUM (Hilbert Uniqueness Method) qui permet de conduire un système d'un état initial à un état final donné, en un temps donné avec un contrôle optimal et un effort minimum. Ensuite les diverses perturbations qui peuvent affecter un système distribué sont étudiées, afin d'examiner la robustesse de la méthode HUM. Un problème modèle ; contrôlabilité exacte de l'équation des ondes ; contrôle par Dirichlet. Formulation générale du problème de la contrôlabilité exacte. Système de l'élasticité et quelques modèles de plaques vibrantes. Equation des ondes : conditions aux limites de Neumann et de type mêlé. Contrôlabilité exacte simultanée. Contrôlabilité exacte de problèmes de transmission. Contrôle interne. Caractérisation du contrôle donné par HUM. Système de l'optimalité et méthode de dualité. Systèmes couplés. Contrôlabilité exacte et pénalisation. Contrôlabilité exacte et pertubations singulières. Perturbations des modes d'action sur les systèmes. Perturbation des domaines. Homogénéisation. Systèmes à mémoire.
AN - INFO/AP
CC - 12 01; 13 13
DE - Théorie contrôle optimal*; Système élastique*; Stabilité; Perturbation; Théorie système; Analyse système; Equation onde; Système commande; Système non linéaire; Théorie perturbation; Stabilisation; Plaque; Condition limité; Système à paramètre réparti*; Contrôlabilité*; Etude dynamique; Optimisation sous contrainte; COPBIB

NO - C-90-F00283
FT - A propos du chaos spatio-temporel : concepts et expériences.
AU - CHIFFAUDEL A.
AF - Ecole Normale Supérieure, Paris (FR)
CS - Ec. Normale Supér., Groupe de Phys. du Solide (FR)
DT - Rapport
LA - FRE
PO - FR
NU - ENS 1989
SO - Rapport de mise au point; 61 p.; 70 Ref.; 15 Fig.; DP. 1988
CTR - Convention IEP 87/82
LO - 05; I605 M 600-1/DRET-IEP 87-822 F
AB - Ce rapport nous éclaire sur la notion de chaos spatio-temporel, c'est-à-dire la perte de cohérence temporelle d'un système non linéaire, à peu de degrés de liberté. Cela nous fait prendre conscience que le désordre peut être compris, formalisé et encadré par des théories des systèmes dynamiques. Cette théorie sera appliquée ici à l'étude des écoulements turbulents.
AN - INFO/RI
CC - 20 04; 14 02
DE - Stabilité écoulement*; Théorie système*; Ecoulement turbulent; Cohérence; Système non linéaire; Instabilité; Chaos*; Equation Kolmogorov

NUMERO SIGNALEMENT	AD-A252 520/2/XAD
TITRE ANGLAIS	Learning Enhanced Flight Control System for High Performance Aircraft.
AUTEUR(S)	NISTLER N. F.
AUTEUR COLLECTIF	Air Force Inst.of Tech., Wright-Patterson AFB, OH.
CLASSIFICATION INT	000805000; 012200
TYPE DE DOCUMENT	Thesis
CODE LANGUE	ENG
CODE PAYS D'ORIGINE	US
NUMERO DE RAPPORT	AFIT/CI/CIA-92-039
SOURCE	Master's thesis; NP. 100; DP. 1992.
CODE JOURNAL NTIS	U9220
CODE TARIF NTIS	NTIS Prices: PC A05/MF A02
RESUME	Numerous approaches to flight control system design have been proposed in an attempt to govern the complex behavior of high performance aircraft.Gain scheduled linear control and adaptive control have traditionally been the most widely used methodologies, but they are not without their limitations.Gain scheduling requires large amounts of a priori design information and costly manual tuning in conjunction with flight tests, while still lacking an ability to accommodate unmodeled **dynamics** and model uncertainty beyond a limited amount of robustness that can be incorporated into the design.Adaptive control is suitable for nonlinear systems with unmodeled **dynamics**, but has deficiencies in accounting for quasi-static state dependencies.Moreover, inherent time delays in adaptive control make it difficult to match the performance of a well-designed gain scheduled controller.An alternative approach that is able to compensate for the inadequacies experienceu with traditional control techniques and to automate the tuning process is desired.Recent Teaming techniques have demonstrated an ability to synthesize multivariable mappings and are thus able to learn a functional approximation of the initially unknown state dependent **dynamic** behavior of the vehicle.By combining a learning component with an adaptive controller, a new hybrid control system that is able to adapt to unmodeled **dynamics** and novel situations, as well as to learn to anticipate quasi-static state dependencies is formed.
CODE CLASSIFICATION	51 05
DESCRIPTEUR(S)	Flight control systems*;Learning*;Accounting;Aircraft;Approach; Deficiencies;Delay;Dynamics;Gain;Limitations;Models;Nonlinear systems;Scheduling;Statics;Test and evaluation;Time;Tuning; Uncertainty
IDENTIFICATEUR(S)	Theses;NTISDODXA

NUMERO SIGNALEMENT	N92-25636/1/XAD
TITRE ANGLAIS	Analysis of Control Trajectories Using Symbolic and Database Computing.
AUTEUR(S)	GROSSMAN R.
AUTEUR COLLECTIF	Chicago Univ., IL.
ORGAN FINANCEMENT	National Aeronautics and Space Administration, Washington, DC.
CLASSIFICATION INT	000917000; C0455749
TYPE DE DOCUMENT	Report
CODE LANGUE	ENG
ORGAN FINANCEMENT	Air Force Office of Scientific Research, Bolling AFB, DC.
CLASSIFICATION INT	043127127; 401997
TYPE DE DOCUMENT	Report
CODE LANGUE	ENG
CODE PAYS D'ORIGINE	US
SOURCE	Final rept. 15 Nov 90-14 Nov 91; NP. 11; DP. 10 Jan 92.
CODE JOURNAL NTIS	U9212
CODE TARIF NTIS	NTIS Prices: PC A03/MF A01
NUMERO ALLOCATION	AFOSR-91-0033
NUMERO PROJET	2304
NUMERO ACTIVITE	A1
NUMERO(S) AGENCE	AFOSR-TR-92-0118
RESUME	Significant progress was made in a number of aspects of nonlinear and stochastic systems.An important problem in the adaptive control of a finite state Markov chain was solved, and significant progress was made along more general directions.A controlled switching diffusion model was developed to study the hierarchical control of flexible manufacturing systems and significant results were obtained.In the area of deterministic nonlinear systems the work continued on nonlinear observers and linearizable **dynamics**.Finally, some important problems in the area of discrete event systems were solved.
CODE CLASSIFICATION	62 03; 72 00
DESCRIPTEUR(S)	Nonlinear systems*;Adaptive control systems*;Control;Diffusion; Dynamics;Models;Numbers;Probability;Switching;Stochastic control
IDENTIFICATEUR(S)	Markov chains;Hierarchical control;Flexible manufacturing systems; NTISDODXA;NTISDODAF

NUMERO SIGNALEMENT	N92-17998/5/XAD
TITRE ANGLAIS	Neural Networks for Aircraft System Identification.
AUTEUR(S)	LINSE D. J.
AUTEUR COLLECTIF	Princeton Univ., NJ.Dept.of Mechanical and Aerospace Engineering.
ORGAN FINANCEMENT	National Aeronautics and Space Administration, Washington, DC.
CLASSIFICATION INT	009938087; P3732113
TYPE DE DOCUMENT	Report
CODE LANGUE	ENG
CODE PAYS D'ORIGINE	US
SOURCE	In NASA. Langley Research Center, Joint University Program for Air Transportation Research, 1990-1991 p 141-154; NP. 14; DP. Dec 91.
CODE JOURNAL NTIS	S3008
CODE TARIF NTIS	NTIS Prices: (Order as N92-17984/5, PC A09/MF A02)
RESUME	Artificial neural networks offer some interesting possibilities for use in control.Our current research is on the use of neural networks on an aircraft model.The model can then be used in a nonlinear control scheme.The effectiveness of network training is demonstrated.
CODE CLASSIFICATION	51 05
DESCRIPTEUR(S)	Aircraft control*;Aircraft models*;Control systems design*;Dynamic control*;Machine learning*;Neural nets*;System identification*; Mathematical models;Nonlinear systems
IDENTIFICATEUR(S)	NTISNASA

NUMERO SIGNALEMENT	PB92-148725/XAD
TITRE ANGLAIS	Observer Design in the Tracking Control Problem of Robots.
AUTEUR(S)	BERGHUIS H.; NIJMEIJER H.; LOEHNBERG P.
	can be used to determine the important **dynamic** characteristics of the Harmonic Drive gear reducer.The PHD, is a planar, three degree of freedom arm with torque sensors integral to each joint allowing joint torque feedback to be implemented.Preliminary testing using the PHD has shown that a simple linear spring model of the Harmonic Drive's flexibility is suitable in many situations.Future work with the system could include a more detailed Harmonic Drive model, as well as development of joint torque feedback schemes for force control.(kr).
CODE CLASSIFICATION	41 03; 62 00
DESCRIPTEUR(S)	Degrees of freedom*;Manipulators*;Accuracy;Control;Detectors; Drives;Dynamics;Feedback;Gears;Harmonics;Humans;Linear systems; Mathematical models;Mobile;Models;Planar structures;Platforms; Reduction;Rob ts;Simulation;Skills;Springs;Torque;Theses
IDENTIFICATEUR(S)	FTS Flight Te,erobotic Servicer;PHD Planar Harmonic Driver; NTISDODXA

NUMERO SIGNALEMENT	N91-13195/3/XAD
TITRE ANGLAIS	Nonregular Solution on the Nonlinear **Dynamic** Disturbance Decoupling Problem with an Application to a Complete Solution of the Nonlinear Model Matching Problem.
AUTEUR(S)	HUIJBERTS H. J. C.
AUTEUR COLLECTIF	Technische Univ.Twente, Enschede (Netherlands).Faculty of Applied Mathematics.
ORGAN FINANCEMENT	National Aeronautics and Space Administration, Washington, DC.
CLASSIFICATION INT	090700007; U1294434
TYPE DE DOCUMENT	Report
CODE LANGUE	ENG
CODE PAYS D'ORIGINE	NL
NUMERO DE RAPPORT	MEMO-862
SOURCE	NP. 23; DP. May 90.
CODE JOURNAL NTIS	S2904
CODE TARIF NTIS	NTIS Prices: PC A03/MF A01
RESUME	The nonregular **Dynamic** Disturbance Decoupling Problem (nDDDP) for nonlinear control systems is presented.A local solution is given by means of a constructive algorithm that is based on Singh's algorithm and the clamped **dynamics** algorithm.The nonlinear Model Matching Problem (MMP) is studied.This problem is defined as follows: given a nonlinear control system, to be referred to as the plant, and another nonlinear control system, to be referred to as a model, can one find a compensator for the plant in such a way that the input-output behavior of the compensated plant matches that of the model.By proving that the solvability of the nonlinear MMP is equivalent to the solvability of an associated nDDDP a complete local solution of this problem is established.
CODE CLASSIFICATION	62 03; 72 00
DESCRIPTEUR(S)	Control theory*;Algorithms;Decoupling;Dynamic control;Dynamical systems;Matching;Nonlinear systems;Compensators;Proving
IDENTIFICATEUR(S)	Foreign technology*;Model matching problem;NTISNASAE;NTISFNNL

NUMERO SIGNALEMENT AD-A226 736/7/XAD
TITRE ANGLAIS Application of Chaos Methods to Helicopter Vibration Reduction Using Higher Harmonic Control.
AUTEUR(S) SARIGUL KLIJN M. M.
AUTEUR COLLECTIF Naval Postgraduate School, Monterey, CA.
CLASSIFICATION INT 019895000; 251450
TYPE DE DOCUMENT Thesis
CODE LANGUE ENG
CODE PAYS D'ORIGINE US
SOURCE Doctoral thesis; NP. 202; DP. Mar 90.
CODE JOURNAL NTIS U9108
CODE TARIF NTIS NTIS Prices: PC A10/MF A02
RESUME Chaos is used to understand complex nonlinear **dynamics**.The geometric and topological methods of Chaos theory are applied, for the first time, to the study of flight test data.Data analyzed is from the OH-6A Higher Harmonic Control (HHC) test aircraft.HHC is an active control system used to suppress helicopter vibrations.Some of the first practical applications of Chaos methods are demonstrated with the HHC data.although helicopter vibrations are mostly periodic, evidence of chaos was found.The presence of a strange attractor was shown by computing a positive Lyapunov exponent and computing a non integer fractal correlation dimension.A broad band Fourier spectrum and a well defined attractor in pseudo phase space are observed.A limit exists to HHC vibration reduction due to the presence of chaos.A new technique based on a relationship between the Chaos methods (the Poincare section and Van der Pol plane) and the vibration amplitude and phase was discovered.This newly introduced technique results in the following: (1) it gives the limits of HHC vibration reduction, (2) it allows rapid determination of best phase for a HHC controller, (3) it determines the minimum HHC controller requirement for any helicopter from a few minutes duration of flight test data, (4) it shows that the HHC controller transfer matrix is linear and repeatable when the vibrations are defined in the Rotor Time Domain and that the matrix is nonlinear and nonrepeatable when the vibrations are defined in the Clock Time Domain.Theses.(jhd).
CODE CLASSIFICATION 51 03; 51 02; 46 05
DESCRIPTEUR(S) Helicopters*;Helicopter rotors*;Vibration*;Amplitude;Control; Control systems;Dynamics;Experimental data;Flight testing;Fourier analysis;Geometry;Harmonics;Lyapunov functions;Nonlinear systems; Reduction;Requirements;Test vehicles;Theses;Time domain;Topology
IDENTIFICATEUR(S) HHC Higher Harmonic Control *;Chaos;Nonlinear dynamics;OH 6A Aircraft;NTISDODXA

NUMERO SIGNALEMENT AD-A226 525/4/XAD
TITRE ANGLAIS Multivariable Methods for the Design, Identification, and Control of Large Space Structures.Volume 1.Estimator Eigenvalue Placement in Positive Real Design.
AUTEUR(S) SLATER G. L.; MCLAREN M. D.
AUTEUR COLLECTIF Cincinnati Univ., OH.Dept.of Aerospace Engineering and Engineering Mechanics.
ORGAN FINANCEMENT Wright Research and Development Center, Wright-Patterson AFB, OH.
CLASSIFICATION INT 006394082; 415940
TYPE DE DOCUMENT Report
CODE LANGUE ENG
CODE PAYS D'ORIGINE US
SOURCE Final rept. Jul 87-Feb 89; See also Volume 3, AD-A226526; NP. 36; DP. Jul 89.
CODE JOURNAL NTIS U9107

NO - C-92-011838
FT - Réponse chaotique de décrochage d'un rotor d'hélicoptère en vol vers l'avant.
ET - Chaotic stall response of helicopter rotor in forward flight.
AU - TANG D. H.; DOWELL E. H.
AF - Duke Univ., Durham (US); Duke Univ., Durham (US)
DT - Publication en série
LA - ENG
PO - US
JT - JOURNAL of FLUIDS and STRUCTURES (GB).
SO - VOL. 6; NO. 3; pp. 311-335; 9 Réf.; 14 Fig.; 1 Tabl.; DP. 1992/05
CD - JOFS2X
SN - 0889-9746
LO - 05; P 2823
AB - Discussion d'un processus typique d'évolution pour la réponse de décrochage des pales d'hélicoptères à un mouvement périodique, apériodique, ou chaotique, et de la condition nécessaire pour l'amorçage de la réponse chaotique. C'est le première étude d'un tel mouvement chaotique dû au décrochage aérodynamique d'une pale d'hélicoptère. Pour cette étude, on a appliqué le modèle non linéaire ONERA de décrochage aérodynamique à l'analyse de la réponse de décrochage des pales d'hélicoptère. Etablissement et solution des équations non linéaires de variables d'état et des équations linéaires de perturbation des variables d'état. Comparaison outre les résultats du modèle ONERA et ceux d'un modèle aérodynamique non linéaire plus simple.
AN - INFO/LV
CC - 01 03; 20 04
DE - PALE ROTOR VOILURE TOURNANTE*; ROTOR HELICOPTERE*; DECROCHAGE AERODYNAMIQUE*; CHAOS; MODELE MATHEMATIQUE; ETUDE THEORIQUE

NO - C-92-011809
FT - Sur le chaos dans les sillages.
ET - On choas in wakes.
AU - NOACK B. R.; ECKELMANN H.
AF - Max Planck Inst., Goettingen (DE); Univ. Goettingen (DE)
DT - Publication en série
LA - ENG
PO - DE
JT - PHYSICA D NONLINEAR PHENOMENA (NL).
SO - VOL. 56; NO. 2/3; pp. 151-164; 41 R f.; 9 Fig.; DP. 1992/05
CD - PDNPDT
SN - 0167-2789
LO - 05; P 2812
AB - Nous faisons la distinction entre écoulements "séparables" au voisinage de corps, qu'on peut décrire approximativement par des systèmes autonomes (AS) à dimensions finies d'équations différentielles ordinaires, et sillage "non-séparable", qui ne possèdent pas cette propriété. Pour les sillages séparables, présentation d'une méthode systématique pour la construction des AS à partir des équations de NAVIER-STOKES, et application à l'écoulement bidimensionnel au voisinage d'un cylindre circulaire. Au moyen du concept de séparabilité, discussion sur la possibilité de bifurcations et de comportement chaotique pour le sillage d'un corps en écoulement non uniforme. On montre que les bifurcations de HOPF et de fourche constituent les instabilités génériques de l'écoulement stationnaire au voisinage d'un corps de taille finie et de l'écoulement bidimensionnel au voisinage d'un cylindre de forme arbitraire. Quand on augmente le nombre de REYNOLDS, les écoulements périodiques correspondants tendent à devenir instables par un scénario intermittent, une cascade à doublement de période, ou une bifurcation de HOPF. En outre, étude de perturbations tridimensionnelles typiques du sillage bidimensionnel stationnaire et périodique d'un cylindre. Des arguments théoriques indiquent qu'il est très improbable que la dynamique des sillages turbulents soit caractérisée par un attracteur étrange de faibles dimensions.
AN - INFO/LV
CC - 20 04
DE - SILLAGE*; CHAOS*; EQUATION NAVIER STOKES; ECOULEMENT STATIONNAIRE; ECOULEMENT UNIFORME; ECOULEMENT BIDIMENSIONNEL

NO - C-92-000820
FT - La dynamique des fluides météorologiques. Modélisation asymptotique. Stabilité et mouvement atmosphérique chaotique.
ET - Meteorological fluid dynamics asymptotic modelling, stability and chaotic atmospheric motion.
AU - ZEYTOUNIAN R. F.
DT - Publication en serie
LA - ENG
PO - ZZ
JT - Lectures notes in physics (DE)
SO - NO m 5; 346 p.; BN . 3-540-54416.1; DP. 1991
CD - LNPHA4
SN - 0075-8450
LO - 05; 8430-1/15
AB - La terre en rotation et son atmosphère. Equations dynamiques et thermiques des mouvements atmosphériques. Phénomènes de propagation d'ondes dans l'atmosphère. Le filtrage des ondes internes. Problèmes d'ajustements instationnaires. Problèmes locaux dynamiques d'onde de lee. Problèmes de couches limites. Stabilité météodynamique. Comportement chaotique déterministe des mouvements atmosphériques.
AN - INFO/VU
CC - 04 02; 20 04
DE - COURANT JET METEOROLOGIE*; STABILITE ECOULEMENT*; PHENOMENE METEOROLOGIQUE; MODELE ECOULEMENT; CIRCULATION ATMOSPHERIQUE; CHAOS

38/61 - (C) C.cedocar
NO - C-90-010973
FT - Transition de l'ordre au chaos dans le sillage d'un aileron.
ET - Transition from order to chaos in the wake of an airfoil.
AU - WILLIAMS S. K.; GHARIB M.
AF - Univ.of California, la Jolla, CA (US); Univ.of California, la Jolla, CA (US)
DT - Publication en serie
LA - ENG
PO - US
JT - journal of fluid mechanics ; (GB)
SO - VOL 213; pp. 29-57; 24 Ref.; 24 Fig.; 7 Phot.; DP. 1990/04
CD - JFLSA7
SN - 0022-1120
LO - 05; P 0484
AB - Présentation d'une étude expérimentale de l'intéraction non linéaire de fréquences multiples dans les sillages forcé d'un aileron. Les vagues avec une ou deux fréquences distinctes se comportent de manière ordonnée, étant verrouillées ou quasi-périodiques. Quand on ajoute une troisième fréquence incommensurable au système, l'écoulement laisse apparaître un comportement chaotique. Antérieurement, on n'avait parlé de cette transition vers le chaos, à trois fréquences, que pour des écoulements en système fermé, à de faibles nombres de REYNOLDS. Cependant, l'écoulement chaotique montre des caractéristiques localisées similaires à celles des écoulements turbulants à nombre de REYNOLDS élevé. Vérification du degré de comportement chaotique en appliquant les idées de la dynamique non linéaire (exposants de LYAPUNOV, sections de POINCARE) aux données expérimentales, reliant aussi la physique fondamentale du système aux concepts d'intéraction de modes et de chaos.
AN - INFO/LV
CC - 20 04; 01 03
DE - Sillage*; Aileron*; Ecoulement non uniforme; Nombre Reynolds; Chaos*

NO - C-89-013080
FT - Etude du chaos spatial et temporel survenant dans les écoulements confinés spatialement.
AU - COULLET P.; GIL L.; LEGA J.; ELPHICK C.; REPAUX D.
AF - Lab. Physique Théorique, Nice (FR); Lab. Physique Théorique, Nice (FR); Lab. Physique Théorique, Nice (FR)
CS - Université de Nice (FR)
DT - Rapport
LA - MUL
PO - FR
NU - Univ. Nice 1989
SO - Rapport final; 50 p.; nombr. Ref.; DP. 1989
CTR - DRET no 86/1511
LO - 05; M 600-1/86-1511
AB - Recueil des publications dans le contrat DRET 86/1511 relatifs aux défauts qui peuvent présenter les structures hors d'équilibre issues d'instabilités. Une forme de turbulence associée aux défauts topologiques. Défauts topologiques des configurations ondulatoires. Transitions dans les systèmes éloignés de l'équilibre : approche de Ginzburg-Landau. Turbulence provoquée par un défaut, ses propriétés statistiques et spatio-temporelles. Défauts et bifurcations sous-critiques.
AN - INFO/VU
CC - 20 04
DE - Stabilité écoulement*; Ecoulement conduit; Ecoulement cavité; Turbulence; Défaut; Chaos; Théorie bifurcation

NO - C-89-009883
FT - Leçons des observations d'écoulement chaotique dans l'atmophère.
ET - Lessons from observations of chaotic flow in the atmosphere.
AU - SCORER R. S.
AF - Imperial College (GB)
DT - Publication en série
LA - ENG
PO - GB
JT - Journal de Mécanique Théorique et Appliquée (FR)
SO - VOL 7; pp. 145-165; 21 Ref.; 3 Fig.; DP. 1988
CD - JMTADB
SN - 0750-7240
LO - 05; P 2250
AB - Contraintes de Reynolds : le mouvement moyen. L'opposition de la K théorie. Diffusion de moment. Vers un meilleur modèle : le mécanisme de mélange. La cascade d'énergie; la vorticité chaotique. Turbulence thermique. Turbulence haute altitude dans l'atmosphère. Fermeture et validation de modèles. Théories statistiques et spectres de puissance. Analyse dimensionnelle et similitude. Mécanismes de concentration naturelle.
AN - INFO/VU
CC - 04 01; 20 04
DE - Turbulence atmosphérique*; Modèle écoulement*; Modélisation*; Chaos

REPORT DOCUMENTATION PAGE

1. Recipient's Reference	2. Originator's Reference	3. Further Reference	4. Security Classification of Document
	AGARD-LS-191	ISBN 92-835-0714-2	UNCLASSIFIED/ UNLIMITED

5. Originator Advisory Group for Aerospace Research and Development
North Atlantic Treaty Organization
7 rue Ancelle, 92200 Neuilly sur Seine, France

6. Title NON LINEAR DYNAMICS AND CHAOS

7. Presented on

8. Author(s)/Editor(s)	9. Date
Various	June 1993
10. Author's/Editor's Address	**11. Pages**
Various	124

12. Distribution Statement *There are no restrictions on the distribution of this document.* Information about the availability of this and other AGARD unclassified publications is given on the back cover.

13. Keywords/Descriptors

Nonlinear systems	Irreversible processes
Fractal geometry	Fluid dynamics
Nonlinear differential equations	Meteorology
Thermodynamics	Flight control

14. Abstract

In the last decade many efforts have been oriented towards the understanding of the unexpected behaviour of systems — linear or non-linear. These could be large (weather systems, biological life) or small (automatic pilot). A new branch of dynamics is now considered; it is called "Chaos". Some general theories have emerged and reconsideration of concepts of non-linear control to determine the stability of such systems is now intensively studied in the scientific community.

It is planned that the following topics will be covered:

— Linear (including time varying coefficients equations) vs non-linear systems. Types of non-linearity: curved characteristics, jumps, bifurcation
— Non linear dynamics; sensibility to initial conditions and/or uncertainties on the system parameters. Robustness
— Neuronal-type machines
— Chaos — Random process behaviour
— Reversibility and irreversibility; Newtonian mechanics and thermodynamics
— Fractals
— Applications:
  — Fluid mechanics, meteorology
  — Aircraft behaviour
  — Mechanical systems.

This Lecture Series, sponsored by the Guidance and Control Panel of AGARD has been implemented by the Consultant and Exchange Programme.

AGARD Lecture Series 191
Advisory Group for Aerospace Research and Development, NATO
NON LINEAR DYNAMICS AND CHAOS
Published June 1993
124 pages

In the last decade many efforts have been oriented towards the understanding of the unexpected behaviour of systems — linear or non-linear. These could be large (weather systems, biological life) or small (automatic pilot). A new branch of dynamics is now considered; it is called "Chaos". Some general theories have emerged and reconsideration of concepts of non-linear control to determine the stability of such systems is now intensively studied in the scientific community.

It is planned that the following topics will be covered:

P.T.O.

AGARD-LS-191

Nonlinear systems
Fractal geometry
Nonlinear differential equations
Random processes
Thermodynamics
Irreversible processes
Fluid dynamics
Meteorology
Flight control

AGARD Lecture Series 191
Advisory Group for Aerospace Research and Development, NATO
NON LINEAR DYNAMICS AND CHAOS
Published June 1993
124 pages

In the last decade many efforts have been oriented towards the understanding of the unexpected behaviour of systems — linear or non-linear. These could be large (weather systems, biological life) or small (automatic pilot). A new branch of dynamics is now considered; it is called "Chaos". Some general theories have emerged and reconsideration of concepts of non-linear control to determine the stability of such systems is now intensively studied in the scientific community.

It is planned that the following topics will be covered:

P.T.O.

AGARD-LS-191

Nonlinear systems
Fractal geometry
Nonlinear differential equations
Random processes
Thermodynamics
Irreversible processes
Fluid dynamics
Meteorology
Flight control

AGARD Lecture Series 191
Advisory Group for Aerospace Research and Development, NATO
NON LINEAR DYNAMICS AND CHAOS
Published June 1993
124 pages

In the last decade many efforts have been oriented towards the understanding of the unexpected behaviour of systems — linear or non-linear. These could be large (weather systems, biological life) or small (automatic pilot). A new branch of dynamics is now considered; it is called "Chaos". Some general theories have emerged and reconsideration of concepts of non-linear control to determine the stability of such systems is now intensively studied in the scientific community.

It is planned that the following topics will be covered:

P.T.O.

AGARD-LS-191

Nonlinear systems
Fractal geometry
Nonlinear differential equations
Random processes
Thermodynamics
Irreversible processes
Fluid dynamics
Meteorology
Flight control

- Linear (including time varying coefficients equations) vs non-linear systems. Types of non-linearity: curved characteristics, jumps, bifurcation
- Non linear dynamics; sensibility to initial conditions and/or uncertainties on the system parameters. Robustness
- Neuronal-type machines
- Chaos – Random process behaviour
- Reversibility and irreversibility; Newtonian mechanics and thermodynamics
- Fractals
- Applications:
  - Fluid mechanics, meteorology
  - Aircraft behaviour
  - Mechanical systems.

This Lecture Series, sponsored by the Guidance and Control Panel of AGARD, has been implemented by the Consultant and Exchange Programme.

ISBN 92-835-0714-2

- Linear (including time varying coefficients equations) vs non-linear systems. Types of non-linearity: curved characteristics, jumps, bifurcation
- Non linear dynamics; sensibility to initial conditions and/or uncertainties on the system parameters. Robustness
- Neuronal-type machines
- Chaos – Random process behaviour
- Reversibility and irreversibility; Newtonian mechanics and thermodynamics
- Fractals
- Applications:
  - Fluid mechanics, meteorology
  - Aircraft behaviour
  - Mechanical systems.

This Lecture Series, sponsored by the Guidance and Control Panel of AGARD, has been implemented by the Consultant and Exchange Programme.

ISBN 92-835-0714-2

- Linear (including time varying coefficients equations) vs non-linear systems. Types of non-linearity: curved characteristics, jumps, bifurcation
- Non linear dynamics; sensibility to initial conditions and/or uncertainties on the system parameters. Robustness
- Neuronal-type machines
- Chaos – Random process behaviour
- Reversibility and irreversibility; Newtonian mechanics and thermodynamics
- Fractals
- Applications:
  - Fluid mechanics, meteorology
  - Aircraft behaviour
  - Mechanical systems.

This Lecture Series, sponsored by the Guidance and Control Panel of AGARD, has been implemented by the Consultant and Exchange Programme.

ISBN 92-835-0714-2

AGARD

NATO OTAN

7 RUE ANCELLE · 92200 NEUILLY-SUR-SEINE

FRANCE

Télécopie (1)47.38.57.99 · Télex 610 176

DIFFUSION DES PUBLICATIONS
AGARD NON CLASSIFIEES

Aucun stock de publications n'a existé à AGARD. A partir de 1993, AGARD détiendra un stock limité des publications associées aux cycles de conférences et cours spéciaux ainsi que les AGARDographies et les rapports des groupes de travail, organisés et publiés à partir de 1993 inclus. Les demandes de renseignements doivent être adressées à AGARD par lettre ou par fax à l'adresse indiquée ci-dessus. *Veuillez ne pas téléphoner.* La diffusion initiale de toutes les publications de l'AGARD est effectuée auprès des pays membres de l'OTAN par l'intermédiaire des centres de distribution nationaux indiqués ci-dessous. Des exemplaires supplémentaires peuvent parfois être obtenus auprès de ces centres (à l'exception des Etats-Unis). Si vous souhaitez recevoir toutes les publications de l'AGARD, ou simplement celles qui concernent certains Panels, vous pouvez demander à être inclu sur la liste d'envoi de l'un de ces centres. Les publications de l'AGARD sont en vente auprès des agences indiquées ci-dessous, sous forme de photocopie ou de microfiche.

CENTRES DE DIFFUSION NATIONAUX

ALLEMAGNE
Fachinformationszentrum,
Karlsruhe
D-7514 Eggenstein-Leopoldshafen 2

BELGIQUE
Coordonnateur AGARD-VSL
Etat-Major de la Force Aérienne
Quartier Reine Elisabeth
Rue d'Evere, 1140 Bruxelles

CANADA
Directeur du Service des Renseignements Scientifiques
Ministère de la Défense Nationale
Ottawa, Ontario K1A 0K2

DANEMARK
Danish Defence Research Establishment
Ryvangs Allé 1
P.O. Box 2715
DK-2100 Copenhagen Ø

ESPAGNE
INTA (AGARD Publications)
Pintor Rosales 34
28008 Madrid

ETATS-UNIS
National Aeronautics and Space Administration
Langley Research Center
M/S 180
Hampton, Virginia 23665

FRANCE
O.N.E.R.A. (Direction)
29, Avenue de la Division Leclerc
92322 Châtillon Cedex

GRECE
Hellenic Air Force
Air War College
Scientific and Technical Library
Dekelia Air Force Base
Dekelia, Athens TGA 1010

ISLANDE
Director of Aviation
c/o Flugrad
Reykjavik

ITALIE
Aeronautica Militare
Ufficio del Delegato Nazionale all'AGARD
Aeroporto Pratica di Mare
00040 Pomezia (Roma)

LUXEMBOURG
Voir Belgique

NORVEGE
Norwegian Defence Research Establishment
Attn: Biblioteket
P.O. Box 25
N-2007 Kjeller

PAYS-BAS
Netherlands Delegation to AGARD
National Aerospace Laboratory NLR
P.O. Box 90502
1006 BM Amsterdam

PORTUGAL
Força Aérea Portuguesa
Centro de Documentação e Informação
Alfragide
2700 Amadora

ROYAUME UNI
Defence Research Information Centre
Kentigern House
65 Brown Street
Glasgow G2 8EX

TURQUIE
Millî Savunma Başkanlığı (MSB)
ARGE Daire Başkanlığı (ARGE)
Ankara

Le centre de distribution national des Etats-Unis (NASA/Langley) *ne* détient PAS de stocks des publications de l'AGARD. D'éventuelles demandes de photocopies doivent être formulées directement auprès du NASA Center for Aerospace Information (CASI) à l'adresse suivante:

AGENCES DE VENTE

NASA Center for
Aerospace Information (CASI)
800 Elkridge Landing Road
Linthicum Heights, MD 21090-2934
United States

ESA/Information Retrieval Service
European Space Agency
10, rue Mario Nikis
75015 Paris
France

The British Library
Document Supply Division
Boston Spa, Wetherby
West Yorkshire LS23 7BQ
Royaume Uni

Les demandes de microfiches ou de photocopies de documents AGARD (y compris les demandes faites auprès du CASI) doivent comporter la dénomination AGARD, ainsi que le numéro de série d'AGARD (par exemple AGARD-AG-315). Des informations analogues, telles que le titre et la date de publication sont souhaitables. Veuiller noter qu'il y a lieu de spécifier AGARD-R-nnn et AGARD-AR-nnn lors de la commande des rapports AGARD et des rapports consultatifs AGARD respectivement. Des références bibliographiques complètes ainsi que des résumés des publications AGARD figurent dans les journaux suivants:

Scientifique and Technical Aerospace Reports (STAR)
publié par la NASA Scientific and Technical
Information Program
NASA Headquarters (JTT)
Washington D.C. 20546
Etats-Unis

Government Reports Announcements and Index (GRA&I)
publié par le National Technical Information Service
Springfield
Virginia 22161
Etats-Unis

(accessible également en mode interactif dans la base de données bibliographiques en ligne du NTIS, et sur CD-ROM)

Imprimé par Specialised Printing Services Limited
40 Chigwell Lane, Loughton, Essex IG10 3TZ